VOLUME: 14 NO: 2 YEAR: 2017

ISSN: 1304-530X

TURKISH JOURNAL OF PHARMACEUTICAL SCIENCES

An Official Journal of the Turkish Pharmacists' Association, Academy of Pharmacy

TURKISH
JOURNAL OF PHARMACEUTICAL SCIENCES

TURKISH
JOURNAL OF PHARMACEUTICAL SCIENCES

AIMS AND SCOPE

The Turkish Journal of Pharmaceutical Sciences is the only scientific periodical publication of the Turkish Pharmacists' Association and has been published since April 2004.
Turkish Journal of Pharmaceutical Sciences is an independent international open access periodical journal based on double-blind peer-review principles. The journal is regularly published 3 times a year. The issuing body of the journal is Galenos Yayinevi/Publishing House.
The aim of Turkish Journal of Pharmaceutical Sciences is to publish original research papers of the highest scientific and clinical value at an international level.
The target audience includes specialists and physicians in all fields of pharmaceutical sciences.
The editorial policies are based on the "Recommendations for the Conduct, Reporting, Editing, and Publication of Scholarly Work in Medical Journals (ICMJE Recommendations)" by the International Committee of Medical Journal Editors (2016, archived at http://www.icmje.org/) rules.

ABSTRACTED/INDEXED IN

Web of Science-Emerging Sources Citation Index (ESCI)
SCOPUS SJR
Chemical Abstracts Service (CAS)
EBSCO
EMBASE
Analytical Abstracts
International Pharmaceutical Abstracts (IPA)
Medicinal & Aromatic Plants Abstracts (MAPA)
TÜBİTAK/ULAKBİM TR Dizin
Türkiye Atıf Dizini

OPEN ACCESS POLICY

This journal provides immediate open access to its content on the principle that making research freely available to the public supports a greater global exchange of knowledge.
Open Access Policy is based on the rules of the Budapest Open Access Initiative (BOAI) http://www.budapestopenaccessinitiative.org/. By "open access" to peer-reviewed research literature, we mean its free availability on the public internet, permitting any users to read, download, copy, distribute, print, search, or link to the full texts of these articles, crawl them for indexing, pass them as data to software, or use them for any other lawful purpose, without financial, legal, or technical barriers other than those inseparable from gaining access to the internet itself. The only constraint on reproduction and distribution, and the only role for copyright in this domain, should be to give authors control over the integrity of their work and the right to be properly acknowledged and cited.

CORRESPONDENCE ADDRESS

Editor-in-Chief, Feyyaz ONUR, Prof.Dr.
Address: Ankara University, Faculty of Pharmacy, Department of Analytical Chemistry, 06100 Tandoğan-Ankara, TURKEY
E-mail: onur@pharmacy.ankara.edu.tr

PERMISSION

Requests for permission to reproduce published material should be sent to the editorial office. Editor-in-Chief, Prof. Dr. Feyyaz ONUR

ISSUING BODY CORRESPONDING ADDRESS

Issuing Body : Galenos Yayınevi
Address: Molla Gürani Mah. Kaçamak Sk. No: 21/1, 34093 İstanbul, TURKEY
Phone: +90 212 621 99 25 Fax: +90 212 621 99 27
E-mail: info@galenos.com.tr

INSTRUCTIONS FOR AUTHORS

Instructions for authors are published in the journal and on the website http://turkjps.org

MATERIAL DISCLAIMER

The author(s) is (are) responsible for the articles published in the JOURNAL.
The editor, editorial board and publisher do not accept any responsibility for the articles.

Publisher Contact
Address: Molla Gürani Mah. Kaçamak Sk. No: 21/1 34093 İstanbul, Turkey
Phone: +90 (212) 621 99 25
Fax: +90 (212) 621 99 27
E-mail: info@galenos.com.tr/yayin@galenos.com.tr
Web: www.galenos.com.tr

Printing at: Özgün Ofset Ticaret Ltd. Şti.
Yeşilce Mah. Aytekin Sk. No: 21 34418 4. Levent, İstanbul, Turkey
Phone: +90 (212) 280 00 09
Printing date: July 2017
ISSN: 1304-530X
E-ISSN: 2148-6247

TURKISH
JOURNAL OF PHARMACEUTICAL SCIENCES

INSTRUCTIONS TO AUTHORS

Turkish Journal of Pharmaceutical Sciences is the official double peer-reviewed publication of The Turkish Pharmacists' Association. This journal is published every 4 months (3 issues per year; April, August, December) and publishes the following articles:

• Research articles

• Reviews (only upon the request or consent of the Editorial Board)

• Preliminary results/Short communications/Technical notes/Letters to the Editor in every field or pharmaceutical sciences.

The publication language of the journal is English.

The Turkish Journal of Pharmaceutical Sciences does not charge any article submission or processing charges.

A manuscript will be considered only with the understanding that it is an original contribution that has not been published elsewhere.

The Journal should be abbreviated as "Turk J Pharm Sci" when referenced.

The scientific and ethical liability of the manuscripts belongs to the authors and the copyright of the manuscripts belongs to the Journal. Authors are responsible for the contents of the manuscript and accuracy of the references. All manuscripts submitted for publication must be accompanied by the Copyright Transfer Form [copyright transfer]. Once this form, signed by all the authors, has been submitted, it is understood that neither the manuscript nor the data it contains have been submitted elsewhere or previously published and authors declare the statement of scientific contributions and responsibilities of all authors.

Experimental, clinical and drug studies requiring approval by an ethics committee must be submitted to the JOURNAL with an ethics committee approval report including approval number confirming that the study was conducted in accordance with international agreements and the Declaration of Helsinki (revised 2013) (http://www.wma.net/en/30publications/10policies/b3/). The approval of the ethics committee and the fact that informed consent was given by the patients should be indicated in the Materials and Methods section. In experimental animal studies, the authors should indicate that the procedures followed were in accordance with animal rights as per the Guide for the Care and Use of Laboratory Animals (http://oacu.od.nih.gov/regs/guide/guide.pdf) and they should obtain animal ethics committee approval.

Authors must provide disclosure/acknowledgment of financial or material support, if any was received, for the current study.

If the article includes any direct or indirect commercial links or if any institution provided material support to the study, authors must state in the cover letter that they have no relationship with the commercial product, drug, pharmaceutical company, etc. concerned; or specify the type of relationship (consultant, other agreements), if any.

Authors must provide a statement on the absence of conflicts of interest among the authors and provide authorship contributions.

All manuscripts submitted to the journal are screened for plagiarism using the 'iThenticate' software. Results indicating plagiarism may result in manuscripts being returned or rejected.

The Review Process

This is an independent international journal based on double-blind peer-review principles. The manuscript is assigned to the Editor-in-Chief, who reviews the manuscript and makes an initial decision based on manuscript quality and editorial priorities. Manuscripts that pass initial evaluation are sent for external peer review, and the Editor-in-Chief assigns an Associate Editor. The Associate Editor sends the manuscript to at least two reviewers (internal and/or external reviewers). The reviewers must review the manuscript within 21 days. The Associate Editor recommends a decision based on the reviewers' recommendations and returns the manuscript to the Editor-in-Chief. The Editor-in-Chief makes a final decision based on editorial priorities, manuscript quality, and reviewer recommendations. If there are any conflicting recommendations from reviewers, the Editor-in-Chief can assign a new reviewer.

The scientific board guiding the selection of the papers to be published in the Journal consists of elected experts of the Journal and if necessary, selected from national and international authorities. The Editor-in-Chief, Associate Editors may make minor corrections to accepted manuscripts that do not change the main text of the paper.

In case of any suspicion or claim regarding scientific shortcomings or ethical infringement, the Journal reserves the right to submit the manuscript to the supporting institutions or other authorities for investigation. The Journal accepts the responsibility of initiating action but does not undertake any responsibility for an actual investigation or any power of decision.

The Editorial Policies and General Guidelines for manuscript preparation specified below are based on "Recommendations for the Conduct, Reporting, Editing, and Publication of Scholarly Work in Medical Journals (ICMJE Recommendations)" by the International Committee of Medical Journal Editors (2016, archived at http://www.icmje.org/).

Preparation of research articles, systematic reviews and meta-analyses must comply with study design guidelines:

CONSORT statement for randomized controlled trials (Moher D, Schultz KF, Altman D, for the CONSORT Group. The CONSORT statement revised recommendations for improving the quality of reports of parallel group randomized trials. JAMA 2001; 285: 1987-91) (http://www.consort-statement.org/);

PRISMA statement of preferred reporting items for systematic reviews and meta-analyses (Moher D, Liberati A, Tetzlaff J, Altman DG, The PRISMA Group. Preferred Reporting Items for Systematic Reviews and Meta-Analyses: The PRISMA Statement. PLoS Med 2009; 6(7): e1000097.) (http://www.prisma-statement.org/);

STARD checklist for the reporting of studies of diagnostic accuracy (Bossuyt PM, Reitsma JB, Bruns DE, Gatsonis CA, Glasziou PP, Irwig LM, et al., for the STARD Group. Towards complete and accurate reporting of studies of diagnostic accuracy: the STARD initiative. Ann Intern Med 2003;138:40-4.) (http://www.stard-statement.org/);

STROBE statement, a checklist of items that should be included in reports of observational studies (http://www.strobe-statement.org/);

MOOSE guidelines for meta-analysis and systemic reviews of observational studies (Stroup DF, Berlin JA, Morton SC, et al. Meta-analysis of observational studies in epidemiology: a proposal for reporting Meta-analysis of observational Studies in Epidemiology (MOOSE) group. JAMA 2000; 283: 2008-12).

GENERAL GUIDELINES

Manuscripts can only be submitted electronically through the Journal Agent website (http://journalagent.com/tjps/) after creating an account. This system allows online submission and review.

TURKISH
JOURNAL OF PHARMACEUTICAL SCIENCES

INSTRUCTIONS TO AUTHORS

The manuscripts are archived according to ICMJE, Web of Science-Emerging Sources Citation Index (ESCI), SCOPUS, Chemical Abstracts, EBSCO, EMBASE, Analytical Abstracts, International Pharmaceutical Abstracts, MAPA(Medicinal & Aromatic Plants Abstracts), Tübitak/ Ulakbim Turkish Medical Database, Türkiye Citation Index Rules.

Format: Manuscripts should be prepared using Microsoft Word, size A4 with 2.5 cm margins on all sides, 12 pt Arial font and 1.5 line spacing.

Abbreviations: Abbreviations should be defined at first mention and used consistently thereafter. Internationally accepted abbreviations should be used; refer to scientific writing guides as necessary.

Cover letter: The cover letter should include statements about manuscript type, single-Journal submission affirmation, conflict of interest statement, sources of outside funding, equipment (if applicable), for original research articles.

REFERENCES

Authors are solely responsible for the accuracy of all references.

In-text citations: References should be indicated as a superscript immediately after the period/full stop of the relevant sentence. If the author(s) of a reference is/are indicated at the beginning of the sentence, this reference should be written as a superscript immediately after the author's name. If relevant research has been conducted in Turkey or by Turkish investigators, these studies should be given priority while citing the literature.

Presentations presented in congresses, unpublished manuscripts, theses, Internet addresses, and personal interviews or experiences should not be indicated as references. If such references are used, they should be indicated in parentheses at the end of the relevant sentence in the text, without reference number and written in full, in order to clarify their nature.

References section: References should be numbered consecutively in the order in which they are first mentioned in the text. All authors should be listed regardless of number. The titles of Journals should be abbreviated according to the style used in the Index Medicus.

Reference Format

Journal: Last name(s) of the author(s) and initials, article title, publication title and its original abbreviation, publication date, volume, the inclusive page numbers. Example: Collin JR, Rathbun JE. Involutional entropion: a review with evaluation of a procedure. Arch Ophthalmol. 1978;96:1058-1064.

Book: Last name(s) of the author(s) and initials, chapter title, book editors, book title, edition, place of publication, date of publication and inclusive page numbers of the extract cited.

Example: Herbert L. The Infectious Diseases (1st ed). Philadelphia; Mosby Harcourt; 1999:11;1-8.

Book Chapter: Last name(s) of the author(s) and initials, chapter title, book editors, book title, edition, place of publication, date of publication and inclusive page numbers of the cited piece.

Example: O'Brien TP, Green WR. Periocular Infections. In: Feigin RD, Cherry JD, eds. Textbook of Pediatric Infectious Diseases (4th ed). Philadelphia; W.B. Saunders Company;1998:1273-1278.

Books in which the editor and author are the same person: Last name(s) of the author(s) and initials, chapter title, book editors, book title, edition, place of publication, date of publication and inclusive page numbers of the cited piece. Example: Solcia E, Capella C, Kloppel G. Tumors of the exocrine pancreas. In: Solcia E, Capella C, Kloppel G, eds. Tumors of the Pancreas. 2nd ed. Washington: Armed Forces Institute of Pathology; 1997:145-210.

TABLES, GRAPHICS, FIGURES, AND IMAGES

All visual materials together with their legends should be located on separate pages that follow the main text.

Images: Images (pictures) should be numbered and include a brief title. Permission to reproduce pictures that were published elsewhere must be included. All pictures should be of the highest quality possible, in

JPEG format, and at a minimum resolution of 300 dpi.

Tables, Graphics, Figures: All tables, graphics or figures should be enumerated according to their sequence within the text and a brief descriptive caption should be written. Any abbreviations used should be defined in the accompanying legend. Tables in particular should be explanatory and facilitate readers' understanding of the manuscript, and should not repeat data presented in the main text.

MANUSCRIPT TYPES

Original Articles

Clinical research should comprise clinical observation, new techniques or laboratories studies. Original research articles should include title, structured abstract, key words relevant to the content of the article, introduction, materials and methods, results, discussion, study limitations, conclusion references, tables/figures/images and acknowledgement sections. Title, abstract and key words should be written in both Turkish and English. The manuscript should be formatted in accordance with the above-mentioned guidelines and should not exceed 16 A4 pages.

Title Page: This page should include the title of the manuscript, short title, name(s) of the authors and author information. The following descriptions should be stated in the given order:

1. Title of the manuscript (Turkish and English), as concise and explanatory as possible, including no abbreviations, up to 135 characters

2. Short title (Turkish and English), up to 60 characters

3. Name(s) and surname(s) of the author(s) (without abbreviations and academic titles) and affiliations

4. Name, address, e-mail, phone and fax number of the corresponding author

5. The place and date of scientific meeting in which the manuscript was presented and its abstract published in the abstract book, if applicable

Abstract: A summary of the manuscript should be written in both Turkish and English. References should not be cited in the abstract. Use of abbreviations should be avoided as much as possible; if any abbreviations are used, they must be taken into consideration independently of the abbreviations used in the text. For original articles, the structured abstract should include the following sub-headings:

Objectives: The aim of the study should be clearly stated.

Materials and Methods: The study and standard criteria used should be defined; it should also be indicated whether the study is randomized or not, whether it is retrospective or prospective, and the statistical methods applied should be indicated, if applicable.

TURKISH
JOURNAL OF PHARMACEUTICAL SCIENCES

INSTRUCTIONS TO AUTHORS

Results: The detailed results of the study should be given and the statistical significance level should be indicated.

Conclusion: Should summarize the results of the study, the clinical applicability of the results should be defined, and the favorable and unfavorable aspects should be declared.

Keywords: A list of minimum 3, but no more than 5 key words must follow the abstract. Key words in English should be consistent with "Medical Subject Headings (MESH)" (www.nlm.nih.gov/mesh/MBrowser.html). Turkish key words should be direct translations of the terms in MESH.

Original research articles should have the following sections:

Introduction: Should consist of a brief explanation of the topic and indicate the objective of the study, supported by information from the literature.

Materials and Methods: The study plan should be clearly described, indicating whether the study is randomized or not, whether it is retrospective or prospective, the number of trials, the characteristics, and the statistical methods used.

Results: The results of the study should be stated, with tables/figures given in numerical order; the results should be evaluated according to the statistical analysis methods applied. See General Guidelines for details about the preparation of visual material.

Discussion: The study results should be discussed in terms of their favorable and unfavorable aspects and they should be compared with the literature. The conclusion of the study should be highlighted.

Study Limitations: Limitations of the study should be discussed. In addition, an evaluation of the implications of the obtained findings/ results for future research should be outlined.

Conclusion: The conclusion of the study should be highlighted.

Acknowledgements: Any technical or financial support or editorial contributions (statistical analysis, English/Turkish evaluation) towards the study should appear at the end of the article.

References: Authors are responsible for the accuracy of the references. See General Guidelines for details about the usage and formatting required.

Review Articles

Review articles can address any aspect of clinical or laboratory pharmaceuticals. Review articles must provide critical analyses of contemporary evidence and provide directions of or future research. Most review articles are commissioned, but other review submissions are also welcome. Before sending a review, discussion with the editor is recommended.

Reviews articles analyze topics in depth, independently and objectively. The first chapter should include the title in Turkish and English, an unstructured summary and key words. Source of all citations should be indicated. The entire text should not exceed 25 pages (A4, formatted as specified above).

CORRESPONDENCE

All correspondence should be directed to the Turkish Journal of Pharmaceutical Sciences editorial board;

Post: Turkish Pharmacists' Association

Address: Willy Brandt Sok. No: 9 06690 Ankara, TURKEY

Phone: +90 312 409 8136

Fax: +90 312 409 8132

Web Page: http://turkjps.org/home/

E-mail: onur@pharmacy.ankara.edu.tr

TURKISH
JOURNAL OF PHARMACEUTICAL SCIENCES

CONTENTS

Original Articles

TURKISH
JOURNAL OF PHARMACEUTICAL SCIENCES

CONTENTS

TURKSH
JOURNAL OF PHARMACEUTICAL SCIENCES

Volume: 14, No: 2, Year: 2017

CONTENTS

Original articles

Review articles

Turk J Pharm Sci 2017;14(2):95-107
DOI: 10.4274/tjps.07078

ORIGINAL ARTICLE

Assessment of Cytotoxicity Profiles of Different Phytochemicals: Comparison of Neutral Red and MTT Assays in Different Cells in Different Time Periods

Fenoliklerin Sitotoksisite Profillerinin Değerlendirilmesi: Farklı Hücrelerde Farklı Zaman Aralıklarında Nötral Kırmızı ve MTT Yöntemlerinin Karşılaştırılması

Merve BACANLI[1]*, Hatice Gül ANLAR[1], A. Ahmet BAŞARAN[2], Nurşen BAŞARAN[1]

[1]Hacettepe University, Faculty of Pharmacy, Department of Pharmaceutical Toxicology, Ankara, Turkey
[2]Hacettepe University, Faculty of Pharmacy, Departments of Pharmacognosy, Ankara, Turkey

ABSTRACT

Objectives: Phenolic compounds exhibit several health protective properties. Galangin, curcumin, pycnogenol, puerarin and ursolic acid are commonly used plant phenolics in folk medicine. The aim of our study was to evaluate the difference between neutral red uptake (NRU) and MTT assays using different plant phenolics (galangin, curcumin, pycnogenol, puerarin and ursolic acid) in healthy and cancer cells in different time periods.

Materials and Methods: In this study, the cytotoxic effects of these phenolic compounds were investigated by NRU and MTT assays in healthy (V79, Chinese hamster fibroblast cell line) and cancer [human cervix epithelial adenocarcinoma cell line Henrietta Lacks (HeLa) and human mammary carcinoma cell line (BT-474)] in 18, 24 and 48 h incubation periods.

Results: Our results demonstrated that galangin, curcumin, pycnogenol, puerarin and ursolic acid decreased cell viability of V79, HeLa and BT-474 cells in a dose-dependent manner in 18, 24 and 48 h incubation periods. However, the cell survival rate was much lower in 48 h incubation period. There was no difference between the results from NRU and MTT assays.

Conclusion: To decide which incubation period and which cytotoxicity study to be used, the cytotoxicity mechanism of the compound must be known.

Key words: MTT, neutral red, plant phenolics

ÖZ

Amaç: Fenolik bileşikler sağlığı koruyucu farklı özellikler gösterir. Galangin, kurkumin, piknogenol, puerarin ve ursolik asit halk tıbbında yaygın olarak kullanılan bitkisel fenoliklerdendir. Bu çalışmanın amacı, nötral kırmızı alım (NKA) ve MTT yöntemleri arasındaki farkı sağlıklı hücreler ve kanser hücrelerinde farklı bitkisel fenoliklerin (galangin, kurkumin, piknogenol, puerarin ve ursolik asit) farklı zaman aralıklarında farklı zaman aralıklarında belirlemektir.

Gereç ve Yöntemler: Bu çalışmada, bu fenolik bileşiklerin sitotoksik etkileri sağlıklı hücreler (Çin hamster fibroblast hücre hattı, V79) ve kanser [insan serviks epitelyal adenokarsinoma hücre hattı, Henrietta Lacks (HeLa) ve insan meme karsinoma hücre hattı (BT-474)] hücrelerinde 18, 24 ve 48 saatlik inkübasyon sürelerinde NKA ve MTT yöntemleriyle değerlendirilmiştir.

Bulgular: Bulgularımız galangin, kurkumin, piknogenol, puerarin ve ursolik asitin V79, HeLa ve BT-474 hücre canlılıklarını 18, 24 ve 48 saatlik inkübasyon sürelerinde doza bağımlı olarak azalttığını göstermiştir. Ancak en az hücre canlılık oranı 48 saatlik inkübasyon sonrası görülmüştür. NKA ile MTT yöntemlerinin sonuçları arasında fark görülmemiştir.

Sonuç: Sitotoksisite analizinde kullanılacak yöntem ve inkübasyon süresinin belirlenmesi için maddelerin sitotoksisite mekanizması bilinmelidir.

Anahtar kelimeler: MTT, nötral kırmızı, bitkisel fenolikler

*Correspondence: E-mail: mervebacanli@gmail.com, Phone: +90 505 259 20 39
ORCID ID: orcid.org/0000-0001-8757-0572
Received: 10.10.2016, Accepted: 20.11.2016

INTRODUCTION

Consumption of great amounts of fruits and vegetables rich in phenolic compounds has been associated with health benefits such as anti-artherogenic, antiinflammatory, anti-microbial, antioxidant, anti-thrombotic, and cardioprotective effects.[1,2] Due to the cytotoxicity profile of many phenolic compounds, it is suggested that these compounds can inhibit the survival of cancer cells. But the data about the cytotoxicity of these compounds in healthy cells are limited.

Galangin (3,5,7-trihydroxyflavone), is present at high concentrations in propolis and in an Indian root, *Alpinia officinarum*, which is a common spice in Asia.[3] It is suggested that galangin has antioxidant, antimutagenic, antiinflammatory, antiviral and anticancer properties.[4,5]

Curcumin (diferuloyl methane), the major yellow pigment from the rhizomes of turmeric (*Curcuma longa L.*), have gained increasing interest because of its chemopreventive properties against human cancers.[6] Turmeric, the powdered rhizome is commonly used as an antiseptic, antidote for poisoning, for treating respiratory disorders, some skin diseases, and as a household remedy for treating sprains and swellings caused by injury.[7,8]

Pycnogenol (PYC) is a standardized natural plant extract obtained from the bark of the French maritime pine *Pinus pinaster* (formerly known as *Pinus maritime*).[9] PYC has been used in European countries as a dietary food supplement. It has strong antioxidant activity and capacity to efficiently scavenge reactive oxygen and nitrogen species.[10]

Puerarin (daidzein-8-C-glucoside) is the main isoflavone derived from the root of *Pueraria lobata* (kudzu root).[11] In experimental models it is also suggested to be used in the prevention and treatment of cardiovascular diseases, diabetes, cancer and osteoporosis.[12]

Ursolic acid (3β-hydroxy-urs-12-en-28-oic acid) is a pentacyclic triterpenoid obtained from plants. It has long been used in traditional Chinese medicine because of its anti-inflammatory, anti-arthritic, cytostatic and anti-proliferative, hepatoprotective effects.[13]

Cytotoxicity assays are widely used in toxicology studies. The NR uptake (NRU) and 3-(4,5-dimethylthiazol-2-yl)-2,5-diphenyltetrazoliumbromide (MTT) assays are commonly used cytotoxicity assays to determine the cytotoxic properties of compounds. NRU assay has been used as an indicator of cytotoxicity in cultures of primary hepatocytes[14] and other cell lines.[15] Living cells take up the neutral red, which is concentrated within the lysosomes of cells.[16] MTT, a water soluble tetrazolium salt, is converted to an insoluble purple formazan by cleavage of the tetrazolium ring by succinate dehydrogenase within the mitochondria. The formazan product is impermeable to the cell membranes and therefore it accumulates in healthy cells.[17]

The aim of our study was to evaluate the difference between NRU and MTT assays using different plant phenolics (galangin, curcumin, PYC, puerarin and ursolic acid) in healthy (V79, Chinese hamster fibroblast cell line) and cancer [human cervix epithelial adenocarcinoma cell line (HeLa) and human mammary carcinoma cell line (BT-474)] cells in different time periods (8, 24 and 48 h).

MATERIALS AND METHODS

Chemicals

The chemicals used in the experiments were purchased from the following suppliers: fetal calf serum (FCS), trypsin-EDTA, penicillinstreptomycin, from Biological Industries (Kibbutz Beit-Haemek, Israel), minimum essential medium (MEM), dimethyl sulfoxide, Triton X-100, phosphate buffered saline (PBS), ethanol, NR, MTT, galangin, curcumin (97%, purity), ursolic acid from Sigma (St Louis, USA), puerarin from Fluka (St. Gallen, Switzerland). PYC®, a registered trade mark of Horphag Research Ltd., (Geneva, Switzerland), was provided by Henkel Corporation (La Grange, IL, U.S.A.).

Cell culture

V79, HeLa and BT-474 cells were seeded in 75 cm^2 flasks in 20 mL MEM supplemented with 10% FCS and 1% penicillin-streptomycin and then grown for 24 h in an incubator at 37°C in an atmosphere supplemented with 5% CO_2.

Determination of cytotoxicity by NRU assay

The cytotoxicity of phenolic compounds was performed in V79, HeLa and BT-474 cell lines by NRU assay following the protocols described by Di Virgilio et al.[18] and Saquib et al.[19]. Following disaggregation of cells with trypsin/EDTA and resuspension of cells in the medium, a total of 10^5 cells/well were plated in 96 well tissue-culture plates. After 24 h incubation, the different concentrations of galangin, curcumin, PYC, puerarin and ursolic acid in medium were added. The cells were incubated for 18, 24 and 48 h at 37°C in 5% CO_2, then the medium was aspirated. The cells were then incubated for an additional 3 h in the medium supplemented with NR (50 µg/mL). The absorbance of the solution in each well was measured in a microplate reader at 540 nm and compared with the wells containing untreated cells. Results were expressed as the mean percentage of cell growth inhibition from three independent experiments. Cell viability was plotted as the percent of control (assuming data obtained from the absence of phenolic compounds as 100%).

Determination of cytotoxicity by MTT assay

MTT assay was performed by the method of Mosmann[17] with the modifications of Holst-Hansen and Brünner[20] and Kuzma et al.[21]. A total of 10^5 cells/well were plated in 96 well tissue-culture plates. After 24 h incubation, cells were exposed to the different concentrations of galangin, curcumin, PYC, puerarin and ursolic acid in medium for 18, 24 and 48 h at 37°C in 5% CO_2 in air. Then, the medium was aspirated and MTT (5 mg/mL of stock in PBS) was added (10 µL/well in 100 µL of cell suspension), and cells were incubated for an additional 4 h with MTT dye. At the end of incubation period, the absorbance of the solution in each well was measured in a microplate reader at 570 nm. Results were expressed as the mean percentage of cell growth from three independent experiments. Cell viability was

plotted as the percent of control (assuming data obtained from the absence of phenolic compounds as 100%).

RESULTS

Determination of cytotoxicity in V79 cell line

A concentration dependent decrease was seen in the survival of cells exposed to galangin, curcumin, PYC, puerarin and ursolic acid in all time periods in both cytotoxicity assays. But in 48 h incubation period, the cell survival is found much lower (Table 1) (Figure 1, 2).

Determination of cytotoxicity in HeLa cell line

A concentration dependent decrease was seen in the survival of cells exposed to galangin, curcumin, PYC, puerarin and ursolic acid in all time periods in both cytotoxicity assays. But in 48 h incubation period, the cell survival is found much lower (Table 2) (Figure 3, 4).

Determination of cytotoxicity in BT-474 cell line

A concentration dependent decrease was seen in the survival of cells exposed to galangin, curcumin, PYC, puerarin and ursolic acid in all time periods in both cytotoxicity assays. But in 48 h incubation period, the cell survival is found much lower (Table 3) (Figure 5, 6).

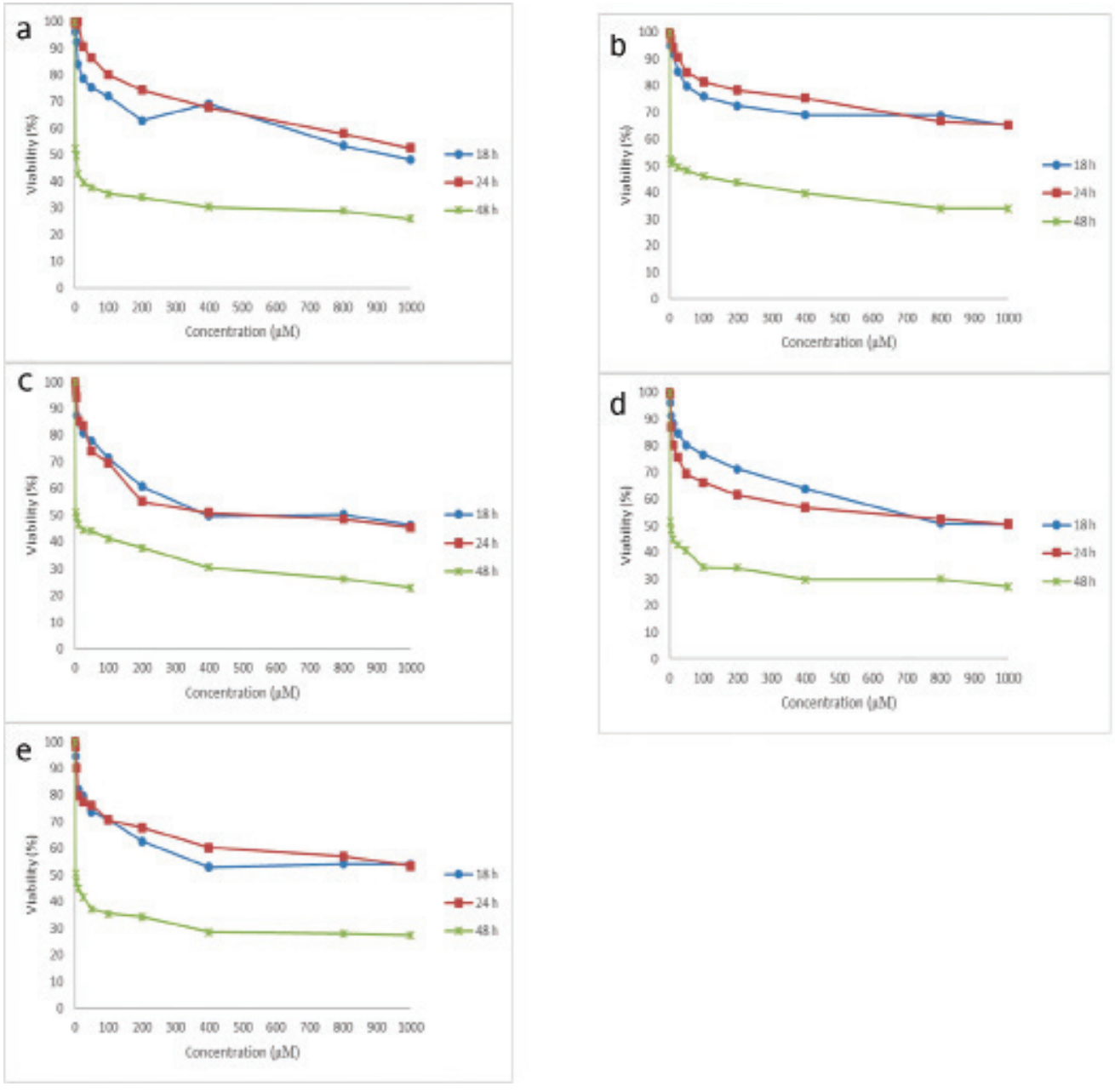

Figure 1. Cytotoxic effects of a) galangin, b) curcumin, c) pycnogenol, d) puerarin and e) ursolic acid in V79 cells by neutral red uptake assay

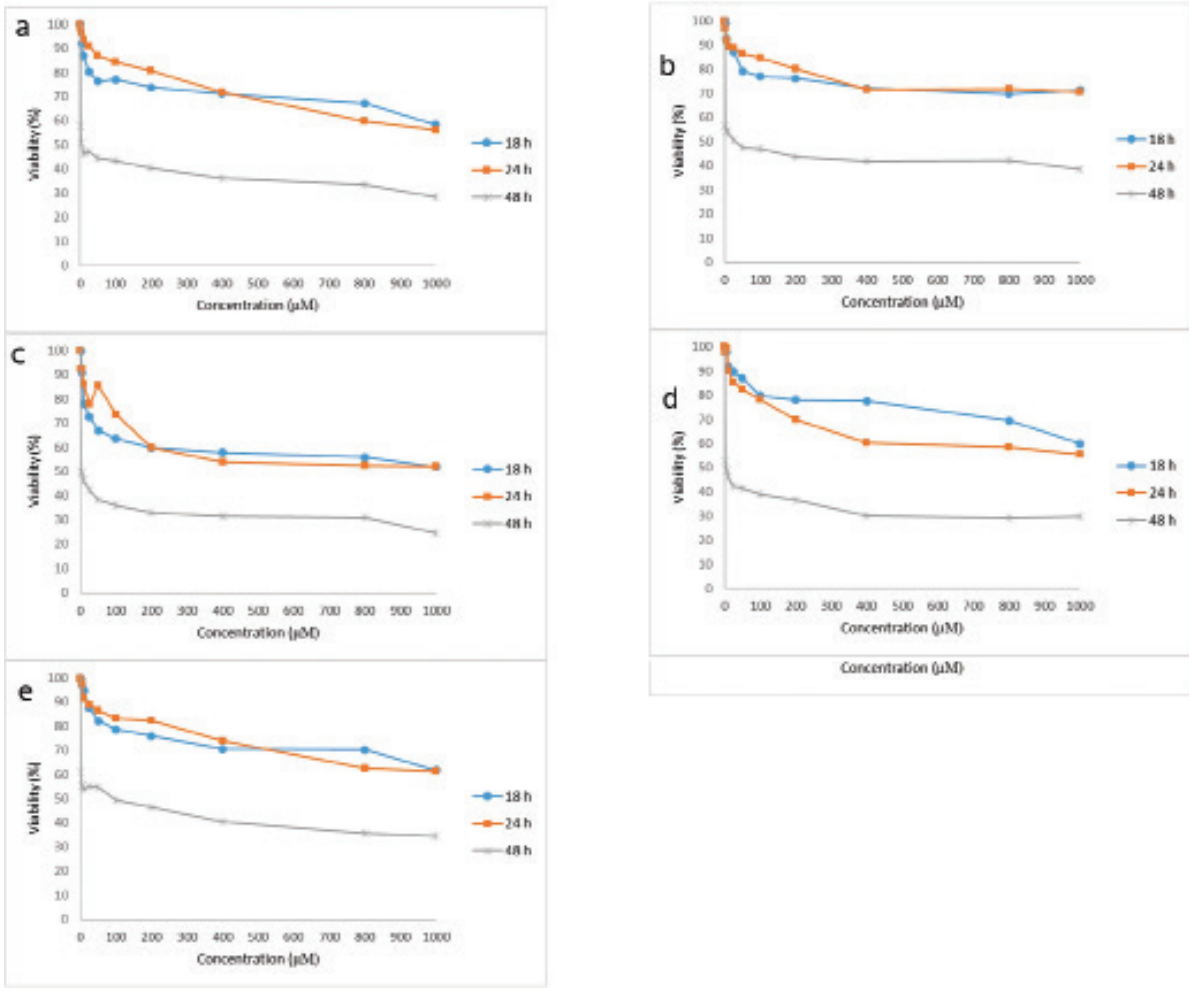

Figure 2. Cytotoxic effects of, a) galangin, b) curcumin, c) pycnogenol, d) puerarin and e) ursolic acid in V79 cells by 3-(4,5-dimethylthiazol-2-yl)-2,5-diphenyltetrazoliumbromide assay

DISCUSSION

The cytotoxic effects of galangin, curcumin, PYC, puerarin and ursolic acid were investigated by NRU and MTT assays in V79, HeLa and BT-474 cells in 18, 24 and 48 h incubation periods. This is the first study about cytotoxic effects of these phenolics in healthy and cancer cell lines with two different assays and different incubation periods. Our results demonstrated that both galangin, curcumin, PYC, puerarin and ursolic acid decreased cell viability of V79, HeLa and BT-474 cells in a dose dependent manner in 18, 24 and 48 h incubation periods. But the cell survival rate was much lower in 48 h incubation period.

In SNU-484 cells, galangin has shown cytotoxic effect in a dose dependent manner and IC_{50} value of galangin in this cell line has found 100 µM.[22] In an another cytotoxicity study with galangin, it has shown that the cytotoxic effect has increased in a dose dependent manner on HepG2 cells.[23] As a result of the small number of studies carried out that galangin has no cytotoxic activity under 100 µM in different methods and different cell lines. Lantto et al.[24] have studied cytotoxicity of curcumin in two different cell lines [neuroblastoma (SH-SY5Y) and fibroblast (CV1-P) cells] by MTT and lactate dehydrogenase (LDH) leakage assays and their results have indicated that curcumin significantly decreased the metabolic activity of these cells.[24] Also, Mehta et al.[25] have showed anti-proliferative effect of curcumin on human breast tumor cell lines BT-20, T-47D, SKBR3 and MCF-7 by MTT assay. The effects of curcumin on the viability of human leukemia cell lines (U937 and Molt4) by MTT assay were also determined and dose dependent cytotoxic effects of curcumin were found.[26] Taner et al.[27] demonstrated the cytotoxic profile of PYC in healthy CHO cells. In this study, PYC has not showed cytotoxic effects at the concentrations of up to 150 µg/mL in CHO cells during 24 h exposure but above this concentration the cytotoxicity of PYC has started and the cell viability was decreased below 50% at 300 µg/mL.[27] There is limited study about cytotoxicity of puerarin. In a single study, it is demonstrated that puerarin has shown cytotoxic effects on HT-29 cells in a dose and time dependent manner.[28] In CaCo-2 cells, the viability of cells has decreased at concentrations higher than 100 µM with ursolic acid exposure for 48 h[29,30] have demonstrated that ursolic acid decreased the cytotoxic effects of ultraviolet B on lymphocytes in trypan blue and MTT methods.

It has been reported that different cytotoxicity assays can give

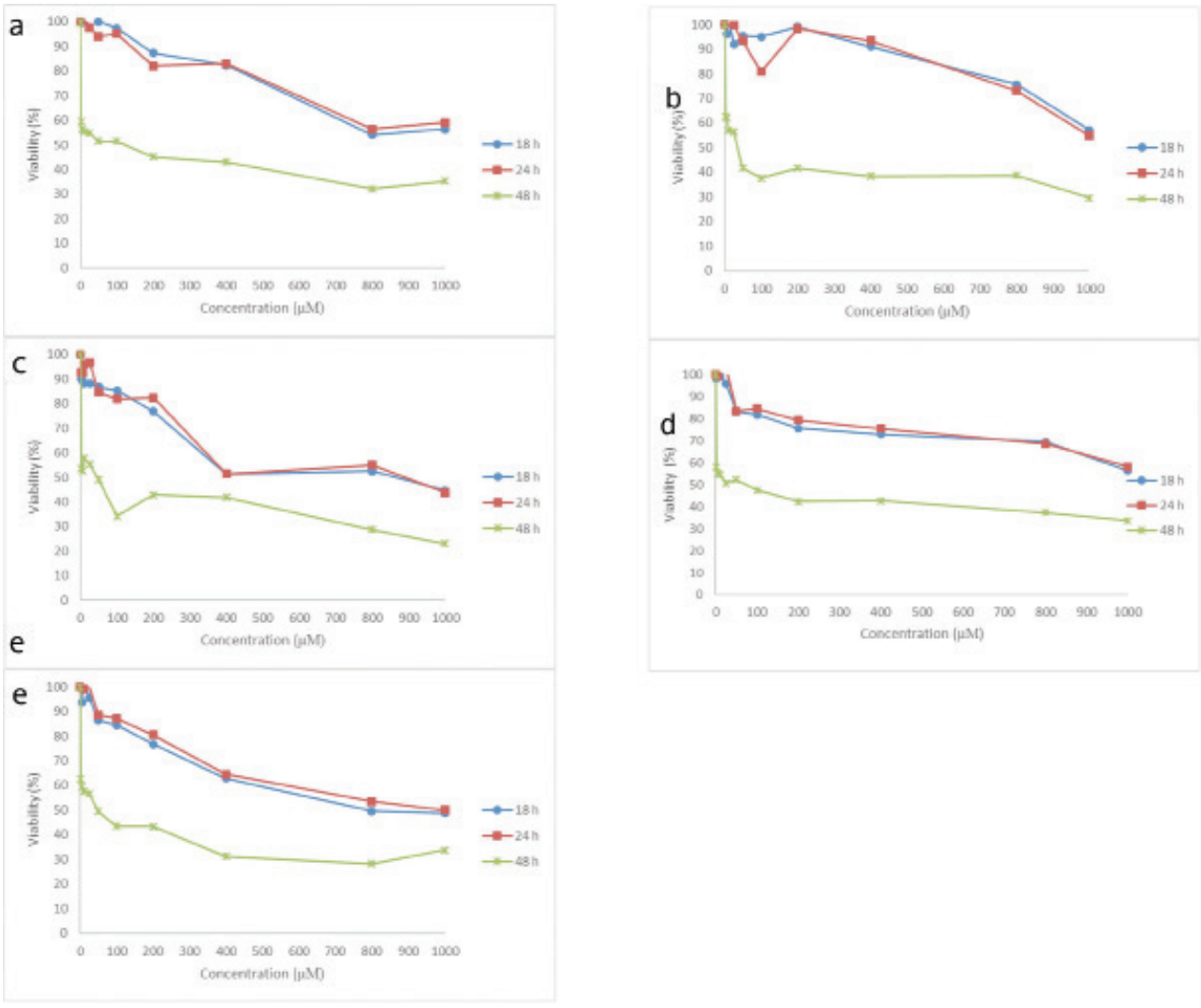

Figure 3. Cytotoxic effects of a) galangin, b) curcumin, c) pycnogenol, d) puerarin and e) ursolic acid in HeLa cells by neutral red uptake assay

different results due to the chemical and the cytotoxicity assay employed.[31] Fotakis and Timbrell[16] have compared four different cytotoxicity assays (LDH, a protein, NRU and MTT assays). Different sensitivity was observed for each assay. The NRU and the MTT assays were found to be the most sensitive in detecting cytotoxic events. Putnam et al.[32] have also studied cytotoxicity of cigarette smoke condensate with eight different (NRU, LDH release, kenacid blue binding, MTT, XTT, acid phosphatase activity, sulforhodamine B binding and resazurin binding) cytotoxicity assays. Four of the more widely used cytotoxicity assays (NRU, MTT, kenacid blue and LDH) were also evaluated at 3, 6, 12 and 18 h time points in this study. They have concluded that assays that measure membrane integrity (LDH) are useful for short exposure times (1 h), NRU assay was the most sensitive for moderate (3-6 h) exposure times; and assays that measure total cell number (NRU and kenacid blue) were more sensitive for longer exposure times (12, 18 and 24 h).[32] But in our study, both phenolics showed similar cytotoxicity profile in NRU and MTT assays in all exposure times.

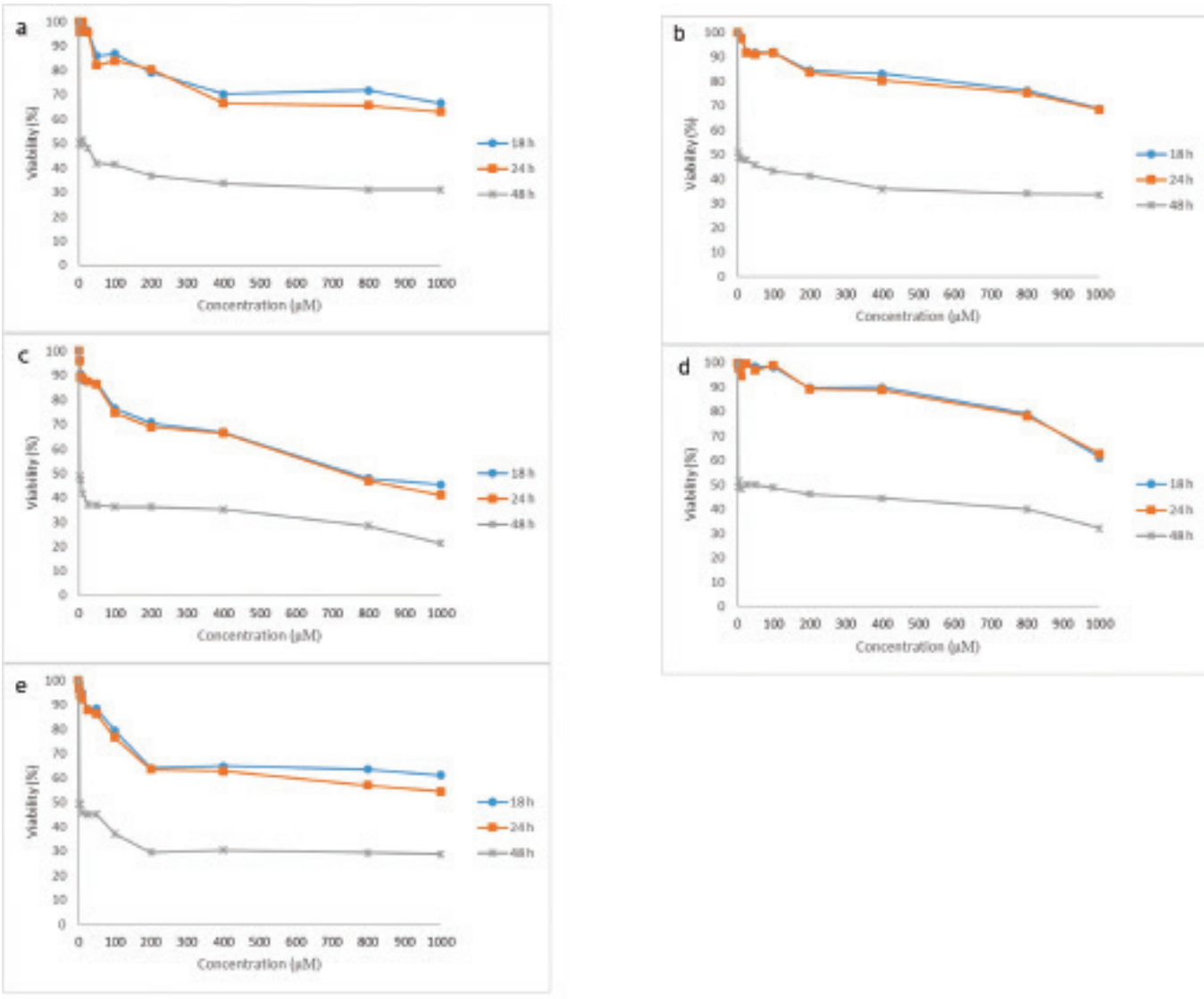

Figure 4. Cytotoxic effects of a) galangin, b) curcumin, c) pycnogenol, d) puerarin and e) ursolic acid in HeLa cells by 3-(4,5-dimethylthiazol-2-yl)-2,5-diphenyltetrazoliumbromide assay

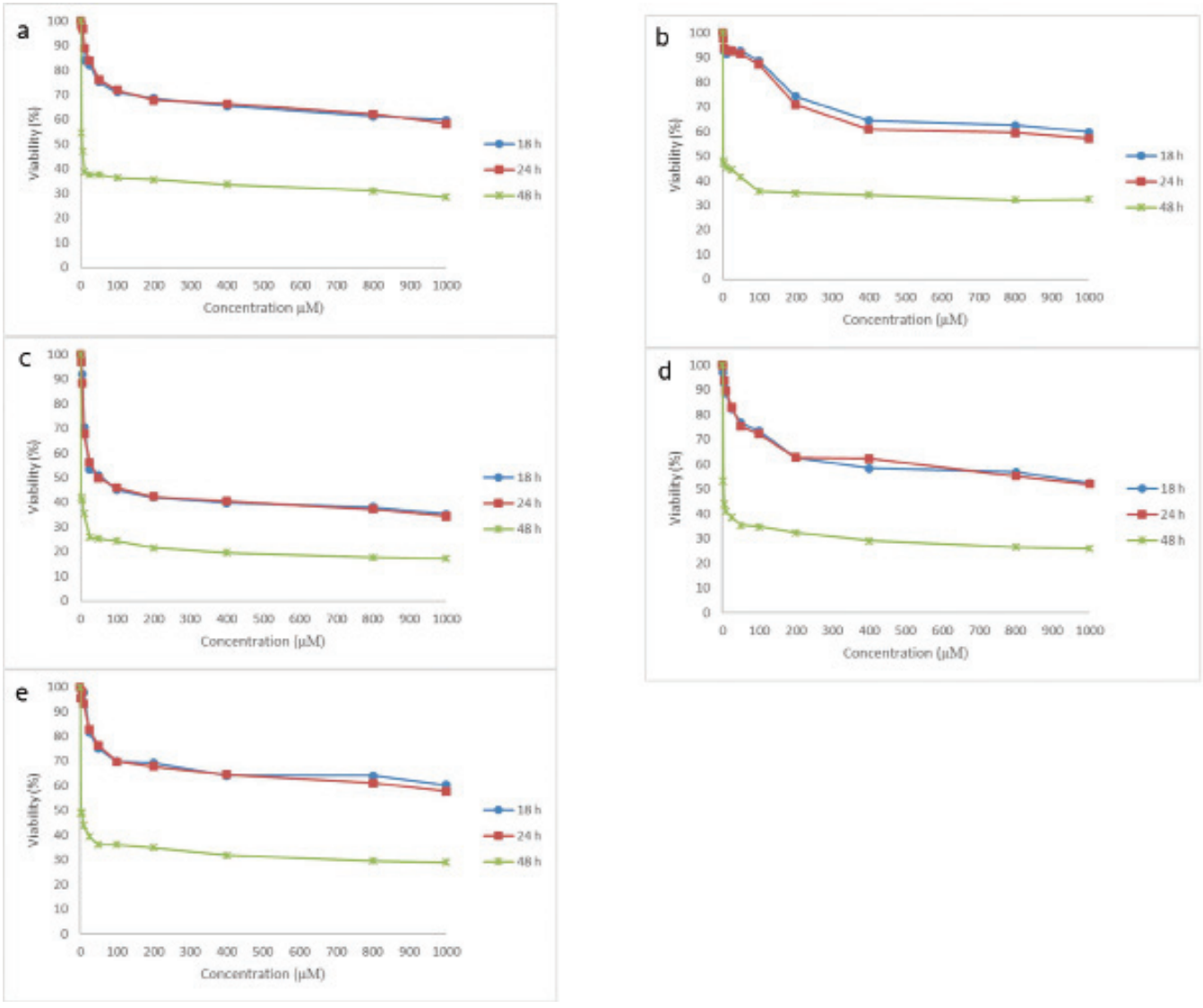

Figure 5. Cytotoxic effects of a) galangin, b) curcumin, c) pycnogenol, d) puerarin and e) ursolic acid in BT-474 cells by neutral red uptake assay

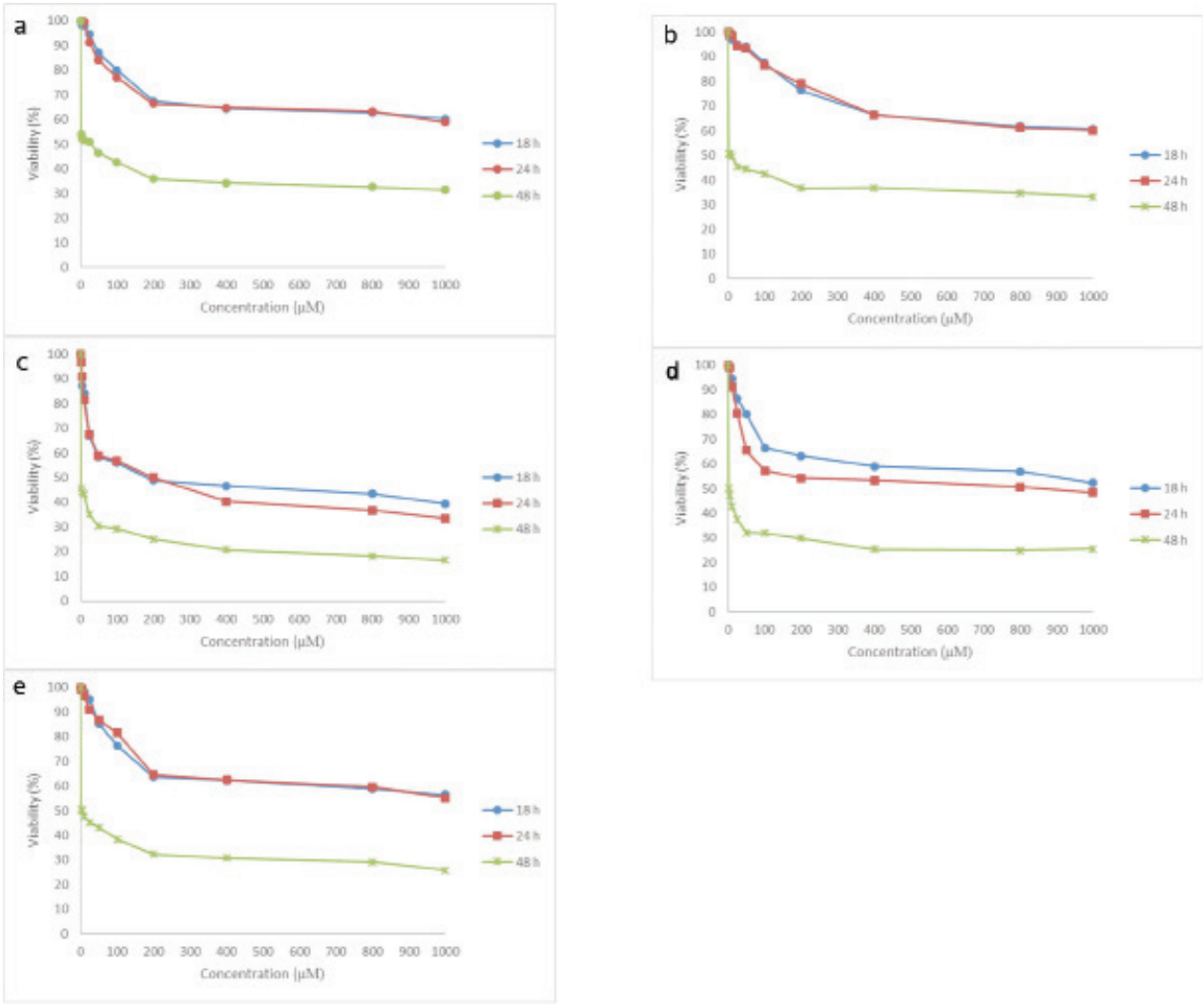

Figure 6. Cytotoxic effects of a) galangin, b) curcumin, c) pycnogenol, d) puerarin and e) ursolic acid in BT-474 cells by 3-(4,5-dimethylthiazol-2-yl)-2,5-diphenyltetrazoliumbromide assay

Table 1. Viability (%) of V79 cells exposed to galangin, curcumin, pycnogenol, puerarin and ursolic acid

	18 h NRU (%)	18 h MTT (%)	24 h NRU (%)	24 h MTT (%)	48 h NRU (%)	48 h MTT (%)
Negative control	100.00	100.000	100.00	100.00	100.00	100.00
1000 μM galangin	48.263	58.388	52.579	56.372	25.898	28.426
800 μM galangin	53.444	67.179	57.996	59.919	28.986	33.411
400 μM galangin	69.153	71.308	67.857	71.913	30.428	36.102
200 μM galangin	62.689	73.759	74.404	80.607	34.105	40.276
100 μM galangin	72.019	77.114	80.059	84.335	35.405	43.396
50 μM galangin	75.271	76.319	86.388	87.156	37.802	44.670
25 μM galangin	78.559	80.393	90.595	90.845	39.569	47.389
10 μM galangin	83.979	86.929	99.880	93.649	42.799	46.417
5 μM galangin	92.412	92.023	99.107	96.603	49.563	50.841
2 μM galangin	96.160	99.959	99.503	98.343	52.244	57.574
1000 μM curcumin	65.148	71.208	65.297	70.663	33.942	38.498
800 μM curcumin	68.951	69.821	66.726	71.680	34.044	42.232
400 μM curcumin	69.098	72.047	75.396	71.555	39.609	41.973
200 μM curcumin	75.950	76.251	81.527	80.240	46.008	43.764
100 μM curcumin	72.478	76.954	78.373	84.750	43.753	46.957
50 μM curcumin	79.845	79.184	85.158	86.513	48.263	47.626
25 μM curcumin	85.430	87.181	90.674	88.853	49.421	50.540
10 μM curcumin	92.100	89.417	94.246	89.146	51.635	53.518
5 μM curcumin	95.002	92.465	97.579	91.759	50.903	54.381
2 μM curcumin	95.241	98.774	99.503	96.821	52.447	56.517
1000 μM pycnogenol	46.298	51.899	45.396	52.039	23.014	24.638
800 μM pycnogenol	50.374	55.883	48.571	52.449	26.203	30.837
400 μM pycnogenol	49.770	57.770	50.972	53.896	30.550	31.506
200 μM pycnogenol	60.812	59.709	55.079	59.941	37.863	33.060
100 μM pycnogenol	71.596	63.510	69.642	73.577	41.174	35.952
50 μM pycnogenol	77.916	66.986	73.948	85.599	43.956	38.261
25 μM pycnogenol	80.984	72.618	83.551	77.793	44.322	42.188
10 μM pycnogenol	85.118	77.989	85.436	86.266	46.597	46.310
5 μM pycnogenol	87.304	90.645	94.424	92.311	49.461	49.396
2 μM pycnogenol	95.352	99.739	97.420	92.460	51.046	49.979
1000 μM puerarin	50.560	59.885	50.521	55.571	27.117	29.802
800 μM puerarin	50.909	69.520	52.480	58.528	29.920	29.258
400 μM puerarin	63.935	77.557	56.805	60.408	29.839	30.082
200 μM puerarin	71.284	78.059	61.567	69.788	34.125	36.750
100 μM puerarin	76.759	79.807	66.230	78.271	34.470	38.995
50 μM puerarin	80.323	87.101	69.464	82.279	40.706	41.368

Table 1. Continue						
25 µM puerarin	84.751	89.632	75.674	85.421	42.758	42.447
10 µM puerarin	88.444	91.722	80.257	90.123	44.891	46.289
5 µM puerarin	91.163	97.930	87.142	99.554	48.446	48.856
2 µM puerarin	96.215	98.212	99.285	97.664	51.635	52.698
1000 µM ursolic acid	54.032	61.724	53.392	61.457	27.483	34.463
800 µM ursolic acid	54.143	70.263	56.984	62.659	28.031	35.607
400 µM ursolic acid	52.958	70.540	60.317	73.896	28.639	40.527
200 µM ursolic acid	62.704	75.929	67.797	82.222	34.348	46.396
100 µM ursolic acid	70.825	78.549	70.615	83.284	35.445	49.288
50 µM ursolic acid	73.764	82.182	76.190	86.534	37.314	54.834
25 µM ursolic acid	79.809	87.348	77.718	88.743	41.765	55.028
10 µM ursolic acid	82.179	94.796	79.781	91.589	44.972	53.949
5 µM ursolic acid	90.685	97.046	90.000	97.643	47.328	55.309
2 µM ursolic acid	94.543	99.417	98.075	99.405	50.741	60.898

NRU: Neutral red uptake assay, MTT: 3-(4,5-dimethylthiazol-2-yl)-2,5-diphenyltetrazoliumbromide

Table 2. Viability (%) of HeLa cells exposed to galangin, curcumin, pycnogenol, puerarin and ursolic acid

	18 h NRU (%)	18 h MTT (%)	24 h NRU (%)	24 h MTT (%)	48 h NRU (%)	48 h MTT (%)
Negative control	100.000	100.000	100.000	100.000	100.000	100.000
1000 µM galangin	58.388	66.607	56.372	63.003	28.426	31.157
800 µM galangin	67.179	71.725	59.919	65.681	33.411	31.117
400 µM galangin	71.308	70.253	71.913	66.483	36.102	33.633
200 µM galangin	73.759	79.332	80.607	80.417	40.276	36.840
100 µM galangin	77.114	86.896	84.335	84.080	43.396	41.520
50 µM galangin	76.319	86.006	87.156	82.111	44.670	41.832
25 µM galangin	80.393	96.149	90.845	95.513	47.389	48.074
10 µM galangin	86.929	101.936	93.649	99.980	46.417	51.415
5 µM galangin	92.023	95.589	96.603	98.088	50.841	49.454
2 µM galangin	99.959	98.790	98.343	96.028	57.574	50.343
1000 µM curcumin	71.208	68.823	70.663	68.510	38.498	33.537
800 µM curcumin	69.821	76.277	71.680	75.226	42.232	33.942
400 µM curcumin	72.047	83.150	71.555	80.417	41.973	35.971
200 µM curcumin	76.251	84.454	80.240	83.619	43.764	41.342
100 µM curcumin	76.954	92.018	84.750	91.786	46.957	43.303
50 µM curcumin	79.184	91.823	86.513	91.292	47.626	45.616
25 µM curcumin	87.181	92.153	88.853	91.797	50.540	47.782
10 µM curcumin	89.417	98.279	89.146	97.770	53.518	48.094
5 µM curcumin	92.465	103.645	91.759	100.508	54.381	49.164

Table 2. Continue

2 μM curcumin	98.774	106.660	96.821	101.788	56.517	51.059
1000 μM pycnogenol	51.899	45.356	52.039	41.157	24.638	21.395
800 μM pycnogenol	55.883	47.984	52.449	46.920	30.837	28.616
400 μM pycnogenol	57.770	66.816	53.896	66.505	31.506	35.315
200 μM pycnogenol	59.709	70.663	59.941	69.048	33.060	36.327
100 μM pycnogenol	63.510	76.332	73.577	74.542	35.952	36.367
50 μM pycnogenol	66.986	86.626	85.599	86.178	38.261	37.132
25 μM pycnogenol	72.618	87.489	77.793	87.498	42.188	37.366
10 μM pycnogenol	77.989	88.233	86.266	88.757	46.310	41.721
5 μM pycnogenol	90.645	90.548	92.311	89.291	49.396	47.381
2 μM pycnogenol	99.739	96.153	92.460	95.739	49.979	48.830
1000 μM puerarin	59.885	61.129	55.571	62.729	29.802	32.204
800 μM puerarin	69.520	79.070	58.528	78.287	29.258	40.004
400 μM puerarin	77.557	89.926	60.408	88.790	30.082	44.395
200 μM puerarin	78.059	89.734	69.788	89.364	36.750	46.133
100 μM puerarin	79.807	98.265	78.271	99.198	38.995	48.719
50 μM puerarin	87.101	98.341	82.279	96.858	41.368	50.011
25 μM puerarin	89.632	99.822	85.421	99.691	42.447	50.123
10 μM puerarin	91.722	99.897	90.123	94.659	46.289	48.228
5 μM puerarin	97.930	100.123	99.554	97.615	48.856	51.415
2 μM puerarin	98.212	99.808	97.664	98.940	52.698	49.053
1000 μM ursolic acid	61.724	61.261	61.457	54.489	34.463	28.750
800 μM ursolic acid	70.263	63.663	62.659	56.967	35.607	29.343
400 μM ursolic acid	70.540	64.994	73.896	62.824	40.527	30.443
200 μM ursolic acid	75.929	64.107	82.222	63.668	46.396	29.507
100 μM ursolic acid	78.549	79.582	83.284	76.726	49.288	37.129
50 μM ursolic acid	82.182	88.356	86.534	86.300	54.834	45.019
25 μM ursolic acid	87.348	88.331	88.743	87.812	55.028	45.086
10 μM ursolic acid	94.796	94.991	91.589	92.253	53.949	45.621
5 μM ursolic acid	97.046	95.286	97.643	94.307	55.309	49.189
2 μM ursolic acid	99.417	99.359	99.405	96.942	60.898	49.610

NRU: Neutral red uptake assay, MTT: 3-(4,5-dimethylthiazol-2-yl)-2,5-diphenyltetrazoliumbromide

Table 3. Viability (%) of BT-474 cells exposed to galangin, curcumin, pycnogenol, puerarin and ursolic acid

	18 h NRU (%)	18 h MTT (%)	24 h NRU (%)	24 h MTT (%)	48 h NRU (%)	48 h MTT (%)
Negative control	100.000	100.000	100.000	100.000	100.000	100.000
1000 µM galangin	59.776	60.333	58.272	58.989	28.589	31.454
800 µM galangin	61.264	62.857	62.119	63.301	31.015	32.675
400 µM galangin	65.408	64.506	66.390	64.763	33.596	34.328
200 µM galangin	68.512	67.449	67.759	66.337	35.500	35.949
100 µM galangin	70.992	79.984	71.915	77.078	36.271	42.579
50 µM galangin	75.184	87.068	76.121	84.103	37.640	46.423
25 µM galangin	82.016	94.622	84.026	91.434	37.514	50.948
10 µM galangin	83.872	98.075	88.900	99.630	38.725	51.458
5 µM galangin	97.472	98.159	96.675	99.958	47.191	52.227
2 µM galangin	98.784	98.915	98.142	100.325	54.603	53.811
1000 µM curcumin	59.824	60.786	57.164	60.100	32.415	33.252
800 µM curcumin	62.490	61.786	59.511	61.181	32.179	34.705
400 µM curcumin	64.496	66.611	60.831	66.434	34.209	36.809
200 µM curcumin	74.351	76.456	70.905	79.126	34.949	36.725
100 µM curcumin	88.653	87.527	87.074	86.588	35.767	42.567
50 µM curcumin	92.603	94.293	91.263	93.445	41.342	44.433
25 µM curcumin	92.960	95.013	92.616	94.414	44.516	45.530
10 µM curcumin	91.536	97.031	93.017	98.698	45.460	49.585
5 µM curcumin	92.544	97.831	93.871	99.296	46.814	50.497
2 µM curcumin	97.648	99.064	97.702	99.930	47.939	50.923
1000 µM pycnogenol	35.200	39.491	34.349	33.512	17.120	16.513
800 µM pycnogenol	38.042	43.412	37.200	36.704	17.589	18.185
400 µM pycnogenol	39.680	46.636	40.456	40.307	19.544	20.785
200 µM pycnogenol	41.920	48.808	42.282	50.040	21.526	25.140
100 µM pycnogenol	44.944	56.079	45.933	56.811	24.312	29.349
50 µM pycnogenol	51.088	58.468	49.845	58.898	25.193	30.355
25 µM pycnogenol	53.408	66.865	56.007	67.550	25.854	35.147
10 µM pycnogenol	70.544	84.243	67.710	81.613	35.484	43.310
5 µM pycnogenol	91.888	87.303	88.443	90.637	40.897	44.223
2 µM pycnogenol	98.240	97.328	96.952	96.720	42.014	45.532
1000 µM puerarin	52.384	52.263	51.964	48.410	25.885	25.584
800 µM puerarin	56.882	57.004	55.175	50.662	26.467	24.906
400 µM puerarin	58.336	59.103	62.184	53.354	29.064	25.390
200 µM puerarin	62.653	63.222	62.642	54.300	32.305	29.887
100 µM puerarin	73.376	66.454	72.290	57.206	34.729	31.926
50 µM puerarin	76.768	80.315	75.240	65.467	35.374	32.109

NRU: Neutral red uptake assay, MTT: 3-(4,5-dimethylthiazol-2-yl)-2,5-diphenyltetrazoliumbromide

CONCLUSION

In conclusion, in this study, the cytotoxic effects of galangin, curcumin, PYC, puerarin and ursolic acid were examined in different cell lines by NRU and MTT assays in 18, 24 and 48 h periods. All of the studied phenolics were decreased the cell viability of both cells with increasing dose. But the cytotoxic effects of phenolics were found more in 48 h incubation period. There is no difference between the results from NRU and MTT assays. Further investigation such as using more cell lines and different reliable cytotoxicity assays and incubations with various concentrations at many time points should be performed to corfirm beneficial and toxic effects of phenolics.

Conflict of Interest: No conflict of interest was declared by the authors.

Financial Disclosure: This work was supported by Hacettepe University Research fund (Contract grant number: 014D07301005).

REFERENCES

1. Balasundram N, Sundram K, Samman S. Phenolic compounds in plants and agri-industrial by-products: Antioxidant activity, occurrence, and potential uses. Food Chem. 2006;99:191-203.
2. Moure A, Cruz JM, Franco D, Domínguez JM, Sineiro J, Domínguez H, Núñez MJ, Parajó JC. Natural antioxidants from residual sources. Food Chem. 2001;72:145-171.
3. Bestwick CS, Milne L. Influence of galangin on HL-60 cell proliferation and survival. Cancer Lett. 2006;243:80-89.
4. Capasso R, Mascolo N. Inhibitory effect of the plant flavonoid galangin on rat vas deferens *in vitro*. Life Sci. 2003;72:2993-3001.
5. Capasso R, Tavares IA. Effect of the flavonoid galangin on urinary bladder rat contractility *in vitro*. J Pharm Pharmacol. 2002;54:1147-1150.
6. Ramachandran C, You W. Differential sensitivity of human mammary epithelial and breast carcinoma cell lines to curcumin. Breast Cancer Res Treat. 1999;54:269-278.
7. Ramsewak RS, DeWitt DL, Nair MG. Cytotoxicity, antioxidant and anti-inflammatory activities of curcumins I-III from Curcuma longa. Phytomedicine. 2000;7:303-308.
8. Srimal RC. Turmeric: a brief review of medicinal properties. Fitoterapia. 1997;68:483-493.
9. Krizkova L, Chovanova Z, Durackova Z, Krajcovic J. Antimutagenic *in vitro* activity of plant polyphenols: Pycnogenol and Ginkgo biloba extract (EGb 761). Phytother Res. 2008;22:384-388.
10. D'Andrea G. Pycnogenol: a blend of procyanidins with multifaceted therapeutic applications? Fitoterapia 2010;81:724-736.
11. Gao Q, Yang B, Ye ZG, Wang J, Bruce IC, Xia Q. Opening the calcium-activated potassium channel participates in the cardioprotective effect of puerarin. Eur J Pharmacol. 2007;574:179-184.
12. Hou SZ, Su ZR, Chen SX, Ye MR, Huang S, Liu L, Zhou H, Lai XP. Role of the interaction between puerarin and the erythrocyte membrane in puerarin-induced hemolysis. Chem Biol Interact. 2011;192:184-192.
13. Martin-Aragon S, de las Heras B, Sanchez-Reus MI, Benedi J. Pharmacological modification of endogenous antioxidant enzymes by ursolic acid on tetrachloride-induced liver damage in rats and primary cultures of rat hepatocytes. Exp Toxicol Pathol. 2001;53:199-206.
14. Fautz R, Husein B, Hechenberger C. Application of the neutral red assay (NR assay) to monolayer cultures of primary hepatocytes: rapid colorimetric viability determination for the unscheduled DNA synthesis test (UDS). Mutat Res. 1991;253:173-179.
15. Morgan CD, Mills KC, Lefkowitz DL, Lefkowitz SS. An improved colorimetric assay for tumor necrosis factor using WEHI 164 cells cultured on novel microtiter plates. J Immunol Methods. 1991;145:259-262.
16. Fotakis G, Timbrell JA. *In vitro* cytotoxicity assays: Comparison of LDH, neutral red, MTT and protein assay in hepatoma cell lines following exposure to cadmium chloride. Toxicol Lett. 2006;160:171-177.
17. Mosmann T. Rapid colorimetric assay for cellular growth and survival: application to proliferation and cytotoxicity assays. J Immunol Methods. 1983;65:55-63.
18. Di Virgilio AL, Iwami K, Watjen W, Kahl R, Degen GH. Genotoxicity of the isoflavones genistein, daidzein and equol in V79 cells. Toxicol Lett. 2004;151:151-162.
19. Saquib Q, Al-Khedhairy AA, Siddiqui MA, Abou-Tarboush FM, Azam A, Musarrat J. Titanium dioxide nanoparticles induced cytotoxicity, oxidative stress and DNA damage in human amnion epithelial (WISH) cells. Toxicol In Vitro. 2012;26:351-361.
20. Holst-Hansen C, Brünner N. MTT-cell proliferation assay. Cell Biology: a Laboratory Handbook. (2nd ed). Academic Press; San Diego; 1998:16-18.
21. Kuzma Ł, Wysokinska H, Rózalski M, Krajewska U, Kisiel W. An unusual taxodione derivative from hairy roots of Salvia austriaca. Fitoterapia. 2012;83:770-773.
22. Kim DA, Jeon YK, Nam MJ. Galangin induces apoptosis in gastric cancer cells via regulation of ubiquitin carboxy-terminal hydrolase isozyme L1 and glutathione S-transferase P. Food Chem Toxicol. 2012;50:684-688.
23. Zhang W, Tang B, Huang Q, Hua Z. Galangin inhibits tumor growth and metastasis of B16F10 melanoma. J Cell Biochem. 2013;114:152-161.
24. Lantto TA, Colucci M, Závadová V, Hiltunen R, Raasmaja A. Cytotoxicity of curcumin, resveratrol and plant extracts from basil, juniper, laurel and parsley in SH-SY5Y and CV1-P cells. Food Chem. 2009;117:405-411.
25. Mehta K, Pantazis P, McQueen T, Aggarwal BB. Antiproliferative effect of curcumin (diferuloylmethane) against human breast tumor cell lines. Anticancer Drugs. 1997;8:470-481.
26. Hashim FJ, Shawkat M, Al-Jewari H. Cytotoxicity of curcumin against leukemic cell lines via apoptosis activity. Curr Res J Biol Sci. 2012;4:60-64.
27. Taner G, Aydın S, Aytaç Z, Başaran AA, Başaran N. Assessment of the cytotoxic, genotoxic, and antigenotoxic potential of Pycnogenol® in *in vitro* mammalian cells. Food Chem Toxicol. 2013;61:203-208.
28. Yu Z, Li W. Induction of apoptosis by puerarin in colon cancer HT-29 cells. Cancer Lett 2006;238:53-60.
29. Ramachandran S, Prasad NR. Effect of ursolic acid, a triterpenoid antioxidant, on ultraviolet-B radiation-induced cytotoxicity, lipid peroxidation and DNA damage in human lymphocytes. Chem Biol Interact. 2008;176:99-107.
30. Ramos AA, Pereira-Wilson C, Collins AR. Protective effects of ursolic acid and luteolin against oxidative DNA damage include enhancement of DNA repair in Caco-2 cells. Mutat Res. 2010;692:6-11.
31. Weyermann J, Lochmann D, Zimmer A. A practical note on the use of cytotoxicity assays. Int J Pharm. 2005;288:369-376.
32. Putnam KP, Bombick DW, Doolittle DJ. Evaluation of eight *in vitro* assays for assessing the cytotoxicity of cigarette smoke condensate. Toxicol In Vitro. 2002;16:599-607.

Turk J Pharm Sci 2017;14(2):108-119
DOI: 10.4274/tjps.60352

ORIGINAL ARTICLE

Self-Emulsifying Formulation of Indomethacin with Improved Dissolution and Oral Absorption

İndomethacinin Geliştirilmiş Çözünürlük ve Sözlü İzolasyon ile Formülasyonunun Özel Emülsifilleştirilmesi

Subhash Chandra Bose PENJURI[1]*, Saritha DAMINENI[2], Nagaraju RAVOURU[3], Srikanth Reddy POREDDY[1]

[1]Mnr College of Pharmacy, Department of Pharmaceutics, Telangana, India
[2]Sultan-ul-uloom College of Pharmacy, Department of Pharmaceutics, Telangana, India
[3]Sri Padmavathi Mahila Visvavidyalayam (Women's University), Institute of Pharmaceutical Technology, Andhra Pradesh, India

ABSTRACT

Objectives: The objective of the present study was to enhance the solubility, dissolution and hence anti-inflammatory activity of poorly soluble drug indomethacin (IMN) by formulating into self emulsifying systems.

Materials and Methods: Self emulsifying formulations were prepared using capmul MCM as oil, tween 80 as surfactant, transcutol P as cosurfactant. Fourier transform infrared spectroscopy and differential scanning calorimetry studies were conducted to know the interaction between drug and excipients. Pseudo ternary phase diagrams were constructed using surfactant and cosurfactant in 1:1 to 1:4 and 2:1 to 4:1 to know the efficient self emulsification region. The formulations were evaluated for their particle size, zeta potential, refractive index, viscosity and cloud point. *In vitro* dissolution studies were conducted in one part of pH 7.2 phosphate buffer and four parts of water. The pharmacokinetic parameters were analysed by Win Nonlin software.

Results: The self emulsification was higher with the ratios 2:1, 3:1 and 1:2 of surfactant and co surfactant and the IMN formulations were prepared. The formulations were stable at different pH and dilutions. The globule size was in the range of 184.1 nm to 340.5 nm, as the ratio of oil, surfactant and cosurfactant mixture has varied effects on the size of globule. The negative charge on the globules of all formulations attributes their stability. The optimized formulation showed better release as compared to marketed product. The AUC of the optimised Self-Emulsifying Drug Delivery System was significantly higher than the marketed product.

Conclusion: Thus, from the present research, self emulsifying systems of IMN provide a useful alternative to enhance dissolution and hence anti inflammatory activity.

Key words: Self emulsifying drug delivery system, pseudo ternary phase diagram, zeta potential, anti-inflammatory activity, indomethacin, AUC

ÖZ

Amaç: Bu çalışmanın amacı, kendiliğinden emülsifiye edici sistemlere formüle ederek, az çözünen ilaç indometazinin (IMN) çözünürlüğünü, çözünmesini ve dolayısıyla anti-inflamatuvar aktiviteyi arttırmaktır.

Gereç ve Yöntemler: Kendi kendine emülsiyon haline getirici formülasyonlar yağ olarak capmul MCM, yüzey aktif madde olarak tween 80, kosürfaktant olarak transcutol P kullanılarak hazırlandı. İlaç ve eksipiyanlar arasındaki etkileşimi bilmek için fourier dönüşüm kızılötesi spektroskopisi ve diferansiyel tarama kalorimetrisi çalışmaları yapılmıştır. Pseudo üçlü faz diyagramları, kendinden emülsiyonlaşmış bölgeyi bilmek için 1:1 ile 1:4 ve 2:1 ile 4:1 arasında yüzey aktif madde ve kosürfaktant kullanılarak oluşturulmuştur. Formülasyonlar, parçacık büyüklüğü, zeta potansiyeli, kırılma indisi, viskozite ve bulut noktası açısından değerlendirildi. *İn vitro* çözünme çalışmaları, pH 7.2 fosfat tamponun bir bölümünde ve dört kısım suda gerçekleştirildi. Farmakokinetik parametreler Win Nonlin yazılımı ile analiz edildi.

Bulgular: Kendiliğinden emülsifikasyon 2:1, 3:1 ve 1:2 oranında surfaktan ve kosürfaktant oranlarına göre daha yüksekti ve IMN formülasyonları hazırlandı. Formülasyonlar, farklı pH ve seyreltmelerde kararlıydı. Küre boyutu, 184.1 nm ile 340.5 nm aralığındaydı, çünkü yağ, yüzey aktif madde ve ko-yüzey aktif madde karışımı oranı kürenin boyutuna farklı etkiler yapmıştır. Tüm formülasyonların globüllerinin üzerindeki negatif yük, kararlılıklarına atıfta bulunmaktadır. Optimize edilmiş formülasyon, pazarlanan ürüne kıyasla daha iyi salınım gösterdi. Optimize edilmiş Kendi Kendine Emülsifiye Edici İlaç Taşıma Sistemi'nin AUC'si pazarlanan ürüne göre önemli derecede yüksekti.

Sonuç: Böylece, mevcut araştırmadan kendi kendine emülsifiye IMN sistemleri, çözünmeyi ve dolayısıyla anti-inflamatuvar aktiviteyi arttırmak için yararlı bir alternatif sağlar.

Anahtar kelimeler: Öz hazırlama için ilaç dağıtım sistemi, sözde üçlü faz diyagramı, zeta potansiyel, anti-inflamatuvar faaliyet, indometazin, AUC

*Correspondence: **E-mail:** penjurisubhash@gmail.com, **Phone:** +919848033974
ORCID ID: orcid.org/0000-0002-9365-0701
Received: 06.10.2016, **Accepted:** 21.11.2016

INTRODUCTION

About 90% of all compounds in today's pharmaceutical drug delivery pipelines are reported to be poorly soluble in water.[1] This poses enormous problems for the industry; for an active pharmaceutical ingredient that cannot reach its molecular target in the body if drug remains undissolved in the gastrointestinal tract (GIT) and is eventually excreted. The ability to increase aqueous solubility is thus a valuable aid to increase the efficacy of certain drugs.[2] So, solubilisation techniques that overcome this issue by increasing the solubility of drugs are becoming more and more important to pharmaceutical industry.[3] Currently a number of technologies are available to deal with the poor solubility, dissolution rate and bioavailability of insoluble drugs. One of the most popular approaches of oral bioavailability and solubility enhancement is the utilization of lipid-based drug delivery systems (LBDDS).[4,5] Self-Emulsifying Drug Delivery System (SEDDS) are proportionate newer LBDDS with huge promise in oral bioavailability enhancement of drugs. These formulations avoid the slow and incomplete dissolution of a drug, increase the extent of its transportation and bypass the P-gp efflux, thereby strengthen drug absorption from the GIT.[6]

The major technique for enhancing bio-availability is SEDDS, which uses lipophilic, pre-concentrated solutions of the active pharmaceutical ingredient and excipients (a liquid carrier, a surfactant and a cosurfactant). They emulsify spontaneously when, come in contact with fluids of GIT to form oil-in-water emulsions or microemulsions under mild agitation.[7] In the design and development of SEDDS, modified long and medium chain triglyceride oils, with different degrees of saturation or hydrolysis are widely used because they offer definite physiological and formulation related advantages, as their degradation products simulate that of the natural end products of intestinal digestion.[8-10]

Surfactants, being amphiphilic in nature, can solubilize high amounts of lipophilic drugs. Usually surfactants will be selected based on hydrophilic-lipophilic balance (HLB) values and safety.[11] The most widely recommended emulsifiers include the non-ionic surfactants with relatively high HLB values. Non-ionic surfactants are considered as safer than the ionic ones.[12-15] Self-emulsification occurs when the entropy change that favors dispersion is greater than the energy required to increase the surface area of the dispersion.[16] Protection of drugs in the gut, reduction in gastric irritation, consistent drug absorption and enhanced oral bioavailability are advantages of SEDDS.[17-21] So the aim of present work was to develop self emulsifying formulations of indomethacin (IMN) to enhance its solubility and hence bioavailability.

MATERIALS AND METHODS

Materials

IMN was a gift obtained from Micro Labs Limited, Bangalore. Mefenamic acid was obtained from Dr. Reddy's Laboratories Ltd. (Hyderabad). Acetonitrile was purchased from Qualigens fine Chemicals (Mumbai). Castor oil, Propylene glycol and PEG 400 was purchased from Merck (Mumbai). Labrafil M 2125, labrasol, Plurol oleique CC 497, Transcutol P and Labrafac WL 1349 were obtained from Gattefosse India Pvt Ltd. (Mumbai). Oleic acid was purchased from Merck (Mumbai). Soya bean oil and sunflower oil were purchased from Genuine chemicals Co. (Mumbai). Isopropyl myristate was purchased from Lobachemie Pvt Ltd (Mumbai). Cremophor RH 40 was obtained from BASF (Mumbai). Tween 80 was purchased from Finar Chemicals (Ahmadabad). Water (HPLC grade) was purchased from Qualigens fine Chemicals (Mumbai).

Bioanalytical method

A HPLC method was used to quantify the amount of IMN in the rat plasma samples obtained during the pharmacokinetic study. The analysis was performed using Intelligent LC 3000 system, sodium acetate buffer pH 3.6 and acetonitrile (40:60) was used as mobile phase with a flow rate of 1 mL/min ODS (C-18), BP 5 µm, 250x4.6 mm was the column used at ambient temperature. The detector wave length and injection volume were 320 nm and 20 mL respectively. Linearity (r^2=0.998) was obtained in the concentration range 0.2-5 µg/mL.[22,23]

Solubility study of IMN in various oils and surfactants

A calibration curve was plotted for IMN in a mixture of ethanol:water (1:1) in the range of 10-50 µg/mL (Beer's Lambert's range) at 320 nm. A good linear relationship was observed between the concentration of IMN and its absorbance in a mixture of ethanol:water (r^2=0.9986, m=0.0186, n=3). Excess amount of IMN was placed in glass vials and mixed manually in 2 mL of various oils/surfactants/cosurfactants. The vials were sonicated for 2 h and centrifuged at 3000 rpm for 20 min, followed by filtration. The filtrate was diluted with mixture of ethanol:water (1:1) and the amount of IMN dissolved in various vehicles was analysed by ultraviolet (UV) spectrophotometric method (Shimadzu, Japan).[24-26]

Determination of emulsification efficiency

Equal amount of surfactant and oil was mixed and gradually heated at 50°C for uniform homogenization. 100 mg of mixture was diluted with 100 mL of water in a stoppered conical flask. Emulsification efficiency was determined by number of inversions required to yield homogenous emulsion. Emulsion was allowed to stand for 2 h and its percentage transmittance was determined at 638 nm by UV-Visible spectrophotometer (Shimadzu, Japan) using distilled water as blank.[27]

Fourier transform infrared spectroscopy

Compatibility studies between IMN, oil and Smix was studied by fourier transform infrared spectroscopy (FTIR) (Perkin Elmer Model 1600, USA). Pure drug and physical mixture were dissolved in dichloromethane separately. By using a capillary tube, a smear/thin film of the samples was placed on the NaCl crystal cell (hexagonal clear, about 2 mm thickness). It was sandwiched with another NaCl crystal cell. The NaCl cells with the sandwiched sample were placed in sample holder. The samples were scanned from 4000 to 400/cm using FTIR spectrophotometer.

Differential scanning calorimetry

Compatibility studies between IMN, oil and Smix was studied by Differential scanning calorimetry [differential scanning calorimetry (DSC)-60, Shimadzu Corporation, Japan]. Liquid samples are placed in dome shaped sample holder and sealed. Then the sample is placed in the right side pocket, with empty cell on left side as blank. Dry nitrogen was used as effluent gas. All samples were scanned at a temperature ramp speed of 5°C/min and the heat flow from 0°C to 200°C.

Construction of pseudoternary phase diagram

Pseudoternary phase diagrams were developed by titrating capmul MCM, tween 80 and transcutol P mixture with water. The trails were conducted using oil and Smix in the ratios 1:1 to 1:9. The surfactant and co surfactant ratios 1:1, 1:2, 1:3, 1:4, 4:1, 3:1, 2:1 were tested in the construction of pseudoternary phase diagrams. After each addition of water the dispersion was observed physically for clarity. Phase diagrams were constructed using Tri-Plot V1-4-2.[28] The ratios with good emulsification were further tested.

Thermodynamic stability studies

Thermodynamic stability studies of formulations were carried by exposing them to heating cooling cycle, centrifugation test and freeze thaw test.[29]

Heating cooling cycle

Formulations were kept at 4°C and then at 40°C in a cyclic way about six times. The formulations were exposed to each temperature for 48 h. Formulations were observed physically for turbidity at the end of test period.

Centrifugation test

Formulations were centrifuged at 3500 rpm for 30 min and observed for any phase separation.

Freeze thaw test

Formulations were kept at -21°C and then at 25°C in a cyclic way about three times. Formulations were observed physically for turbidity at the end of test period. Stable formulations were considered for further evaluation.

Determination of dispersion ability

1 mL of each formulation was added in 500 mL of water at 37±1°C. A standard stainless steel dissolution paddle is used with rotating speed of 50 rpm which provided gentle agitation. The *in vitro* performance of the formulations is visually assessed using the grading system as given in Table 1.[30]

Drug precipitation study

IMN SEDDS were taken into 250 mL water and mixed under continuous stirring (100 rpm) on magnetic stirrer. The formed emulsion was then observed visually after a period of 24 h for the precipitation of drug. The self-emulsifying systems were then considered as stable (without precipitation) or unstable (with precipitation).[31]

Preparation of SEDDS

Based on the solubility, emulsification ability and pseudo-ternary phase diagram studies excipients were selected. Formulation was limited to only the SEDDS that passed the thermodynamic stability studies, dispersion ability and precipitation study. Accurately weighed amount of IMN was dissolved initially in capmul MCM (oil). Tween 80 and transcutol P (surfactant and cosurfactant) mixture were accurately weighed and added slowly to the drug-oil mixture. The mixture was heated at 40°C on a magnetic stirrer, until IMN was perfectly dissolved. Then the mixture was sealed in a glass capped vial and stored at room temperature until used.

Evaluation of SEDDS

Drug content

A calibration curve was plotted for IMN in a mixture of ethanol: water (1:1) in the range of 10-50 µg/mL (Beer's Lambert's range) at 320 nm. A good linear relationship was observed between the concentration of IMN and its absorbance in a mixture of ethanol:water (r^2=0.9986, m=0.0186, n=3). Drug from pre-weighed SEDDS is extracted by dissolving in ethanol:water (1:1) for IMN respectively and the drug content was analyzed by UV spectrophotometer (Shimadzu, Japan).[23]

Refractive index and percent transmittance

1 mL of formulation diluted to 100 mL with water and a drop of it was placed on the Abbe's refractometer prism, RI value was determined in the presence of a visible light source (Tungsten lamp). The percent transmittance of formulations was measured at 650 nm using UV spectrophotometer (Shimadzu, Japan). Distilled water was used as a blank.[32]

Viscosity

0.5 gm of SEDDS was diluted to 10 times with distilled water and viscosity of the resultant emulsion was measured using Brookfield viscometer with spindle # CPE40.[31]

Effect of pH and robustness to dilution

SEDDS were subjected to 100 fold dilution with distilled water, 0.1 N HCl and phosphate buffer pH 6.8. The resultant diluted emulsions were checked for coalescence of globules and phase separation after 24 h storage.[33]

Table 1. Visual assessment of efficiency of self emulsification

Grade	Dispersibility & appearance	Time of self emulsification
1	Rapid forming microemulsion which is clear or slightly bluish in appearance	<1 min
2	Rapid forming, slightly less clear emulsion which has bluish white appearance	<2 min
3	Bright white emulsion (similar to milk in appearance)	<3 min
4	Dull, greyish whitish emulsion with a slightly oily appearance that is slow to emulsify	>3 min
5	Exhibit poor or minimal emulsification with large oil globules present on the surface	>3 min

Size analysis and homogeneity of SEDDS

The mean globule size, zeta potential and polydispersity index of SEDDS were measured by photon correlation spectroscopy instrument (Zetasizer 3000HS, Malvern Instruments Corp., U.K.) at 25°C.[34] For measurement, SEDDS was pre-diluted by addition of 0.6 mL of SEDDS to 90 mL of distilled water under slow agitation at room temperature (25°C). The system was analyzed by dispersing it in 100 mL distilled water as dispersant. Analysis was done in triplicate and mean results are presented. The sizing and zeta potential of the SEDDS was determined in a small volume module. Samples were directly placed into the module and the data was collected for 10 min. All studies were repeated in triplicates, with good agreement being found between the measurements.

Turbidimetric evaluation

Equal quantity of SEDDS and 0.1 N HCl was mixed under continuous stirring (50 rpm) on magnetic hot plate at 37±0.5°C temperature. The turbidity was measured by using a turbidimeter (Digital nephelo-turbidity meter 132, Systronics, India).[35,36]

Cloud point measurement

The cloud point value of optimized formulations were determined and compared. Each formulation was diluted with water in the ratio of 1:100 and placed in a water bath with gradual increase (2°C/min) in temperature (from 25 to 80°C). Cloud point was measured as the temperature at which there was a sudden appearance of cloudiness as seen visually.[27]

In vitro release study

A calibration curve was plotted for IMN in one part of 7.2 pH phosphate buffer and four parts of water in the range of 10-50 µg/mL (Beer's Lambert's range) at 320 nm. A good linear relationship was observed between the concentration of IMN and its absorbance in one part of 7.2 pH phosphate buffer and four parts of water (r^2=0.9997, m=0.0189, n=3). *In vitro* release of optimized formulations capsules filled with (SEDDS), marketed product and pure drug each containing 25 mg of IMN were carried using USP type 1 dissolution apparatus (Model No TDT-08L, Electrolab, Mumbai). One part of pH 7.2 Phosphate buffer and four parts of water was used as dissolution medium maintained at 37±0.5°C with the basket rotating at 100 rpm. Samples (10 mL) were withdrawn at regular intervals and the same volume of fresh dissolution medium was replaced to maintain sink condition.[25] The samples were filtered, diluted and analyzed UV spectrophotometrically at 320 nm (Shimadzu, Japan). Dissolution studies were performed and the mean cumulative percentage of IMN was calculated and plotted against time. *In vitro* dissolution data was statistically analysed by one way ANOVA followed by turkey post hoc test for multiple comparison using graph pad prism. Differences were considered to be significant at a level of $p<0.05$. Dissolution profile of optimized formulations and marketed product was compared on the basis of their similarity factor (f2) and difference factor (f1).

In vitro diffusion study

A calibration curve was plotted for IMN in in one part of 7.2 pH phosphate buffer and four parts of water in the range of 10-50 µg/mL (Beer's Lambert's range) at 320 nm. A good linear relationship was observed between the concentration of IMN and its absorbance in one part of 7.2 pH phosphate buffer and four parts of water (r^2=0.9997, m=0.0189, n=3). *In vitro* diffusion studies of optimized SEDDS and marketed products were carried by dialysis method. 250 mL of one part of pH 7.2 phosphate buffer and four parts of water was used as diffusion medium for IMN-B1. Temperature was maintained at 37°C with the paddle speed of 100 rpm. Samples were withdrawn at regular intervals of time for 12 h and drug concentration was analyzed by UV spectrophotometer (Shimadzu, Japan). The data was statistically analysed by t test ($p<0.05$) using graph pad prism.[31]

Pharmacodynamic studies

Anti-inflammatory studies

The anti-inflammatory activity of optimized and marketed formulations of IMN was evaluated by the carrageenan-induced rat hind paw edema method by using Digital plethysmometer (PLM-01 plus, Orchid Scientifics, India). Study protocol was approved by IAEC (Reg. No. IAEC/SUCP/CPCSEA/08/2013). The animals were divided into three groups (six animals in each group) for anti-inflammatory studies.[37,38] Wistar strain male albino rats weighing between (150-200 g) were used. The animals were in a light controlled 12 hours cycle with free access to food and water. Animals were fasted overnight before experiment with free access to water. Animals were divided into three groups of six animals each. Group 1 (control) received water. Group 2 received 10 mg/kg formulated SEDDS and group 3 received 10 mg/kg marketed product. After one hour, paw edema was induced by injecting 50 µL of 1% w/v carrageenan into the sub planar region of the left hind paw. Paw volume was determined after 5 h in all groups. Difference in the paw volume, determined before and after injection of the edema-provoking agent indicated the severity of edema. One control group and reference group were used in this study. Volumes of right hind paw of controls and treated animals were measured with a plethysmometer and the percentage inhibition of inflammatory reaction was determined for each animal by comparison with control and calculated by the following formula.

$$\% \text{ inhibition of edema} = \frac{\left(V_{control} - V_{test}\right)}{V_{control}} \times 100$$

Where,

$V_{control}$ = mean edema of rats in control group

V_{test} = mean edema volume of rats in tested group

Pharmacokinetic evaluation

Pharmacokinetic study protocol was approved by the IAEC (Reg. No. IAEC/MNRCOP/CPCSEA/09-04-2013). The oral pharmacokinetics of IMN was assessed in wistar rats. Animals were fasted overnight with free access to water for at least 12 h before dosing. After collecting the zero hour blood sample (blank), the formulations were given orally (10 mg/kg body weight). The animals were then anesthetized and blood

samples were withdrawn from the tail vein and placed in heparinised centrifuge tubes. The plasma was then separated and assayed for the concentration of IMN by HPLC. Table 2 shows the specifications of animals used for *in vivo* study. The pharmacokinetic parameters were calculated using WinNonlin software.[39,40] The animals were divided into three groups;

Group 1: IMN suspension [pure IMN in 1% carboxymethylcellulose (CMC)] administered animals.

Group 2: IMN-B1 administered animals.

Group 3: Marketed product (in 1% CMC) administered animals.

Stability study

Stability studies were conducted according to the ICH Q1A (R2) guidelines. Formulations were packed in a screw capped bottle and were kept in stability chamber at a temperature of 40±2˚C and 75±5% RH for 6 months. Samples were withdrawn at the end of 1, 2, 3 and 6 months and analyzed for drug content, homogeneity, clarity, globule size and release. Zero time samples were used as control for the study.[41,42]

RESULTS AND DISCUSSION

Selection of oil, surfactant and cosurfactant

Solubility of indomethacin in oils, surfactants and co surfactants

The selection of oil, surfactant and cosurfactant for the formulation of SEDDS was initially based on the solubility of IMN in these excipients. IMN solubility in various oils and surfactants is shown in Table 3. Capmul MCM showed maximum solubility of IMN so it was selected as oil; labrasol and tween 80 which showed good solubility were selected as surfactants for further study. The solubility of IMN in surfactant and oil is important, as cosurfactants on dilution with water may separate out resulting in micellar dispersion, thus reducing the solvent capacity for IMN.[43] So, all the cosurfactants were further used in the study.

Emulsification ability

The oil, surfactant and cosurfactants which showed good solubility were tested for their emulsification ability. Capmul MCM showed good solubility of IMN which helps to prevent precipitation in the intestinal fluids[44], so the emulsification efficiency of this oil is studied with surfactants labrasol, tween 80 and cosurfactants transcutol P, plurol oleique CC, PG and PEG 400 which showed good solubility of IMN. The emulsification efficiency results as indicated by inversions and percentage transmittance are given in Table 4. Better emulsification efficiency is given by lesser number of inversions.[8] The number of inversions required for tween 80, labrasol, transcutol P, PEG 400, PG and plurol oleique CC was found to be 9, 15, 6, 8, 11 and 17 respectively.

Percentage transmittance of labrasol and tween 80 was 94.8 and 99.1 respectively. As the emulsification efficiency and solubility of IMN was greater with tween 80, it was selected as surfactant in the further study. The percentage transmittance of cosurfactants transcutol P, PEG 400, PG and plurol oleique CC was found to be 96.5, 93.7, 88.3 and 82 respectively. Based on the solubility and emulsification of IMN with oil, transcutol P was selected as cosurfactant.

Compatibility studies

The FTIR spectra of IMN and physical mixture are shown in Figure 1. The characteristic peaks of IMN are unchanged and

Table 2. Animal specifications for *in vivo* study

Species	Wistar rats
Weight	150-200 gm
Gender	Male/Female
No. of animals in each group	6
Total time of the study	24 h
No. of blood samples from each animal	12
Sampling intervals (h)	0.5, 1, 1.5, 2, 3, 4, 5, 6, 8, 12, 16, 24
Volume of the blood sample	0.1 mL

Table 3. Solubility of IMN in various oils/surfactants

Oil/surfactant	Solubility (mg/mL)	Oil/surfactant	Solubility (mg/mL)
Castor oil	11.48±1.26	Tween 80	119.34±1.20
Oleic acid	6.79±2.71	Cremophor RH 40	90.72±1.82
Labrafil M2125	15.16±0.93	Labrasol	167.38±0.87
Sunflower oil	10.32±1.59	Transcutol P	192.1±1.39
Soya bean oil	18.48±1.15	Plurol oleique CC	150.17±2.01
Labrafac lipophile WL 1349	29.23±0.96	PG	121.21±1.99
IPM	35.14±1.84	PEG 400	98.57±0.58
Capmul MCM	51.87±2.11		

Mean ± standard deviation, n=3, IMN: Indomethacin

Table 4. Emulsification efficiency of surfactants and cosurfactants with capmul MCM

Surfactant/cosurfactant	Number of inversions	Percentage transmittance
Tween 80	9±2	99.1
Labrasol	15±2	94.8
Transcutol P	6±3	96.5
Plurol oleique CC	17±3	82.0
PG	11±2	88.3
PEG 400	8±2	93.7

Mean ± standard deviation, n=3

prominently observed in FTIR spectra of physical mixture suggesting that there was no interaction between IMN and excipients. DSC thermograms of pure IMN and physical mixture are presented in Figure 2. The DSC thermograms showed sharp melting peak for IMN, at 161°C. A small endothermic peak with low intensity was observed at 161°C in physical mixture, may be due to reduction in drug crystallinity and molecular dispersion of IMN in the lipid excipients.

Construction of pseudoternary phase diagram

Pseudoternary diagrams form the basis for selection of composition of components for SEDDS. They were constructed with capmul MCM as oil, mixture of tween 80 and transcutol P as surfactant mixture with IMN and water (Figure 3). The process of self micro emulsification was observed to be spontaneous as the energy required to form is less. The selected surfactant mixture is a combination of low and high HLB value, which makes it a more efficient SEDDS.[43,45]

The microemulsion region was observed in pseudo ternary diagrams. The phase diagrams which showed maximum self emulsification region were with tween 80 and transcutol P in the ratios 2:1, 3:1 and 1:2. Increase in tween 80 concentration (2:1 to 3:1) showed spontaneous and better emulsification which may be due to formation of monolayers of surfactant on the emulsion globules which increases the stability. A slight increase in cosurfactant ratio (1:2) showed good emulsification region as, transcutol P may have fluidized the surfactant making it flexible to form microemulsion. So the S:Co ratios of 2:1, 3:1 and 1:2 which showed maximum self micro emulsification region were used and various formulations were made for further study shown in Table 5.

Dispersion ability

An efficient SEDDS formulation disperses very fast in seconds provided the condition of gentle stirring.[8] The dispersion rate

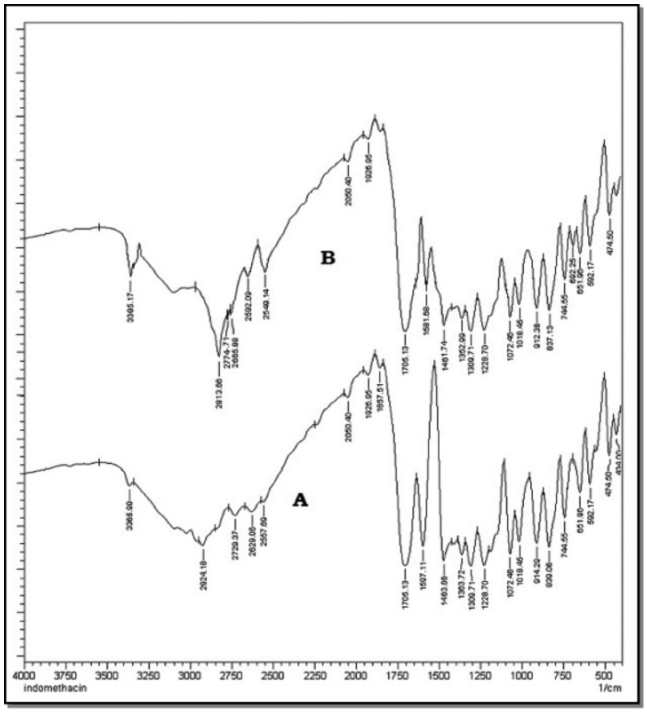

Figure 1. FTIR spectra of A: indomethacin and B: physical mixture

FTIR: Fourier transform infrared spectroscopy

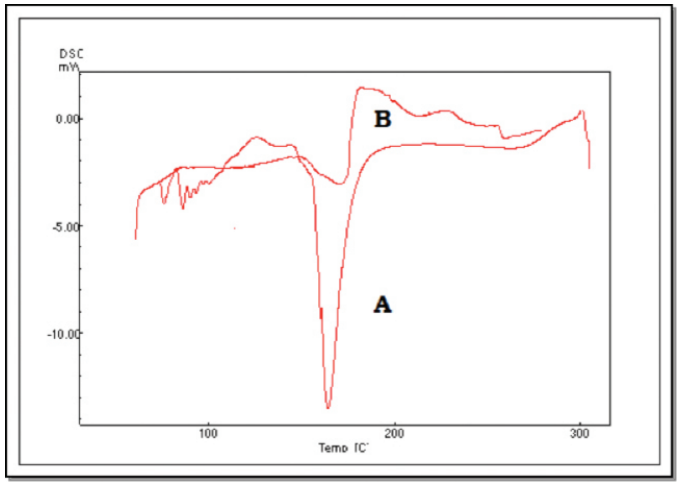

Figure 2. Differential scanning calorimetry thermograms of A: indomethacin and B: physical mixture

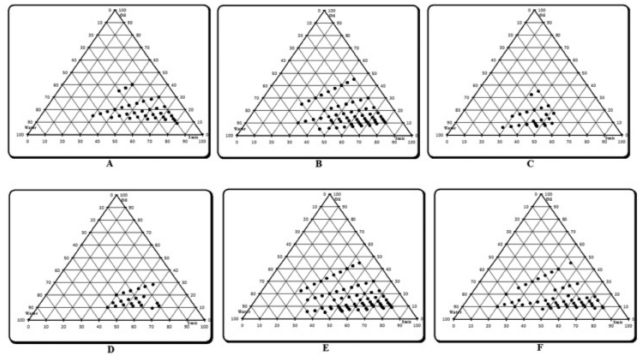

Figure 3. Pseudoternary phase diagram showing the o/w emulsion region of capmul, tween 80 and transcutol P at Smix ratio of A is 1:1, B is 1:2, C is 1:3, D is 1:4, E is 2:1, F is 3:1

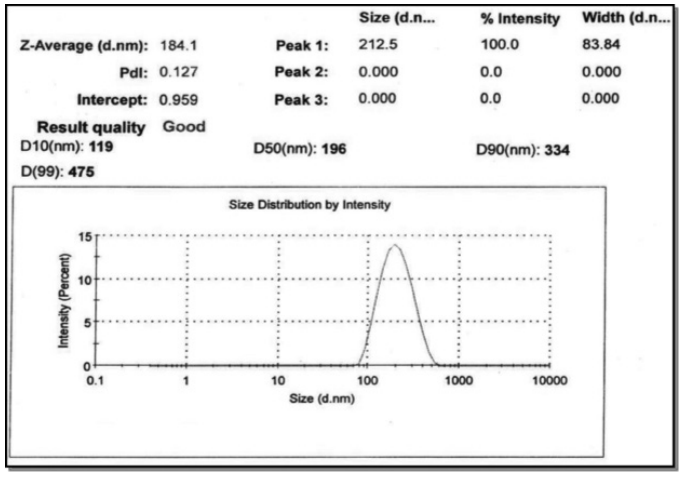

Figure 4. Globule size data of IMN-B1

IMN: Indomethacin

depends on the interfacial barrier at the oil and dilution medium interface. Tween 80 and transcutol P at the ratios 2:1, 3:1 and 1:2 showed good dispersion as shown in Table 6 may be due to formation of stable interfacial film. Formulations which showed dispersibility grade of 1 and 2 were selected for further study.

Thermodynamic stability and precipitation study

The stability of the formulations affects the performance and instability may result in precipitation or phase separation. The effect of metastable forms, which are difficult to find, can be eliminated by the thermodynamic studies. The formulations were subjected to centrifugation, heating, cooling cycles, freeze thaw test. Results were shown in Table 6. The concentration of surfactant and cosurfactant has varied effects and is important for a stable microemulsion formation. Formulations which have passed the thermodynamic stability study, dispersion test and drug precipitation study were optimised and further evaluated. IMN-A1, IMN-A2, IMN-A3, IMN-B1, IMN-B2 and IMN-C2 were selected as optimized formulations as they passed the stability study.

Evaluation of optimized IMN SEDDS formulations

Drug content

The IMN content in the formulations is given in Table 7 which showed uniform distribution. All the formulations have drug content in the range 99.1±1.92 to 100.3±0.91%.

Percentage transmission and refractive index

Refractive index of the formulations was in the range of 1.434-1.447, nearly same as that of water as shown in Table 7. The percentage transmission was found to be in the range 95.4 to 99.2. The results indicated that the optimized SEDDS formulations are translucent and clear dispersions.

Viscosity

The viscosity of optimised formulations is shown in Table 7. Viscosity of the system plays an important role in drug release. It was reported that low viscosity of the systems will result in o/w emulsions. The viscosity of the formulations was in the range of 0.656 cps to 0.932 cps.

Dilution and pH effect

All the formulations were stable when diluted to 100 times with water, 0.1N HCl and pH 6.8 phosphate buffer. There was no phase separation or precipitation which indicates the non ionic surfactants used were stable to change in pH and the concentration of electrolyte.[46] This is necessary for stable emulsion system as it gets in contact with various physiological fluids in the system.

Table 5. Composition of SEDDS formulations

S: Co S	**2:1**					
O: Smix	1:1	1:2	1:3	1:4	1:5	1:6
Tween 80	325	433.4	487.6	520	541.7	557.2
Transcutol P	162.5	216.6	243.7	260	270.8	278.6
Capmul MCM	487.5	325	243.7	195	162.5	139.3
Indomethacin	25	25	25	25	25	25
Formulation code	IMN-A1	IMN-A2	IMN-A3	IMN-A4	IMN-A5	IMN-A6
S: Co S	**3:1**					
O: Smix	1:1	1:2	1:3	1:4	1:5	1:6
Tween 80	365.6	487.5	548.4	585	609.3	626.7
Transcutol P	121.9	162.5	182.8	195	203.1	208.9
Capmul MCM	487.5	325	243.7	195	162.5	139.3
Indomethacin	25	25	25	25	25	25
Formulation code	IMN-B1	IMN-B2	IMN-B3	IMN-B4	IMN-B5	IMN-B6
S: Co S	**1:2**					
O: Smix	1:1	1:2	1:3	1:4	1:5	1:6
Tween 80	162.5	216.6	243.7	260	270.8	278.6
Transcutol P	325	433.4	487.6	520	541.7	557.2
Capmul MCM	487.5	325	243.7	195	162.5	139.3
Indomethacin	25	25	25	25	25	25
Formulation code	IMN-C1	IMN-C2	IMN-C3	IMN-C4	IMN-C5	IMN-C6

IMN: Indomethacin, SEDDS: Self-Emulsifying Drug Delivery System

Emulsion globule size and zeta potential analysis

Diffusion of drug can be faster from smaller emulsion globules, which increases dissolution of drug into aqueous medium. The average globule size distribution of the optimised formulations is given in Table 8. The globule size was in the range of 184.1 nm to 340.5 nm, the ratio of oil, surfactant and cosurfactant mixture has varied effects on the size of globule.

IMN-A1 to IMN-A3, IMN-B1 to IMN-B2 showed an increase in globule size which may be due increase in tween 80 concentration in the formulation, which results in more penetration of water into the emulsion globules resulting in larger size.[47]

IMN-C2 showed a globule size of 237.8 nm, which may be attributed to a higher ratio of transcutol P. Formulation IMN-B1, has shown the smallest size globules (Figure 4). The polydispersibility index of the formulations was less than 1 indicating the uniformity of size distribution within the formulation.[48]

The optimised formulations were checked for their zeta potential and tabulated in Table 8. Zeta potential values were in the range of -7.55 to -8.48 mV. From the results, the negative charge on the globules of all formulations attributes their stability, by causing repulsion between them and thus preventing their coalescence (Figure 5).[49]

Turbidimetric evaluation

The turbidity which attributes to the clarity and uniformity of emulsification, hence stability of the formulation was measured. A measure of turbidity also gives the knowledge of globule size.[50] The turbidity values are shown in Table 8. The lower values indicate that prepared systems were clear and may have

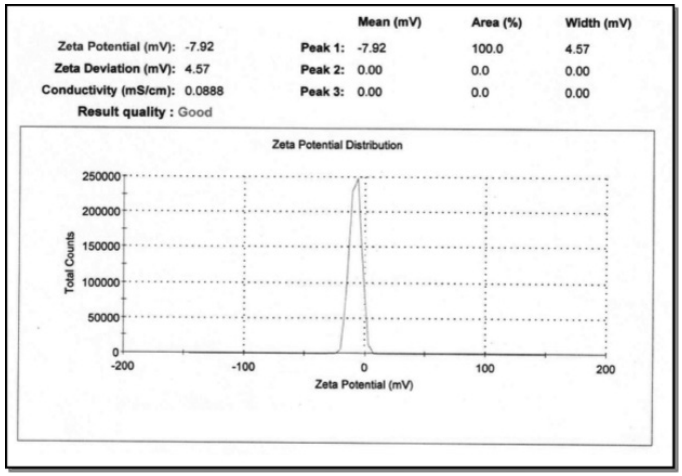

Figure 5. Zeta potential data of IMN-B1

IMN: Indomethacin

Table 6. Results of thermodynamic stability studies, visual dispersion grading

Formulation code	Centrifuge	Heating/Cooling cycle	Freeze thaw	Dispersion grade	Inference
IMN-A1	Pass	Pass	Pass	2	Pass
IMN-A2	Pass	Pass	Pass	2	Pass
IMN-A3	Pass	Pass	Pass	2	Pass
IMN-A4	Pass	Pass	Pass	2	Pass
IMN-A5	Pass	Fail	Pass	3	Fail
IMN-A6	Pass	Fail	Fail	3	Fail
IMN-B1	Pass	Pass	Pass	2	Pass
IMN-B2	Pass	Pass	Pass	2	Pass
IMN-B3	Pass	Pass	Pass	2	Pass
IMN-B4	Pass	Pass	Pass	2	Pass
IMN-B5	Pass	Fail	Pass	2	Fail
IMN-B6	Fail	Pass	Pass	3	Fail
IMN-C1	Pass	Fail	Fail	2	Fail
IMN-C2	Pass	Pass	Pass	2	Pass
IMN-C3	Pass	Pass	Pass	2	Pass
IMN-C4	Pass	Fail	Pass	2	Fail
IMN-C5	Fail	Pass	Pass	3	Fail
IMN-C6	Pass	Fail	Pass	3	Fail

Mean ± standard deviation, n=3, IMN: Indomethacin

lower globule size.[51] The decrease in turbidity can be due to the decrease in emulsion globule size.

Cloud point

The point at which cloudiness appears is known as cloud point. At a temperature higher than the cloud point, formulation may undergo phase separation which is due to dehydration of polyethylene oxide moiety of the non-ionic surfactant. So, cloud point of the formulation should be more than 37°C. IMN formulations showed cloud point at high temperature >37°C (Table 8), indicating stability at physiological temperature.

In vitro dissolution study

Faster release of IMN from SEDDS was observed which may be due to dissolved state of IMN, spontaneous formation of microemulsion and smaller globule size, as compared to plain IMN shown in Figure 6.

Formulation IMN-B1 showed the maximum release which may due to its oil and surfactant mixture concentration, which leads to rapid emulsification of oil for finer globules. Nanosized globule provides larger effective surface area for diffusion of solubilised IMN from SEDDS to dissolution media.[44] In dissolution study formulation IMN-B1 showed maximum release of drug (100.12±1.31%) in 40 min. The data was analyzed by *t test* and significant difference ($p<0.05$) was observed between means at 10 to 50 min.

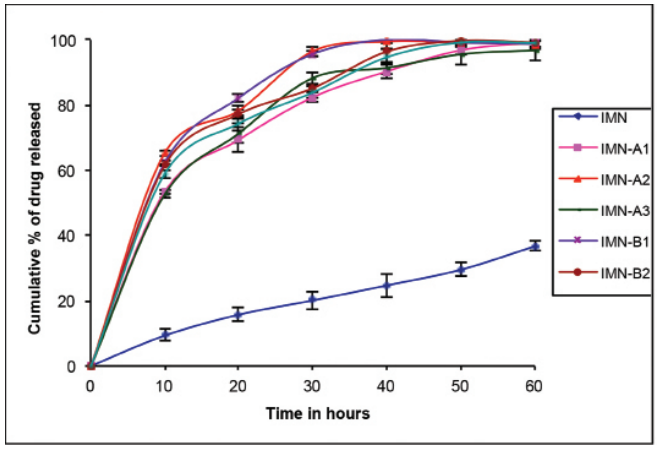

Figure 6. *In vitro* dissolution profiles of indomethacin formulations

In comparison to marketed product dissolution profile of IMN-B1 showed 100.12±1.31% of drug release at the end of 40 min, where as marketed product showed 93.68±2.29% release at the end of 60 min. The data was analyzed by *t test* and significant difference was observed between means.

The dissolution profile of the IMN-B1 SEDDS was compared with the marketed product of powder filled capsule by similarity (f2) and dissimilarity factor (f1). The low value of f2 (15%) and more f1 (45%) indicates the dissolution profiles of optimized and marketed product were not similar. The IMN SEDDS has improved dissolution rate of IMN than the powder filled capsule product.

In vitro diffusion study

In vitro diffusion study for IMN-C1 and marketed product were carried out for 12 h. The percentage release was found to be 81.51±4.56 and 57.96±4.75 for IMN-C1 and marketed product respectively (Figure 7). The data of *in vitro* diffusion data was analyzed by *t test* and significant difference was observed between means.

Anti-inflammatory activity

The percentage inhibition and paw edema in rats showed a significant inhibition ($p<0.001$) compared to control. IMN-B1 showed significant inhibition ($p<0.05$ and $p<0.01$) compared to marketed product due to increased absorption of IMN from lipids. IMN-B1 and marketed product showed the maximum activity at the end of 5th hour of oral administration. Percentage inhibition of IMN-B1 and marketed product was found to be 76.73±2.84 and 64.73±6.83 respectively. The present study revealed that IMN-B1 showed better anti-inflammatory activity over the marketed product.

Table 7. Drug content, refractive Index, percentage transmission and viscosity of IMN SEDDS

Formulation code	Drug content (%)	Refractive index	Percentage transmission	Viscosity (cps)
IMN-A1	99.58±1.27	1.446±0.02	97	0.932±1.31
IMN-A2	99.1±1.92	1.434±0.03	99.2	0.845±2.71
IMN-A3	100.3±0.91	1.445±0.02	96.3	0.656±2.11
IMN-B1	99.71±0.84	1.447±0.02	95.4	0.906±3.01
IMN-B2	99.73±1.25	1.444±0.03	96	0.872±1.28
IMN-C2	99.65±0.94	1.439±0.03	97.5	0.737±0.94

Mean ± standard deviation, n=3, SEDDS: Self-Emulsifying Drug Delivery System, IMN: Indomethacin

Pharmacokinetic studies

Figure 8 depicts the mean plasma concentration-time profiles of pure IMN, IMN-B1 and marketed product. The plasma level profiles were significantly increased for IMN-B1 and marketed product compared to pure IMN. C_{max} was found to be 1.9±0.22, 7.87±0.33 and 3.58±0.27 µg/mL for pure IMN, IMN-B1 and marketed product respectively (Table 9). C_{max} of IMN-B1 and marketed product was 4.14 and 1.88 times higher than that of pure IMN respectively. Time required to reach maximum concentration was found to be 2.33±0.58, 1.33±0.29 and 1.5 hr for pure IMN, IMN-B1 and marketed product respectively.

The low AUC value of pure IMN and marketed product may be due to less absorption into the body. On the contrary, IMN-B1 showed high AUC values indicating increased/better absorption of drug and hence improved bioavailability of IMN from SEDDS. The $t_{1/2}$ and Vd of IMN was more with the optimized IMN-B1 indicating better drug distribution. The time taken to reach maximum concentration was lesser with IMN-B1 which indicates fast absorption.

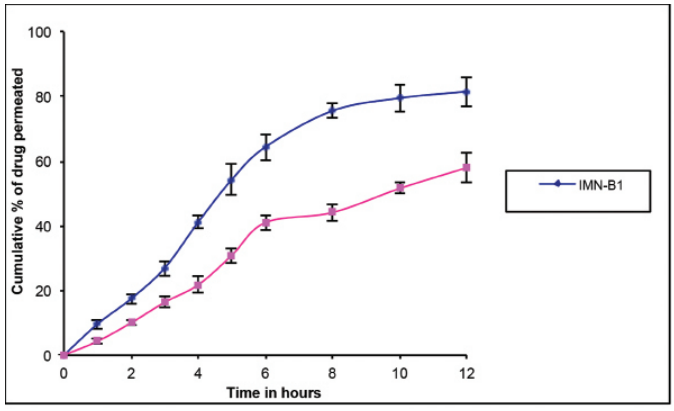

Figure 7. *In vitro* diffusion profile of IMN-B1 and marketed product
IMN: Indomethacin

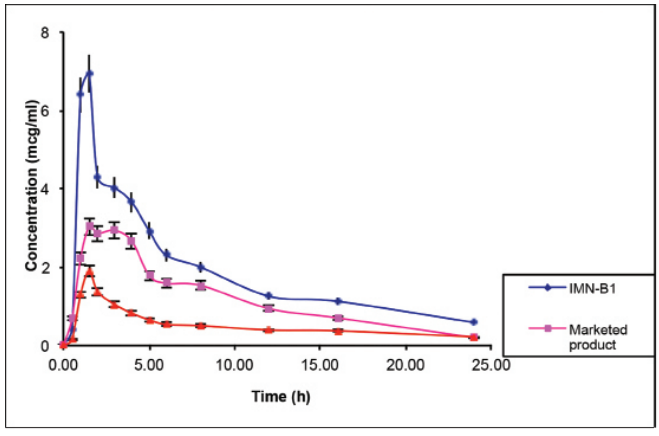

Figure 8. Mean plasma concentration - time profiles of indomethacin

Stability study

No change in the physical parameters such as homogeneity and clarity was observed during the stability study. A slight increase in globule size to 193 nm has been observed which may be due to aggregation of globules. The PDI was within 1 which reflects the uniformity. The drug content and dissolution behaviour of prepared formulation was well within the limits during the storage and significant difference ($p<0.05$) was observed between means of drug content at 3rd and 6th month.

CONCLUSION

In the present study prepared self emulsifying formulations showed enhanced release of IMN when compared to the marketed capsules. SEDDS formed micro emulsion dispersed

Table 9. Pharmacokinetic parameters of IMN in rats after oral dose of 10 mg/kg

Parameter	Oral administration		
	Pure IMN	IMN-B1	Marketed product
C_{max} (µg/mL)	1.9±0.22	7.87±0.33***	3.58±0.27***###
t_{max} (hr)	2.33±0.58	1.33±0.29	1.50
$AUC_{0\rightarrow t}$ (hr/µg/mL)	12.27±1.59	43.18±14.03*	28.09±3.86
$AUC_{0\rightarrow \infty}$ (hr/µg/mL)	16.8±1.98	60.12±22.85*	30.03±5.66
$t_{1/2}$ (hr)	7.8±1.24	7.73±1.80	5.59±2.17

Mean ± standard deviation, n=6, *p<0.05, **p<0.01, ***p<0.001 vs. pure IMN; #p<0.5, ###p<0.001 vs. IMN-B1, IMN: Indomethacin

Table 8. Globule size, PDI, zeta potential, turbidity and cloud point of IMN SEDDS

Formulation	Globule size (nm)	PDI	Zeta potential (mV)	Turbidity (NTU)	Cloud point (°C)
IMN-A1	201.7±1.83	0.153±1.32	-7.55±2.81	10.53±2.79	74-75
IMN-A2	253.6±2.55	0.264±1.71	-7.83±2.15	19.14±3.06	71-73
IMN-A3	340.5±1.74	0.421±2.11	-7.94±1.84	20.84±3.57	70-71
IMN-B1	184.1±2.07	0.127±1.67	-7.92±2.11	BLD	63-65
IMN-B2	226.3±1.79	0.199±1.83	-8.48±1.33	14.27±3.11	62-63
IMN-C2	237.8±1.19	0.151±1.06	-8.1±1.47	17.79±2.85	62-63

Mean ± standard deviation, n=3, BLD: Below limit of detection, SEDDS: Self-Emulsifying Drug Delivery System, IMN: Indomethacin

rapidly with a size range 184.1 nm to 340.5 nm, showing good emulsification. The anti inflammatory activity and pharmacokinetic study showed improved activity as compared to marketed product due to solubilisation of drug by the self emulsification process. Further results show a possible chance of improvement in bioavailability of IMN with the formulated SEDDS. Thus this technique helps in improving solubility and can be applied to similar drugs used in the treatment of various diseases.

ACKNOWLEDGEMENTS

We thank the Sultan-ul-Uloom educational Society and MNR educational trust, Hyderabad for their valuable support to carry out this research work.

Conflict of Interest: No conflict of interest was declared by the authors.

REFERENCES

1. Lipinski CA. Poor aqueous solubility: an industry wide problem in drug discovery. Am Pharm Rev. 2002;5:82-88.
2. Yalkowsky S. Technique of solubilization of drugs, drugs and the pharmaceutical sciences. New York; Marcel Dekker; 1981.
3. Amidon GL, Lennernas L, Shah VP, Crison JR. A theoretical basis for a biopharmaceutic drug classification: the correlation of *in vitro* drug product dissolution and *in vivo* bioavailability. Pharm Res. 1995;12:413-420.
4. Humberstone AJ, Charman WN. Lipid-based vehicles for the oral delivery of poorly water soluble drugs. Adv Drug Deliv Rev. 1997;25:103-128.
5. Gursoy RN, Benita S. Self-emulsifying drug delivery systems (SEDDS) for improved oral delivery of lipophilic drugs. Biomed Pharmacother. 2004;58173-182.
6. Porter CJ, Charman WN. Intestinal lymphatic drug transport: an update. Adv Drug Deliv Rev. 2001;50:61-80.
7. Gao P, Morozowich W. Development of supersaturatable self-emulsifying drug delivery system formulations for improving the oral absorption of poorly soluble drugs. Expert Opin Drug Deliv. 2006;3:97-110.
8. Pouton CW, Porter CJ. Formulation of lipid-based delivery systems for oral administration: materials, methods and strategies. Adv Drug Deliv Rev. 2008;60:625-637.
9. Porter CJ, Trevaskis NL, Charman WN. Lipids and lipid-based formulations: optimizing the oral delivery of lipophilic drugs. Nat Rev Drug Discov. 2007;6:231-248.
10. Chen ML. Lipid excipients and delivery systems for pharmaceutical development: a regulatory perspective. Adv Drug Deliv Rev. 2008;60:768-777.
11. Devani M, Ashford M, Craig DQ. The emulsification and solubilisation properties of polyglycolysed oils in self-emulsifying formulations. J Pharm Pharmacol. 2004;56:307-316.
12. Chistyakov BE. Theory and practical application aspects of surfactants. Studies in Interface Science. 2001;13:511-618.
13. Li P, Ghosh A, Wagner RF, Krill S, Joshi YM, Serajuddin AT. Effect of combined use of nonionic surfactant on formation of oil-in-water microemulsions. Int J Pharm. 2005;288:27-34.
14. Lind ML, Jacobsen J, Holm R, Müllertz A. Intestinal lymphatic transport of halofantrine in rats assessed using a chylomicron flow blocking approach: the influence of polysorbate 60 and 80. Eur J Pharm Sci. 2008;35:211-218.
15. Rang MJ, Miller CA. Spontaneous emulsification of oils containing hydrocarbon, nonionic surfactant, and oleyl alcohol. J Colloid Interface Sci. 1999;209:179-192.
16. Reiss H. Entropy induced dispersion of bulk liquids. J Colloid Interface Sci. 1975;53:61-70.
17. Khoo SM, Humberstone AJ, Porter CJH, Edwards GA, Charman WN. Formulation design and bioavailability assessment of lipidic self-emulsifying formulations of halofantrine. Int J Pharm. 1998;167:155-164.
18. Yetukuri K, Sudheer P. Approaches to development of solid self micro emulsifying drug delivery system: formulation techniques and dosage forms: a review. Int J Pharm Sci Res. 2012;3:3550-3558.
19. Sarpal K, Pawar BY, Bansa AK. Self-emulsifying drug delivery systems: a strategy to improve oral bioavailability. Current Research in Pharmaceutical Sciences. 2010;11:42-49.
20. Nidhi M, Shikha S. New strategy for solubilization of poorly soluble drug-SEDDS. Der Pharmacia Lettre. 2009;1:60-67.
21. Kawakami K, Yoshikawa T, Hayashi T, Nishihara Y, Masuda K. Microemulsion formulation for enhanced absorption of poorly soluble drugs. II. *In vivo* study. J Control Release. 2002;81:75-82.
22. Boon V, Glass B, Nimmo A. High-performance liquid chromatographic assay of indomethacin in porcine plasma with applicability to human levels. J Chromatogr Sci. 2006;44:41-44.
23. Li T, Fang L, Ren C, Wang M, Zhao L. Determination of transdermally and orally applied indomethacin in rat plasma and excised skin and muscle samples. AJPS. 2008;3:269-275.
24. Balakrishnan P, Lee BJ, Oh DH, Kim JO, Hong MJ, Jee JP, Kim JA, Yoo BK, Woo JS, Yong CS, Choi HG. Enhanced oral bioavailability of dexibuprofen by a novel solid self emulsifying drug delivery system (SEDDS). Eur J Pharm Biopharm. 2009;72:539-545.
25. Ministry of Health and Family welfare. Indian Pharmacopoeia (6th ed). Ghaziabad: The Indian Pharmacopoeia commission; 2010.
26. Hong JY, Kim JK, Song YK, Park JS, Kim CK. A new self-emulsifying formulation of itraconazole with improved dissolution and oral absorption. J Control Release. 2006;110:332-338.
27. Avachat AM, Patel VG. Self nanoemulsifying drug delivery system of stabilized ellagic acid-phospholipid complex with improved dissolution and permeability. Saudi Pharm J. 2015;23:276-289.
28. Nabi SSU, Shakeel F, Talegaonkar S, Ali J, Baboota S, Ahuja A, Khar RK, Mushir A. Formulation development and optimization using nanoemulsion technique: a technical note. AAPS Pharm Sci Tech. 2007;8:1-6.
29. Shafg S, Shakeel F, Talegaonkar S, Ahmad FJ, Khar RK, Ali M. Development and bioavailability assessment of ramipril nanoemulsion formulation. Eur J Pharm Biopharm. 2007;66:227-243.
30. Khoo SM, Humberstone AJ, Porter CJH, Edwards GA, Charman WN. Formulation design and bioavailability assessment of lipidic self-emulsifying formulations of halofantrine. Int J Pharm. 1998;167:155-164.
31. Patel D, Sawant KK. Oral bioavailability enhancement of acyclovir by self microemulsifying drug delivery systems (SMEDDS). Drug Dev Ind Pharm. 2007;33:1318-1326.

32. Ramadan E, Borg TH, Abdelghani GM, Saleh N. Formulation and evaluation of acyclovir microemulsions. Bull Pharm Sci. 2013;36:31-47.

33. Kallakunta VR, Bandari S, Jukanti R, Veerareddy PR. Oral self emulsifying powder of lercanidipine hydrochloride: formulation and evaluation. Powder Technol. 2012;221:375-382.

34. Cho HJ, Ku WS, Termsarasab U, Yoon I, Chung CW, Moon HT, Kim DD. Development of udenafil-loaded microemulsions for intranasal delivery: *In vitro* and *in vivo* evaluations. Int J Pharm. 2012;423:153-160.

35. Taha EI, Al-Saidan S, Samy AM, Khan MA. Preparation and *in vitro* characterization of self-nanoemulsified drug delivery system (SNEDDS) of all-trans-retinol acetate. Int J Pharm. 2004;285:109-119.

36. Nazzal S, Nutan M, Palamakula A, Shah R, Zaghloul AA, Khan MA. Optimization of a self-nanoemulsified tablet dosage form of ubiquinone using response surface methodology: effect of formulation ingredients. Int J Pharm. 2002;240:103-114.

37. Lichtenberger LM, Romero JJ, Dial EJ, Moore JE. Naproxen-PC: a GI safe and highly effective anti-inflammatory. Inflammopharmacology. 2009;17:1-5.

38. Liles JH, Flecknell PA. The use of non-steroidal anti-inflammatory drugs for the relief of pain in laboratory rodents and rabbits. Lab Anim. 1992;26:241-255.

39. Boon V, Glass B, Nimmo A. High-performance liquid chromatographic assay of indomethacin in porcine plasma with applicability to human levels. J Chromatogr Sci. 2006;44:41-44.

40. Saritha D, Penjuri SCB, Nagaraju R. Formulation and evaluation of self emulsifying drug delivery system (SEDDS) of Indomethacin. Int J Res Pharm Sci. 2014;4:17-23.

41. Bachhav YG, Patravale VB. SMEDDS of glyburide: formulation, *in vitro* evaluation, and stability studies. AAPS Pharm Sci Tech. 2009;10:482-487.

42. Patel AR, Vavia PR. Preparation and *in vivo* evaluation of SMEDDS (self-microemulsifying drug delivery system) containing fenofibrate. AAPS J. 2007;9:344-352.

43. Pouton CW. Lipid formulations for oral administration of drugs: non-emulsifying, self-emulsifying and self-microemulsifying drug delivery systems. Eur J Pharm Sci. 2000;11:93-108.

44. Pouton CW. Formulation of poorly water-soluble drugs for oral administration: physicochemical and physiological issues and the lipid formulation classification system. Eur J Pharm Sci. 2006;29:278-287.

45. Craig DQM, Baker SA, Banning D, Booth SW. An investigation into the mechanisms of self-emulsification using particle size analysis and low frequency dielectric spectroscopy. Int J Pharm. 1995;11:103-110.

46. Osborne DW, Middleton CA, Rogers RL. Alcohol-free microemulsions. J Dispers Sci Technol. 1988;9:415-423.

47. Pouton CW. Formulation of self-emulsifying drug delivery systems. Adv Drug Deliv Rev. 1997;25:47-58.

48. Zhang P, Liu Y, Feng N, Xu J. Preparation and evaluation of self-emulsifying drug delivery system of oridonin. Int J Pharm. 2008;355:269-276.

49. Roland I, Piel G, Delattre L, Evrard B. Systematic characterization of oil-in- water emulsions for formulation design. Int J Pharm. 2003;263:85-94.

50. Groves MT, Mustafa RM. Measurement of the spontaneity of self emulsifiable oils. J Pharm Pharmcol. 1974;26:671-681.

51. Pouton CW. Self-emulsifying drug delivery systems: assessment of the efficiency of emulsification. Int J Pharm. 1985;27:335-348.

Turk J Pharm Sci 2017;14(2):120-126
DOI: 10.4274/tjps.87587

ORIGINAL ARTICLE

Development, Internal and External Validation of Naproxen Sodium Sustained Release Formulation: an Level A *In Vitro-In Vivo* Correlation

Naproksen Sodyum Süreli Serbest Formülasyonun Geliştirilmesi, İç ve Dış Olarak Doğrulaması: Bir Düzey A *İn Vitro-İn Vivo* Korelasyon

Ramesh NARAYANASAMY*, Ramakrishna SHABARAYA

Srinivas College of Pharmacy, Farengipete Post, Mangalore, Karnataka, India

ABSTRACT

Objectives: The aim of the present study was to develop and validate an *in vitro-in vivo* correlation (IVIVC) for naproxen sodium-sustained release tablets and to compare their plasma concentrations over time with the immediate-release tablets.

Materials and Methods: *In vitro* release rate data were obtained for each tablet by using the USP Apparatus II, paddle stirrer at 50 rpm in pH 7.4 phosphate buffer. A four-way crossover study was conducted in 6 healthy subjects by administering naproxen sodium sustained release 375 mg and 500 mg of immediate release tablets. Series of blood samples were collected over 24 hours and estimated by using the validated liquid chromatography tandem-mass spectrometry method.

Results: The similarity factor was calculated and it was found that values between, 50 and 100 indicates similarity of the profiles. Assessment of predicted and observed bioavailability was performed and prediction errors (PE) % calculated, as per the Food Drug Administration guidelines, the average absolute PE% of C_{max} and AUC of individual formulation was found below 15% for establishment of IVIVC, based on internal prediction strongly suggesting that the naproxen sodium IVIVC models are valid. During external validation the predicted curve for the naproxen sodium sustained-release tablets was found to be identical to immediate release tablets and considered as valid.

Conclusion: IVIVC can serve as a surrogate for *in vivo* bioavailability study and supports biowaivers, supports and validates the dissolution methods and specification settings and assists in quality control during scale-up and post-approval changes. It may be used to predict the variation in site change, process changes and to predict the absorption performance of naproxen sodium products with different release rates.

Key words: IVIVC, naproxen sodium, sustained release, dissolution, *in vivo* bioavailability study, internal and external predictability

ÖZ

Amaç: Bu çalışmanın amacı, naproksen sodyumun sürekli salım tableti için *in vitro-in vivo* korelasyon (IVIVC) geliştirmek, doğrulamak ve zamana bağlı plazma konsantrasyonlarını derhal salınan tabletle karşılaştırmaktır.

Gereç ve Yöntemler: *İn vitro* salım hızı verileri, pH 7.4 fosfat tampon içinde 50 dev/dakikada, USP Apparatus II, palet karıştırıcısı kullanılarak her bir tablet için elde edilmiştir. Naproksen sodium 375 mg sürekli salım ve 500 mg derhal salım tabletleri 6 sağlıklı kişiye uygulanarak dört yönlü bir çaprazlama çalışması gerçekleştirilmiştir. Yirmi dört saat boyunca toplanan kan örnekleri valide edilmiş sıvı kromatografisi tandem-kütle spektrometresi yöntemi kullanılarak tayin edilmiştir.

Bulgular: Hesaplanan ve 50-100 arasında bulunan değerler benzerlik faktörlerini göstermektedir. C_{max} ve AUC ortalama değerlerine yakın bulunmuştur. Tahmin edilen ve gözlemlenen biyoyararlanım değerlendirmesi yapıldı ve Gıda İlaç İdaresi yönetmeliklerine göre % tahmin hataları (PE) hesaplandı; iç tahmin ile IVIVC'nin oluşturulması için C_{max}'ın ortalama mutlak %PE'si ve formülasyonun bireysel formülasyonun AUC'si %15'in altında bulundu, naproksen sodyumun IVIVC modelleri geçerlidir. Dış validasyon sırasında, naproksen sodyumun sürekli salım tableti için öngörülen eğri, derhal salım tableti ile aynı bulunması geçerli olduğunu göstermektedir.

Sonuç: Bu IVIVC, *in vivo* biyoyararlanım araştırması için vekil olarak hizmet edebilir ve biyolojik yönlendiricileri destekler, çözünme yöntemlerini ve spesifikasyon ayarlarını destekler ve onaylar, ölçek büyütme ve onay sonrası değişiklikler sırasında kalite kontrolünde yardımcı olur. Yer değişikliği, proses değişiklikleri ve farklı emisyon oranlarına sahip naproksen sodyum ürünlerinin emme performansını tahmin etmek için kullanılabilir.

Anahtar kelimeler: IVIVC, naproksen sodyum, sürekli salım, çözünme, *in vivo* biyoyararlanım çalışması, iç ve dış öngörülebilirlik

*Correspondence: **E-mail:** ramesh7779@gmail.com, **Phone:** 91 824 2232700
Received: 12.12.2016, **Accepted:** 26.01.2017

INTRODUCTION

In vitro-in vivo correction is a predictive mathematical model relating the relationship between an *in vitro* property of a dosage form and an *in vivo* response.[5] *In vitro-in viv*o correlation (IVIVC) is most widely established by using formulations with different release rates i.e. slow, medium and fast, data on the *in vitro* release rates and *in vivo* plasma concentration-time profiles of developed formulations, and by using deconvolution techniques to confirm the link between dissolution rate and fraction absorbed. The Food Drug Administration (FDA) guidelines has discussed the three categories of IVIVC models: namely, level A, B, and C models. Level A is a linear is most widely used as it is developed point to point correlation and stands for *in vitro* and *in vivo* absorption rate of the drug. Level A can be developed on both deconvolution and convolution-based methods. Level B compares the mean *in vitro* dissolution time to the mean *in vivo* residence time or the mean *in vivo* dissolution time. Level C is a single point comparison of dissolution time point to one pharmacokinetic parameter [e.g. C_{max}, area under the curve (AUC), and T_{max} time of the maximum plasma concentration]. Level D is a rank order analysis.[5] The development and validation of IVIVC is vital for optimization of sustained release dosage form as it predicts the *in vivo* release profile of the sustained release (SR) dosage form based on *in vitro* data.[9]

Various IVIVC studies have been published for a number of formulations, including Busprion, propranolol, nevirapine, metoprolol and other drugs.[6-17] The concepts and methods used in establishing the IVIVC are reviewed elsewhere.[4,5] According to BCS classification naproxen sodium comes under class 2 drug and in addition naproxen is relatively having a short life suggest suitable applicant for modified release formulation.[1,2] The present work is intended to formulate naproxen sodium sustained release tablet, develop and validate the internal and external predictability of level A IVIVC models. *In vitro* dissolution study was performed to check the release profile and bioavailability study conducted to check the rate and extent of absorption of developed naproxen sodium sustained release and marketed immediate release tablet. Further established and validated IVIVC models can be used as a surrogate for the bioequivalence study, minimize the time and cost for manufacturers, a quality control tool to measure the product performance, a waiver for human studies when the minor changes are done as specified in the scale-up and post-approval changes (SUPAC)- immediate release and SUPAC-modified release guidance.

MATERIALS AND METHODS

Chemicals and reagents

Naproxen sodium, HPMC K100M supplied as a gift sample by Strides Arcolab Limited, Bangalore and Colorcon Asia Pvt. Limited, Goa, India. All other materials like talc, magnesium stearate, ethyl cellulose were procured from local dealer.

In vitro dissolution study and data analysis

The drug release profiles were examined by using by using the United States Pharmacopeia (USP) dissolution apparatus (type 2, paddle) pH 1.2, 4.5, 5.5, 6.8 and 7.4 at 50 & 75 rpm (rotation per min). The dissolution studies were performed on six tablet of naproxen sodium 375 mg SR tablets (i.e. slow, medium and fast) and naproxen sodium 500 mg tablet (marketed immediate release). Samples were drawn at 0.0, 0.5, 1.0, 1.5, 2.0, 3.0, 4.0, 6.0, 8.0, 12.0, 18.0 and 24.0 hours and analyzed by using UV spectroscopy at a wavelength of 332 nm. The percentage fraction dissolved and percentage release at various time points were determined. The similarity of dissolution profiles were evaluated for fast versus slow, slow versus medium and medium versus fast by using the similarity factor (f2).

In vivo bioavailability study and data analysis

This was an single center, randomized, single-dose, open-label, 4-way crossover, bioavailability study to compare the rate and extent of absorption of a naproxen sodium 375 mg SR tablets (i.e. slow, medium and fast) and naproxen sodium 500 mg tablet (marketed immediate release), in six healthy male subjects under fasting conditions. Samples were collected at 0.0, 0.5, 1.0, 1.5, 2.0, 2.5, 3.0, 3.5, 4.0, 4.5, 5.0, 5.5, 6.0, 8.0, 10.0, 12.0, 16.0 and 24.0 hours post dose sample. A washout period of 7 days between the dosing of four periods. The study was approved by ethics committee and informed consent were provided by subjects prior enrolled into the study and. Validation of the method was carried out after the development of the liquid chromatography mass spectrometry (LCMS) methods. Validation performed as per the USFDA guidelines i.e. specificity/selectivity, carry over, linearity, precision and accuracy, recovery, dilution integrity, ruggedness, stabilities like freeze thaw stability, bench top stability, long term stability, stock solution stability. A simple and sensitive validated LCMS/MS method used for estimation of plasma sample by using protein precipitate extraction. The calibration curves were linear in the range of 1.167 µg/mL to 163.729 µg/mL for naproxen sodium. Bioavailability study evaluated through plasma concentration data by using pharmacokinetic parameters like C_{max}, AUC, T_{max}, half lifeand estimation performed by using Phoenix 6.4.0 version software.

IVIVC model development

Linear regression analysis was used to study the relationship between the drug dissolved and the drug absorbed in percentage. A correlation was established for naproxen sodium 375 mg SR tablets (i.e. slow, medium and fast) formulations (M/F, S/F, and S/M). A linear regression done by using a least squares method to estimate the regression parameters. Determination coefficient (r^2) was evaluated. The deconvolution procedure was used to obtain *in vivo* input profiles of naproxen sodium from the sustained release dosage forms. The percent of dissolved is plotted against the dissolution sampling points of target formulation to check whether developed IVIVC model is valid.

IVIVC validation

The objective is to predict the outcome of *in vivo* profile with a given model and target formulation of *in vitro* profile. Internal validation provides basis for the acceptability of the model and

external validation is superior and gives the self-confidence in the model. As per the FDA guidance on IVIVC for level A criteria as follows: for internal validation the mean absolute percent prediction error i.e. for C_{max} and AUC should not exceed 10%, and for individual formulation should not exceed 15%. For external validation the prediction errors i.e. C_{max} and AUC, for the formulation should not exceed 10%, 10% to 20% indicates in conclusive predictability and demonstrate the requirement for further study. The percent prediction errors (PE) for C_{max} and AUC were calculated as follows:

$$\%PE_{C_{max}} = \left(\frac{C_{max}\,(observed) - C_{max}\,(prediction)}{C_{max}\,(observed)} \right) x\ 100 \quad (1)$$

$$\%PE_{AUC} = \left(\frac{AUC\,(observed) - AUC\,(prediction)}{AUC\,(observed)} \right) x\ 100 \quad (2)$$

RESULT AND DISCUSSION

In vitro dissolution study

The *in vitro* dissolution studies were performed at different pH conditions (namely pH 1.2, 4.5, 5.5, 6.8, 7.4) to select appropriate pH condition. The results of dissolution studies at different pH conditions with 50 rpm, at pH 1.2 and 50 rpm, drug release was partial and utmost 11% released from the formulations (F1-F6; SR tablets composition are mentioned in Table 1) within 3 hours as shown in the Figure 1. At pH 4.5, the drug release was very slow till 24 hours. The release was incomplete for all the formulations (F1-F6; SR tablets) as shown in the Figure 2. At pH 5.5 homogeneous and slow release of drug from all the 6 formulations (F1-F6; SR tablets) over the period of 24 h, 80.59-99.86% of drug was released as shown in the Figure 3. At pH 6.8 and 7.4 about 86.79-97.32% as shown in the Figure 4 and 86.95-95.81% release of drug was observed as shown in the Figure 5. Hence pH 5.5 selected for *in vitro* dissolution studies for naproxen sodium. There is no significant changes observed in drug release when performed with 75 rpm. The *in vitro* drug release studies performed as per the USP method i.e. pH 7.4 pH condition at 50 rpm for naproxen sodium SR tablets (i.e. F2 slow, F5 medium and F4 fast). The *in vitro* release characteristics of the fast, medium, and slow sustained release tablet of naproxen sodium were determined and presented in Figure 6. The similarity factor (r^2) was calculated fast versus slow 52.52, fast versus medium 69.87 and medium versus slow 64.08 respectively.[4]

The percentage fraction dissolved for naproxen sodium are in the rank order of marketed immediate release, fast, medium and slow sustained release tablets and are presented in the Figure 6.

In vivo bioavailability study and data analysis

The mean pharmacokinetic profile for all formulations are presented in Table 2. The rank order release in the dissolution testing was obvious in the plasma concentration profile of

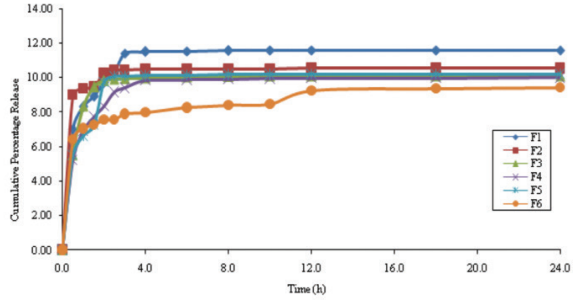

Figure 1. Percentage cumulative release profiles of naproxen sodium sustained release formulations (F1-F6) at pH 1.2 and 50 rpm

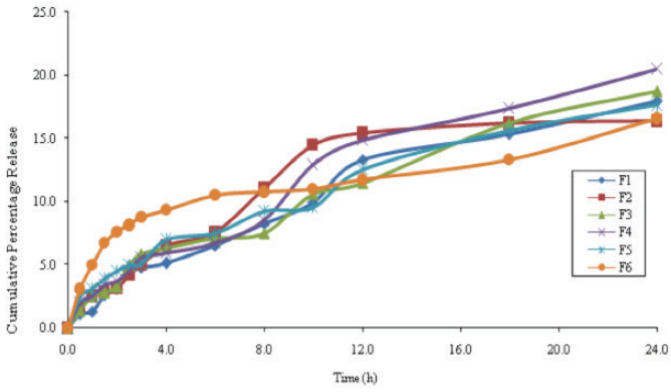

Figure 2. Percentage cumulative release profiles of naproxen sodium sustained release formulations (F1-F6) at pH 4.5 and 50 rpm

Table 1. Composition of naproxen sodium formulation (F1-F6)

Formulation	Naproxen sodium	HPMC K100M	Talc (1.5%)	Magnesium stearate (1.5%)	Talc (1%)	Magnesium stearate (1%)	Ethyl cellulose
F1	375	75 mg	-	-	4.50 mg	4.50 mg	-
F2	375	150 mg	-	-	5.25 mg	6.00 mg	-
F3	375	225 mg	-	-	5.25 mg	6.00 mg	-
F4	375	37.5 mg	6.75 mg	6.75 mg	-	-	37.5 mg
F5	375	37.5 mg	7.87 mg	7.87 mg	-	-	37.5 mg
F6	375	37.5 mg	9.00 mg	9.00 mg	-	-	37.5 mg

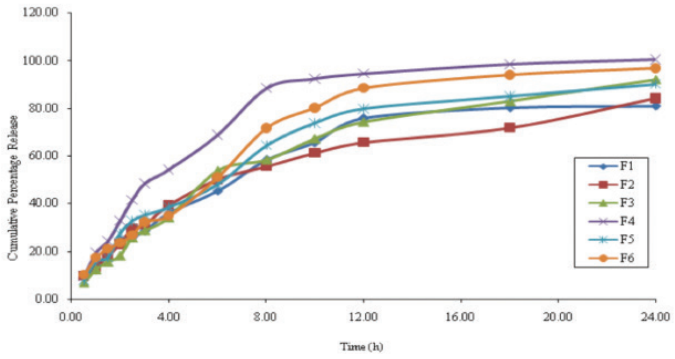

Figure 3. Percentage cumulative release profiles of naproxen sodium sustained release formulations (F1-F6) at pH 5.5 and 50 rpm

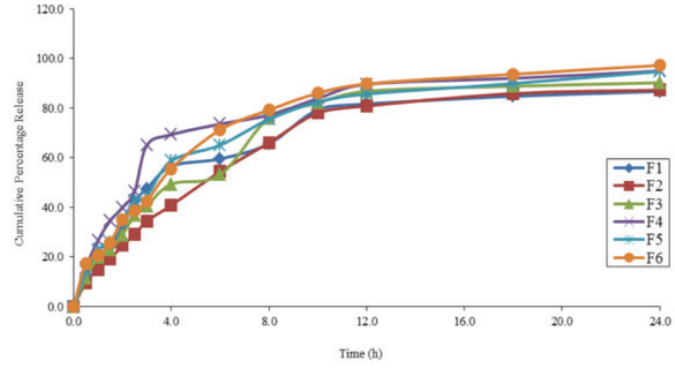

Figure 4. Percentage cumulative release profiles of naproxen sodium sustained release formulations (F1-F6) at pH 6.8 and 50 rpm

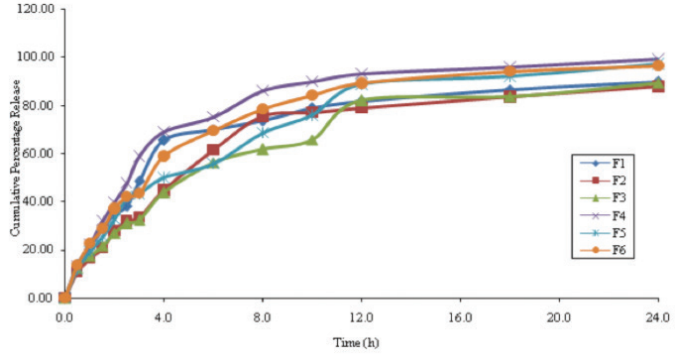

Figure 5. Percentage cumulative release profiles of naproxen sodium sustained release formulations (F1-F6) at pH 7.4 and 50 rpm

naproxen sodium as in the Figure 7. AUC of naproxen slow release and medium release tablet was significantly higher compare to immediate release and fast release tablet. There is significant difference observed in naproxen slow and medium sustained release tablet compare to marketed immediate release and fast sustained tablet. AUC of naproxen sustained release tablets was much higher than immediate release tablet, may due to change in location of naproxen sodium absorption in gastrointestinal tract.

In vitro-in vivo correlation development

Level A *in vitro* and *in vivo* correlation was developed by comparing percent dissolved versus the percent absorbed of naproxen sodium fast, medium and slow sustained release and marketed immediate release tablets. The IVIVC plot was constructed using percentage of drug dissolved at pH 7.4

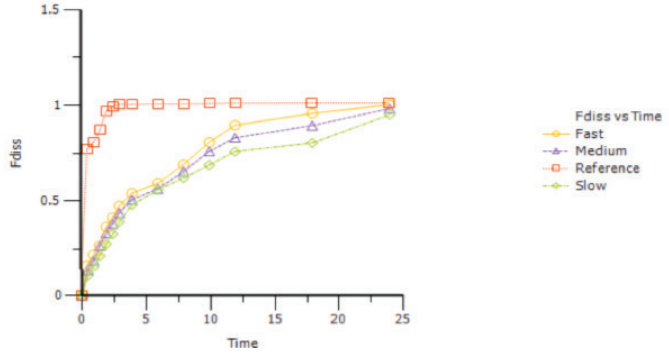

Figure 6. Percentage fraction dissolved versus time for naproxen sodium IR tablet and SR tablets (i.e. F2 slow, F5 medium and F4 fast)

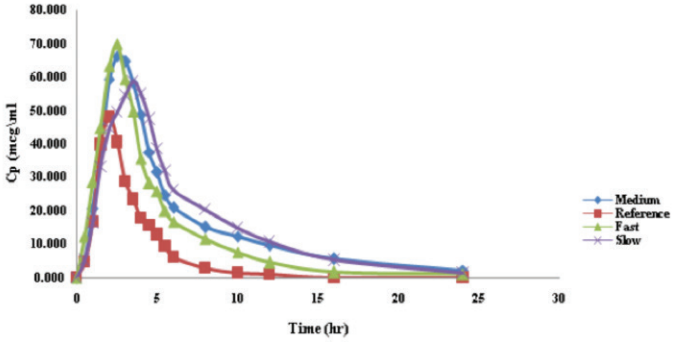

Figure 7. Mean plasma concentrations versus time of naproxen sodium for marketed immediate release and sustained release tablet (fast, medium and slow)

Table 2. Mean pharmacokinetic parameter of naproxen sodium for marketed immediate release and sustained release tablet (fast, medium and slow)

Formulation	T_{max} (hr)	C_{max} (ug/mL)	AUC (hr*ug/mL)
Immediate release tablet	1.833±0.258	54.209±10.685	147.483±36.265
Fast sustained release tablet	2.167±0.258	73.767±4.889	307.561±7.775
Medium sustained release tablet	2.667±0.258	68.879±4.562	391.273±82.259
Slow sustained release tablet	3.583±0.376	63.199±3.141	391.499±69.217

AUC: Area under the curve

buffer dissolution media at 50 rpm versus the percentage of drug absorbed. The slope of the best-fit line was examined using linear regression analysis and coefficient of correlation (r^2). IVIVC model linear regression of percentage dissolved and percentage absorbed for naproxen sodium sustained release tablet presented in the Figure 8-10. The correlation coefficient (r^2) for naproxen sodium SR tablets medium versus slow was 0.987, fast versus medium was 0.948, and naproxen sodium SR tablets fast versus medium was 0.96 respectively. Good linear regression relationship observed between all the three test formulation. Edington et al.[9] described the dissolution methodology which discriminates between the formulation and mimics the *in vivo* release profile in development of IVIVC.

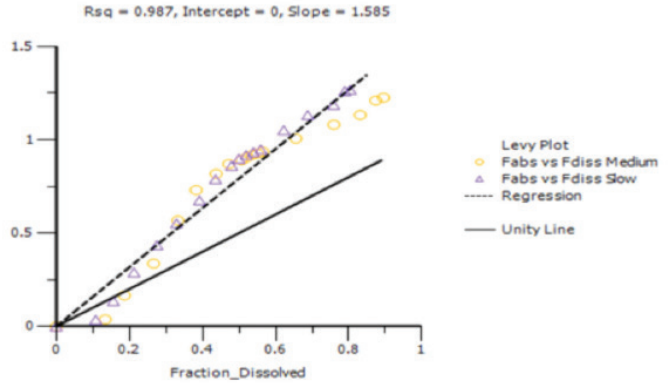

Figure 8. *In vitro-in vivo* correlation model linear regression percentage dissolved and percentage absorbed for naproxen sodium medium and slow sustained release tablet

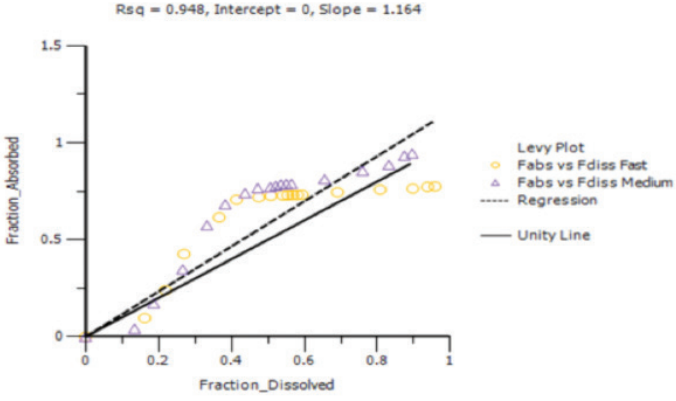

Figure 9. *In vitro-in vivo* correlation model linear regression percentage dissolved and percentage absorbed for naproxen sodium fast and medium sustained release tablet

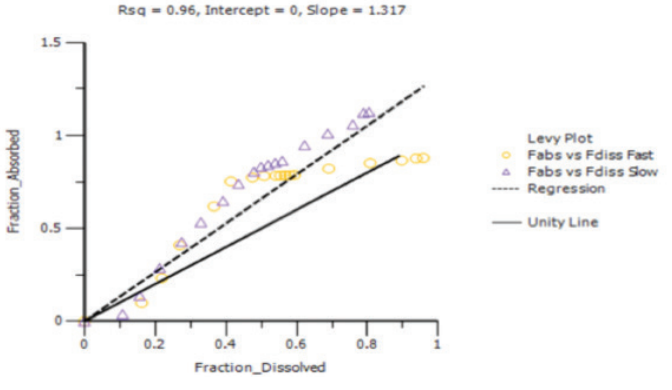

Figure 10. *In vitro-in vivo* correlation model linear regression percentage dissolved and percentage absorbed for naproxen sodium fast and slow sustained release tablet

IVIVC validation

The internal validation of the IVIVC was examined by using the mean *in vitro* dissolution data and mean *in vivo* pharmacokinetics of the naproxen sodium sustained release tablets (i.e. slow, medium fast) corresponds to fast/medium/slow SR tablets. Each of IVIVC model predicted naproxen sodium plasma concentration versus time profiles were compared to the experimental data using prediction error metrics. The observed plasma concentration of naproxen sodium sustained release tablets (i.e. slow, medium and fast) are presented in the Figure 11-13, good correlation found between the observed and predicted plasma concentration.

Internal validation

The validity of correlation assessed by determining how well the IVIVC model predict the rate and extent of naproxen sodium as characterized by C_{max} (maximum plasma concentration) and AUC (area under the plasma concentration-time curve from time zero to the time of the last quantifiable concentration). The prediction error estimated by using naproxen sodium slow SR tablets as a target formulation refer the Table 3. C_{max} and AUC were found close to the mean values. The prediction error estimated by using naproxen sodium fast sustained release tablets as a target formulation refer the Table 4. C_{max} and AUC were found close to the mean values. The prediction error estimated by using naproxen sodium medium sustained release tablets as a target formulation refer the Table 5. C_{mavx} and AUC were found close to the mean values. As per the FDA for IVIVC the average absolute prediction error should be 10% and in addition individual formulation should not exceed 15%. In the present study relatively low prediction error for C_{max} and AUC observed strongly suggest that the naproxen sodium IVIVC models are valid. Cross validation between the naproxen sodium sustained release tablets showed well within

Table 3. Prediction errors (%) associated with C_{max} and AUC for naproxen sodium fast vs. slow sustained release tablets

Formulation	Parameter	PE%
Fast	AUC	4.852
Fast	C_{max}	-21.187
Medium	AUC	0.794
Medium	C_{max}	-26.879
Slow	AUC	-5.643
Slow	C_{max}	-33.069

AUC: Area under the curve, PE: Prediction errors

the acceptance limits and provides the self confidence to next stage of validation.

External validation

IVIVC for naproxen sodium immediate release tablet was used as a target formulation to predict the plasma concentration of naproxen sodium sustained release tablets (i.e. slow, medium and fast). Figure 14-16 shows the plasma concentration versus time of predicted formulation (immediate release tablet) with naproxen sodium fast, medium and slow SR tablet. The predicted curve for the naproxen sodium SR tablets (i.e. slow, medium and fast) are identical to immediate release tablet and considered model is valid.

Table 4. Prediction errors (%) associated with C_{max} and AUC for naproxen sodium fast vs. medium sustained release tablets

Formulation	Parameter	PE%
Fast	AUC	-18.760
Fast	C_{max}	-35.896
Medium	AUC	14.180
Medium	C_{max}	-40.250
Slow	AUC	6.8779
Slow	C_{max}	-44.696

AUC: Area under the curve, PE: Prediction errors

Table 5. Prediction errors (%) associated with C_{max} and AUC for naproxen sodium medium vs. slow sustained release tablets

Formulation	Parameter	PE%
Fast	AUC	-5.852
Fast	C_{max}	-31.281
Medium	AUC	-9.495
Medium	C_{max}	-35.501
Slow	AUC	-15.271
Slow	C_{max}	-39.791

AUC: Area under the curve, PE: Prediction errors

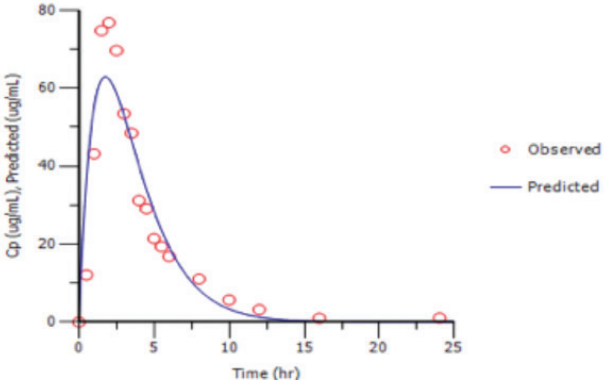

Figure 11. Observed and predicted plasma concentration for naproxen sodium fast sustained release tablet

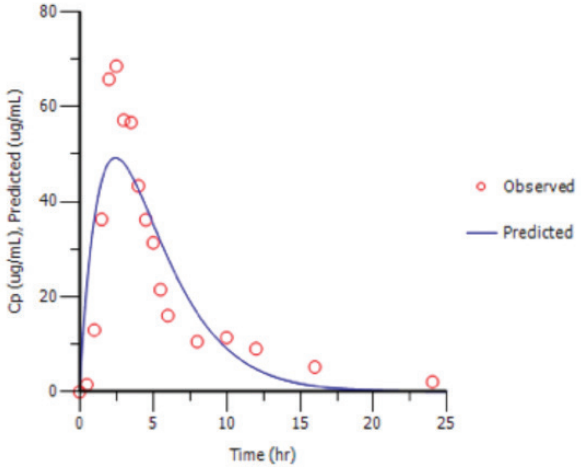

Figure 12. Observed and predicted plasma concentration for naproxen sodium medium sustained release tablet

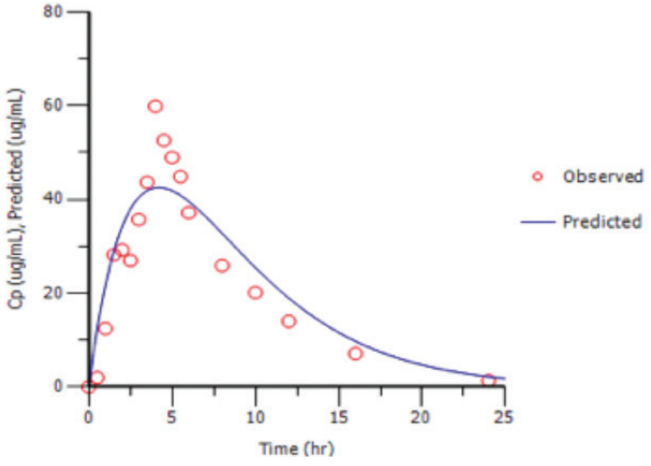

Figure 13. Observed and predicted plasma concentration for naproxen sodium slow sustained release tablet

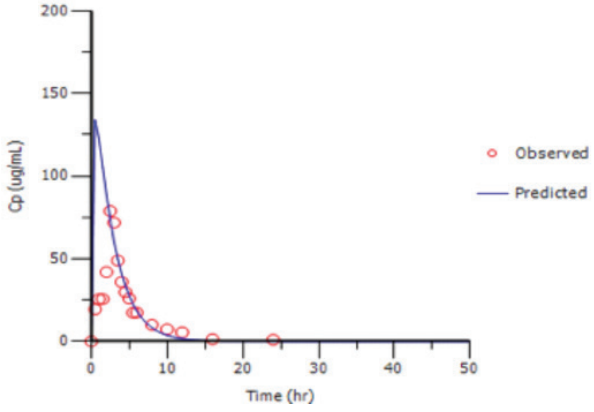

Figure 14. Plot of plasma concentration versus time of predicted formulation with naproxen sodium fast sustained release tablet

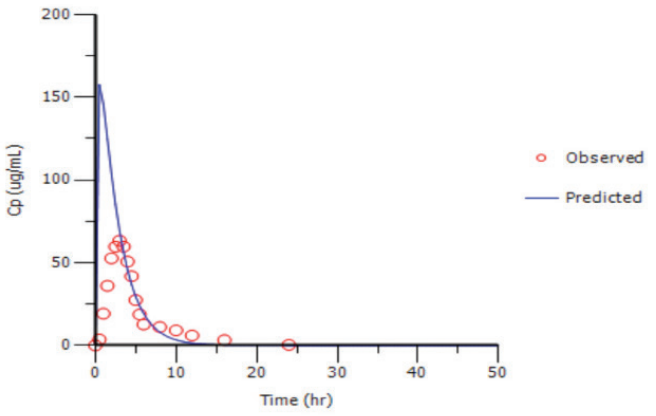

Figure 15. Plot of plasma concentration versus time of predicted formulation with naproxen sodium slow sustained release tablet

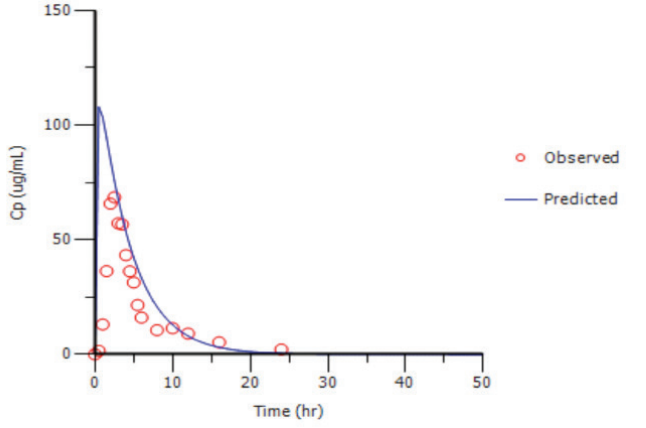

Figure 16. Plot of plasma concentration versus time of predicted formulation with naproxen sodium medium sustained release tablet

CONCLUSION

This study established and validated the internal and external predictability of an IVIVC relationship for naproxen sodium formulation. Meaningful relationship was observed between the *in vitro* and *in vivo* parameters, thus indicates an exceptional IVIVC model for naproxen sodium SR tablets (i.e. slow, medium and fast). The resulted prediction errors are within the acceptance limit as per the USFDA guidelines for both C_{max} and AUC. It can support dissolution data to predict the *in vivo* absorption, act as a biowaiver for bioequivalence and bioavailability studies and serve as a model for evaluating the naproxen sodium sustained release formulation. It can supports and validates the use of dissolution methods and specification settings, assisting in quality control which will be supportive for SUPAC.

ACKNOWLEDGEMENTS

The authors gratefully acknowledge administration of Srinivas College of Pharmacy, SeQuent Research Limited & Strides Arcolab Ltd, Colorcon Asia Pvt Limited, India and Phoenix Winonlin Certara software Hyderabad, India for granting support to carry out the work.

Conflict of Interest: No conflict of interest was declared by the authors.

REFERENCES

1. De Haan P, Lerk CF. Oral controlled release dosage forms. A review. Pharm Weekbl Sci. 1984;6:57-67.
2. Rashid HO, Kabir AKL, Hossaina Z, Rouf ASS. Design and Formulation of Once Daily Naproxen Sustained Release Tablet Matrix from Methocel K 15M CR and Methocel K 100M CR. Iranian Journal of Pharmaceutical Sciences Autumn. 2009:5:215-224.
3. Yasmin D, Rahman R, Akter M. Formulation development of directly compressed Naproxen SR tablet using Kollidon SR and Avicel PH 102 polymer. International Current Pharmaceutical Journal. 2013;2:112-114.
4. Huntjens DR, Spalding DJ, Danhof M, Della Pasqua OE. Correlation between *in vitro* and *in vivo* concentration-effect relationships of naproxen in rats and healthy volunteers. Br J Pharmacol. 2006;148:396-404.
5. Extended Release Oral Dosage Forms: Development, Evaluation, and Application of I*n Vitro/In Vivo* Correlations. U.S. Department of Health and Human Services Food and Drug Administration Center for Drug Evaluation and Research (CDER) September 1997 BP 2. http://www.fda.gov/cder/guidance/index.htm.
6. Takka S, Sakr A, Goldberg A. Development and validation of an *in vitro-in vivo* correlation for buspirone hydrochloride extended release tablets. J Control Release. 2003;88:147-157.
7. Huang YB, Tsai YH, Yang WC, Chang JS, Wu PC, Takayama K. Once-daily propranolol extended-release tablet dosage form: formulation design and *in vitro/in vivo* investigation. Eur J Pharm Biopharm. 2004;58:607-614.
8. Macha S, Yong CL, Darrington T, Davis MS, MacGregor TR, Castles M, Krill SL. *In vitro-in vivo* correlation for nevirapine extended release tablets. Biopharm Drug Dispos. 2009;30:542-550.
9. Edington ND, Marroum P, Uppoor R, Hussain A, Augsburger L. Development and internal validation of an *in vitro-in vivo* correlation for a hydrophilic metoprolol extended release tablet formulation. Pharm Res. 1998;15:466-473.
10. Sankalia JM, Sankalia MG, Mashru RC. Drug release and swelling kinetics of directly compressed glipizide sustained release matrices: establishment of level A IVIVC. J Control Release. 2008;129:49-58.
11. Dutta S, Qiu Y, Samara E, Cao G, Granneman GR. Once a day extended release dosage form of divalproex sodium III: development and validation of a level A *in vitro-in vivo* Correlation. J Pharm Sci. 2005;94:1949-1956.
12. Li ZQ, He X, Gao X, Xu YY, Wang YF, Gu H, Ji RF, Sun SJ. Study on dissolution and absorption of four dosage forms of isosorbide mononitrate: level A *in vitro-in vivo* correlation. Eur J Pharm Biopharm. 2011;79:364-371.
13. Frick A, Möller H, Wirbitzki E. Biopharmaceutical characterization of oral controlled modified-release drug products. *In vitro/in vivo* correlation of roxatidine. Eur J Pharm Biopharm. 1998;46:313-319.
14. Dalton JT, Straughn AB, Dickason DA, Grandolfi GP. Predictive ability of level A *in vitro-in vivo* correlation for ringcap controlled-release acetaminophen tablets. Pharm Res. 2001;18:1729-1734.
15. Qiu Y, Gupta P, Briskin J, Cheskin H, Semla S. Sustained-release multiparticulate formulations of Zileuton. I. *In vitro* and *in vivo* evaluation. Intional Journal of Pharmaceutics. 1996;143:179-185.
16. Qui Y, Cheskin H, Briskin J, Engh K. Sustained-release hydrophilic matrix tablets of zileuton: formulation and *in vitro/in vivo* studies. J Contrl Rel. 1997;45:249-256.
17. Mandal U, Ray KK, Gowda V, Ghosh A, Pal TK. *In-vitro* and *in-vivo* correlation for two gliclazide extended-release tablets. J Pharm Pharmacol. 2007;59:971-976.
18. Balan G, Timmins P, Greene DS, Marathe PH. *In-vitro in-vivo* correlation models for glibenclamide after administration of metformin/glibenclamide tablets to healthy human volunteers. J Pharm Pharmacol. 2000;52:831-838.

Turk J Pharm Sci 2017;14(2):127-133
DOI: 10.4274/tjps.85057

ORIGINAL ARTICLE

Subcutaneous Toxicity of Agmatine in Rats

Sıçanlarda Subkütan Agmatin Toksisitesi

Tayfun UZBAY[1]*, Fatma Duygu KAYA YERTUTANOL[1], Ahmet MİDİ[2], Burcu ÇEVRELİ[1]

[1]Üsküdar University, Neuropsychopharmacology Application and Research Center, (NPARC), İstanbul, Turkey
[2]Bahçeşehir University, Faculty of Medicine, Department of Pathology, İstanbul, Turkey

ABSTRACT

Objectives: The aim of this study was to investigate the effects of repetitive agmatine administration on sensorimotor gating in rats first but, as unexpected, ulcerative necrotic cutaneous lesions appeared, thus, the study was directed primarily to clarify these results.

Materials and Methods: In the first set of experiments, we administered agmatine (40, 80 and 160 mg/kg) and saline (control group) subcutaneously to male Wistar albino rats (n=8 for each group) for 14 consecutive days. Ulcerative necrotic cutaneous lesions appeared following the third day of agmatine administration. We decided to explore the potential toxic dermal effects of agmatine and conducted second set of experiments with two groups (n=8) to compare the effects of subcutaneous vs. intraperitoneal agmatine (80 mg/kg) injection to understand if the injection route determines the toxicity.

Results: Our results showed that prolonged subcutaneous but not intraperitoneal administration of agmatine leads to a delayed dermal reaction in rats. Histopathologic examination of skin samples revealed cutaneous aseptic necrosis at the injection site whereas blood tests were found to be normal.

Conclusion: This finding is important to point out the risks of prolonged subcutaneous administration of agmatine to rats within the concept of animal welfare. In addition, the results raise questions about the possible risks of over-the-counter use of agmatine among humans although the agent is taken via oral route.

Key words: Agmatine, skin reaction, subcutaneous route, toxicity, rat

ÖZ

Amaç: Bu çalışmanın amacı sıçanlarda ilk kez tekrarlayan agmatin uygulamasının sensorimotor kapılama sistemi üzerine etkilerini incelemekti, ancak subkütan uygulamada karşımıza çıkan beklenmedik ülseratif nekrotik lezyonlar bu konuya odaklanmamıza neden oldu.

Gereç ve Yöntemler: İlk grup deneylerde, erkek Wistar albino sıçanlara 14 gün süreyle subkütan yoldan agmatin (40, 80 ve 160 mg/kg) veya salin (kontrol grubu) enjeksiyonu yapıldı (n=8 her bir grup). Uygulamaların üçüncü gününden itibaren agmatin verilen gruplarda ülseratif nekrotik deri lezyonları gözlendi. Bu etkilerin dermal bir reaksiyona bağlı olup olmadığını anlamak için ayrı bir denek grubuna aynı protokolle agmatin (80 mg/kg) intraperitoneal yoldan verildi (n=8 her bir grup).

Bulgular: Bulgularımız subkütan yoldan verilen agmatinin geç dönemde ortaya çıkan bir dermal reaksiyona neden olurken, intraperitoneal uygulamanın böyle bir etki oluşturmadığına işaret etti. Lezyon gözlenen deneklerden alınan deri örneklerinin histopatolojik incelemesinde, enjeksiyon yerindeki deride aseptik nekroz saptanırken, bu deneklerin kan testleri normal bulundu.

Sonuç: Bu bulgu sıçanlarda uzun süreli subkütan agmatin uygulamasının denek refahı bakımından risk oluşturan toksik bir etkiye neden olduğuna işaret etmektedir. Bu bulgu insanlarda oral yoldan reçetesiz olarak alınabilen agmatinin bazı potansiyel riskleri olabileceği konusunda sorular ortaya çıkarmaktadır.

Anahtar kelimeler: Agmatin, deri reaksiyonu, subkütan yol, toksisite, sıçan

*Correspondence: **E-mail:** uzbayt@yahoo.com, **Phone:** +90 312 304 47 67
Received: 17.11.2016, **Accepted:** 02.02.2017

INTRODUCTION

Agmatine is a polyamine that is produced through decarboxylation of L-arginine by the enzyme arginine decarboxylase. It interacts to various receptors and has been accepted as a new neurotransmitter in brain. In experimental studies, agmatine exhibited neuroprotective, anticonvulsant, antinociceptive, anxiolytic and antidepressant-like actions in central nervous system (CNS). It also generates some favorable effects on cerebral damages and withdrawal syndromes involved in addictive drugs.[1-6]

Agmatine binds α2-adrenoceptors and imidazoline receptors and blocks ligand-gated cation channels like cholinergic, nicotinic, serotonergic and NMDA receptors.[6] One of the important psychiatric disorders is schizophrenia. Schizophrenia is a severe mental disorder regarding impairment of sensorimotor gating system.[7] In some studies, a single dose of 160 mg/kg agmatine by ip route was found to disrupt the prepulse inhibition (PPI) of acoustic startle reflex in rats.[8] Disruption of PPI is related to sensorimotor gating deficits. In addition, plasma levels of agmatine in patients with schizophrenia were found to be almost three-fold elevated compared to healthy subjects.[9] Because PPI is an available tool for sensorimotor gating deficits, agmatine may have some toxic effects on sensorimotor system which is not proven yet.

Although various studies on experimental animals indicated that agmatine has some beneficial pharmacological effects[5,6] several polyamines such as putresin, spermine and spermidine which are also metabolites of agmatine elicit some toxic effects in both animals and human.[10-16] It is well-known that fermented foods contain high levels of polyamines such as cheese, fermented fish and meat, wine, beer, and fermented vegetables and some non-fermented foods such as fish, meat, fruits, juices, and vegetables have a considerable amount of polyamines.[17] Some bioamines are also considered as an indicator of microbial contamination in foods.[18] Agmatine which is produced especially during the fermentation of alcohol (wine and beer in particular) is known to increase the histamine toxicity in humans.[18-20]

Although polyamines may have possible toxic effects, some polyamines such as agmatine is used as over the counter medications or dietary supplement products. Agmatine has been used as a dietary supplement for promoting the functions of both the peripheral and CNS.[21-23] There are several agmatine containing commercial products that are marketed as nutraceuticals.

In our laboratory, investigating the effects of repetitive (14 days) administration of different doses of agmatine on sensorimotor gating were decided in rats. After we started the test protocol with 160 mg/kg/day alternating intraperitoneal/subcutaneous injections of agmatine, we noticed severe skin lesions of rats after subcutaneous injections. These lesions appeared in all subjects at the second or third day of drug administration. The same lesions were also seen in other agmatine groups but not in the subjects of saline treated control group. In this context, we organized a second set of experiments to investigate this skin reaction in detail. Because this statement may have important public health relevance, the main goal of the present study if agmatine administration by subcutaneous route has some unpredictable harmful effects in rats. Here we report the injection site reaction (ISR) after subcutaneous administration of agmatine in rats and discuss the possible toxic effects of agmatine.

MATERIALS AND METHODS

Animals and laboratory conditions

In this study, adult male Wistar albino rats were used as the test animals. The animals were obtained from Üsküdar University Experimental Research Unit (ÜSKÜDAB, İstanbul, Turkey). All experiments were performed in Neuropsychopharmacology Application and Research Center of Üsküdar University. Animals were kept under controlled conditions (temperature, 22±2˚C; humidity, 50±5%; and a 12 h light/dark cycle, lights on from 07:00 to 19:00 h). The animals had free access to tap water and standardized pellet food throughout the procedures. All experiments were performed at the same time of day and during the light period. All the experiments were conducted according to the ethical rules in Helsinki Declaration and Guide for the Care and Use of Laboratory Animals as adopted by the National Institutes of Health, USA, which was published and released in 1996. In addition, this study was approved by the Local Ethic Committee of the Üsküdar University on 20.10.2015 with a decision number 2015-07. The ethical permissions included in additional tests.

Study protocol

The test animals assigned into several groups randomly (n=8 for each group). The study had two sets of experiments that began with four groups (Table 1). Agmatine sulfate (Sigma Chemicals Co, USA) was dissolved in 1 mL saline and administered 160, 80 and 40 mg/kg/day to animals for 14 consecutive days in two times a day. In order to prevent the risk of peritonitis, the drug was injected intraperitoneally in the morning and subcutaneously in the evening. Saline was injected as a vehicle two times a day to the control group. At the third day of agmatine treatments, skin lesions were appeared almost in all animals.

After 14 days of agmatine administration, all animals were decapitated under anesthesia (xylazine plus ketamine) and both blood samples and skin biopsies were collected. Complete blood count, renal and liver function tests were performed to assess metabolic function. The skin biopsies were evaluated by an experienced pathologist.

After the experiments were terminated, second set experiments were performed with two new groups of animals (n=8 for each group) to determine whether the lesions were related to the route of administration of agmatine. Agmatine 80 mg/kg/day was given intraperitoneally to one group and subcutaneously to the second group for one week. Post-mortem examination of the abdominal cavity and organs following the termination of experiments revealed any obvious abnormalities. Saline

injections were done by the same routes of agmatine in all experiments.

RESULTS

Skin lesions

At the second or third day after the initiation of injections, most of the dorsal skin of the animals of agmatine 160 mg/kg/day group was observed to turn black without any hair loss. One or two days after this observation, annular hemorrhagic ulcerative lesions appeared on the dorsal skin with prominent hair loss over it. The lesion sites were limited to injections sites and around. All animals had one or more lesions with diameter of 1.5 cm to 2.5 cm (Table 1). During the 14 days period, old lesions healed with crust formation resulting hair loss over it but new lesions continue to emerge with ongoing drug administration. Only 6 animals in the agmatine 80 mg/kg/day group showed similar lesions with diameter of 1 cm to 2 cm (Table 1). On the other hand, similar lesions within the same range of diameters were observed in the 5 animals of the agmatine 40 mg/kg/day group (Table 1). There were no skin lesions in the saline treated group. The general health of all animals was good and vital signs were between normal ranges.

In the second set of experiments, no skin lesions were observed in the animals of intraperitoneal agmatine 80 mg/kg/day treated group. On the other hand, all animals of the subcutaneous agmatine 80 mg/kg/day treated group developed the similar skin lesions with a diameter of 1.5-2.5 cm on the second day which continue to progress and the number of the lesions were between one and three (Table 1). A skin lesion at the fifth day of agmatine administration is shown in Figure 1. These experiments revealed that subcutaneous administration of agmatine may have toxic effects on rats.

Blood tests

There were no prominent differences between control and agmatine groups in terms of complete blood count, C-reactive protein, renal and liver function tests (for liver and kidney function test results see Table 2). Blood tests were not performed during second set of experiments.

Biopsies

In half of the cases, there were changes secondary to bacterial infection (purulent exudate collection, bacteria cluster, prominent dermal edema and neutrophil infiltration). These changes were also present in subcutaneous tissue. Non-complicated cases showed subcutaneous vascular thrombosis, epidermal and dermal necrosis, hyalinization in the dermal collagen, mild perivascular lymphocyte infiltration, and basal epidermal separation in the epithelia that located around the ulcer (Figure 2). The histopathologic examination of lesions was compatible with injection site cutaneous aseptic necrosis.

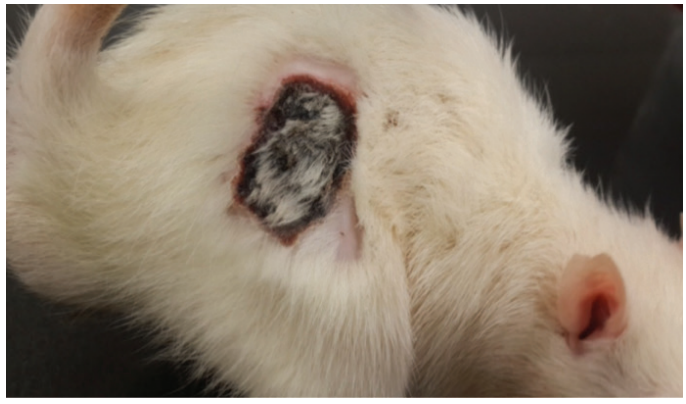

Figure 1. A lesion at the back skin of a subject in group 5

Table 1. Summary of study protocol

Experiments	Groups n=8	Agent	Total Dose	Total given volume*	Route	Duration (days)	Animals with skin reactions (n)	Number of skin lesions (n)	Lesion size (cm)	Blood tests	Biopsies
First set of experiments	1	Agmatine	160 mg/kg/day	1 mL/day	Alternate i.p./s.c.**	14	8	1 or 2	1.5-2.5	+	+
	2	Agmatine	80 mg/kg/day	1 mL/day	Alternate i.p./s.c.	14	6	1 or 2	1-2	+	+
	3	Agmatine	40 mg/kg/day	1 mL/day	Alternate i.p./s.c.	14	5	1	1-2	+	+
	4	Saline	-	1 mL/day	Alternate i.p./s.c.	14	-	-	-	+	-
Second set of experiments	5	Agmatine	80 mg/kg/day	1 mL/day	s.c.	7	8	1 or 3	1.5-2.5	-	-
	6	Agmatine	80 mg/kg/day	1 mL/day	i.p.	7	-	-	-	-	-

*Agmatine was dissolved in saline and given as 0.5 mL solution to subjects two times a day.
**ip.: Intraperitoneal; s.c.: Subcutaneous

Table 2. Liver and kidney function test results of rats

Group	Rat	AST U/L	ALT U/L	BUN mg/dL	Creatinine mg/dL
1	1	156.6	69.3	11.8	0.2
	2	180.1	61.5	13.6	0.2
Agmatine	3	236.5	83.9	13.3	0.2
160 mg/kg/day	4	181.5	61.8	13.4	0.2
	5	156.6	67.9	12.1	0.2
	6	146.0	47.7	12.0	0.2
	7	211.7	124.9	14.2	0.2
	8	239.5	82.6	12.1	0.2
2	1	118.3	79.8	19.1	0.2
	2	134.6	81.5	16.8	0.2
Agmatine	3	142.2	97.8	20.0	0.3
80 mg/kg/day	4	114.6	89.9	17.2	0.2
	5	116.5	87.1	16.2	0.2
	6	130.8	81.6	16.4	0.2
	7	111.5	69.5	16.8	0.2
	8	111.7	92.3	18.5	0.3
3	1	109.3	68.1	19.4	0.3
	2	141.0	75.0	20.8	0.3
Agmatine	3	108.6	76.1	17.8	0.2
40 mg/kg/day	4	113.7	81.1	17.0	0.3
	5	108.0	75.6	22.1	0.3
	6	129.7	71.6	19.8	0.2
	7	131.2	98.9	23.1	0.2
	8	131.4	82.4	19.6	0.3
4	1	241.6	74.3	18.8	0.5
	2	226.8	60.4	14.9	0.2
Saline	3	142.7	60.0	14.7	0.2
	4	321.3	96.7	18.9	0.3
	5	187.3	68.5	19.6	0.5
	6	142.0	69.5	16.2	0.3
	7	178.7	64.4	14.8	0.2
	8	219.9	62.7	14.8	0.3

AST: Aspartate aminotransferase; ALT: Alanine aminotransferase; BUN: Blood urea nitrogen

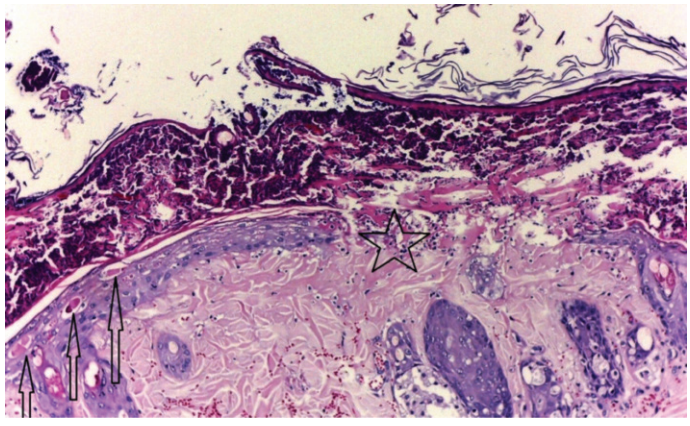

Figure 2. Splitting at the dermoepidermal junction in epidermis, purulent exudate on surface with neutrophil infiltration, necrotic cells in epidermis (an arrow), epidermal necrosis and ulcer with fibrinopurulent exudate (indicated with a star), dermal collagen hyalinization, hemorrhage in dermis in 160 mg/kg/day agmatine group (hematoxylin and eosin stain x100)

DISCUSSION

Our results clearly showed that subcutaneous agmatine administration to rats caused a serious skin reaction with prominent lesions. This is the first observation reported in literature that demonstrates the toxic effects of repetitive agmatine administration to rats. This unexpected and harmful effect of agmatine seems to be related to the route of administration due to the lack of similar observation by intraperitoneal route. In addition, we detected multiple lesions with cutaneous and subcutaneous changes by histopathological methods, thus this unexpected effect seems to be a regular ISR.

Polyamines are positively charged molecules that are prevalent among living organisms and derived from ornithine, methionine, arginine and lysine.[24] They bind to several negatively charged molecules in cells to conduct vital processes. They have various roles in cell function as cell growth and proliferation, regulation of ion channels, protein and nucleic acid synthesis, regulation of gene expression, protection of cell components and anti-oxidative effects.[25-30] On the other hand, polyamine levels are under critical control to prevent its potential toxic effects. It is indicated that beside direct effects of excess polyamine levels, some reactive aldehydes and reactive oxygen species that are produced with the catabolism of polyamines may also lead to toxicity.[31] In a tissue culture study, it was shown that accumulation of polyamines may result in an apoptotic process where hydrogen peroxide is overproduced.[32] The neurotoxicity, nephrotoxicity, hepatotoxicity, inflammatory effects can occur because of polyamine oxidation.[31]

Agmatine, a polyamine, is a widely-used workout supplement especially among body builders. The use of agmatine as an ergogenic aid is based on its nitric oxide modulating, cardio protective and hypoglycemic effects.[33,34] Beside this, it was reported that agmatine has potentiating effect on morphine-induced analgesia in mice.[3] Therefore, analgesic features of agmatine which encourage people to push the sports limits made this polyamine very popular among athletes. The agmatine sulfate powders or pills generally contain 250-750 mg agmatine sulfate per serving where daily intake can be up to 7500 mg/day.[35] There are limited studies or case reports which stated that long-term agmatine use is safe in humans.[23,35] In one case, a daily dose of 2.67 g oral agmatine sulfate for 5 years was reported to be safe without evidence of any adverse effects. The authors indicated that the periodic physical examinations and laboratory analyses revealed no adverse reactions.[23] In another randomized, double-blind, placebo-controlled clinical study including patients with lumbar disc-associated radiculopathy, the same dose of oral agmatine (2.67 g) were given for 14 days. In this study, only three patients had mild-to-moderate diarrhea and nausea as adverse effects.[35] On the other hand, limited animal studies also introduced evidence about the safety of agmatine.[36] In an animal study, oral agmatine sulfate administration with a daily dose of 100 mg/kg/day of adult Wistar albino rats for 95 days was reported to be also safe.[36] In other two studies performed on Sprague-Dawley rats agmatine sulfate were administrated at 40 mg/kg dose intraperitoneally as once daily injections for 42 and 17 consecutive days. No

skin lesions were reported.[37,38] From the available evidence, it appears that oral and intraperitoneal administration of agmatine does not lead to a major toxicity in rodents and human beings.

On the contrary, we observed severe skin lesions with agmatine administration in rats. Adverse cutaneous drug reactions are skin and/or mucosa reactions with various morphologies which are triggered with systemic administration of drugs in appropriate doses. These reactions may be classified as non-immunologic and immunologic drug reactions. Non-immunologic drug reactions have not immunologic processes and sensitization is not required for this kind of reactions.[39,40] However immunologic drug reactions have type 1, type 2, type 3 or type 4 immunologic processes in sensitive individuals.[39] The adverse drug reactions triggered with subcutaneous administration of drugs are called ISRs. These may include mild reactions like erythema and induration or may progress to ulcerations as in our study. The possible immune reaction that underlies the ISR is type IV (delayed) hypersensitivity which is mediated by antigen-specific effector T cells and becomes apparent 48-72 h after antigen exposure.[41] Although immuno-histochemical analysis was not performed, delayed onset of lesions (48-72 hours after administration of agmatine) and histopathologic results suggest that this process could be associated with type 4 hypersensitivity reaction.

Delayed hypersensitivity reactions of skin are often induced by dermal or intradermal exposure to small lipophilic chemicals (haptens) with a molecular weight less than 500 Daltons.[42] Haptens are molecules that can not elicit an immune response due to their small molecular weight often less than 1 kDa and need to bind to a protein to become antigenic.[41] Probably agmatine sulfate served as a hapten with its small molecular weight (228 Da) and lipophilic structure and bind to the dermal proteins to form neoantigens. Although the sensitizing potential of a hapten can not be reliably determined by its chemical structure, it was shown that most haptens react with amine (NH_2) or thiol (SH) groups of skin proteins.[43] Another possible mechanism can be the metabolization of the potential haptens to reactive metabolites by cutaneous enzymes, however agmatine metabolizing enzymes are absent in cutaneous tissue. Also, one can point out the potential toxic effect of sulfate component of agmatine, but there are several well-known drugs that are used safely via subcutaneous injection such as morphine sulfate and heparine sulfate in humans. To our knowledge, the repeated subcutaneous administration of sulfate containing agents to rodents seem to be harmless to the skin or other tissues of the subjects.[44,45] Hence we assume that sulfate component doesn't seem to be responsible for mentioned skin lesions in this study.

Because lower doses of agmatine were related to a less number of injured rats, the harmful effect of agmatine observing in our study seems to be dose dependent. Thus, we did not test lower doses of agmatine than 40 mg/kg in the present study. Because all our subjects in the 160 mg/kg/day ip/sc agmatine treated group and 80 mg/kg/day sc agmatine treated group developed similar skin lesions, we claim that agmatine act as a potent hapten in cutaneous/subcutaneous tissue. There are some drugs which may lead to ISRs in human like HIV-1 fusion inhibitor enfuvirtide, interferons, anti-TNF drugs adalimumab and etanercept.[46-49] Most of these ISRs are mild as erythema and self-limited, whereas necrotic ulcerative lesions of skin are rare. There are human cases of cutaneous necrotic ulcers related with subcutaneous administration of polyethylene-glycol modified (pegylated) interferon-a-2b,[50,51] interferon beta-1b,[52] and enoxaparine sodium.[53] Nevertheless, the overall rate of skin ulcers among ISRs is relatively rare. On the other hand, agmatine administration elicited severe lesions in a dose-dependent manner in most of the animals in our study, which may be specific to rats for sure. The lack of immuno-histochemical evaluation of skin samples is the major limitation of this study. Even so, this study is important because although agmatine is reported to be safe in mammals, we showed its potential toxic effects in rats when administrated subcutaneously.

CONCLUSION

In conclusion, our results suggest that subcutaneous injection of agmatine cause harmful skin reaction in rats. As subcutaneous administration is one of the commonly used delivery routes among animals, researchers should be cautious with this route while using agmatine. Further research is needed to reveal the underlying mechanism of agmatine related cutaneous/subcutaneous toxicity via using immunohistochemical methods. Although this study doesn't provide any data related to the potential toxicity of agmatine among humans and agmatine is commonly used via oral route, we suggest that health professional need to be attentive to possible uncommon routes of administration of agmatine.

ACKNOWLEDGEMENTS

This study has been partially supported by Scientific and Technological Research Council of Turkey (TUBITAK) (Project No: SBAG - 110S344). We also thank our colleague İlknur Bozkurt M.D. from NP-İstanbul Neuropsychiatry Hospital who provided biochemistry analysis of the blood samples of the rats.

Conflict of Interest: No conflict of interest was declared by the authors.

REFERENCES

1. Cabella C, Gardini G, Corpillo D, Testore G, Bedino S, Solinas SP, Cravanzola C, Vargiu C, Grillo MA, Colombatto S. Transport and metabolism of agmatine in rat hepatocyte cultures. Eur J Biochem. 2001;268:940-947.
2. Gilad GM, Salame K, Rabey JM, Gilad VH. Agmatine treatment is neuroprotective in rodent brain injury models. Life Sci. 1995;58:41-46.
3. Yesilyurt O, Uzbay IT. Agmatine potentiates the analgesic effect of morphine by an α2-adrenoceptor-mediated mechanism in mice. Neuropsychopharmacology. 2001;25:98-103.
4. Zomkowski AD, Hammes L, Lin J, Calixto JB, Santos AR, Rodrigues AL. Agmatine produces antidepressant-like effects in two models of depression in mice. Neuroreport. 2002;13:387-391.
5. Uzbay T. A new target for diagnosis and treatment of CNS disorders: agmatinergic system. Curr Med Chem. 2012;19:5116-5121.

6. Uzbay T. The pharmacological importance of agmatine in the brain. Neurosci Biobehav Rev. 2012;36:502-519.
7. Geyer MA, Krebs-Thomson K, Braff DL, Swerdlow NR. Pharmacological studies of prepulse inhibition models of sensorimotor gating deficits in schizophrenia: a decade in review. Psychopharmacology. 2001;156:117-154.
8. Uzbay T, Kayir H, Goktalay G, Yildirim M. Agmatine disrupts prepulse inhibition of acoustic startle reflex in rats. J Psychopharmacol. 2010;24:923-929.
9. Uzbay T, Goktalay G, Kayir H, Eker SS, Sarandol A, Oral S, Buyukuysal L, Ulusoy G, Kirli S. Increased plasma agmatine levels in patients with schizophrenia. J Psychiatr Res. 2013;47:1054-1060.
10. Tabor CW, Rosenthal SM. Pharmacology of spermine and spermidine; some effects on animals and bacteria. J Pharmacol Exp Ther. 1956;116:139-155.
11. De Vera N, Serratosa J, Artigas F, Martínez E. Toxic effects of putrescine in rat brain: Polyamines can be involved in the action of excitotoxins. Amino Acids. 1992;3:261-269.
12. Creaven PJ, Perez R, Pendyala L, Meropol NJ, Loewen G, Levine E, Berghorn E, Raghavan D. Unusual central nervous system toxicity in a phase I study of N1N11 diethylnorspermine in patients with advanced malignancy. Invest New Drugs. 1997;15:227-234.
13. Ray RM, Viar MJ, Yuan Q, Johnson LR. Polyamine depletion delays apoptosis of rat intestinal epithelial cells. Am J Physiol Cell Physiol. 2000;278:480-489.
14. Sharmin S, Sakata K, Kashiwagi K, Ueda S, Iwasaki S, Shirahata A, Igarashi K. Polyamine cytotoxicity in the presence of bovine serum amine oxidase. Biochem Biophys Res Commun. 2001;282:228-235.
15. Wilding G, King D, Tutsch K, Pomplun M, Feierabend C, Alberti D, Arzoomanian R. Phase I trial of the polyamine analog N1, N14-diethylhomospermine (DEHSPM) in patients with advanced solid tumors. Invest New Drugs. 2004;22:131-138.
16. Wunderlichová L, Buňková L, Koutný M, Jančová P, Buňka F. Formation, degradation, and detoxification of putrescine by foodborne bacteria: a review. Compr Rev Food Sci Food Safety. 2014;13:1012-1030.
17. Silla Santos MH. Biogenic amines: their importance in foods. Int J Food Microbiol. 1996;29:213-231.
18. Halász A, Baráth Á, Holzapfel WH. The biogenic amine content of beer; the effect of barley, malting and brewing on amine concentration. Z Lebensm Unters F A. 1999;208:418-423.
19. Ibe A, Saito K, Nakazato M, Kikuchi Y, Fujinuma K, Nishima T. Quantitative determination of amines in wine by liquid chromatography. J Assoc Anal Chem. 1990;74:695-698.
20. Galgano F, Caruso M, Favati F, Romano P. HPLC determination of agmatine and other amines in wine. J Int Sci Vigne Vin (France). 2003;37:237-242.
21. Berenholz L, Segal S, Gilad VH, Klein C, Yehezkeli E, Eviatar E, Kessler A, Gilad GM. Agmatine treatment and vein graft reconstruction enhance recovery after experimental facial nerve injury. J Peripher Nerv Syst. 2005;10:319-328.
22. Halaris A, Plietz J. Agmatine: metabolic pathway and spectrum of activity in brain. CNS Drugs. 2007;21:885-900.
23. Gilad GM, Gilad VH. Long-term (5 years), high daily dosage of dietary agmatine evidence of safety: a case report. J Med Food. 2014;17:1256-1259.
24. Miller-Fleming L, Olin-Sandoval V, Campbell K, Ralser M. Remaining mysteries of molecular biology: The role of polyamines in the cell. J Mol Biol. 2015;427:3389-3406.
25. Williams K. Interactions of polyamines with ion channels. Biochem J. 1997;325:289-297.
26. Bettuzzi S, Davalli P, Astancolle S, Pinna C, Roncaglia R, Boraldi F, Tiozzo R, Sharrard M, Corti A. Coordinate changes of polyamine metabolism regulatory proteins during the cell cycle of normal human dermal fibroblasts. FEBS Lett. 1999;446:18-22.
27. Davidson NE, Hahm HA, McCloskey DE, Woster PM, Casero RA Jr. Clinical aspects of cell death in breast cancer: the polyamine pathway as a new target for treatment. Endocr Relat Cancer. 1999;6:69-73.
28. Tabib A, Bachrach U. Role of polyamines in mediating malignant transformation and oncogene expression. Int J Biochem Cell Biol. 1999;31:1289-1295.
29. Hou MH, Lin SB, Yuann JM, Lin WC, Wang AH, Kan Ls L. Effects of polyamines on the thermal stability and formation kinetics of DNA duplexes with abnormal structure. Nucleic Acids Res. 2001;29:5121-5128.
30. Kaur-Sawhney R, Tiburcio AF, Altabella T, Galston AW. Polyamines in plants: an overview. J Cell Mol Biol. 2003;2:1-12.
31. Pegg AE. Toxicity of polyamines and their metabolic products. Chem Res Toxicol. 2013;26:1782-1800.
32. Zou T, Rao JN, Liu L, Xiao L, Cui YH, Jiang Z, Ouyang M, Donahue JM, Wang JY. Polyamines inhibit the assembly of stress granules in normal intestinal epithelial cells regulating apoptosis. Am J Physiol Cell Physiol. 2012;303:102-111.
33. Raasch W, Schäfer U, Qadri F, Dominiak P. Agmatine, an endogenous ligand at imidazoline binding sites, does not antagonize the clonidine–mediated blood pressure reaction. Br J Pharmacol. 2002;135:663-672.
34. Piletz JE, Aricioglu F, Cheng JT, Fairbanks CA, Gilad VH, Haenisch B, Halaris A, Hong S, Lee JE, Li J, Liu P, Molderings GJ, Rodrigues AL, Satriano J, Seong GJ, Wilcox G, Wu N, Gilad GM. Agmatine: clinical applications after 100 years in translation. Drug Discov Today. 2013;18:880-893.
35. Keynan O, Mirovsky Y, Dekel S, Gilad VH, Gilad GM. Safety and efficacy of dietary agmatine sulfate in lumbar disc-associated radiculopathy. An open-label, dose-escalating study followed by a randomized, double-blind, placebo-controlled trial. Pain Med. 2010;11:356-368.
36. Gilad GM, Gilad VH. Evidence for oral agmatine sulfate safety a 95-day high dosage pilot study with rats. Food Chem Toxicol. 2013;62:758-762.
37. Rushaidhi M, Collie ND, Zhang H, Liu P. Agmatine selectively improves behavioural function in aged male Sprague-Dawley rats. Neuroscience. 2012;218:206-215.
38. Rushaidhi M, Zhang H, Liu P. Effects of prolonged agmatine treatment in aged male Sprague-Dawley rats. Neuroscience. 2013;234:116-124.
39. Shimizu H. Shimizu's Textbook of Dermatology. 1st ed. Hokkaido-Japan: Hokkaido University Press, Nakayama Shoten, 2007.
40. Nayak S, Acharjya B. Adverse cutaneous drug reaction. Indian J Dermatol. 2008;53:2-8.
41. Adam J, Pichler WJ, Yerly D. Delayed drug hypersensitivity: models of T-cell stimulation. Br J Clin Pharmacol. 2011;71:701-707.
42. Dearman RJ, Kimber I. Factors influencing the induction phase of skin sensitization. Am J Contact Dermat. 2003;14:188-194.

43. Alvarez-Sánchez R, Basketter D, Pease C, Lepoittevin JP. Studies of chemical selectivity of hapten, reactivity, and skin sensitization potency. 3. Synthesis and studies on the reactivity toward model nucleophiles of the 13C-labeled skin sensitizers, 5-chloro-2-methylisothiazol-3-one (MCI) and 2-methylisothiazol-3-one (MI). Chem Res Toxicol. 2003;16:627-636.

44. Alleva FR, Balazs T. Toxic effects of postnatal administration of streptomycin sulfate to rats. Toxicol Appl Pharmacol. 1978;45:855-859.

45. Habs M, Schmähl D. Carcinogenicity of bleomycin sulfate and peplomycin sulfate after repeated subcutaneous application to rats. Oncology. 1984;41:114-119.

46. Zeltser R, Valle L, Tanck C, Holyst MM, Ritchlin C, Gaspari AA. Clinical, histological, and immunophenotypic characteristics of injection site reactions associated with etanercept: a recombinant tumor necrosis factor alpha receptor: Fc fusion protein. Arch Dermatol. 2001;137:893-899.

47. Lalezari JP, Henry K, O'Hearn M, Montaner JS, Piliero PJ, Trottier B, Walmsley S, Cohen C, Kuritzkes DR, Eron JJ Jr, Chung J, DeMasi R, Donatacci L, Drobnes C, Delehanty J, Salgo M; TORO 1 Study Group. Enfuvirtide, an HIV-1 fusion inhibitor, for drug-resistant HIV infection in North and South America. N Engl J Med. 2003;348:2175-2185.

48. Dalmau J, Pimentel CL, Puig L, Peramiquel L, Roe E, Alomar A. Cutaneous necrosis after injection of polyethylene glycol-modified interferon alfa. J Am Acad Dermatol. 2005;53:62-66.

49. Bavbek S, Ataman Ş, Bankova L, Castells M. Injection site reaction to adalimumab: Positive skin test and successful rapid desensitisation. Allergol Immunopathol (Madr). 2013;41:204-206.

50. Kurzen H, Petzoldt D, Hartschuh W, Jappe U. Cutaneous necrosis after subcutaneous injection of polyethylene-glycol-modified interferon alpha. Acta Derm Venereol. 2002;82:310-312.

51. Rosina P, Girolomoni G. Cutaneous necrosis complicating the injection of pegylated interferon alpha-2b in a patient with chronic hepatitis C. Acta Dermatovenerol Croat. 2008;16:35-37.

52. Faghihi G, Basiri A, Pourazizi M, Abtahi-Naeini B, Saffaei A. Multiple cutaneous necrotic lesions associated with Interferon beta-1b injection for multiple sclerosis treatment: A case report and literature review. J Res Pharm Pract. 2015;4:99-103.

53. Issa AA, Simman R. Lovenox induced tissue necrosis, a case report and literature review. J Am Coll Clin Wound Spec. 2015;5:66-68.

Turk J Pharm Sci 2017;14(2):134-140
DOI: 10.4274/tjps.54227

ORIGINAL ARTICLE

Comparative Anatomical Studies on Three Endemic *Ononis* L. (*Leguminosae*) Species Growing in Turkey

Türkiye'de Yetişen Üç Endemik *Ononis* L. (*Leguminosae*) Türü Üzerinde Karşılaştırmalı Anatomik Çalışmalar

Ayşe BALDEMİR[1]*, Maksut COŞKUN[2]

[1]Erciyes University, Faculty of Pharmacy, Department of Pharmaceutical Botany, Kayseri, Turkey
[2]Ankara University, Faculty of Pharmacy, Department of Pharmaceutical Botany, Ankara, Turkey

ABSTRACT

Objectives: The leaf and stem anatomical characteristics of three endemic *Ononis* L. (*Leguminosae*) species were studied for the first time for the evaluated in terms of systematic of similarities and differences in these taxa.

Materials and Methods: *Ononis sessilifolia* Bornm., *Ononis basiadnata* Hub.-Mor. and *Ononis macrosperma* Hub.-Mor. were collected from different provinces of Turkey. In this anatomical study, transversal and superficial sections from the leaves and transversal sections from stems of the species were taken and examined by appropriate reagends. Illustrations were obtained by using an Olympus U-DA 2K 17149 drawing tube attached to an Olympus BX50 microscope. The microphotographs were taken by a Leica DM 4000 B microscope.

Results: *O. macrosperma* is bifacial leaf, the others are monofacial leaf. The leaf of *O. basiadnata* has eglandular trihomes. If the anatomical similarities between species are to be listed, *Rubiaceae* type stoma was observed in all three species and solitary crystals were found in stem and leaf sections.

Conclusion: Anatomical characteristics, such as mesophyll structure, transmission bundles and crystal structures, may contribute to the taxonomy of *Ononis* species for future work.

Key words: *Ononis*, leaf and stem anatomy, endemic, *Leguminosae*, Turkey

ÖZ

Amaç: Üç endemik *Ononis* L. (*Leguminosae*) türünün yaprak ve gövde anatomik özellikleri, bu taksonlarda benzerliklerin ve farklılıkların sistematik olarak değerlendirilmesi için ilk kez çalışılmıştır.

Gereç ve Yöntemler: *Ononis sessilifolia* Bornm., *Ononis basiadnata* Hub.-Mor. ve *Ononis macrosperma* Hub.-Mor. türleri Türkiye'nin farklı illerinden toplanmıştır. Bu anatomik çalışmada, türlerin gövdelerinden enine, yapraklardan ise enine ve yüzeysel alınmış ve uygun reaktiflerle incelenmiştir. Çizimler Olympus BX50 mikroskoba bağlı bir Olympus U-DA 2K 17149 çizim tüpü kullanılarak yapılmıştır. Mikrofotoğraflar Leica DM 4000 B mikroskobu ile çekilmiştir.

Bulgular: *O. macrosperma* bifasiyal yaprak, diğerleri monofasiyal yapraktır. *O. basiadnata*'nın yaprağı örtü tüyüne sahiptir. Türler arasındaki anatomik benzerlikler sıralanacak olursa, her üç türde *Rubiaceae* türü stoma ve gövde ve yaprak kesitlerinde ise tekli kristaller görülmüştür.

Sonuç: Mezofil yapısı, iletim demetleri ve kristal yapıları gibi anatomik özellikler, gelecekteki çalışmalar için *Ononis* türlerinin taksonomisine katkıda bulunabilir.

Anahtar kelimeler: *Ononis*, yaprak ve gövde anatomisi, endemik, *Leguminosae*, Türkiye

*Correspondence: **E-mail:** aysebaldemir@gmail.com, **Phone:** +90 352 207 66 66
ORCID ID: orcid.org/0000-0003-2473-4837
Received: 20.05.2016, **Accepted:** 02.02.2017

INTRODUCTION

Leguminosae, third largest family of flowering plants, is cosmopolitan family and absent only from Antarctica. Many species in this family are cultivated for food in the different regions of worldwide, such as beans, peas, peanuts, and soybean.[1,2] The genus *Ononis* L. belonging to the *Leguminosae* is represented by 75 taxa worldwide. The genus have 17 species of which 4 taxons are endemic in Turkey.[3-5] In different regions of our country, the species of *Ononis* are used in folk medicine to diuretic, antiseptic and antimicrobial effects.[6] In addition, the aerial part of *Ononis arvensis L.* has been used in traditional medicine to treat urinary tract infections and skin diseases. In the literature, there have been a few anatomical and morphological studies on some *Ononis* species.[7-12] Anatomical investigations are of great importance in the identification of medicinal plants.[13] Leaf epidermal studies are useful in determining their anatomical characteristics thus helping in the evaluation of a taxonomic relationship according to similarities and differences between species.[14]

In this study, the anatomical and morphological properties of three endemic *Ononis* species (*Ononis sessilifolia* Bornm., *Ononis basiadnata* Hub. - Mor. and *Ononis macrosperma* Hub. - Mor.) were studied comparatively. In addition, new and extended findings on three species of *Ononis* are presented in comparison with the definitions given in Metcalfe and Chalk[15] and anatomical structures of the other *Ononis* species.

EXPERIMENTAL

Plant materials

Plant materials were gathered from the localities indicated in Table 1. Voucher specimens are deposited in the Herbarium of the Faculty of Pharmacy at the University of Ankara, Turkey (AEF).

Table 1. Locations and herbarium numbers of the studied *Ononis* species

Species	Locations	Herbarium number
Ononis sessilifolia	C5 Niğde: Çamardı, Demirkazık, Narpızlı plateau, channel around, rocky slopes, s.l. 2073 m, 13.06.2007, Ayşe and Şükrü Baldemir	(AEF 23979)
Ononis basiadnata	C4 İçel: Gülnar-Mut road, exit of Gülnar, fields, among maquis, s.l. 1140 m. 08.06.2007, Ayşe and Şükrü Baldemir	(AEF 23968)
Ononis macrosperma	C2 Antalya: Elmalı, Çığlıkara, entrance of Sinekçibeli, rocky slopes, *Cedrus libani* forest, s.l. 1684 m. 29.5.2008, Ayşe and Şükrü Baldemir	(AEF 24698)

Anatomical studies

The microscopical studies were carried out on material (aerial parts of *Ononis* species) in 70% alcohol. Free hand sections were taken, stained and mounted in Sartur reagent[16] and chloralhydrate solution.

Anatomical drawings of the transversal and superficial sections were sketched using an Olympus U-DA 2K 17149 drawing tube attached to an Olympus BX50 microscope. The microphotographs were taken by a Leica DM 4000 B microscope and some of them were composed by the Adobe Photoshop 7.0 program.

RESULTS AND DISCUSSION

Anatomical studies

Leaf anatomy of O. sessilifolia

Cross section of leaf blade

The leaf is monofacial. The upper epidermis cells are square or rectangular-shaped, and are single-layered with anticlinal walls. Underneath the epidermis there are generally two layers of palisade parenchyma but sometimes there is a single-layer. The spongy parenchyma with 2-3 layers is formed of thin walled, isodiametric parenchymatous cells with few intercellular spaces. Glandular hairs with a multicellular stalk and a multicellular head are observed. The lower epidermis cells are covered with a thin cuticle. Stomata occur on both sides of the leaves (Figure 1).

Cross section of the midrib

The lower epidermis cells are smaller than the upper ones and are covered with a thin cuticle. Underneath the epidermis there are generally two layers of palisade parenchyma but sometimes there is a single-layer. Sclerenchyma cells generally form crescent-shaped groups surrounding phloem (the thin-walled irregular constellation of small cells) and the xylem (wider vessels and tracheids) is underneath it. Solitary crystals which are very variable in size and shape (styloids) are characteristically observed and frequently form a sheath along the outer boundary of the pericyclic sclerenchyma (Figure 1).

Surface of the lower and upper epidermis

The lower epidermal cells are similar to those in the upper epidermis in point of small rectangular shape and thin-walled structure. Rubiaceae type stomata (each stoma is surrounded by 2 or more subsidiary cells) have 3-4 subsidiary cells. There are glandular hairs on both the upper and lower epidermis (Figure 1).

Leaf anatomy of O. basiadnata

Cross section of leaf blade

The leaf is monofacial. The upper epidermis cells are rectangular-shaped, single-layered with thin anticlinal walls, and have a smooth cuticle. Similar to *O. sessilifolia*, underneath the epidermis there are generally two layers of palisade parenchyma but sometimes there is a single-layer. Spongy cells with 2-3 layers, thin walled and isodiametric

parenchymatous cells, are irregulary arranged. Glandular hairs is more dense with respect to *O. sessilifolia* can be classified into two types: those, with a multicellular stalk (1-4 row cells) and a multicellular glandular (1-5 row cells) head and those with a multicellular stalk and an unicellular glandular head. Also, eglandular hairs are observed densely (Figure 2).

Cross section of the midrib (the central vein of a leaf)

The lower epidermis cells are square or rectangular shape and thin walled structure, smaller than the upper ones and are covered with a thin cuticle. Sclerenchyma cells generally form crescent-shaped groups surrounding phloem which thin-walled irregular constellation of small cells and the xylem with vessels and tracheids is underneath it. Unlike *O. sessilifolia*, solitary crystals are also abundantly present in the parenchyma cells of *O. basiadnata* species. Similarly to *O. sessilifolia*, crystals are characteristically observed in the pericyclic sclerenchyma cells. Also, these crystals have been found in the mesophyll (Figure 2).

Surface of the lower and upper epidermis

Glandular and eglandular hairs are observed to densely cover both the upper and lower epidermis. The stomata have 3-4 subsidiary cells which is Rubiaceae type (Figure 2).

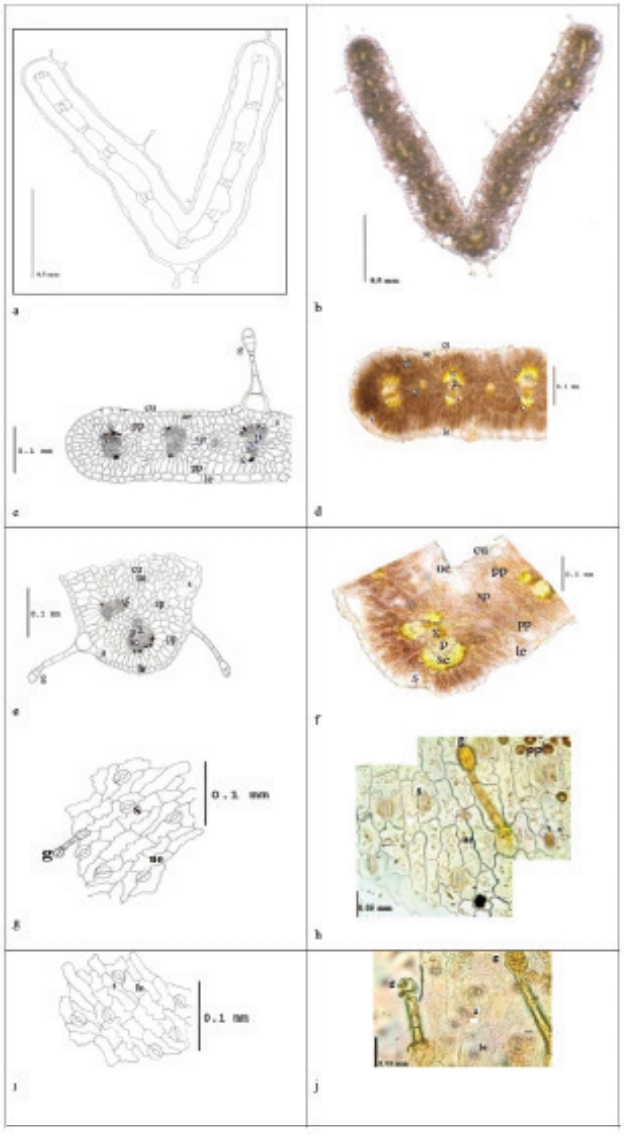

Figure 1. *O. sessilifolia*, a,b) Schematic drawing of the transverse section of the leaf and photo; c,d) Schematic drawing of transverse section of leaf blade and photo; e,f) Schematic drawing of transverse section of midrib and photo; g,h) Drawing of upper surface view of leaf and photo; ı,j) Drawing of lower surface view of leaf and photo

cu: Cuticle, g: Glandular hair, ue: Upper epidermis, c: Crystal, pp: Palisade parenchyma, sp: Spongy parenchyma, sc: Sclerenchyma, p: Phloem, x: Xylem, s: Stomata, le: Lower epidermis

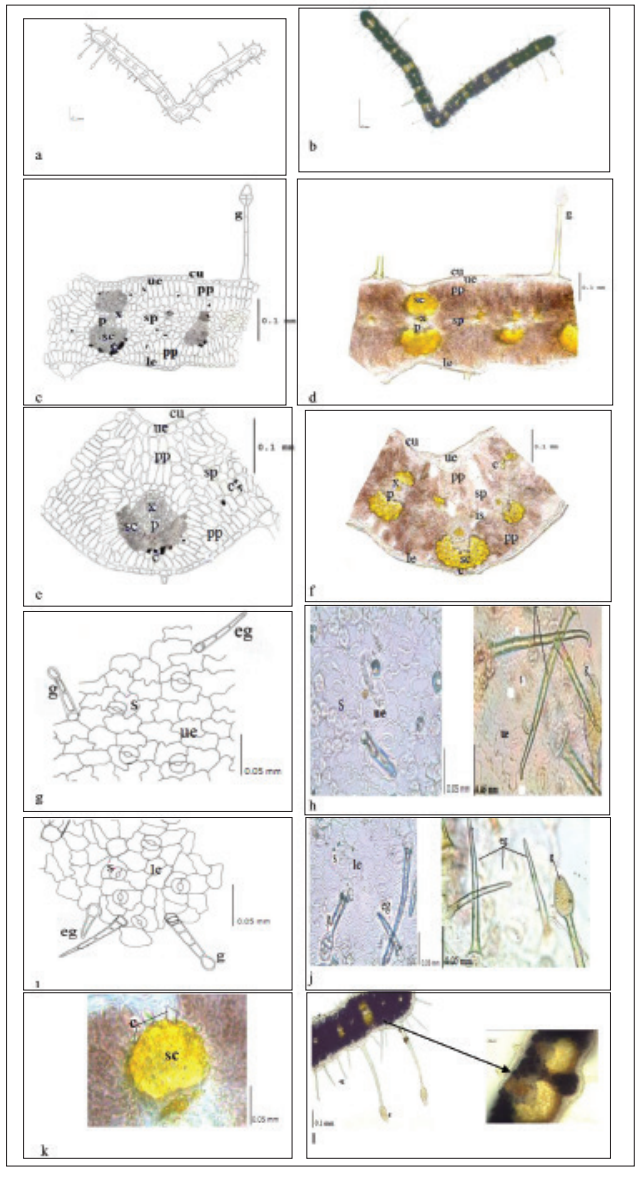

Figure 2 *O. basiadnata*, a,b) Schematic drawing of the cross section of the leaf and photo; c,d) Schematic drawing of transverse section of leaf blade and photo; e,f) Schematic drawing of transverse section of midrib and photo; g,h) Drawing of upper surface view of leaf and photo; ı,j) Drawing of lower surface view of leaf and photo; k) prismatic crystals in sclerenchyma, l) general view of glandular and eglandular hairs, vascular bundles in mesophyll

cu: Cuticle, g: Glandular hair, eg: Eglandular hair, ue: Upper epidermis, c: Crystal, pp: Palisade parenchyma, sp: Spongy parenchyma, sc: Sclerenchyma: p: Phloem, x: Xylem, s: Stomata, le: Lower epidermis

Leaf anatomy of O. macrosperma

Cross section of leaf blade

The leaf is bifacial. The upper and lower epidermis cells consist of a single layer of square or rectangular-shaped cells with thin walls. The cuticle is thin. Underneath the epidermis there is usually two layers of palisade parenchyma. The spongy parenchyma consists of 4-5 layers of usually isodiametrical cells with few intercellular spaces. Glandular hairs have two types. The first type consists of glandular hairs with a multicellular stalk and a multicellular round-head. The second type consists of a multicellular stalk and a unicellular glandular head. They are sparsely observed relative to the other two species. Rubiaceae type stomata are observed (Figure 3).

Cross section of the midrib

The upper and lower epidermis cells are square or rectangular-shaped cells, and are single-layered with anticlinal walls. The palisade parenchyma cells have a single layer or two layers. The spongy mesophyll with 2-4 layers consists of isodiametric parenchymatous cells with few intercellular spaces. There are sclerenchyma cells which generally surrounded phloem and the xylem is underneath phloem. As in the two other species, solitary crystals with various shapes and sizes (styloids) are observed and frequently form a sheath along the outer boundary of the pericyclic sclerenchyma (Figure 3).

Surface of the lower and upper epidermis

The lower epidermal cells are similar to those in the upper epidermis. Unlike the upper epidermis, striated cuticle is observed on the lower epidermis. The stomata generally have 3 subsidiary cells. Glandular hairs are sparsely observed on both the upper and lower epidermis (Figure 3).

Stem anatomy of O. sessilifolia

Cross sections from the stems are rounded. The cuticle is thin-layered. The epidermis consists of a single-layer of square or short rectangular cells. Parenchyma cells which have a great number of large and small prismatic crystals are 3-4 lines. The pericycle is end of the parenchyma cells and it is not clear. Sclerenchyma cells which are clustered crescent-shaped and are interconnected with the end portions are arranged in a circle. Crystals are lined up on the sclerenchyma cells individually. The vascular bundles are surrounded with pith and pith rays which are number of 4-6. Phloem is composed of small and irregularly shaped cells. The cambium formes 1 or 2 rows at the start of the xylem. However, it is not very obvious and endodermis layer is not apparent. While the phloem is located on the outer side of the cambium, the xylem is located on its inner side. Pith is formed by rounded and large parenchymatic cells. Also, this part is identified charactersitically by secretory cells in places. The stem has many glandular (a multicellular stalk (1-4 row cells), a multicellular head (1-3 row cells) and fewer eglandular (unicellular and multicellular) hairs. Eglandular trichomes are generally multicellular and long (Figure 4).

Stem anatomy of O. basiadnata

The cross sections of the stem are rounded. The cuticle is thin layered with a crenate margin. The epidermis consists of a single layer of rectangular cells. Parenchyma cells are oval-shaped and have 3-5 lines. The sclerenchyma cells, cluster crystals and vascular bundles (generally 9-11 numbers) resemble those of *O. sessilifolia*. Endodermis layer is not clear. The pith area is narrower than that of *O. sessilifolia* and number of pith rays are 5-7. Eglandular hairs were determined to be more intense than glandular hairs. Also, starch was observed in the parenchyma cells. Locations of the phloem and xylem are similar to *O. sessilifolia*. Pericycle is end of the parenchyma cells, schlerenchymatous, occasionally parenchymatous (Figure 5).

Stem anatomy of O. macrosperma

The cross sections of the stem are rounded. The cuticle is thin layered. The epidermis consists of single-layered cells. The parenchyma cells are oval-shaped with 4-6 lines. The sclerenchyma cells, cluster crystals and numbers of the

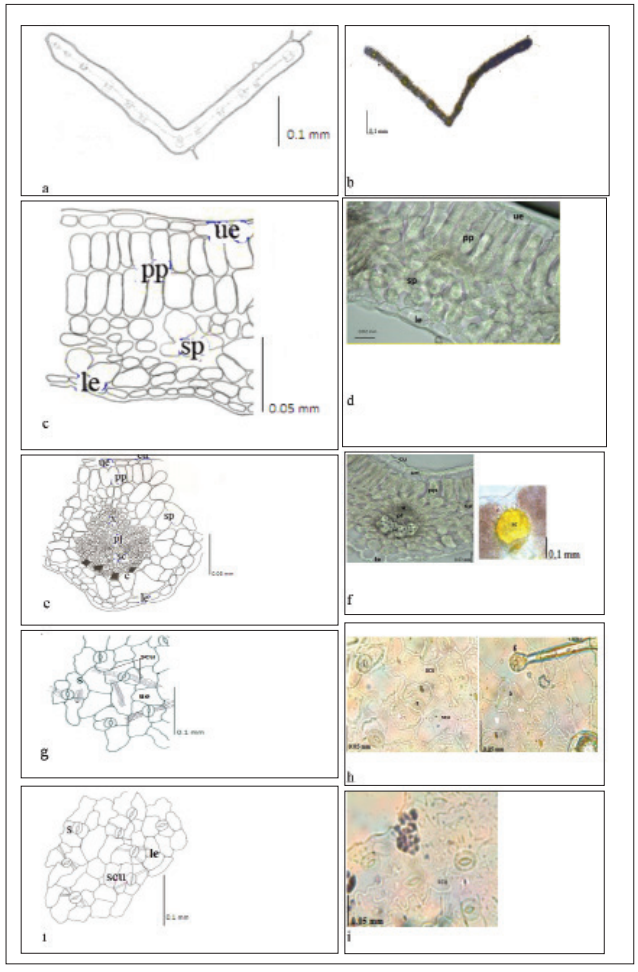

Figure 3. *O. macrosperma*, a,b) Schematic drawing of the cross section of the leaf and photo; c,d) Schematic drawing of transverse section of leaf blade and photo; e) Schematic drawing of transverse section of midrib; f) midrib photo and prismatic crystals in sclerenchyma; g,h) Drawing of upper surface view of leaf and photo; ı,j) Drawing of lower surface view of leaf and photo

cu: Cuticle, ue: Upper epidermis, c: Crystal, pp: Palisade parenchyma, sp: Spongy parenchyma, sc: Sclerenchyma, pl: Phloem, x: Xylem, s: Stomata, le: Lower epidermis, g: Glandular hair, ue: Upper epidermis, scu: Striated cuticle

vascular bundles are generally 9-10 and properties of the phloem and xylem similar to the other two species. Lines of pith rays are commonly 3-4. However, crystals are scarce in comparison to the other two species (*O. sessilifolia* and *O. basiadnata*). The pith area is narrower than that of *O. sessilifolia*.

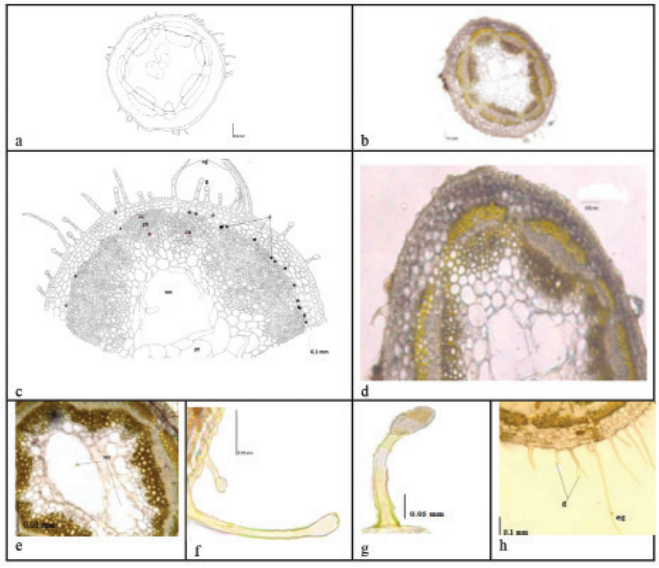

Figure 4. *O. sessilifolia*, transverse section of stem, a,b) Schematic drawing and photo; c,d) Anatomical drawing and photo; e) Secretory cells in pith; f,g) Glandular hairs; h) Glandular and eglandular hairs

e: Epiderma, p: Parenchyma cells, sc: Sclerenchyma, pl: Phloem, ca: Cambium, x: Xylem, sec: Secretory cells, pt: Pith, g: Glandular hair, eg: Eglandular hair, c: Crystal

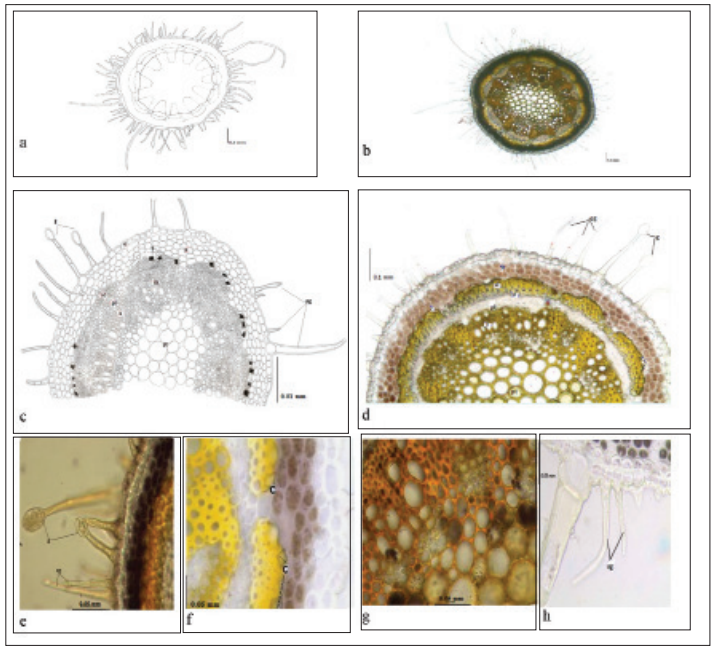

Figure 5. *O. basiadnata* transverse section of stem, a,b) Schematic drawing and photo; c,d) Anatomical drawing and photo; e) Glandular and eglandular hairs; f) Crystals in sclerenchyma; g) Starch granules in parenchymva cells; h) Eglandular hairs

e: Epiderma, p: Parenchyma cells, sc: Sclerenchyma, pl: Phloem, ca: Cambium, x: Xylem, pt: Pith, g: Glandular hair, eg: Eglandular hair, c: Crystal

Also, secretory cells were detected in the pith *O. sessilifolia*. Glandular and eglandular hairs were seen less frequently than in the other two species. Starch was detected densely in parenchymatic tissue (Figure 6).

In this study, the anatomical properties of three endemic *Ononis* species were investigated. As it stated in Metcalfe (1965), the three species of *Ononis* have Rubiaceae type stomata (Figure 1-3). Taia (2004) investigated in leaf characters within tribe *Trifolieae* (Family *Leguminosae*). Unlike to our study, it was found that *Ononis* species (*Ononis natrix* L., *Ononis vaginalis* Vahl, *Ononis reclinata* L., *Ononis sicula* Guss., *Ononis pubescens* L., *Ononis serrata* Forssk.) have diacytic, paracytic, brachyparacytic stomata type. In addition, these species have only multicellular glandular hair. However, in our study, leaf section of *O. basiadnata* was found eglandular hair (Figure 2). The type of vascular bundle in the leaf is similar to that in the stem at three *Ononis* species. *O. basiadnata* was the most intense in terms of glandular and eglandular hairs (Figure 5, Table 2). The other two species, *O. sessilifolia* and *O. macrosperma* followed it, respectively. The arrangements and type of crystals in stem section were very similar to the leaf anatomy. Furthermore, in stem anatomical studies of *O. macrosperma* and *O. sessilifolia*, the secretory cells in the pith region were detected (Figure 4, 6, Table 3).

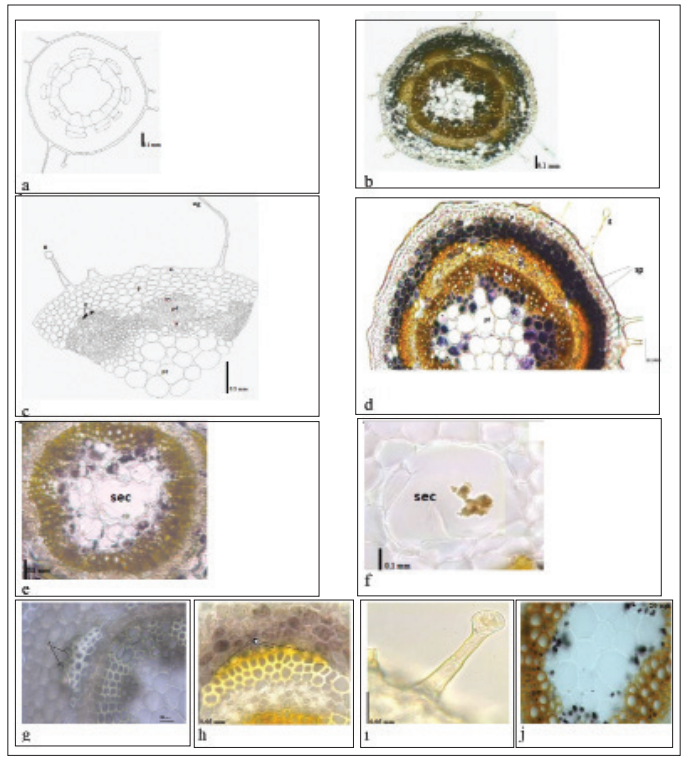

Figure 6. *O. macrosperma* O. macrosperma transverse section of stem, a,b) Schematic drawing and photo; c,d) Anatomical drawing and photo; e, f) Secretory cells in pith; g,h) Crystals in sclerenchyma; ı) Glandular hair; j) Starch granules in parenchyma cells

e: Epiderma, p: Parenchyma cells, sc: Sclerenchyma, pl: Phloem, ca: Cambium, x: Xylem, sec: Secretory cells, pt: Pith, g: Glandular hair, eg: Eglandular hair, c: Crystal

Table 2. Comparison of stem cross sections in 3 *Ononis* taxa growing in Turkey

Taxa	Epidermal cells	Eglandular trichomes	Glandular trichomes	Cortex parenchyma	Pericycle	Crystals of calcium oxalate	Pith
Ononis sessilifolia	Square or rectangular	Usually multi-cellular (4-5 cell) and long	Multicellular stalk and head; multi-cellular stalk and unicellular head; unicellular stalk and head	3-5 layers, cylindrical or oval cells, starch (-)	End of the parenchyma cells, schlerenchymatous, occasionally parenchymatous	Individually, lined up on the schlerenchyma cells	Pith area is wide, rounded and large parenchymatic cells, secretory cells (+)
Ononis basiadnata	Usually rectangular	Densely, unicellular and multi-cellular (2-4 cell), short and long	Multicellular stalk and unicellular head, short and long	4-5 layers, rectangular or oval cells, starch (+)	End of the parenchyma cells, schlerenchymatous, occasionally parenchymatous	Individually, lined up on the schlerenchyma cells	Pith area is narrow, rounded and large parenchymatic cells, secretory cell (-)
Ononis macrosperma	Usullay small and rectangular	Sparcely, long and multi-cellular (2-4 cell)	Sparcely, multicellular stalk and unicellular head	4-6 layers, oval cells, starch (+)	End of the parenchyma cells, schlerenchymatous, occasionally parenchymatous	Sparcely and individually lined up on the schlerenchyma cells	Pith area is narrow, rounded and large parenchymatic cells, secretory cells (+)

Table 3. Comparison of leaf cross and surface in 3 *Ononis* taxa growing in Turkey

Taxa	Leaf structure	Lower and upper epidermal cells	Eglandular trichomes	Glandular trichomes	Crystals of calcium oxalate	Palisade parenchyma	Spongy parenchyma	Stomata
Ononis sessilifolia	Monofacial	The lower epidermal cells are similar to those in the upper epidermis which is square or rectangular, usually small, these are covered with a thin cuticle.	-	Long: multicellular stalk and head, usually 2-3-celled head	Solitary crystals (Styloids) in pericyclic schlerenchyma	Usually 2 layers, short and cylindrical, starch (+)	Isodiametric parenchymatous cells, starch (+)	Rubiaceae type stomata, with 3-4 subsidiary cells
Ononis basiadnata	Monofacial	The lower epidermis (rectangular) cells are smaller than the upper ones (rectangular) and these are covered with a thin cuticle.	Densely, simple, short: unicellular; long: multicellular	Densely, long: multicellular stalk and head; multicellular stalk and unicellular head	Solitary crystals (Styloids) in pericyclic schlerenchyma generally; and in mesophyll	Usually 2 layers and short cylindrical, starch (+)	Isodiametric, starch (+)	Rubiaceae type stomata, with 3-4 subsidiary cells
Ononis macrosperma	Bifacial	The lower epidermal cells are similar to those in the upper epidermis which is square or rectangular, striated cuticle is seen both upper and lower surface	-	long: multicellular stalk and multicellular round-head, multicellular stalk and unicellular round-head	Solitary crystals (Styloids) in pericyclic schlerenchyma	Usually 2 layers and cylindrical, starch (+)	Isodiametric, starch (+)	Rubiaceae type stomata, with mainly 3 subsidiary cells

CONCLUSION

This study is original in that, similar and different anatomical features of the three endemic *Ononis* species growing in Turkey are revealed in detail for the first time. Our investigations showed that anatomical studies also proved to be very important in providing information of taxonomic importance. It is hoped that this study will form a basis for future research on the other *Ononis* species in Turkey. Furthermore, anatomical studies should be supported by molecular, morphologic and chemical studies.

Conflict of Interest: No conflict of interest was declared by the authors.

REFERENCES

1. Doyle JJ, Luckow MA. The rest of the iceberg. Legume diversity and evolution in a phylogenetic context. Plant Physiology. 2003;131:900-910.
2. Heywood VH, Brummitt RK, Culham A, Seberg O. *Leguminosae* (*Fabaceae*) In: Flowering Plant Families of the World. New York; Firefly Books; 2007:185-188.
3. Davis PH. Flora of the Turkey and the East Aegean Islands. (3rd Ed) Edinburgh University Press. London; 1970:375-384.
4. Güner A. A Checklist of the Flora of Turkey (Vascular Plants), Nezahat Gokyigit Botanic Garden Publication. Flora series I; İstanbul; 2012:482-484.
5. Evans WC. Trease and Evans Pharmacognosy, WB. 15th ed. Printed in China; 2002:26.
6. Baytop T. Plants with Therapy in Turkey (Past and Present). Nobel Tıp Kitabevleri; İstanbul; 1999:251.
7. Langer R, Engler S, Kubelka W. Comparative root anatomy of some perennial taxa of the genus *Ononis* L. Pharmazie. 1995;50:627-629.
8. Duke JA, Bogenschutz MJ, Ducellier J, Duke PAK. Handbook of Medicinal Herbs. 2th ed. London; 2002.
9. Taia WK. Leaf characters within tribe *Trifoliae* (*Family Leguminosae*). J Bio Sci. 2004;7:1463-1472.
10. Baldemir A, Pınar NM, Suludere Z, Coşkun M. Türkiye'de doğal olarak yetişen endemik üç *Ononis* L. (*Fabaceae*) türünün polen ve tohum morfolojisi. J Fac Pharm Ankara. 2009;38:89-102.
11. Agullo JC, Juan A, Alonso M, Terrones A, Crespo MB. Taxonomic status of *Ononis tridentata* (*Fabaceae*) from Morocco, resolved by multivariate morphometric analyses. Plant Biosyst. 2013;147:645-653.
12. Baldemir A, Coşkun M. Comparative morphological studies on three endemic *Ononis* L. (*Leguminosae*) species growing in Turkey. Bio Di Con. 2016;9:82-91.
13. Arıhan O, Güvenç A. Studies on the anatomical structure of stems of willow (*Salix* L.) species (*Salicaceae*) growing in Ankara province, Turkey. Turk J Bot. 2011;35:535-551.
14. Ogie-Odia EA, Eseigbe D, Ilechie MN, Erhabor J, Ogbebor E. Foliar epidermal and phytochemical studies of the grasses *Cymbopogon citratus* (Stapf.), *Axonopus compressus* (P. Beauv.) and *Eragrostis tremula* (S.W. Beauv) in Ekpoma, Edo state, Nigeria. Sci World J. 2010;5:20-25.
15. Metcalfe CR, Chalk L. Anatomy of the dicotyledones. Oxford; Clarendon Press; 1965.
16. Çelebioğlu S, Baytop T. A new reagent for microscopial investigation of plant Publication of the Institute of Pharmacognosy. İstanbul; 1949.

Turk J Pharm Sci 2017;14(2):141-147
DOI: 10.4274/tjps.81994

ORIGINAL ARTICLE

Assessment of Vitronectin, Soluble Epithelial-Cadherin and TGF-β1 as a Serum Biomarker with Predictive Value for Endometrial and Ovarian Cancers

Endometrial ve Ovaryum Kanserinde Tanısal Değer Yönünden Serum Biyobelirteci Olarak Vitronektin, Solubl Epitel-Kaderin ve TGF-β1'in Değerlendirilmesi

Taylan TURAN[1], Meral TORUN[1], Funda ATALAY[2], Aymelek GÖNENÇ[1]*

[1]Gazi University, Faculty of Pharmacy, Department of Biochemistry, Ankara, Turkey
[2]Ankara Oncology Training and Research Hospital, Clinic of Obstetrics and Gynecology, Ankara, Turkey

ABSTRACT

Objectives: Extracellular matrix components, including vitronectin (VN), soluble epithelial-cadherin (sE-cadherin) and transforming growth factor-beta 1 (TGF-β1), play a key role in the invasion and metastasis of cancer. The objective of the study was to determine the clinical significance of serum levels of these molecules in patients with endometrial and ovarian cancers.

Materials and Methods: Serum levels of VN, sE-cadherin and TGF-β1 in patients with endometrial (n=28) and ovarian cancers (n=40) and healthy controls (n=41) were measured by ELISA using commercial kits.

Results: A significant difference was found in VN, sE-cadherin and TGF-β1 levels between patients and healthy controls ($p<0.01$, $p<0.01$ and $p<0.05$, respectively). Serum VN and sE-cadherin levels were decreased significantly in both endometrial and ovarian cancer patients compared to controls ($p<0.01$, $p<0.01$, respectively). Conversely, TGF-β1 levels were increased significantly in patients with ovarian cancer as compared to controls ($p<0.01$). There was no significant difference between healthy controls and endometrial cancer patients.

Conclusion: In conclusion, our study reveals that serum VN, sE-cadherin and TGF-β1 levels can be candidate targets for providing new diagnostic procedures in endometrial and ovarian cancers.

Key words: Vitronectin, sE-cadherin, TGF-β1, endometrial cancer, ovarian cancer

ÖZ

Amaç: Vitronektin, çözünür epitelyal-cadherin (sE-cadherin) ve transforming büyüme faktörü-beta 1'i (TGF-β1) içeren ekstrasellüler matriks elemanları kanserin invazyonu ve metastazında anahtar rol oynamaktadır. Bu çalışmada endometriyal ve over kanserli hastalarda bu moleküllerin serum düzeylerinin klinik önemini belirlemek amaçlanmıştır.

Gereç ve Yöntemler: Bu çalışmada, 28 endometriyum kanseri hastası, 40 over kanseri hastası ve 41 sağlıklı kontrol grubuna ait serum vitronektin (VN), sE-cadherin ve TGF-β1 düzeyleri ELISA yöntemiyle ticari kitler kullanılarak ölçülmüştür.

Bulgular: Total hasta grubunda, sağlıklı kontrollere kıyasla VN, sE-cadherin ve TGF-β1 düzeylerinde anlamlı bir farklılık bulunmuştur (sırasıyla $p<0,01$; $p<0,01$ ve $p<0,05$). Serum VN ve sE-cadherin düzeyleri hem endometriyal hem de over kanseri hastalarında kontrol grubuna kıyasla önemli ölçüde düşük bulunmuştur ($p<0,01$). Buna karşın, TGF-β1 düzeyleri, kontrol grubuna kıyasla over kanserinde anlamlı derecede yükselmiştir ($p<0,01$), ancak sağlıklı kontroller ile endometriyal kanserli hastalar arasında anlamlı bir fark bulunamamıştır.

Sonuç: Çalışmamız serum VN ve sE-cadherin düzeylerinin, endometriyal ve over kanserlerinde yeni tanı yöntemleri sağlamak için aday hedefler olabileceğini ortaya koymaktadır.

Anahtar kelimeler: Vitronektin, sE-cadherin, TGF-β1, endometriyal kanser, over kanseri

*Correspondence: **E-mail:** aymelek70@gmail.com, **Phone:** +90 312 202 31 52 - +90 533 713 13 67
ORCID ID: orcid.org/0000-0003-2741-7087
Received: 24.03.2017, **Accepted:** 13.04.2017

INTRODUCTION

Currently, cancer ranks the second most common cause of death following cardiovascular diseases.[1] Among the gynecological malignancies; endometrial and ovarian cancers have the highest mortality rate.[2] In Turkey the most frequently detected gynecological cancer is endometrium cancer.[3] According to The Association of Public Health Professionals report in Turkey the ovarian cancer is the seventh most common cause of cancer related mortality with a frequency of 5%.[4]

The adherence of cells to the extracellular matriks (ECM) underlies maintenance of tissue integrity, cellular movement, and extracellular recognition processes.[5] It is well known that cancer cell formation and dispersion is closely associated with loss of cell-cell adhesion and tissue integrity, due to excessive proteolytic degradation of the ECM, and altered cell-ECM adhesion.[6] Thus, in recent years, some relatively small molecules have generated great interest as a new research target in tumor pathogenesis. Vitronectin (VN) is a major plasma glycoprotein that execute multiple functions in the regulation of cell differentiation, proliferation, and morphogenesis as a cell adhesion molecule.[7] Recent studies have been shown that VN has a role in pathophysiological processes and its biosynthesis may be regulated in disease states.[8,9] Plenty of *in vitro* studies suggest that tumor invasion is enhanced with modulated VN activities in some cancer types.[10,11]

Epithelial-cadherin (E-cadherin) is an epithelial adhesion molecule, the intact function of which is crucial for the establishment and maintenance of epithelial tissue polarity, structural integrity, cell proliferation and recognition.[12] E-cadherin consists of an extracellular domain, a transmembrane segment, and a cytoplasmic domain.[13] It plays a pivotal role in the suppression of tumor invasion and metastasis.[14] Decreased E-cadherin expressions were observed in epithelial tumor cells, and its expression levels were found to be closely linked to loss of cell to cell adhesion and carcinogenesis.[15] But, there are conflicting results about soluble E-cadherin (sE-cadherin) levels in cancer. Some suggest that serum sE-cadherin levels were higher,[16] while others were revealed that sE-cadherin levels were significantly lower[17] in patients compared to controls.

Transforming growth factor-beta (TGF-β) is a member of a family of multifunctional polypeptides and has a significant role in regulating cell growth and differentiation, apoptosis, cell motility, ECM production, angiogenesis, and cellular immunity.[18] TGF-β are widely expressed in all tissues and has a dual role in cancer, acting both as a tumor suppressor in the early stages of tumorigenesis by arresting cell cycle progression in late G_1 phase in epithelial cells and as a promoter of an epithelial to mesenchymal transition that has been associated with increased tumor growth, cell motility, invasion and metastasis.[19] Some studies have found that TGF-β1 is quickly activated and released into the blood and serum and tissue levels of it are significantly enhanced in cancer patients.[20,21] Increased TGF-β1 levels were reported in various cancers.[22,23]

There are inadequate published data to verify the importance of serum VN, sE-cadherin and TGF-β1 concentrations in endometrial and ovarian cancers, up to now. Therefore, the investigation of changes in VN, sE-cadherin and TGF-β1 expressions and compare patients with healthy individuals was aimed for both diagnostic and protective purposes in these cancers.

MATERIALS AND METHODS

Patients

Newly diagnosed sixty eight gynecological cancer patients (mean age 58.62±1.70 years) and forty one age-matched healthy volunteers (mean age 56.56±1.78 years) were collected from Ankara Oncology Training and Research Hospital, Ankara, Turkey. Control group consists of 41 healthy individual with no systemic or benign/malign diseases. Patients with gynecological cancer were divided into two groups; forty of the patients (n=40) were ovarian cancer and the rest of them were endometrial cancer (n=28). None of the patients had any additional disease or had previously undergone any treatment and none of the control groups had a history of gynecological cancer. The study was approved by Gazi University Oncology Training and Research Hospital Medical Ethics Committee, and written informed consent was obtained from the patients or their relatives. The Declaration of Helsinki was adhered to in this study. Gynecological cancer was diagnosed by pathology reports, definitely.

Methods

Sample collection and analysis

Peripheral venous blood samples were collected from the patients and healthy controls and immediately placed into sterile test tubes. The blood samples were centrifugated at 1000Xg for 15 min at 4°C to obtain serum and kept in eppendorf tubes at -80°C until analysis. In the present study, the serum levels of VN, sE-cadherin and TGF-β1 from the patients with endometrial and ovarian cancers and healthy controls were analyzed and compared by ELISA.

Measurement of serum vitronectin levels

The VN levels in serum were measured spectrophotometrically by using a commercial assay kit, according to the manufacturer's instructions (GenWay, Nancy Ridge Drive San Diego, CA, USA). To carry out the immunological reaction, 100 µL of antibody-peroxidase conjugate solution was pipetted into each well of antibody coated microtiterplate, and subsequently 50 µL of standard or diluted sample (500-1000 fold) solution was transferred to the plate. Then the plate was sealed with a foil and incubated for 2 hours at room temperature by gentle mixing. Each well was aspirated and washed four times with 400 µL of washing buffer. 100 µL substrate solution was added to each well, then incubated at room temperature for 15 min for substrate incubation. After incubation period, 100 µL stop solution was added into each well in the same order as for substrate and the plate was tapped gently to mix. After stopping the reaction, optical density at 450 nm of each well was measured by Standard microplate reader, and a blank well was set as zero. According to the standard concentrations and

corresponding optical density values, the standard curve was obtained. The concentration of the VN in each sample was determined by interpolating from the VN concentration (X axis) to the absorbance value (Y axis). The range of standard curve is 5-320 ng/mL. The intra-assay CV is <4.4% and the inter-assay precision is <5.6%.

Measurement of serum sE-cadherin levels

The sE-cadherin levels in serum were measured spectrophotometrically by using a commercial assay kit, according to the manufacturer's instructions (Aviscera Bioscience, Suite C Santa Clara, CA, USA). 100 µL of Dilution Buffer was pipetted to Blank Wells and the same voume of standard, diluted sample (20 fold) or positive control was added per well. Then plate was covered with plate sealer and incubated for 2 hours on micro-plate shaker at room temperature. Subsequently, each well was aspirated and washed four times with 300 µL 1X Washing Buffer. 100 µL detection antibody working solution was added to each well, then incubated at room temperature for 2 hours on micro-plate shaker. Later on, aspiration and washing step were repeated for four times. After the washing step, 100 µL of Streptavidin-Horseradish Peroxidase Conjugate was transferred to each well and the plate was incubated again on micro-plate shaker, at room temperature for 45 min. Next, aspiration and washing steps were repeated for four times. 100 µL substrate solution was pipetted to each well and incubated one more time, on micro-plate shaker, at room temperature for 10 min by protecting the plate from light. And finally, the reaction was stopped by adding 100 µL of stop solution into the wells. Optical density of each well was determined within 15 min, using a micro-plate reader at 450 nm. By plotting the concentrations of standards against optical values, standard curve was obtained. The corresponding sample concentrations were then determined by comparing the optical density values of samples to the standard curve. The range of standard curve is 187.5-12000 pg/mL and the sensitivity is 93 pg/mL. The intra-assay precision is <4.8% and the inter-assay precision is <6.6%.

Measurement of serum TGF-β1 levels

The TGF-β1 levels in serum were measured spectrophotometrically by using a commercial assay kit, according to the manufacturer's instructions (BOSTER Biological Tech., Fremont, Pleasanton, USA). 100 µL of prepared with different concentration human TGF-β1 standard solutions were pipetted into the precoated 96-well plate. For control well, 100 µL sample diluent buffer was used. And 100 µL of properly diluted sample (7 fold) of serum was transferred to each empty well. After sealing the plate with a cover, it was incubated at 37˚C for 90 min. Plate content was discarded. Following, 100 µL biotinylated anti-human TGF-β1 antibody working solution was poured into each well and the plate was incubated again at 37˚C for 1 hour. Then, the plate in question was washed three times with 0.01 M tris-buffered saline (TBS). After the third washing, 100 µL prepared ABC working solution was added into each well and the plate was incubated again at 37˚C for 30 min. Plate washed five times with the enough volume of 0.01 M TBS. 90 µL prepared TMB color developing agent was trasferred into each well and the plate incubate at 37˚C in dark for 25 min. Then, 100 µL TMB stop solution was added and the optical density of each well was read at 450 nm in a micro-plate reader within 30 min after adding the stop solution. According to the standard concentrations and corresponding optical density values, the standard curve was drawn. The corresponding sample concentrations were then determined by comparing the optical density values of samples to the standard curve. The range of standard curve is 15.6-1000 pg/mL and the sensitivity is <1 pg/mL. The intra-assay precision is <4.1% and the inter-assay precision is <6.0%.

Measurement of other blood parameters

Serum levels of total cholesterol, high-density lipoprotein (HDL)-cholesterol and triglycerides were measured spectrophotometrically on the Roche-Hytachi P-800 autoanalyser by using a commercial kit (Roche, Mannheim, Germany) in all subjects recruited in the study. Concentration of serum low-density lipoprotein (LDL)-cholesterol was calculated by the standard Friedewald formula.[24]

Statistical analysis

SPSS packed programme (version 17 software, SPSS Inc. Chicago, Illinois, USA) was used for statistical analyses. The results were presented as mean ± standard deviation. Student's t-test was used to compare the results between groups. Mann-Whitney U test was used to evaluate the results between subgroups. Pearson correlation coefficients were calculated for relationship between measured parameters. The value of $p<0.05$ was considered as statistically significant, in all statistical analyses.

RESULTS

General characteristics and some biochemical parameters of patients and control groups were presented in Table 1. No significant difference was determined between groups in terms of age and quetelet index ($p>0.05$).

Table 1. General characteristics and biochemical parameters from gynecological cancer and control

	Total patients	Healthy controls	p value
Total number of subjects	68	41	p>0.05
Age (years)	58.62±1.21	58.39±1.25	p>0.05
Quetelet index (kg/m^2)	28.72±0.40	27.85±0.59	p>0.05
	Biochemical parameters		
Total cholesterol (mg/dL)	200.35±6.48	205.10±5.21	p>0.05
HDL-cholesterol (mg/dL)	ç.97±1.57	43.32±2.09	p>0.05
LDL-cholesterol (mg/dL)	128.36±5.01	134.80±4.39	p>0.05
Triglycerides (mg/dL)	155.93±9.22	189.51±14.96	p>0.05

HDL: High-density lipoprotein, LDL: Low-density lipoprotein

Similarly, no significant differences were determined in the comparison of total cholesterol, HDL-cholesterol LDL-cholesterol and triglyceride levels between total patients and healthy controls (p>0.05).

Serum VN (112.72±4.34 μg/mL) and sE-cadherin (5.15±0.40 ng/mL) levels of patients were found to be significantly lower than healthy controls (134.87±4.59 μg/mL and 23.48±2.12 ng/mL recpectively) (p<0.01). However, in patients, serum TGF-β1 levels (173.74±12.31 pg/mL) were found to be higher than healthy controls (133.50±14.37 pg/mL) (p<0.05, Figure 1).

In patients with endometrial and ovarian cancer, serum VN levels (117.07±5.59 μg/mL and 109.68±6.27 μg/mL, respectively) were found to be lower than healthy controls (134.87±4.59 μg/mL) (p<0.01) (Figure 2). The lower VN levels were determined in ovarian cancer group compared to endometrial cancer group. Similarly serum sE-cadherin levels in endometrial and ovarian cancer patient groups (4.76±0.63 ng/mL and 5.42±0.53 ng/mL, respectively) were found to be lower than healthy controls (23.48±2.12 ng/mL) (p<0.01), but the sE-cadherin levels were found to be lower in patients with endometrial cancer in comparison to ovarian cancer patient group. Serum TGF-β1 levels were found to be increased significantly in ovarian cancer patiens when compared to control group (180.31±11.61 pg/mL and 133.50±14.37 pg/mL, recpectively) (p<0.05). However, no significant difference was found between endometrial cancer patients and healthy controls (164.36±25.10 pg/mL and 133.50±14.37 pg/mL, recpectively) (p>0.05) (Figure 2).

Using bivariate correlation analysis of the measured parameters, positive correlations were found between serum VN and sE-cadherin levels (r=0.775, p<0.01) (Figure 3a) and negative correlations were found between both VN and TGF-β1 (r=-0.379, p<0.05) (Figure 3b) and sE-cadherin and TGF-β1 (r=-0.373, p<0.05) (Figure 3c) in control group.

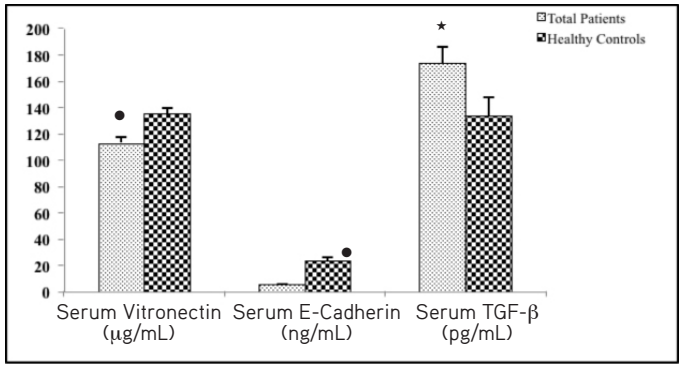

Figure 1. The comparison of serum concentrations of VN, sE-cadherin and TGF-β1 between total patient group and control group

●: A significant difference from control group (p<0.01), ★: A significant difference from control group (p<0.05), VN: Vitronectin, TGF- β1: Transforming growth factor-beta 1, sE-cadherin: Soluble epithelial-cadherin

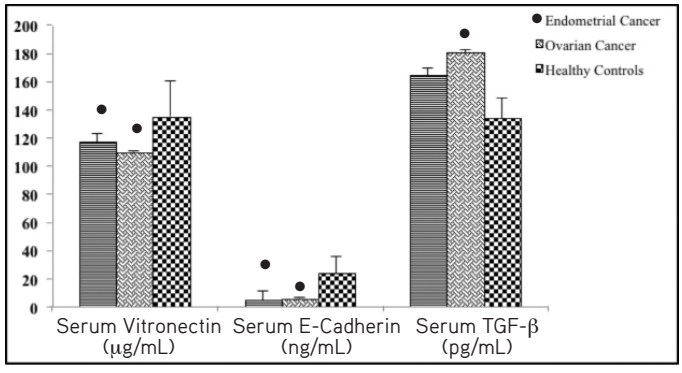

Figure 2. The comparison of serum concentrations of VN, sE-cadherin and TGF-β1 between endometrial and ovarian cancers and control group

●: A significant difference from control group (p<0.01), VN: Vitronectin, TGF- β1: Transforming growth factor-beta 1, sE-cadherin: Soluble epithelial-cadherin

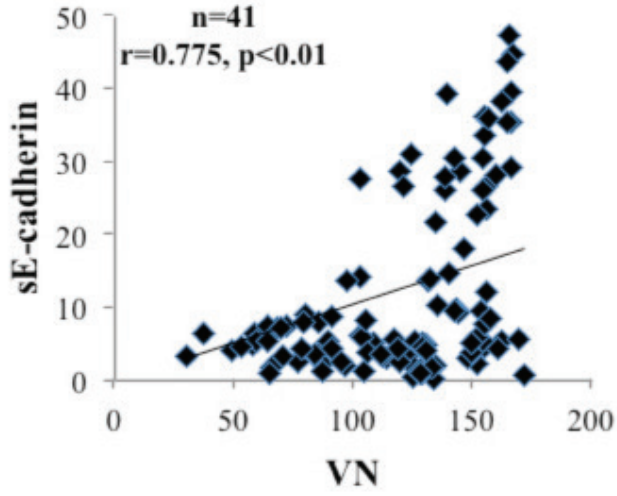

Figure 3a. Correlation between serum VN and sE-cadherin in control group, The solid line represents the calculated regression line with a correlation coefficient (r) of 0.775

VN: Vitronectin, sE-cadherin: Soluble epithelial-cadherin

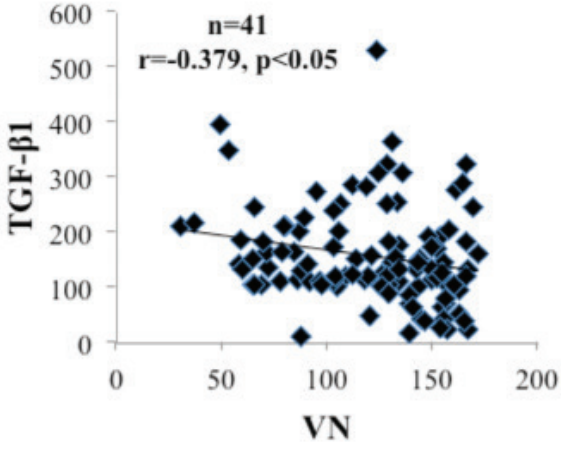

Figure 3b. Correlation between serum VN and TGF-β1 in control group, The solid line represents the calculated regression line with a correlation coefficient (r) of -0.379

VN: Vitronectin, TGF- β1: Transforming growth factor-beta 1,

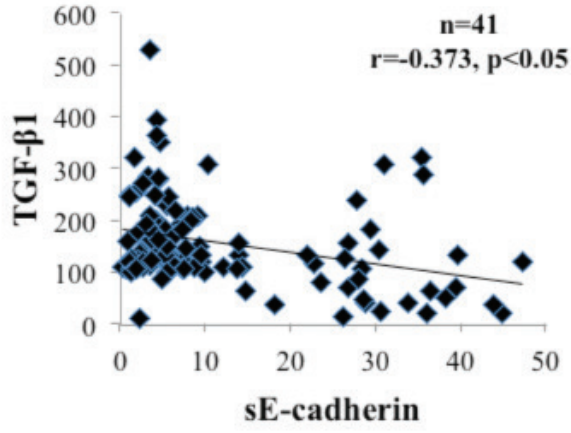

Figure 3c. Correlation between serum sE-cadherin and TGF-β1 in control group, The solid line represents the calculated regression line with a correlation coefficient (r) of -0.373

TGF- β1: Transforming growth factor-beta 1, sE-cadherin: Soluble epithelial-cadherin

DISCUSSION

Endometrial and ovarian cancers are the most common of the gynecologic malignancies in women. Regulation of cellular adhesion is provided by signaling pathways between tumor cells and the ECM. Cellular adhesion is controlled by the cell surface receptor family and integrins. VN, sE-cadherin and TGF-β1 are important components of the ECM proteins. Thus, we mainly tried to demonstrate the clinical significance of serum levels of these molecules in terms of diagnostic purpose in endometrial and ovarian cancers.

There are inconsistent results in the literature concerning serum VN levels in various cancer types. In one of the studies, Kadowaki et al.[25] showed that serum VN levels were elevated in breast cancer patients. They concluded that serum VN level is very valuable for evaluating clinical assessment of breast cancer. Contrary to the aforementioned study, Hao et al.[26] found that the mean value of serum VN level in patients with breast cancer at early and late stages were lower than normal individuals. Yamada et al.[27] studied the plasma concentration of VN in control subjects and hepatocellular carcinoma (HCC). They obtain similar lower plasma VN levels in patients with HCC as compared to control group. No significant difference in VN levels was reported by Tugcu et al.[28] between control and patient groups in various types of cancers apart from gynecological cancers. In this study concerning the VN levels when compared to control group a significant difference was found both for endometrial and for ovarian cancer patient groups. Decrease in serum VN levels may be attributed to matrix metalloproteinase-2 secreted by tumor cells in ECM.

Cell to cell adhesion is basically mediated by cadherins. There are conflicting results in the literature about sE-cadherin in cancer. Elevated sE-cadherin levels were reported in gastric cancer by Katayama et al.[29], later on it was confirmed by Gofuku et al.[30] In newly diagnosed bladder cancer patients, serum sE-cadherin levels were found to be significantly higher than normal controls and they suggested that high levels of sE-cadherin correlate with higher grade tumors.[31] Similarly, Liang et al.[16] were revealed that the serum sE-cadherin in breast cancer patients were significantly higher than controls. Shirahama et al.[32] indicated that the levels of serum sE-cadherin did not vary significantly from controls in basal cell carcinoma. In colorectal patients, Velikova et al.[33] determined that there was no statistically significant difference between sE-cadherin levels between controls and patients. However, Bonaldi et al.[17] suggested that sE-cadherin was lower in patients with prostate cancer compared to controls. Several studies concluded that decreased expression of E-cadherin facilitated tumor invasion and metastasis in various tumors such as ovarian, endometrial and cervical cancers.[34,35] In our study we determined that sE-cadherin levels were decreased in both cancer groups. We think that low serum sE-cadherin levels may be result of decreased E-cadherin expression in these gynecological cancers.

For many cancer, circulating levels of TGF-β1 have been measured up to now. Elevated serum TGF-β1 levels have been observed in various cancer types and have been linked to cancers in previous studies. Shim et al.[20] evaluated the serum levels of TGF-β1 in patients with colorectal carcinoma versus healthy controls and their results showed that TGF-β1 serum levels in patients were significantly higher than controls. TGF-β1 has been reported to be enhanced in serum in invasive breast cancer patients.[36] In a similar manner, it was demonstrated that serum concentrations of TGF-β1 in gastric cancer patients were significantly higher than controls.[37] Han et al.[23] were revealed that patients with cholangiocarcinomas, HCCs and gastric carcinomas presented increased serum TGF-β1 levels than non-cancer counterparts. It has been shown that the blockage of TGF-β causes upregulation of E-cadherin resulting in the reduction of migration and invasion of carcinoma cells[38] and then TGF-β1 expression negatively correlated with E-cadherin expression.[39] Our results are consistent with the literature in terms of elevated serum TGF-β1 levels and reduced sE-cadherin levels. It was assumed that increased TGF-β1 levels may be associated with decreased E-Cadherin expression in endometrial and ovarian cancers.[40]

CONCLUSION

As a conclusion, our study revealed that when compared to control group serum levels of VN and sE-cadherin are significantly decreased whereas TGF-β1 level is elevated in patients with gynecological cancer. In ovarian cancer, we have found marked increase of TGF-β1 and decrease of VN. A remarkable decrease in sE-cadherin concentration has been determined in patients with endometrial cancer. Although large-scale studies are required, it was suggested that alterations in serum levels of mentioned relatively small molecules in ovarian and endometrial cancer may be associated with disease progression. Therefore these molecules may be promising targets for both diagnosis and therapy.

Conflict of Interest: No conflict of interest was declared by the authors.

REFERENCES

1. Jemal A, Siegel R, Ward E, Murray T, Xu J, Thun MJ. Cancer statistics, 2007. CA Cancer J Clin. 2007;57:43-66.
2. Nguyen L, Cardenas-Goicoechea SJ, Gordon P, Curtin C, Momeni M, Chuang L, Fishman D. Biomarkers for early detection of ovarian cancer. Womens Health (Lond). 2013;9:171-187.
3. Turgut A, Ozler A, Sak ME, Evsen MS, Soydinç HE, Alabalık U, Gül T. Retrospective analysis of the patients with gynecological cancer: 11-Year Experience. J Clin Exp Invest. 2012;3:209-213.
4. Ergör G. Non Contagious Diseases in Turkey. Cancer Mortality. In: Unal B, ed. Turkish Public Health Report. 2012:286-287.
5. Preissner KT. Structure and Biological Role of Vitronectin. Annu Rev Cell Biol. 1991;7:275-310.
6. De Wever O, Mareel M. Role of tissue stroma in cancer cell invasion. J Pathol. 2003;200:429-447.
7. Tomasini BR, Mosher DF. Vitronectin. Prog Hemost Thromb. 1990;10:269-305.
8. Juliano RL, Varner JA. Adhesion molecules in cancer: the role of integrins. Curr Opin Cell Biol. 1993;5:812-818.
9. Madsen CD, Sidenius N. The interaction between urokinase receptor and vitronectin in cell adhesion and signalling. Eur J Cell Biol. 2008;87:617-629.
10. Kashyap AS, Hollier BG, Manton KJ, Satyamoorthy K, Leavesley DI, Upton Z. Insulin-like growth factor-I: vitronectin complex-induced changes in gene expression effect breast cell survival and migration. Endocrinology. 2011;152:1388-1401.
11. Pola C, Formenti SC, Schneider RJ. Vitronectin-alphavbeta3 integrin engagement directs hypoxia-resistant mTOR activity and sustained protein synthesis linked to invasion by breast cancer cells. Cancer Res. 2013;73:4571-4578.
12. Mărgineanu E, Cotrutz CE, Cotrutz C. Correlation between E-cadherin abnormal expressions in different types of cancer and the process of metastasis. Rev Med Chir Soc Med Nat Iasi. 2008;112:432-436.
13. Chetty R, Serra S. Nuclear E-cadherin immunoexpression: from biology to potential application in diagnostic pathology. Adv Anat Pathol 2008;15:234-240.
14. Ho CM, Cheng WF, Lin MC, Chen TC, Huang SH, Liu FS, Chien CC, Yu MH, Wang TY, Hsieh CY. Prognostic and predictive values of E-cadherin for patients of ovarian clear cell adenocarcinoma. Int J Gynecol Cancer. 2010;20:1490-1497.
15. Holcomb K, Delatorre R, Pedemonte B, McLeod C, Anderson L, Chambers J. E-cadherin expression in endometrioid, papillary serous, and clear cell carcinoma of the endometrium. Obstet Gynecol. 2002;100:1290-1295.
16. Liang Z, Sun XY, Xu LC, Fu RZ. Abnormal expression of serum soluble E-cadherin is correlated with clinicopathological features and prognosis of breast cancer. Med Sci Monit. 2014;20:2776-2782.
17. Bonaldi C, Azzalis LA, Junqueira VB, de Oliveira CG, Vilas Boas VA, Gáscon TM, Gehrke FS, Kuniyoshi RK, Alves BC, Fonseca FL. Plasma levels of E-cadherin and MMP-13 in prostate cancer patients: correlation with PSA, testosterone and pathological parameters. Tumori. 2015;101:185-188.
18. Massague J. TGF-β signal transduction. Annu Rev Biochem. 1998;67:753-791.
19. Akhurst RJ, Derynck R. TGF-β signaling in cancer-a double-edged sword. Trends Cell Biol. 2001;11:44-51.
20. Shim KS, Kim KH, Han WS, Park EB. Elevated serum levels of transforming growth factor-beta1 in patients with colorectal carcinoma: its association with tumor progression and its significant decrease after curative surgical resection. Cancer. 1999;85:554-561.
21. Zhao J, Liang Y, Yin Q, Liu S, Wang Q, Tang Y, Cao C. Clinical and prognostic significance of serum transforming growth factor-beta1 levels in patients with pancreatic ductal adenocarcinoma. Braz J Med Biol Res. 2016;25:49.
22. Loh JK, Lieu AS, Su YF, Cheng CY, Tsai TH, Lin CL, Lee KS, Hwang SL, Kwan AL, Wang CJ, Hong YR, Howng SL, Chio CC. The alteration of plasma TGF-β1 levels in patients with brain tumors after tumor removal. Kaohsiung J Med Sci 2012;28:316-321.
23. Han B, Cai H, Chen Y, Hu B, Luo H, Wu Y, Wu J. The role of TGFBI (βig-H3) in gastrointestinal tract tumorigenesis. Mol Cancer. 2015;14:64.
24. Friedewald WT, Levy RI, Fredrıckson DS. Estimation of the concentration of low-density lipoprotein cholesterol in plasma, without use of the preparative ultracentrifuge. Clin Chem. 1972;18:499-502.
25. Kadowaki M, Sangai T, Nagashima T, Sakakibara M, Yoshitomi H, Takano S, Sogawa K, Umemura H, Fushimi K, Nakatani Y, Nomura F, Miyazaki M. Identification of vitronectin as a novel serum marker for early breast cancer detection using a new proteomic approach. J Cancer Res Clin Oncol. 2011;137:1105-1115.
26. Hao W, Zhang X, Xiu B, Yang X, Hu S, Liu Z, Duan C, Jin S, Ying X, Zhao Y, Han X, Hao X, Fan Y, Johnson H, Meng D, Persson JL, Zhang H, Feng X, Huang Y. Vitronectin: a promising breast cancer serum biomarker for early diagnosis of breast cancer in patients. Tumour Biol. 2016;7:8909-8916.
27. Yamada S, Kobayashi J, Murawaki Y, Suou T, Kawasaki H. Collagen-binding activity of plasma vitronectin in chronic liver disease. Clin Chim Acta. 1996;252:95-103.
28. Tugcu D, Devecioglu O, Unuvar A, Ekmekci H, Ekmekci OB, Anak S, Ozturk G, Akcay A, Aydogan G. Plasma Levels of Plasminogen Activator Inhibitor Type 1 and Vitronectin in Children With Cancer. Clin Appl Thromb Hemost. 2016;22:28-33.
29. Katayama M, Hirai S, Kamihagi K, Nakagawa K, Yasumoto M, Kato I. Soluble E-cadherin fragments increased in circulation of cancer patients. Br J Cancer. 1994;69:580-585.
30. Gofuku J, Shiozaki H, Doki Y, Inoue M, Hirao M, Fukuchi N, Monden M. Characterization of soluble E-cadherin as a disease marker in gastric cancer patients. Br J Cancer. 1998;78:1095-1101.
31. Griffiths TR, Brotherick I, Bishop RI, White MD, McKenna DM, Horne CH, Shenton BK, Neal DE, Mellon JK. Cell adhesion molecules in bladder cancer: soluble serum E-cadherin correlates with predictors of recurrence. Br J Cancer. 1996;74:579-584.
32. Shirahama S, Furukawa F, Wakita H, Takigawa M. E- and P-cadherin expression in tumor tissues and soluble E-cadherin levels in sera of patients with skin cancer. J Dermatol Sci. 1996;13:30-36.
33. Velikova G, Banks RE, Gearing A, Hemingway I, Forbes MA, Preston SR, Hall NR, Jones M, Wyatt J, Miller K, Ward U, Al-Maskatti J, Singh SM, Finan PJ, Ambrose NS, Primrose JN, Selby PJ. Serum concentrations of soluble adhesion molecules in patients with colorectal cancer. Br J Cancer. 1996;77:1857-1863.
34. Varras M, Skafida E, Vasilakaki T, Anastasiadis A, Akrivis C, Vrachnis N, Nikolopoulos G. Expression of E-cadherin in primary endometrial carcinomas: clinicopathological and immunohistochemical analysis of 30 cases. Eur J Gynaecol Oncol. 2013;34:31-35.

35. Zhou XM, Zhang H, Han X. Role of epithelial to mesenchymal transition proteins in gynecological cancers: pathological and therapeutic perspectives. Tumour Biol. 2014;35:9523-9530.

36. Sheen-Chen SM, Chen HS, Sheen CW, Eng HL, Chen WJ. Serum levels of transforming growth factor beta1 in patients with breast cancer. Arch Surg. 2001;136:937-940.

37. Li X, Yue ZC, Zhang YY, Bai J, Meng XN, Geng JS, Fu SB. Elevated serum level and gene polymorphisms of TGF-beta1 in gastric cancer. J Clin Lab Anal. 2008;22:164-171.

38. Fransvea E, Angelotti U, Antonaci S, Giannelli G. Blocking transforming growth factor-beta up-regulates E-cadherin and reduces migration and invasion of hepatocellular carcinoma cells. Hepatology. 2008;47:1557-1566.

39. Liu GL, Yang HJ, Liu T, Lin YZ. Expression and significance of E-cadherin, N-cadherin, transforming growth factor-β1 and Twist in prostate cancer. Asian Pac J Trop Med. 2014;7:76-82.

40. Cho IJ, Kim YW, Han CY, Kim EH, Anderson RA, Lee YS, Lee CH, Hwang SJ, Kim SG. E-cadherin antagonizes transforming growth factor β1 gene induction in hepatic stellate cells by inhibiting RhoA-dependent Smad3 phosphorylation. Hepatology. 2010;52:2053-2064.

Turk J Pharm Sci 2017;14(2):148-156
DOI: 10.4274/tjps.52523

ORIGINAL ARTICLE

Desloratadine-Eudragit® RS100 Nanoparticles: Formulation and Characterization

Desloratidin-Euragit® RS100 Nanopartikülleri: Formülasyon ve Karakterizasyon

Evrim YENİLMEZ

Anadolu University, Faculty of Pharmacy, Department of Pharmaceutical Technology, Eskişehir, Turkey

ABSTRACT

Objectives: The objective of the present study was to formulate Desloratadine-Eudragit® RS100 nanoparticles and investigate the characteristics of the prepared nanoparticles.

Materials and Methods: The nanoparticles were prepared by spray drying method and the quantification of desloratadine (DL) was carried out with a high performance liquid chromatography (HPLC) method.

Results: DL was successfully loaded to polymer and the developed HPLC method was found to be linear, reproducible, precise, accurate, specific and selective. Characterization of the nanoparticles including entrapment efficiency, particle size, zeta potential, morphology, polidispersity index, solid state characterizations and drug release was performed. *In vitro* release studies of DL loaded nanoparticles were also examined in the simulated intestinal fluid (pH 7.4). *In vitro* release of DL from nanoparticle formulations followed Korsemeyer-Peppas model.

Conclusion: A validated HPLC method was developed for the determination of DL. Proposed spray drying method can be successfully applicable to the nanoparticle preparation containing DL. In addition, the release studies of all nanoparticles and active substance have been studied comparatively. Hence, it could be concluded that DL loaded nanoparticles seem to be a promising drug delivery system for the active agent.

Key words: Desloratadine, Eudragit® RS100, HPLC, nanoparticle

ÖZ

Amaç: Bu çalışmanın amacı, Desloratadin-Eudragit® RS100 nanopartiküllerini formüle etmek ve hazırlanan nanopartiküllerin özelliklerini araştırmaktır.

Gereç ve Yöntemler: Nanopartiküller püskürterek kurutma yöntemi ile hazırlanmış ve miktar tayini yüksek basınçlı sıvı kromatografisi (YBSK) yöntemi ile yapılmıştır.

Bulgular: Desloratadin (DL) başarıyla polimere yüklenmiş ve geliştirilen YBSK yönteminin doğrusal, tekrarlanabilir, hassas, doğru, spesifik ve selektif olduğu bulunmuştur. Önerilen püskürterek kurutma yöntemi, DL içeren nanopartikül preparatının hazırlanmasında başarı ile kullanılmıştır. Nanopartiküllerin karakterizasyonu partikül boyutu, zeta potansiyel, morfoloji, polidispersite indeksi, katı hal karakterizasyonları ve etkin madde salımı dahil olmak üzere yapılmıştır. DL yüklü nanopartiküllerin *in vitro* salım çalışmaları, simüle edilmiş barsak vasatında (pH 7.4) incelenmiştir. Nanopartikül formülasyonlarından DL'nin *in vitro* salımı, Korsemeyer-Peppas modeline uymaktadır.

Sonuç: DL miktar tayini için YBSK yöntemi geliştirilmiştir. Önerilen püskürterek kurutma yöntemi, DL içeren nanopartikül preparatına başarıyla uygulanmıştır. Ayrıca, tüm nanopartiküllerin ve etkin maddenin salım çalışmaları karşılaştırmalı olarak incelenmiştir. Bu nedenle, DL yüklü nanopartiküllerin etkin madde için umut verici bir ilaç taşıyıcı sistem olduğu sonucuna varılabilir.

Anahtar kelimeler: Desloratadin, Eudragit® RS100, YBSK, nanopartikül

*Correspondence: **E-mail:** evrimakyi@anadolu.edu.tr, **Phone:** +90 532 557 54 09
ORCID ID: orcid.org/0000-0002-7979-0089
Received: 28.03.2017, **Accepted:** 03.06.2017

INTRODUCTION

Perennial allergic rhinitis affects up to 21% of the general population in some countries.[1] With the prevalence of the disease increasing, even greater numbers of the population will be affected in the future. Convenient treatment is so important to ease the signs and symptoms of allergic rhinitis like sneezing, rhinorrhea, nasal congestion and to improve patients quality of life. Desloratadine (DL) is a tricyclic antihistamine. It has an orally active nonsedating, peripheral histamine H1-receptor antagonist. DL inhibited histamine release from human mast cells *in vitro*. It has been used to treat allergy symptoms.[2] Old histamine H1 receptor antagonists have the potential for adverse central nervous system effects and are characterized by poor receptor specificity.[3] DL is slightly soluble in water and it has a reduced drug dissolution rate in gastrointestinal fluid following oral administration, and consequently, reduced bioavailability.[4]

In the recent decades nanoparticles containing drugs have gained increasing interest in pharmaceutic fields owing to their potential for site-specific drug delivery. The drugs are incorporated into a polymeric matrix, covalently bind to the polymer backbone or form electrolyte complexes of oppositely charged polymer-drug systems.[5] Drug dissolution rate could be controlled with different approaches such as formulation of nanoparticles.[6]

Eudragit® RS100 is a co-polymer of poly (ethylacrylate, methyl-methacrylate and chlorotrimethyl-ammonioethyl methacrylate), contains 4.5-6.8% of quaternary ammonium groups.[7] Biodegradable drug delivery systems consist of non-toxic, biodegradable polymers and are well tolerated by the human body. They are preferred for increasing the absorption of active substance, for increasing bioavailability and for targeting therapeutic agents to specific organs.[8] Eudragit RS-100 is a widely used polymer for the preparation of controlled release oral pharmaceutical dosage forms.[5,6,9] As a result, Eudragit® RS100 is a promising polymer for the transport of the active substance to the targeted region.

In this study, we investigate the possibility of the preparation of stable DL loaded nanoparticles by using spray-drying method without any cross-linked agent. The physicochemical properties of the obtained nanoparticles were characterized. In addition, the performed formulation and characterization studies results will be helpful to the future planned *in vivo* studies and in order to formulate DL nanoparticles to alternative dosage forms such as tablets or capsules for the usage in antihistaminic treatment.

MATERIALS AND METHOD

Materials

DL was a kind gift from Morepen Labs. (New Jesey, USA), Eudragit® RS100 was purchased from Evonic India Pvt. Ltd. Methanol and acetonitrile were obtained from Merck Chemical Co. (Germany). All the other chemicals were of analytical grade.

Preparation of nanoparticles

In this study, nanoparticles of DL with the different ratios of DL/Eudragit® RS100 were prepared using Buchi B-190 mini spray dryer (Büchi, Switzerland).[10,11] The spray dryer was connected to the Inert Loop B-295 (Büchi Labortechnik AG, Flawil, Switzerland) because of the organic solvent. Carbondioxide gas was used at a flow rate of 120 L/min. The inlet temperature was selected as 120°C for having maximum dried nanoparticles.[12,13] The residual oxygen level in the system was controlled below 4%. The fully weighed Eudragit polymer was dissolved in methanol by mixing at magnetic stirrer for 2 hours at 250 rpm. After the clear solution was obtained, DL was added and stirred for 10 more min at 250 rpm stirring speed. The transparent solution was run using 30 min of methanol for conditioning the device to the desired level in terms of parameters such as spraying, pump level, inlet temperature, outlet temperature, gas flow and ambient temperature. After the required conditions had been met, the clear solution was transferred to a dry nano-spray dryer, peristaltic pump with an inlet temperature of 120°C and an outlet temperature of 64°C and delivered to a drying zone with a 4 µm nozzle diameter. After the drying nanoparticles were collected in the collection chamber.

Characterization studies

The particle size distribution and zeta potential of the nanoparticles were measured at 25°C by dynamic light scattering (DLS) (Malvern Zetasizer-Nano ZS, Malvern Instruments Limited, UK). The morphology of the nanoparticles were carried out by with scanning electron microscope (SEM) and also fourier transform infrared spectroscopy (FTIR) analysis were done, respectively. The stability of spheres was tested using differential scanning calorimeter (DSC) analysis and nuclear magnetic resonance analysis (^{1}H-NMR) analysis. In order to determine release properties *in vitro* drug release mechanism was examined in the simulated biological fluid at pH 7.4. Encapsulation efficiency was also analyzed for the determination of the drug amount in the nanoparticle formulations.

Measurement of particle size and zeta potential

The particle size, size distribution and zeta potential of the nanoparticles were measured at 25°C by DLS (Malvern Zetasizer-Nano ZS, Malvern Instruments Limited, Worcestershire, UK). Samples of all nanoparticles were dispersed in double-distilled water (adjusted to a constant conductivity of 50 µS•cm^{-1} using 0.9% NaCl) just prior to analyses. All analyses were repeated in triplicate.

Scanning electron microscopy analysis

The particle shape and surface properties of the freshly prepared nanoparticle formulation and DL were investigated by SEM (Zeiss Ultra Plus Fesem, Germany) after spreading the formulation and DL onto the double-sided carbon tape pre-affixed on a specimen stub and were then allowed to dry at room-temperature. Samples were coated with a thin layer of gold (100 Å) by a sputter coater under 50 mA for 2 min before observed under SEM. Images were taken at high vacuum mode with varying magnifications at an accelerating voltage of 3.0 kV.

Differential scanning calorimetry

Thermal analysis of the DL formulation was carried out in

a pressure-assisted aluminum sample vessel using DSC (Schimadzu DSC-60, Japan) apparatus at a flow rate of nitrogen of 50 mL/dk^{-1} and at a temperature 25°C to a final temperature of 180°C at 10°C min^{-1} against aluminum reference. DSC experiments with pure DL were previously carried out to identify the melting point peak. As a control, physical mixtures of DL and polymer were also analyzed.[14]

Fourier transform infrared spectroscopy

The FTIR spectrum of the DL formulations were determined at a wavelength of 4000-500 cm^{-1} using FTIR (Schimadzu IR Prestige-21, Japan) instrument.

Nuclear magnetic resonance

^{1}H-NMR of the DL formulation prepared was carried out by dissolving in deutero chloroform (CDCl3), NMR (Bruker 500 MHz UltraShield NMR, Germany).

Entrapment efficiency

In order to determine the amount of DL in drug loaded nanoparticles, drug entrapment efficiency study was studied by validated high performance liquid chromatography (HPLC) method with the ultraviolet (UV) detection set in 262 nm. A reversed phase Lichrospher C18 column (150x2.3 mm i.d., pore size 5 µm) was used. The mobile phase consisted of a mixture of acetonitrile:water (60:40 v/v) and the flow rate was set at 0.8 mL/min. In the first step, in order to find free DL, the spray-dried nanoparticles (5 mg) were dissolved in 2 mL of distilled water in Eppendorf tube. After being held in the ultrasonic bath for 20 min, the upper transparent part was collected by centrifuging for 5 min at 13.000 rpm and the sample was analyzed through the necessary dilutions (1:1) with mobile phase. In the second step, 2 mL of the mobile phase, in which DL and Eudragit® RS100 are soluble, is added to the remaining residue formulation in the Eppendorf tube. Five min ultrasonic bath is used to obtain a clear solution and the sample was also analyzed through the necessary dilutions (1:1) with mobile phase in order to determine the amount of active substance entrapped. The experiments were repeated 3 times for each formulation. Before the injections, all solutions were previously filtered through a membrane filter (pore size 0.22 µm, Millipore). Entrapment efficiency (EE) was calculated using equation given below.[15]

EE (%)= Total DL - Free DL/Total DL x 100

In vitro drug release studies

Studies were performed in simulated intestinal fluid (SIF: pH 7.4), for a period of 24 h.[16-18] A dialysis (cellulose membrane) method was used to identify release behavior of nanoparticles. 5 mg nanoparticle formulation was weighed into the dialysis bag with 1 mL of dissolution medium. The dialysis bag which was sealed with clamps was placed in 50 mL of the SIF at 37±0.5°C under sink conditions and stirred at 100 rpm using magnetic stirrer. In order to determine the amount of DL released from the dialysis bag at different time intervals (5 min, 10 min, 15 min, 30 min, 45 min, 1 h, 2 h, 3 h, 4 h, 5 h 6 h, 24 h), 1 mL of the samples were picked up and then replaced with the 1 mL of fresh SIF. The concentration of drug released to the medium was determined by measuring the absorbance at 262 nm using HPLC Shimadzu liquid chromatography equipped with a model LC-10ATVP binary pump and model SPD-M10AVP PDA detector using the stationary phase 150x4.6 mm LiChrospher® 100 RP-18 octadecyl silane column (5 µm particle size) (Merck, Darmstadt, Germany) with integration by LC Solution Version 1.23 SP1 Software (Shimadzu Corporation, Kyoto, Japan). The mobile phase consisted of acetonitrile:water (60:40). The mobile phase was prepared daily and degassed by sonication under reduced pressure and filtered through 0.45 µm membrane filter. The flow rate was set at 0.8 mL/min resulting in a run time of 7 min per sample. The injection volume was 20 µL. Detection was performed at 262 nm and samples were analyzed at room temperature. In order to study the mechanism of drug release from nanoparticles, the release data were fitted to different equations with DDSolver programme.

RESULTS AND DISCUSSION

In the current study, a simple spray drying methods was used for the preperation of formulations. Differrent amounts of drug/polymer was formulated as given in Table 1.

Solubility characteristic of a drug is one of the main factor to decide about the method of encapsulation.[5] Spray drying methods was selected for the formulations.[10-12] Spray-drying parameters are given in Table 2.

All the prepared formulations were in nanometer size and the size distributions were relatively monodisperse in all the formulations with the polydispersity index (PDI) values between 0.113±0.25-0.412±0.30 (Table 3). Most researchers recognize PDI values ≤0.3 as optimum values; however, values ≤0.5 are also acceptable. According to our Results given in Table 3 formulations were in homogenous size distributions even after DL was loaded to polymer.[14,15,19]

Table 1. Composition of DL loaded eudragit RS®100 nanoparticles

Formulation code	DL (g)	Eudragit RS®100 (g)	Methanol (mL)
E1	0.1	1	100
E2	0.2	1	100
E3	0.3	1	100
Placebo	-	1	100

DL: Desloratadine

Table 2. Spray-drying parameters

Inlet air temperature (°C)	120
Aspirator rate (% flow) (m^3=h)	50-100%
Nozzle diameter (µm)	4
Outlet air temperature (°C)	64

Particle size is one of the important physical properties of colloidal systems. Particle size distribution of the formulation is especially significant in the physical stability (Figure 1) and activity of colloidal systems was also found that the size of nanoparticles plays a key role in their adhesion to and interaction with biological cells.[20]

The mean particle size of DL loaded nanoparticles of all formulations ranged from 312±1.32 nm to 485±1.05 nm with a relative monodisperse distribution (Table 3). Smaller particles have higher surface area/volume ratio, which makes it easier for the encapsulated drug to be released from the nanoparticles by diffusion and surface erosion and also have advantages for the drug loaded nanoparticles to penetrate into, and permeate through the physiological drug barriers.[21] The acceptable value for PDI is 0.05-0.7; values greater than 0.7 indicate very broad size distribution and probably no suitability for DLS technique.[19,20] Smaller size helps in targeting and increased penetration of drug through biological membranes.[22] Since it was reported that, change in the organic phase ratio may result the change in the viscosity of the system, which in turn can change the characteristics of the nanoparticles (e.g., particle size, encapsulation efficiency, surface morphology, etc.), therefore, different ratios of formulations were evaluated. It was noticed that the mean particle size increase with increases of drug concentration. Increase in particle size with the increase in drug concentration might have occurred due to the fact that it produces a significant increase in the viscosity and thus leading to an increase of the nanoparticle size, polymer concentration had profound effect on average particle size. This effect can be attributed to the effect of polymer concentration on the viscosity of the polymeric solution and need more energy to disperse the system.[23,24]

Table 3. Drug loading and particle size distribution of nanoparticle formulations

Formulations	Particle size (nm) ±SD	PDI ± SD	Zeta potential ±SD	Entrapment efficiency ±SD
E1	312±1.32	0.319±1.03	22.50±2.01	75.95±1.13
E2	412±0.29	0.354±0.34	25.10±1.74	64.07±1.40
E3	485±1.05	0.412±0.30	28.80±0.56	88.50±1.12
Placebo	112±1.73	0.113±0.25	15.40±0.83	-

PDI: Polydispersity index, SD: Standard deviation

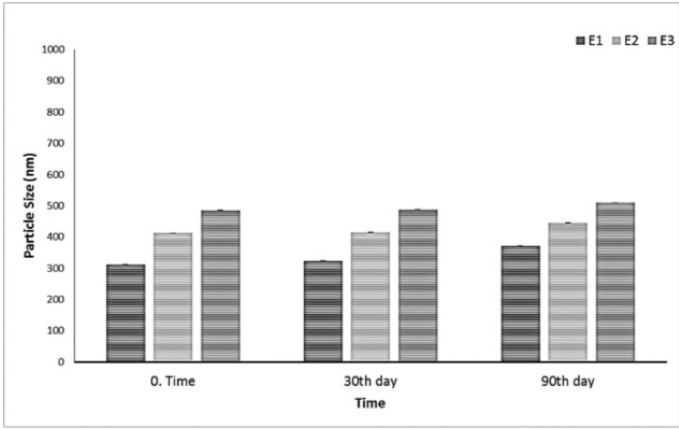

Figure 1. Particle size distribution of formulations during 3 months storage at 25˚C

The measurement of the zeta potential allows predictions of storage stability of colloidal dispersions.[20,21] Zeta potential of nanoparticles is commonly used to characterize the surface property of nanoparticles. The mean zeta potential of all formulations ranged from 15.40±0.83 mV to 28.80±0.56 mV, which may be attributed to the positive charges on polymer matrices indicating good physical stability as shown in Table 3. Cationic property of nanoparticles was determined due to the effect of positively charged quaternary ammonium groups in Eudragit® RS100 interact with the negatively charged mucus and open up the tight junctions of epithelial cells to allow the paracellular transport pathway resulting in an increase in bioavailability.[25,26] As a result of the stability studies of the formulations over 3 months, no statistically significant change was observed ($p>0.05$). This indicates the stability of the formulations.

From the SEM, it was observed that nanoparticles were usually spherical (Figure 3). The surface of the drug-loaded Eudragit RS100 nanoparticles manifested the presence of drug particles.[27]

DSC has shown to be an important tool to quickly obtain information about possible interactions between the active

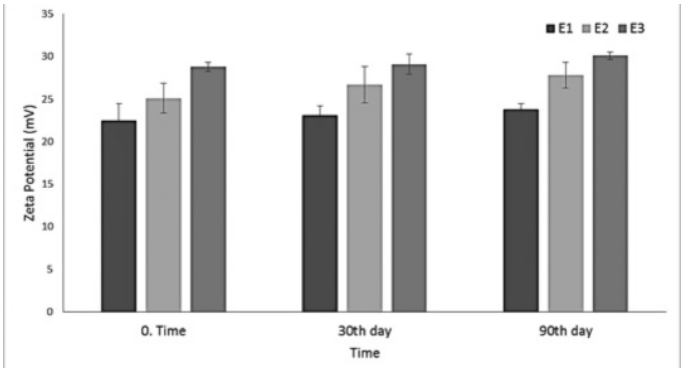

Figure 2. Zeta potential cahange of formulations during 3 months storage at 25˚C

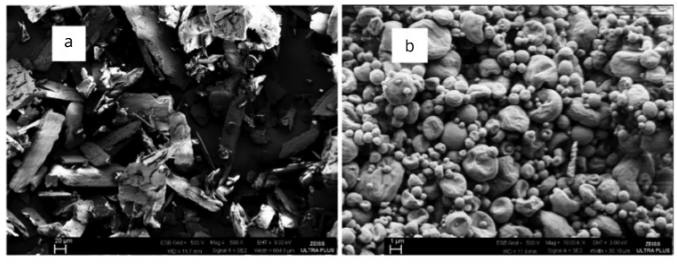

Figure 3. a) Scanning electron microscope photography of drug, b) scanning electron microscope photography of drug-loaded Eudragit RS100 nanoparticles (E1)

and the excipients, according to the appearance, shift, or disappearance of endothermic or exothermic peaks.[28] DSC gives an insight into melting and recrystallization behaviors of polymeric nanoparticles. No loss in typical peaks or no appearances of new peaks were recorded upon DSC analyses. This indicates that there was no physical or chemical interaction or incompatibility between the formulations prepared.[29] Accordingly, DSC measurements were performed on each of the components, both in their pure forms and the corresponding drug loaded forms (Figure 4).

FTIR spectroscopy is used as an important technique to investigate possible chemical interactions between drug and active substance. The formation of new absorption bands and the expansion of the absorption bands give the main signals of the interaction between the drug and the active substance.[28] The FTIR spectra show that the characteristic bands of DL and polymer individually were not altered in binary mixtures, which indicates no interactions between DL and the selected polymer when contact is established in spray dryer. The spectra of DL show prominent bands at 1.141 and 1.435 cm^{-1}, which is attributed to the C-C stretching of aromatic rings, while the bands at 1.172 and 778 cm^{-1} correspond to C-N amines and C-Cl stretching, respectively and is given in Figure 5.

These results are in agreement with other published datas.[27,29] The spectra of DL loaded polymer formulations show the same absorption bands, indicating that the DL did not decompose in the range of applied temperatures and successfully loaded to polymers. Therefore, DL is sufficiently thermally stable to allow analysis by the DSC method.

^{1}H-NMR investigations were used to obtain information about the mobility and structure of both the nanoparticle system and the incorporated drug. Comparing the drug-loaded nanoparticle formulations with each other no essential difference could be observed. On the other hand, the signals of pure drug are also seen in the same as the drug loaded formulations. This indicates that the active substance has been successfully loaded into the formulations. Peaks in 7-8 ppm interval belong to aromatic C-H peaks, peaks in 3-4 ppm belongs to -CH3 in the spectrum of DL.[30,31] Similar spectra were also obtained for the spectra of drug loaded nanoparticle formulations indicating the successful incorporation of drug into the nanoparticles. Physicochemical characterization was undertaken both by DSC and ^{1}H-NMR measurements. The combination of both analytical methods proved very suitable to obtain information about the structure of the DL loaded polymers.[31,32]

A simple and validated HPLC method was adopted and developed for the determination of DL. The method was validated for accuracy, precision and linearity with reference to the International Council for Harmonisation guidelines.[33] The separation and resolution of the peaks of the blank reagent and the formulation could be achieved using a mixture of acetonitrile:water (60:40 v/v) as the mobile phase with UV detection at 262 nm.[34] The method was found to be linear and reproducible. For the developed method the linear regression anaysis of the datas gave the following equation

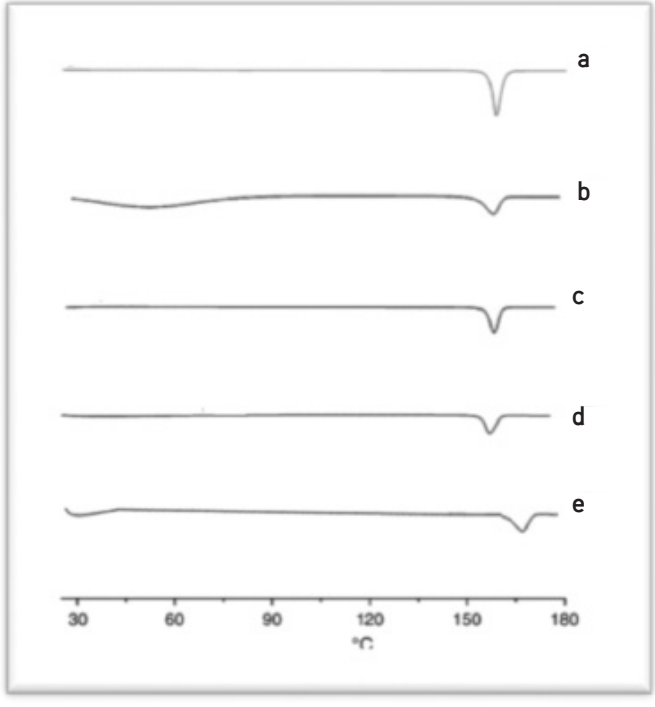

Figure 4. Differential scanning calorimeter curves of desloratadine (A), E1 (B), E2 (C), EC (D) and Eudragit® RS100 (E)

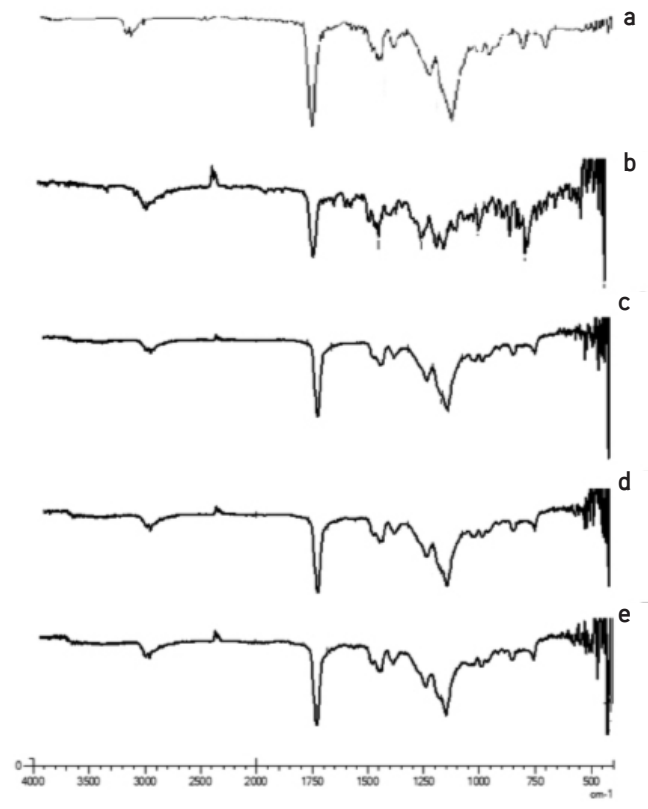

Figure 5. FTIR bands of Eudragit® RS100 (A), desloratadine (B), E1 (C), E2 (D) and E3 (E) formulations

A= 4096.6x+13453 with a correlation coefficient of, r=0.9999. Calibration curve of DL was constructed by plotting absorbance versus concentration which showed linearity over the concentration ranges of 100-700 µg/mL (Figure 7). The limit of quantification was determined as 0.290 µg/mL^{-1}, and the limit of detection was calculated as 0.628 µg/mL^{-1}.[35] Meanwhile the developed method was spesific for the determination of DL. The developed method is found to be precise, accurate, specific and selective. The method was also found to be linear and reproducible. According to the conditions described, the retention time was about 1.7 min for DL.

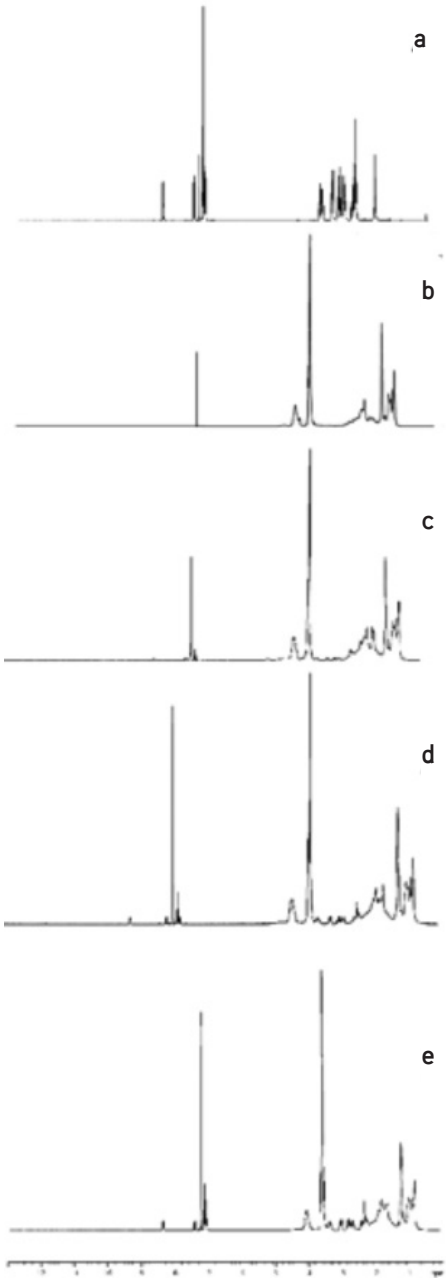

Figure 6. ^{1}H-NMR-spectrum of Eudragit® RS100 (A), DL (B), E1 (C), E2 (D) and E3 (E) formulations

The accuracy of the proposed method was assessed by recovery studies at different concentrations of 100 µg/mL^{-1}, 400 µg/mL^{-1}, 700 µg/mL^{-1}. The recovery studies were carried out by adding the known amount of standard solution of the pure drug. The solutions were analysed by proposed method, the results were given in Table 4.

The precision of the method was assessed by carrying out six replicate determination of three different concentrations of DL both inter-day and intra-day. The results are shown in Table 5. The method was found to be precise as indicated by the results showing % relative standard deviation less than 2.

The encapsulation efficiency explains that it is the percentage of the amount of the drug that loaded to drug carrier agent. In this study, the % EE of formulations E1, E2 and E3 were found as 75.95±1.13, 64.07±1.40 and 88.50±1.12 respectively. Drug-polymer composition is most likely the main factor for release rate, however it seems that a complex phenomena between drug and polymer molecules may occur, including entrapment of drug within polymer molecules and the adsorption of drug molecules on the surface of polymeric matrix as a result of electrostatic adhesions.[5,21]

Eudragit® RS100 as a water-insoluble carrier was identified to be able to control drug release in both nanoparticles and solid dispersions.[9,35] Figure 8 demonstrates the DL release profiles from Eudragit® RS100 polymers. There were no noteworthy differences between formulations as stated by the release profiles. All the nanoparticles revealed slower drug release rate in comparison with the intact drug. The release rate was not affected by increasing the Eudragit® RS100 relative amount in the nanoparticles. The released profiles of DL loaded formulations exhibited a burst release in one hour time which was attributed to the drug loaded the surface of nanoparticles.[5,20]

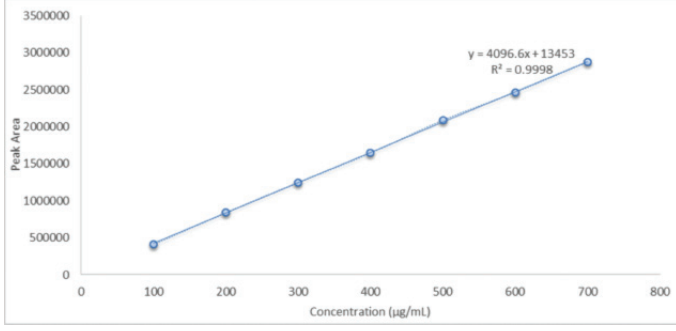

Figure 7. Calibration curve of desloratadine

Table 4. Accuracy results of desloratadine

Concentration (µg/mL)	Mean Rec. %	Difference %	SD	RSD	SE	CI (95%)
100	100.3	0.344	0.833	0.831	0.340	0.874
400	100.6	0.626	0.152	0.152	0.062	0.160
700	100.1	0.154	0.158	0.158	0.064	0.166

SD: Standard deviation, RSD: Relative standard deviation, SE: Standard error, CI: Confidence level

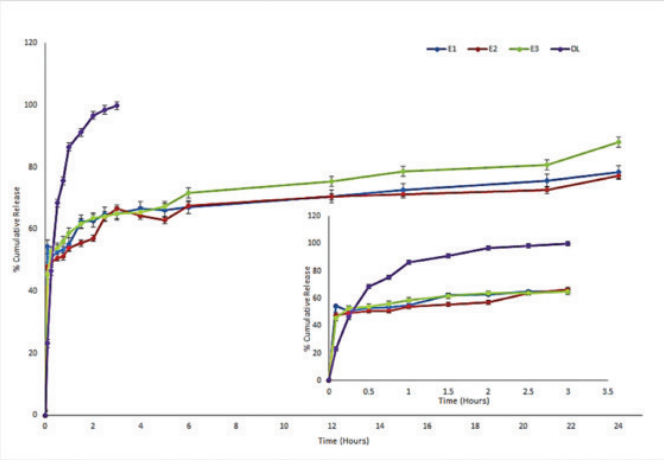

Figure 8. *In vitro* release of formulations and pure desloratadine (n=7)

Table 5. The results of intra-day and Inter-day precision of desloratadine

Concentration		Intra-day		Inter-day
150 µg/mL	**Day 1**	**Day 2**	**Day 3**	
SD	0.833	0.264	0.176	0.270
RSD	0.830	0.263	0.175	0.027
CI (95%)	0.874	0.277	0.184	0.134
300 µg/mL	**Day 1**	**Day 2**	**Day 3**	
SD	0.610	0.763706	0.763	0.399607
RSD	0.151	0.190509	0.190	1.553771
CI (95%)	0.641	0.801461	0.801	0.19872
500 µg/mL	**Day 1**	**Day 2**	**Day 3**	
SD	1.110	0.765	0.352	0.742
RSD	0.158	0.109	0.050	1.479
CI (95%)	1.165	0.803	0.369	0.369

SD: Standard deviation, RSD: Relative standard deviation, CI: Confidence level

When nanoparticles of microcrystalline drug particles, are exposed to aqueous media, the carrier dissolves and the drug is released as a fine colloidal dispersion, thus resulting in higher surface area and consequently, enhanced dissolution rate and bioavailability of poorly water soluble drugs.[36,37]

In order to study the mechanism of drug release from nanoparticles, the release data were fitted to different equations with DDSolver programme (Table 6).[38] Furthermore a kinetic parameter can be used to study the influence of formulation factors on the drug release for optimization as well as control of release.[38] The kinetic models used were zero-order, first-order, Higuchi, Korsemeyer-Peppas models. According to highest k and r^2 values and according to lowest AIC values, *in vitro* release of all DL loaded polymer formulations followed Korsemeyer-Peppas model.[39] This model indicates a diffusion controlled drug release mechanism from polymer matrix.[40]

CONCLUSION

As indicated with this study, formulations of DL-Eudragit® RS100 nanoparticles applying single spray drying procedure is able to improve the physicochemical characteristics of the drug. The HPLC method that was validated for DL was also found to be a simple and rapid method. The DSC and NMR studies confirmed the decrease of drug crystallinity in the nanoparticles. The intermolecular interaction between DL and Eudragit® RS100 was identified in the FTIR spectrum of the nanoparticles. DL was successfully formulated as a model drug in this study. It was shown that all nanoparticles displayed a slowed release pattern with a burst release in comparison with the pure drug powder. The advances in the formulation technology of nanoparticle delivery systems has been widely accepted approach as compared to conventional immediate release formulations of the same drug. Hence it could be concluded that DL loaded nanoparticles seem to be a promising delivery system for the drug.

Additionally, formulation studies that we have undertaken in this study will be helpful to the future planned *in vivo* studies to convert DL nanoparticles into alternative dosage forms such as tablets or capsules for use in antihistaminic treatment.

Table 6. Mathematical modelling of desloratadine loaded nanoparticles

Kinetic model	E1			E2			E3		
	k	r^2	AIC*	k	r^2	AIC*	k	r^2	AIC*
Zero order model	0.005	-0.005	0.178	0.005	-0.005	0.177	0.005	-0.004	0.178
First order model	0.000	-0.003	0.169	0.000	-0.003	0.168	0.000	-0.002	0.167
Hixson Crowell Model	0.000	-0.003	0.172	0.000	-0.003	0.170	0.000	-0.002	0.170
Korsmeyer Peppas model	**0.059**	**0.001**	**0.081**	**0.056**	**0.001**	**0.080**	**0.058**	**0.001**	**0.070**
Higuchi Model	0.023	-0.002	0.164	0.022	-0.002	0.162	0.024	-0.001	0.163

*AIC: Akaike information criterion

ACKNOWLEDGEMENT

The author would like to thank to BIBAM (Anadolu University) management for spray dryer equipments and the author would like to thank to Exp. Serkan Levent from Anadolu University, Faculty of Pharmacy, Department of Pharmaceutical Chemistry for NMR and FTIR analyses.

Conflict of Interest: No conflict of interest was declared by the author.

REFERENCES

1. Simons FE, Prenner BM, Finn A Jr; Desloratadine Study Group. Efficacy and safety of desloratadine in the treatment of perennial allergic rhinitis. J Allergy Clin Immunol. 2003;111:617-622.
2. Zheng J, Rustum AM. Rapid separation of desloratadine and related compounds in solid pharmaceutical formulation using gradient ion-pair chromatography. J Pharm Biomed Anal. 2010;51:146-152.
3. Veronez IP, Daniel JSP, Junior CEC, Garcia JS, Trevisan MG. Development, characterization, and stability studies of ethinyl estradiol solid dispersion. J Therm Anal Calorim. 2014;120:573-581.
4. Kolašinac N, Kachrimanis K, Homšek I, Grujić B, Đurić Z, Ibrić S. Solubility enhancement of desloratadine by solid dispersion in poloxamers. Int J Pharm. 2012;436:161-170.
5. Adibkia K, Javadzadeh Y, Dastmalchi S, Mohammadi G, Niri FK, Alaei-Beirami M. Naproxen-eudragit RS100 nanoparticles: preparation and physicochemical characterization. Colloids Surf B Biointerfaces. 2011;83:155-159.
6. Adibkia K, Mohajjel Nayebi A, Barzegar-Jalali M, Hosseinzadeh S, Ghanbarzadeh S, Shiva A. Comparison of the Analgesic Effect of Diclofenac Sodium-Eudragit® RS100 Solid Dispersion and Nanoparticles Using Formalin Test in the Rats. Adv Pharm Bull. 2015;5:77-81.
7. Kiliçarslan M, Baykara T. The effect of the drug/polymer ratio on the properties of the verapamil HCl loaded microspheres. Int J Pharm. 2003;252:99-109.
8. Bodmeier R, Chen H. Preparation and characterization of microspheres containing the anti-inflammatory agents, indomethacin, ibuprofen, and ketoprofen. J Control Release. 1989;10:167-175.
9. Barzegar-Jalali M, Alaei-Beirami M, Javadzadeh Y, Mohammadi G, Hamidi A, Andalib S, Adibkia K. Comparison of physicochemical characteristics and drug release of diclofenac Sodium-Eudragit® RS100 nanoparticles and solid dispersions. Powder Technology. 2012;219:211-216.
10. Lee SH, Heng D, Ng WK, Chan HK, Tan RB. Nano spray drying: a novel method for preparing protein nanoparticles for protein therapy. Int J Pharm. 2011;403:192-200.
11. Li X, Anton N, Arpagaus C, Belleteix F, Vandamme TF. Nanoparticles by spray drying using innovative new technology: the Büchi nano spray dryer B-90. J Control Release. 2010;147:304-310.
12. Pradhan R, Kim SY, Yong CS, Kim JO. Preparation and characterization of spray-dried valsartan-loaded Eudragit® E PO solid dispersion microparticles. Asian J Pharm Sci. 2016;11:744-750.
13. Paudel A, Loyson Y, Van den Mooter G. An investigation into the effect of spray drying temperature and atomizing conditions on miscibility, physical stability, and performance of naproxen-PVP K 25 solid dispersions. J Pharm Sci. 2013;102:1249-1267.
14. Gill P, Moghadam TT, Ranjbar B. Differential Scanning Calorimetry Techniques: Applications in Biology and Nanoscience. J Biomol Tech. 2010;21:167-193.
15. Karabey-Akyurek Y, Nemutlu E, Bilensoy E, Oner L. An Improved and Validated HPLC Method for the Determination of Methylprednisolone Sodium Succinate and its Degradation Products in Nanoparticles. Curr Pharm Anal. 2017;13:162-168.
16. Borges O, Cordeiro-da-Silva A, Romeijn SG, Amidi M, de Sousa A, Borchard G, Junginger HE. Uptake studies in rat Peyer's patches, cytotoxicity and release studies of alginate coated chitosan nanoparticles for mucosal vaccination. J Control Release. 2006;114:348-358.
17. Kalaria DR, Sharma G, Beniwal V, Ravi Kumar MN. Design of biodegradable nanoparticles for oral delivery of doxorubicin: *in vivo* pharmacokinetics and toxicity studies in rats. Pharm Res. 2009;26:492-501.
18. Kawadkar J, Chauhan Meenakshi K, Ram A. Evaluation of potential of Zn-pectinate gel (ZPG) microparticles containing mesalazine for colonic drug delivery. DARU. 2010;18:211-220.
19. Büyükköroğlu G, Kaytaz Şenel B, Karabacak RB. Preparation and *In Vitro* Evaluation of DNA-Bonded Polymeric Nanoparticles as New Approach for Transcutaneous Vaccination. Lat Am J Pharm. 2017;36:730-739.
20. Kırımlığlu-Yurtdaş G, Yazan Y. Formulation and *In Vitro* Characterization of Polymeric Nanoparticles Designed for Oral Delivery of Levofloxacin Hemihydrate. Eur Int J Scie Technol. 2016;5:148-157.
21. Thagele R, Mishra A, Pathak AK. Formulation and characterization of clarithromycin based nanoparticulate drug delivery system. Int J Pharm Life Sci. 2011;2:510-515.
22. Vasir JK, Reddy MK, Labhasetwar VK. Nanosystems in Drug Targeting: Opportunities and Challenges. Curr Nanosci. 2005;1:47-64.
23. Sharma N, Madan P, Lin S. Effect of process and formulation variables on the preparation of parenteral paclitaxel-loaded biodegradable polymeric nanoparticles: A co-surfactant study. Asian J Pharm Sci. 2016;11:404-416.
24. Yeo Y, Baek N, Park K. Microencapsulation methods for delivery of protein drugs. Biotechnology and Bioprocess Engineering. 2001;6:213-230.
25. Trivedi P, Verma A, Garud N. Preparation and characterization of aceclofenac microspheres. Asian J Pharm. 2008;2:110-115.
26. Ubrich N, Schmidt C, Bodmeier R, Hoffman M, Maincent P. Oral evaluation in rabbits of cyclosporin-loaded Eudragit RS or RL nanoparticles. Int J Pharm. 2005;288:169-175.
27. Joshi AS, Patil CC, Shiralashetti SS, Kalyane NV. Design, characterization and evaluation of Eudragit microspheres containing glipizide. Drug Invention Today. 2013;5:229-234.
28. Daniel JSP, Veronez IP, Rodrigues LL, Trevisan MG, Garcia JS. Risperidone-solid-state characterization and pharmaceutical compatibility using thermal and non-thermal techniques. Thermochimica Acta. 2013;568:148-155.
29. Büyükköroğlu G, Yazan EY, Öner AF. Preparation and physicochemical characterizations of solid lipid nanoparticles containing DOTAP® for DNA delivery. Turk J Chem. 2015;39:1012-1024.
30. Devane MA, Shaikh SR. Formulation and evaluation of Desloratadine orodispersible tablets by using ß-cyclodextrin and superdisintegrants. J Pharm Res. 2011:4;3327-3330.
31. Mu S, Liu Y, Gong M, Liu DK, Liu CX. Synthesis and biological evaluation of substituted desloratadines as potent arginine vasopressin V2 receptor antagonists. Molecules. 2014;19;2694-2706.

32. Ali SM, Upadhyay SK, Maheshwari A. NMR spectroscopic study of the inclusion complex of desloratadine with β-cyclodextrin in solution. J Incl Phenom Macrocycl Chem. 2007;59:351-355.

33. ICH-Q2 (R1) International Conference on Harmonisation of Technical Requirements for Registration of Pharmaceuticals for Humen Use 2005; http//www.ich.org [Accessed: 20.02.2015].

34. El-Enany N, El-Sherbiny D, Belal F. Spectrophotometric, spectrofluorometric and HPLC determination of desloratadine in dosage forms and human plasma. Chem Pharm Bull (Tokyo). 2007;55:1662-1670.

35. "Guidance for Industry Bioanalytical Method Validation, US Department of Health and Human Services, Food and Drug Administration," Center for Drug Evaluation and Research, Rockville, MD, May, 2001. http://www.fda.gov/eder/guidance/4252fnl.pdf (accessed September 1, 2004).

36. Lee VH. Nanotechnology: challenging the limit of creativity in targeted drug delivery. Adv Drug Deliv Rev. 2004;56:1527-1528.

37. Serajuddin, A. Solid dispersion of poorly water-soluble drugs: Early promises, subsequent problems, and recent breakthroughs. J Pharm Sci. 1999;88:1058-1066.

38. Zhang Y, Huo M, Zhou J, Zou A, Li W, Yao C, Xie S. DDSolver: an add-in program for modeling and comparison of drug dissolution profiles. AAPS J. 2010;12:263-271.

39. Barzegar-Jalali M, Adibkia K, Valizadeh H, Shadbad MR, Nokhodchi A, Omidi Y, Mohammadi G, Nezhadi SH, Hasan M. Kinetic analysis of drug release from nanoparticles. J Pharm Pharm Sci. 2008;11:167-177.

40. Singhvi G, Singh M. Review: *in vitro* drug release characterization models. Int J Pharm Stud Res. 2011;2:77-84.

Turk J Pharm Sci 2017;14(2):157-163
DOI: 10.4274/tjps.25743

ORIGINAL ARTICLE

Antibacterial, Antitubercular and Antiviral Activity Evaluations of Some Arylidenehydrazide Derivatives Bearing Imidazo[2,1-*b*]thiazole Moiety

İmidazo[2,1-*b*]tiyazol Çekirdeği Taşıyan Bazı Arilidenhidrazit Türevlerinin Antibakteriyel, Antitüberküler ve Antiviral Aktivite Tayinleri

Nuray ULUSOY GÜZELDEMİRCİ[1]*, Berin KARAMAN[1], Ömer KÜÇÜKBASMACI[2]

[1]İstanbul University, Faculty of Pharmacy, Department of Pharmaceutical Chemistry, İstanbul, Turkey
[2]İstanbul University, Cerrahpaşa Faculty of Medicine, Department of Microbiology, İstanbul, Turkey

ABSTRACT

Objectives: The aim of this study was to determine the probable antibacterial, antitubercular, and antiviral activities of some N^2-arylidene-(6-(4-chlorophenyl)imidazo[2,1-*b*]thiazol-3-yl) acetic acid hydrazides **(3a-j)**. Further structural optimization of the identified lead structures can lead us to new more active potential antibacterial, antitubercular, and antiviral agents.

Materials and Methods: Antibacterial activities of the title compounds against *Staphylococcus aureus* ATCC 29213, *Pseudomonas aeruginosa* ATCC 27853 and *Escherichia coli* ATCC 25922. These molecules were also evaluated for their *in vitro* antitubercular activity against *Mycobacterium tuberculosis* H37Rv (ATCC 27294) using the BACTEC 460 radiometric system and BACTEC 12B medium. Moreover, all the compounds **(3a-j)** were also evaluated against some DNA and RNA viruses in Madin-Darby Canine Kidney, Crandell-Rees Feline Kidney (CRFK), Vero, human embryonic lung (HEL) and HeLa cells.

Results: Among the tested compounds, **3i** displayed the highest efficacy against *S. aureus* and *E. coli*. Compound **3j**, 5-nitro-2-furfurylidene derivative showed the highest antituberculosis activity (IC_{50}: 6.16 µg/mL and IC_{90}: 14.390 µg/mL). Compound **3i** showed the most potent antiviral activity against feline corona virus in CRFK cell cultures (antiviral EC_{50}: 7.5 µM and SI>13). Furthermore, compounds **3c** and **3g** displayed activity against herpes simplex virus-1 and vaccinia virus in HEL cell cultures (antiviral EC_{50} values of 9; 16 and 20; 14 µM, respectively).

Conclusion: On the basis of aforementioned results, it can be conluded that imidazo[2,1-*b*]thiazole derivatives bearing hydrazone moieties serve as promising chemical probes to design therapeutic agents with antibacterial, antitubercular, and antiviral properties.

Key words: Imidazo[2,1-*b*]thiazole, arylidenehydrazide, antibacterial activity, antitubercular activity, antiviral activity

ÖZ

Amaç: Bu çalışmanın amacı, bazı N^2-ariliden-(6-(4-klorofenil)imidazo[2,1-*b*]tiyazol-3-il) asetik asit hidrazitlerinin **(3a-j)** olası antibakteriyel, antitüberküler ve antiviral aktivitelerinin tayin edilmesidir. Tanımlanmış yapıların ileri yapısal optimizasyonu, bizi daha aktif potansiyel antibakteriyel, antitüberküler ve antiviral ajanlara ulaştırabilir.

Gereç ve Yöntemler: Söz konusu bileşiklerin antibakteriyel aktiviteleri, *Staphylococcus aureus* ATCC 29213, *Pseudomonas aeruginosa* ATCC 27853 ve *Escherichia coli* ATCC 25922'ye karşı tayin edilmiştir. Bu moleküllerin, *Mycobacterium tuberculosis* H37Rv (ATCC 27294) karşı *in vitro* antitüberküler aktiviteleri de BACTEC 460 radiometrik sistem ve BACTEC 12B ortamı kullanılarak tayin edilmiştir. Dahası, bileşiklerin tümü **(3a-j)**, Madin-Darby Canine Kidney, Crandell-Rees Feline Kidney (CRFK), Vero, insan embriyonik akciğeri (HEL) ve HeLa hücrelerinde bazı DNA ve RNA virüslerine karşı tayin edilmiştir.

*Correspondence: E-mail: nulusoy@istanbul.edu.tr, Phone: +90 532 574 92 63
ORCID ID: orcid.org/0000-0002-4495-4282
Received: 16.08.2016, Accepted: 23.10.2016

Bulgular: Test bileşikleri arasında, **3i**, *S. aureus* ve *E. coli*'ye karşı en yüksek etkinliği göstermiştir. 5-Nitro-2-furfuriliden türevi **3j** bileşiği, en yüksek antitüberküler aktivite göstermiştir (IC_{50}: 6.16 µg/mL ve IC_{90}: 14.390 µg/mL). Bileşik **3i**, en güçlü antiviral aktiviteyi CRFK hücre kültürlerinde feline corona virüse karşı göstermiştir (antiviral EC_{50}: 7.5 µM ve SI>13). Ayrıca, **3c** ve **3g** bileşikleri HEL hücre kültürlerinde, herpes simpleks virüs-1 ve aşı virüsüne karşı aktivite göstermişlerdir (antiviral EC_{50} değerleri sırasıyla 9; 16 ve 20; 14 µM'dir).

Sonuç: Yukarıda sözü edilen sonuçlara dayanarak, hidrazon çekirdeği taşıyan imidazo[2,1-*b*]tiyazol türevleri, antibakteriyel, antitüberküler ve antiviral özelliklere sahip terapötik ajanlar tasarlamak için umut verici kimyasal problar olarak yarar sağlayabilir.

Anahtar kelimeler: İmidazo[2,1-*b*]tiyazol, arilidenhidrazid, antibakteriyel aktivite, antitüberküler aktivite, antiviral aktivite

INTRODUCTION

Infectious diseases caused by bacteria have increased dramatically in recent years. Despite many significant advances in antibacterial therapy, the widespread use and misuse of antibiotics have led to the emergence of bacterial resistance to antibiotics, which is a serious threat to public health. On the other hand, tuberculosis (TB), still remains the leading cause of worldwide death among infectious diseases.[1,2] In 2014, there were an estimated 9.6 million new TB cases: 5.4 million among men, 3.2 million among women and 1.0 million among children.[3] Additionally, viral infections caused by the rapid emergence of antiviral drug resistant strains have become a serious threat globally.[4] Many diseases are actually caused by the different members of DNA- and RNA-containing viruses. Among DNA-containing viruses, the herpes group of viruses, particularly herpes simplex virus-1 (HSV-1) primarily causes encephalitis, stomatitis, ocular infections and HSV-2 primarily causes genital lesions, skin eruptions or cytomegalovirus is related with severe morbidity and mortality in patients at risk for disease because of immune system disabilities and varicella-zoster virus is the ethiological agent of chickenpox and shingles.[5,6] Influenza (INF) viruses, parainfluenza-3 virus, alphaviruses (e.g. sindbis virus), respiratory syncytial virus (RSV) and vesicular stomatitis virus (VSV) are examples of enveloped single-stranded RNA-containing viruses. VSV causes an economically important disease in horses and cattle.[7] Both RSV and parainfluenza-3 virus are an important cause of respiratory tract infections.[8,9]

Among the heterocyclic rings containing bridgehead nitrogen atom, imidazo[2,1-*b*]thiazoles derivatives are especially attractive because of their different biological activities such us antibacterial,[10] antituberculosis,[11] antiviral,[12] anticancer,[13] antiinflammatory[14] and diuretic[15] activities. On the other hand, arylidenehydrazide moiety are also associated with various biological properties including antibacterial,[16] antitubercular,[17] antiviral,[18] anticancer,[19] antiinflammatory and analgesic[20] activities.

In continuation of our previous studies on the biological properties of imidazo[2,1-*b*]thiazole derivatives,[21-27] in this study, we reported the antibacterial, antitubercular and antiviral activity evaluation of some arylidenehydrazide derivatives bearing imidazo[2,1-*b*]thiazole moiety.

MATERIALS AND METHODS

Chemistry

All chemicals were purchased from Merck (Darmstadt, Germany) or Sigma-Aldrich (St. Louis, MO, USA) chemical companies. Using a Büchi B-540 melting point apparatus (Flawil, Switzerland) with open capillaries, melting points were determined and are uncorrected. Elemental analyses were performed on a Thermo Finnigan Flash EA 1112 elemental analyser. Infrared spectra were recorded (in KBr) using a Perkin Elmer Spectrum 100 fourier transform infrared (FTIR) spectrometer and Shimadzu IRAffinity-1 FTIR spectrophotometer. ^{1}H and ^{13}C-nuclear magnetic resonance spectra were obtained on Varian UNITY INOVA 500 MHz spectrometer using dimetil sulfoxide-d_6 as an internal standard. All chemical shifts were reported as δ (ppm) values and spin-spin couplings (J) were exposed in Hz. MS (ESI-) were determined on a Finnigan LCQ Advantage Max mass spectrometer.

General synthesis of N^2-arylidene-(6-(4-chlorophenyl) imidazo[2,1-b]thiazol-3-yl)acetic acid hydrazides (**3a-3j**)[28]

A solution of 0.005 mol compound **2** and 0.005 moL of an appropriate aromatic aldehyde in 100 mL ethanol was heated under reflux for 5 h. The precipitate obtained was purified either by recrystallization from ethanol or by washing with hot ethanol.

Biological activity

Antibacterial activity

Minimum inhibitory concentrations (MICs) were determined by the microbroth dilution method using the National Committee for Clinical Laboratory Standards recommendations.[29] Mueller-Hinton broth (Oxoid, Hemakim, Turkey) was used as the test medium. An inoculum of approximately $5x10^5$ CFU cm^{-3} was delivered per well. Serial twofold dilutions of the test compounds (128-0.25 µg/mL) and extra dilutions (256-0.25 µg/mL) for antibiotic standards were prepared. Plates were incubated for 16-20 h at 35°C in an ambient air incubator. The lowest concentration of the test compounds inhibiting visible growth was taken as the MIC value.

Antitubercular activity

In vitro evaluation of antitubercular activity

Primary screening was conducted at 6.25 mg/mL against *Mycobacterium tuberculosis* $H_{37}Rv$ in BACTEC 12B medium using a broth microdilution assay the Microplate Alamar Blue Assay (MABA).[30] Compounds exhibiting fluorescence were tested in the BACTEC 460 radiometric system.[31] Compounds effecting <90% inhibition in the primary screen were not generally evaluated further. Compounds demonstrating at least 90% inhibition in the primary screen were re-tested at lower concentrations against *M. tuberculosis* $H_{37}Rv$ in order

to determine the actual MIC using MABA. The MIC was defined as the lowest concentration effecting a reduction in fluorescence of 90% relative to the controls. Concurrently with the determination of MICs, compounds were tested for cytotoxicity (IC_{50}) in VERO cells at concentrations £6.25 mg/mL or 10 times the MIC for *M. tuberculosis* H_{37}Rv (solubility in media permitting). After 72 h exposure, viability was assessed on the basis of cellular conversion of 3-(4,5-dimethylthiazol-2-yl)-2,5-diphenyl tetrazolium bromide into a formazan product using the Promega CellTiter 96 Non-radioactive Cell Proliferation Assay. Compounds for which the selectivity index (IC_{50}: MIC ratio) SI>10 were assumed to possess *in vitro* activity confirmed in the BACTEC 460 at 6.25 mg/mL.

Microplate alamar blue susceptibility assay

Antimicrobial susceptibility testing was performed in black, clear-bottomed, 96-well microplates (black view plates; Packard Instrument, Meriden, Connecticut, USA) in order to minimize background fluorescence. Outer perimeter wells were filled with sterile water to prevent dehydration in experimental wells. Initial drug dilutions were prepared in either dimethyl sulfoxide or distilled deionized water, and subsequent twofold dilutions were performed in 0.1 mL of 7H9GC (no Tween 80) in the microplates. BACTEC 12B-passaged inocula were initially diluted 1:2 in 7H9GC, and 0.1 mL was added to wells. Subsequent determination of bacterial titers yield $1x10^6$ CFU/mL in plate wells for H_{37}Rv. Frozen inocula were initially diluted 1:20 in BACTEC 12B medium followed by a 1:50 dilution in 7H9GC. Addition of 1/10 mL to wells resulted in a final bacterial titers of $2.0x10^5$ CFU/mL for H_{37}Rv. Wells containing drug only were used to detect autofluorescence of compounds. Addition control wells consisted of bacteria only (B) and medium only (M). Plates were incubated at 37˚C. Starting at day 4 of incubation, 20 mL of 10x Alamar Blue solution (Alamar Biosciences/Accumed, Westlake, Ohio, USA) and 12.5 mL of 20% Tween 80 were added to one B well an done M well, and plates were reincubated 37˚C. Wells were observed at 12 and 24 h for a color change from blue to pink and for a reading of ≥50.000 fluorescence units (FU). Fluorescence was measured in a Cytofluor II microplate fluorometer (Perseptive Biosystems, Framingham, Massachusetts, USA) in bottom-reading mode with excitation at 530 nm and emission at 590 nm. If the B wells became pink by 24 h, reagent was added to the entire plate. If the well remained blue or £50.000 FU was measured, additional M and B wells were tested daily until a color change occurred, at which time reagents were added to all remaining wells. Plates were then incubated at 37˚C, and results were recorded at 24 h post-reagent addition. Visual MICs were defined as the lowest concentration of drug that had prevented a color change. For fluorometric MICs, a background subtraction was performed on all wells with a mean of triplicate M wells. Percent inhibition was defined as 1-(test well FU/mean FU triplicate B wells) x 100. The lowest drug concentration effecting an inhibition of ≥90% was considered the MIC.

BACTEC radiometric method of susceptibility testing

Inocula for susceptibility testing were either from a positive BACTEC isolation vial with a growth index (GI) of 500 or more, or a suspension of organisms isolated earlier on a conventional medium. The culture was well mixed with a syringe and 0.1 mL of a positive BACTEC culture was added to each of the vials containing the test compounds (6.25 mg/mL). The standard vials contained rifampicin (0.25 mg/mL). A control vial was inoculated with a 1:100 dilution of the culture. Each vial was tested immediately on a BACTEC instrument to provide CO_2 in the headspace. The vials were incubated at 37˚C and tested daily with a BACTEC instrument. When the GI in the control read at least 30, the increase in GI (ΔGI) from the previous day in the control was compared with that in the drug vial. The following formula was used to interpret the results:

ΔGI control > ΔGI drug = susceptible

ΔGI control < ΔGI drug = resistant

If a clear susceptibility pattern (the difference of ΔGI of control and the drug bottle) was not seen at the time the control GI was 30 the vials were read for 1 or 2 additional days to establish a definite pattern of ΔGI differences.

Antiviral activity

The compounds (**3a**-**j**) were evaluated for activity against diverse RNA- and DNA-viruses, using the following cell-based assays[32]: (a) Madin-Darby Canine Kidney (MDCK) cells infected with INF A/H1N1 subtype (A/Ned/378/05), INF A/H3N2 subtype (A/HK/7/87) or INF B (B/Ned/537/05); (b) Crandell-Rees Feline Kidney (CRFK) cells infected with feline corona virus (FCoV) or feline herpes virus (FHV); (c) African green monkey kidney Vero cells infected with parainfluenza-3 virus, reovirus-1, Sindbis virus, Coxsackie B4 virus or Punta toro virus; (d) human embryonic lung (HEL) fibroblast cells infected with HSV-1 or -2, an acyclovir-resistant HSV-1 strain, vaccinia virus, VSV; (e) human cervixcarcinoma Henrietta Lacks (HeLa) cells infected with VSV, coxsackie B4 virus or RSV.

To perform the antiviral assays, the virus was added to subconfluent cell cultures in 96-well plates, and at the same time, the test compounds were added at serial dilutions. Appropriate reference compounds were included, i.e. the virus entry inhibitor dextran sulfate 5000, the broad antiviral agent ribavirin, the antiherpetic drug ganciclovir, and the HIV inhibitor azidothymidine. After 3-6 days incubation at 37˚C (or 35˚C in the case of INF virus), the cultures were examined by microscopy to score the compounds' inhibitory effect on virus-induced cytopathic effect or their cytotoxicity. For some viruses, antiviral and cytotoxic activities were confirmed by the colorimetric 3-(4,5-carboxymethoxyphenyl)-2-(4-sulfophenyl)-2H-tetrazolium cell viability assay.

RESULTS AND DISCUSSION

The key intermediate **2** was prepared from ethyl (6-(4-chlorophenyl)imidazo[2,1-*b*]thiazol-3-yl)acetate hydrobromide (**1**) and hydrazine hydrate following the literature method.[33] The synthetic route of the compounds is outlined in Scheme 1. Condensation of **2** with appropriate aromatic aldehyde afforded the corresponding *N*^{2}-arylidene-(6-(4-

chlorophenyl)imidazo[2,1-*b*]thiazol-3-yl)acetic acid hydrazides (**3a-j**).[28]

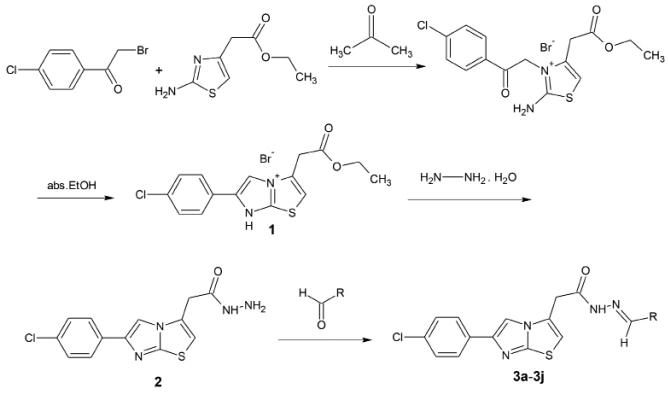

Scheme 1. Synthesis of the title compounds **(3a-j)**

Compounds **3a-j** were evaluated for *in vitro* antibacterial activity against *Staphylococcus aureus* ATCC 29213, *Pseudomonas aeruginosa* ATCC 27853 and *Escherichia coli* ATCC 25922 using the microbroth dilution method[29]. As can be seen in Table 1, **3i** (2,4-dichlorobenzylidene derivative) showed the highest activity against *S. aureus* ATCC 29213 and *E. coli* ATCC 25922 (*MIC*: 2 µg/mL, 64 µg/mL, respectively).

Compounds **3a-j** were evaluated against *M. tuberculosis* $H_{37}Rv$ (ATCC 27294) in BACTEC 12B medium using a broth microdilution assay, the MABA. The primary antituberculosis screening was performed in accordance with the protocol of the Tuberculosis Antimicrobial Acquisition and Coordinating Facility Southern Research Institute[30]. Rifampin was used as the control drug in the tests. Compounds demonstrating a percent inhibition of bacterial growth of greater than or equal to 90% in the primary screen were retested against *M. tuberculosis* $H_{37}Rv$, to determine the actual MIC in the MABA. The MIC was defined as the lowest concentration effecting a reduction in fluorescence of 90%, relative to controls. This value was determined from the dose-response curve as the IC_{90} using a curve fitting program. Any IC_{90} value of ≤10 µg/mL was considered "Active" for antitubercular activity. Compounds active in the initial screen were tested for IC_{50} in Vero cells. Cytotoxicity was determined from the dose-response curve as the IC_{50} using a curve fitting program. Concurrent with the determination of MICs, compounds were tested for cytotoxicity in Vero cells at concentrations 10x the MIC for *M. tuberculosis* $H_{37}Rv$. Most of the tested compounds showed weakly antitubercular activity and cytotoxicities of the compounds were found to be very high (Table 2).

The compounds (**3a-j**) were also evaluated against INF A/H1N1 subtype (A/Ned/378/05), INF A/H3N2 subtype (A/HK/7/87), INF B (B/Ned/537/05) in MDCK, FCoV, FHV in CRFK, parainfluenza-3 virus, reovirus-1, sindbis virus, coxsackie B4 virus, punta toro virus in Vero, HSV-1 (KOS), HSV-2 (G), HSV-1 TK KOS ACV, vaccinia virus, VSV, in HEL and VSV, coxsackie B4 virus and RSV in HeLa cell cultures. As can be seen in Table 3, the most active compound was R=2,4-dichlorophenyl substituted **3i**. It inhibited FCoV with EC_{50} of 7.5 µM. R=4-hydroxyphenyl substituted derivative **3c**, inhibited HSV-1 (KOS), HSV-2 (G), HSV-1 TK KOS ACV, vaccinia virüs and VSV with EC_{50} of 9, 27, 32, 16 and 32 µM, respectively. R=3-methoxy-4-hydroxyphenyl substituted 3g *showed* EC_{50} values of 20 and 14 µM for HSV-1 (KOS) and v virus, respectively (Table 4). However, tested compounds (**3a-j**) didn't show any inhibition against INF A/H1N1 subtype (A/Ned/378/05), INF A/H3N2 subtype (A/HK/7/87), INF B (B/Ned/537/05), parainfluenza-3

Table 1. Antibacterial activity of compounds 3a-j (MIC mg/mL)

Comp./ *microorg.	R	A	B	C
3a	C6H5	128	>128	128
3b	$C_6H_4(OH)(2-)$	>128	>128	>128
3c	$C_6H_4(OH)(4-)$	128	128	>128
3d	$C_6H_4(OCH3)(4-)$	64	128	128
3e	$C_6H_4(NO_2)(4-)$	>128	>128	>128
3f	$C_6H_4(N(CH_3)_2)(4-)$	128	>128	128
3g	$C_6H_3(OCH_3)(OH)(3,4-)$	128	>128	>128
3h	$C_6H(OCH_3)_2(2,5-)$	>128	>128	128
3i	$C_6H(Cl_2)(2,4-)$	32	>128	64
3j	5-nitro-2-furyl	128	128	128
Amikacin	-	1	1	2

MIC: Minimum inhibitory concentrations, *A: *Staphylococcus aureus* ATCC 29213, B: *Pseudomonas aeruginosa* ATCC 27853, C: *Escherichia coli* ATCC 25922

Table 2. Antimycobacterial activity screening results of 3a-j (MIC mg/mL)

Compound	Assay	IC_{50} (mg/mL)	IC_{90} (mg/mL)	Activity
3a	n.t.	n.t.	n.t.	n.t.
3b	MABA	>100	>100	Inactive
3c	MABA	22.710	33.060	Weakly active
3d	MABA	69.170	>100	Weakly active
3e	MABA	>100	>100	Inactive
3f	MABA	>100	>100	Weakly active
3g	MABA	20.670	36.860	Weakly active
3h	MABA	44.720	>100	Weakly active
3i	MABA	>100	>100	Inactive
3j	MABA	6.16	14.390	Weakly active
Rifampicin			0.125	

MIC: Minimum inhibitory concentrations, MABA: Microplate Alamar Blue Assay, n.t.: not tested

virus, reovirus-1, sindbis virus, coxsackie B4 virus, punta toro virüs, VSV, coxsackie B4 virus and RSV strains (i.e. minimal antivirally effective concentration ≥5-fold lower than minimal cytotoxic concentration) (Table 5).

CONCLUSION

In this work, a series of arylidenehydrazide derivatives bearing imidazo[2,1-*b*]thiazole moiety was evaluated for antibacterial, antitubercular and antiviral activities. The results showed that some compounds exhibited antibacterial, antimycobacterial and antiviral activities with different percentage of inhibition. Therefore, we have identified a novel series of imidazo[2,1-*b*] thiazoles, which may develop into the potential class of antibacterial, anti-tubercular and antiviral agents.

ACKNOWLEDGEMENTS

We thank Prof. Lieve Naesens from the Rega Institute for Medical Research, Katholieke Universiteit Leuven, B-3000 Leuven, Belgium for evalution of antiviral activity. We thank Dr. Joseph A. Maddry from the Tuberculosis Antimicrobial Acquisition and Coordinating Facility (TAACF), National Institute of Allergy and Infectious Diseases Southern Research Institute, Alabama, USA, for the evaluation of anti-TB activity. The present work was supported by İstanbul University Scientific Research Projects (Project No: 49399).

Table 3. Anti-feline corona virus and anti-feline herpes virus activity and cytotoxicity of the compounds 3a-j in Crandell-Rees Feline Kidney cell cultures

Compound	CC_{50}[a] (μM)	EC_{50}[b] (μM)	
		FCoV	FHV
3a	>100	>100	>100
3b	50.6	>20	>20
3c	20.7	>20	>20
3d	>100	>100	>100
3e	4.4	>4	>4
3f	50.8	>20	>20
3g	24.5	>20	>20
3h	>100	>100	>100
3i	>100	7.5	54.8
3j	9.7	>4	>4
HHA (μg/mL)	>100	5.3	8.8
UDA (μg/mL)	>100	17.7	12.9
Ganciclovir (μM)	>100	>100	3.6

FCoV: Feline corona virüs, FHV: Feline herpes virüs, HHA: Hippeastrum hybrid agglutinin, UDA: Urtica dioica agglutinin, MTS: 3-(4,5-dimethylthiazol-2-yl)-5(3-carboxymethonyphenol)-2-(4-sulfophenyl)-2H-Tetrazolium, [a]50% cytotoxic concentration, as determined by measuring the cell viability with the colorimetric, formazan-based MTS assay, [b]50% effective concentration, or concentration producing 50% inhibition of virus-induced, cytopathic effect, as determined by measuring e cell viability with the colorimetricformazan-based MTS assay

Table 4. Antiviral activity and cytotoxicity of the compounds 3a-j in human embryonic lung cell cultures

Compound	MCC[a] (μM)	EC_{50}[b] (μM)				
		Herpes simplex virus-1 (KOS)	Herpes simplex virus-2 (G)	Herpes simplex virus-1 TK KOS ACV^r	Vaccinia virus	Vesicular stomatitis virus
3a	>100	>100	>100	>100	>100	>100
3b	>100	>100	>100	>100	>100	>100
3c	≥100	9	27	32	16	32
3d	100	>20	>20	>20	>20	>20
3e	>100	>100	>100	>100	>100	>100
3f	>100	>100	>100	>100	>100	>100
3g	500	20	>100	>100	14	>100
3h	100	>20	>20	>20	>20	>20
3i	100	>20	>20	>20	>20	>20
3j	>100	>100	>100	>100	>100	>100
Brivudin	>250	0.05	199	10	10	>250
Ribavirin	>250	2	2	2	10	>250
Cidofovir	>250	0.7	1.1	3.5	>250	>250
Ganciclovir	>100	0.03	0.03	0.1	>100	>100

[a]Required to cause a microscopically detectable alteration of normal cell morphology, [b]Required to reduce virus-induced cytopathogenicity by 50%

Table 5. Antiviral activity and cytotoxicity of the compounds 3a-j in Vero cell cultures

Compound	MCC[a] (μM)	EC_{50}[b] (μM)				
		Parainfluenza-3 virus	Reovirus-1	Sindbis virus	Coxsackie virus B4	Punta Toro virus
3a	>100	>100	>100	>100	>100	>100
3b	100	>20	>20	>20	>20	>20
3c	20	>4	>4	>4	>4	>4
3d	>100	>100	>100	>100	>100	>100
3e	20	>4	>4	>4	>4	>4
3f	>100	>100	>100	>100	>100	>100
3g	40	>8	>8	>8	>8	>8
3h	100	>20	>20	>20	>20	>20
3i	≥20	>20	>20	>20	>20	>20
3j	100	>20	>20	>20	>20	>20
DS-5000 (μM)	>100	>100	>100	15	>100	20
(S)-DHPA (μM)	>250	>250	>250	>250	>250	>250
Ribavirin (μM)	>250	29	146	>250	>250	112

[a]Required to cause a microscopically detectable alteration of normal cell morphology, [b]Required to reduce virus-induced cytopathogenicity by 50%

Conflict of Interest: No conflict of interest was declared by the authors.

REFERENCES

1. Krasnov VP, Vigorov AY, Musiyak VV, Nizova IA, Gruzdev DA, Matveeva TV, Levit GL, Kravchenko MA, Skornyakov SN, Bekker OB, Danilenko VN, Charushin VN. Synthesis and antimycobacterial activity of *N*-(2-aminopurin-6-yl) and *N*-(purin-6-yl) amino acids and dipeptides, Bioorg Med Chem Lett. 2016;26:2645-2648.
2. Bhowruth V, Dover LG, Besra GS. Tuberculosis chemotherapy: recent developments and future perspectives. Prog Med Chem. 2007;45:169-203.
3. WHO Global Tuberculosis Report, 2015. http://apps.who.int/iris/bitstream/10665/191102/1/9789241565059_eng.pdf (accessed August, 2016).
4. Xue S, Ma L, Gao R, Lin Y, Li Z, Synthesis and antiviral activity of some novel indole-2-carboxylate derivatives. Acta Pharm Sin B. 2014;4:313-321.
5. El-Sabbagh OI, Baraka MM, Ibrahim SM, Pannecouque C, Andrei G, Snoeck R, Balzarini J, Rashad AA. Synthesis and antiviral activity of new pyrazole and thiazole derivatives. Eur J Med Chem. 2009;44:3746-3753.
6. Gudmundsson KS, Johns BA, Allen SH. Pyrazolopyridines with potent activity against herpesviruses: effects of C5 substituents on antiviral activity. Bioorg Med Chem Lett. 2008;18:1157-1161.
7. Romanutti C, Castilla V, Coto CE, Wachsman MB. Antiviral effect of a synthetic brassinosteroid on the replication of vesicular stomatitis virus in Vero cells, Int J Antimicrob Agents. 2007;29:311-316.
8. Andries K, Moermans M, Grevers T, Willebrords R, Sommen C, Lacrampe J, Janssens F, Wyde PR. Substituted benzimidazoles with nanomolar activity against respiratory syncytial virüs. Antiviral Res. 2003;60:209-219.
9. Wyde PR, Chetty SN, Timmerman P, Gilbert BE, Andries K. Short duration aerosols of JNJ 2408068 (R170591) administered prophylactically or therapeutically protect cotton rats from experimental respiratory syncytial virus infection. Antiviral Res. 2003;60:221-231.
10. Juspin T, Laget M, Terme T, Azas N, Vanelle P. TDAE-assisted synthesis of new imidazo[2,1-*b*]thiazole derivatives as anti-infectious agents, Eur J Med Chem. 2010;45:840-845.
11. Andreani A, Granaiola M, Leoni A, Locatelli A, Morigi R, Rambaldi M. Synthesis and antitubercular activity of imidazo[2,1-*b*]thiazoles. Eur J Med Chem. 2001;36:743-746.
12. Barradas JS, Errea MI, D'Accorso NB, Sepúlveda CS, Damonte EB. Imidazo [2,1-*b*]thiazole carbohydrate derivatives: Synthesis and antiviral activity against Junin virus, agent of Argentine hemorrhagic fever. Eur J Med Chem. 2011;46:259-264.
13. Ding H, Chen Z, Zhang C, Xin T, Wang Y, Song H, Jiang Y, Chen Y, Xu Y, Tan C. Synthesis and cytotoxic activity of some novel *N*-pyridinyl-2-(6-phenylimidazo[2,1-*b*]thiazol-3-yl)acetamide derivatives, Molecules. 2012;17:4703-4716.
14. Abdelal AM, Gineinah MM, Tayel MM, Tantawy A. Imidazo[2,1-*b*]thiazoles: Synthesis and antiinflammatory activity of some new 3,5-disubstituted 6-phenylimidazo[2,1-*b*]thiazoles. Sci Pharm. 1993;61:21.
15. Andreani A, Rambaldi M, Mascellani G, Rugarli Pi. Synthesis and diuretic activity of imidazo[2,1-*b*]thiazole acetohydrazones. Eur J Med Chem. 1987;22:19-22.
16. Küçükgüzel ŞG, Rollas S, Erdeniz H, Kiraz M. Synthesis, characterization and antimicrobial evaluation of ethyl 2-arylhydrazono-3-oxobutyrates. Eur J Med Chem. 1999;34:153-160.
17. Eldehna WM, Fares M, Abdel-Aziz MM, Abdel-Aziz HA, Design, synthesis and antitubercular activity of certain nicotinic acid hydrazides. Molecules. 2015;20:8800-8815.

18. Narang R, Narasimhan B, Sharma S, Sriram D, Yogeeswari P, De Clercq E, Pannecouque C, Balzarini J. Synthesis, antimycobacterial, antiviral, antimicrobial activities, and QSAR studies of nicotinic acid benzylidene hydrazide derivatives. Med Chem Res. 2012;21:1557-1576.

19. Sundaree S, Vaddula BR, Tantak MP, Khandagale SB, Shi C, Shah K, Kumar D. Synthesis and anticancer activity study of indolyl hydrazide-hydrazones. Med Chem Res. 2016;25:941-950.

20. Navidpour L, Shafaroodi H, Saeedi-Motahar G, Shafiee A. Synthesis, anti-inflammatory and analgesic activities of arylidene-2-(3-chloroanilino) nicotinic acid hydrazides. Med Chem Res. 2014;23:2793-2802.

21. Ulusoy Güzeldemirci N, Şatana D, Küçükbasmacı Ö. Synthesis, characterization, and antimicrobial evaluation of some new hydrazinecarbothioamide, 1,2,4-triazole and 1,3,4-thiadiazole derivatives. J Enzyme Inhib Med Chem. 2013;28:968-973.

22. Ulusoy Güzeldemirci N, Küçükbasmacı Ö. Synthesis and antimicrobial activity evaluation of new 1,2,4-triazoles and 1,3,4-thiadiazoles bearing imidazo[2,1-*b*]thiazole moiety. Eur J Med Chem. 2010;45:63-68.

23. Gürsoy E, Güzeldemirci NU. Synthesis and primary cytotoxicity evaluation of new imidazo[2,1-*b*]thiazole derivatives. Eur J Med Chem. 2007;42:320-326.

24. Ulusoy N, Kiraz M, Küçükbasmacı Ö. New 6-(4-bromophenyl)-imidazo[2,1-*b*]thiazole derivatives: Synthesis and antimicrobial activity. Monatsh Chem. 2002;133:1305-1315.

25. Ulusoy N. Synthesis and antituberculosis activity of cycloalkylidenehydrazide and 4-aza-1-thiaspiro[4.5]decan-3-one derivatives of imidazo[2,1-*b*]thiazole. Arzneim-Forsch/Drug Res. 2002;52:565-571.

26. Ulusoy N, Çapan G, Ötük G, Kiraz M. Synthesis and antimicrobial activity of new 6-phenylimidazo[2,1-*b*]thiazole derivatives. Boll Chim Farmaceutico. 2000;139:167-172.

27. Çapan G, Ulusoy N, Ergenç N, Kiraz M. New 6-phenylimidazo[2,1-*b*] thiazole derivatives: Synthesis and antifungal activity. Monatsh Chem. 1999;130:1399-1407.

28. Karaman B, Ulusoy Güzeldemirci N. Synthesis and biological evaluation of new imidazo[2,1-b]thiazole derivatives as anticancer agents. Med Chem Res. 2016;25:2471-2484.

29. Clinical and Laboratory Standards Institute. Performance standards for antimicrobial testing, (15th ed). Informational supplement. M100-S15. Wayne, PA; Clinical and Laboratory Standards Institute; 2005.

30. Collins LA, Franzblau SG. Microplate alamar blue assay versus BACTEC 460 system for high-throughput screening of compounds against *Mycobacterium tuberculosis* and *Mycobacterium avium*. Antimicrob Agents Chemother. 1997;41:1004-1009.

31. Inderleid CB. Antibiotics in Laboratory Medicine. In: Lorian V, ed. (3rd ed). Williams & Wilkins; Baltimore; 1991:134.

32. Krečmerová M, Holý A, Pohl R, Masojidková M, Andrei G, Naesens L, Neyts J, Balzarini J, De Clercq E, Snoeck R. Ester prodrugs of cyclic 1-(S)-[3-hydroxy-2-(phosphonomethoxy)propyl]-5-azacytosine: synthesis and antiviral activity. J Med Chem. 2007;50:5765-5772.

33. Harraga S, Nicod L, Drouhin JP, Xicluna A, Panouse JJ, Seilles E, Robert JF. Imidazo[2,1-*b*]thiazole derivatives. XI. Modulation of the CD2-receptor of human T trypsinized lymphocytes by several imidazo[2,1-*b*]thiazoles. Eur J Med Chem. 1994;29:309-315.

Turk J Pharm Sci 2017;14(2):164-168
DOI: 10.4274/tjps.43434

ORIGINAL ARTICLE

Activation of Two Different Drugs Used in Alzheimer's Disease Treatment on Human Carbonic Anhydrase Isozymes I and II Activity: an *In Vitro* Study

Alzheimer Hastalığının Tedavisinde Kullanılan İki Farklı İlacın İnsan Karbonik Anhidraz I ve II İzoenzim Aktiviteleri Üzerindeki Aktivasyonu: *İn Vitro* Çalışma

Esra DİLEK

Erzincan University, Faculty of Pharmacy, Department of Biochemistry, Erzincan, Turkey

ABSTRACT

Objectives: Human carbonic anhydrase I and II (hCAI, II) isoenzymes were purified from human erythrocyte. Kinetic interactions between the enzymes and memantine and donepezil, two different drugs used in Alzheimer's disease (AD) treatment, were investigated.

Materials and Methods: The purification procedure was composed of preparation of homogenate (or hemolysate) and affinity chromatography on Sepharose 4B-L-tyrosine-sulfanilamide.

Results: Both drug exhibited *in vitro* activator effects on hCAI and II enzymes activity. Strong activations were found for these compounds: The CA values of memantine and donepezil against hCAI were 0.013 µM and 1.8 µM, respectively. The K_A values of memantine and donepezil against hCAII were 0.045 µM and 3.7 µM, respectively.

Conclusion: Since the levels of CA isoenzymes are low in patients with AD or in the older population, increasing activities of these isoenzymes are important for these patients. The effect of these drugs used in AD treatment was thought to be caused by positive changes in the levels of carbonic anhydrase isoenzymes.

Key words: Human CAI, human CAII, enzyme activation, memantine, donepezil

ÖZ

Amaç: İnsan karbonik anhidraz I ve II (hCAI ve II) izoenzimleri insan eritrositlerinden saflaştırıldı. Alzheimer hastalığının (AH) tedavisinde kullanılan memantin ve donepezil ilaçlarının bu enzimlerle olan kinetik etkileşimleri incelendi.

Gereç ve Yöntemler: Saflaştırma prosedürü homojenat (ya da hemolizat) hazırlama ve Sefaroz-4B-L-tirozin-sülfonamid afinite kromotografisi yönteminden oluşmaktadır.

Bulgular: Her iki ilaç da CAI ve II izoenzim aktiviteleri üzerinde *in vitro* aktivatör etkisi gösterdi. Bu bileşikler için güçlü aktivasyon değerleri elde edildi: hCAI izoenzimine karşı memantin ve donepezil için CA değerleri sırasıyla 0.013 µM ve 1.8 µM. hCAII izoenzimine karşı memantin ve donepezil için K_A değerleri sırasıyla 0.045 µM and 3.7 µM.

Sonuç: AH ve yaşlı nüfusta CA izoenzim seviyeleri düşük olduğu için, bu hastalarda bu izoenzimlerin aktivitelerinin artması önem arz etmektedir. Bahsi geçen bu iki ilacın AH tedavisindeki etkisini CA izoenzimleri seviyesinde yapmış olduğu pozitif artış ile göstermiş olduğu düşünülmüştür.

Anahtar kelimeler: İnsan CAI, insan CAII, enzim aktivasyonu, memantin, donepezil

*Correspondence: **E-mail:** edilek@erzincan.edu.tr, **Phone:** +90 530 696 84 60
ORCID ID: orcid.org/0000-0002-3629-5168
Received: 05.09.2016, **Accepted:** 02.11.2016

INTRODUCTION

Carbonic anhydrases (CA) (CA, EC 4.2.1.1) are belong to family of metalloenzyme and have 16 isoforms in mammals. They catalyze from the reversible hydration of CO_2 to the bicarbonate ion and protons and are expressed as pH regulatory enzyme in most tissues especially in erythrocytes.[1-6] Many such CA isozymes which make these processes are important therapeutic targets with the potential to be inhibited/activated for the treatment of diseases such as glaucoma, edema, obesity, osteoporosis, epilepsy and cancer.[2-8] Activation of several these isoenzymes was reported to be a possible therapy for increasing of synaptic efficacy. This increase might represent the new approach for the treatment of Alzheimer's disease (AD). At the same time, it may ensure to improvement aging, spatial learning and memory therapy.[9]

AD is characterized clinically as a progressive dementia. The neurobiological mechanisms influencing the progressive impairments in memory and intellectual performance that are the hallmarks of AD are not well understood. In addition, the levels of several CA isozymes, including human carbonic anhydrase (hCAI), are diminished in patients affected by AD or in the older population.[10]

Several classes of CA activators are known. One of them is histamine. Histamine is an organic compound including nitrogen and both mediates local immune responses and acts as a neurotransmitter. It was reported to increase the activity of CA and to attend the proton shuttling process.[11] Function of CA activators is to bind at the entrance of the enzyme active site, at the same time to ease the proton transfer processes between active site and solvent system. Histidine, phenylalanine, sildenafil citrate have been shown to be potential activators of different CA isozymes. D-3,4-dihydroxyphenylalanine; dextrodopa (D-DOPA), L-Tyr, and 4-amino-L-Phe act as perfect activators for CAs like the histamine. But LHis, L-Trp, L-Adrenaline, and dopamine have been demonstrated weak activating effects for different CAs.[2,12-15]

Generally it is known that activators bind to different site from the inhibitors within the enzyme active cavity.[11,16] Also, they participate in facilitated the proton transfer processes between active site and solvent system, shuttling protons with groups which have an appropriate pKa such as the carboxylate groups.[17]

Memantine is an antagonist of N-methyl-D-aspartate glutamate receptors as uncompetitively. It is proposed to treat of patients with moderate to severe AD. Additionally, benefits of memantine in AD are reported.[18,19] Memantine was chosen because of its similarity to histamine which is activator of CA isoenzymes (Figure 1). Both compounds have -NH_2 group. Donepezil is a drug used in the palliative treatment of AD. It is approved for treatment in patients with mild to moderate AD.[20,21]

In light of the above information, we thought that these drugs could activate hCAI and II isoenzymes. We have purified hCAI and hCAII from human erythrocytes and analyzed the *in vitro* effects of these drugs memantine (1) and donepezil (2) on these isoenzymes. We used the esterase activity of hCAI and hCAII and 4-nitrophenyl acetate (NPA) as substrate. We are justified in our opinion. Because we found that memantine (1) and donepezil (2) are a potent activator of hCAI and hCAII.

RESULTS AND DISCUSSION

CA purification, assay and activation

We used a simple one step method which is the Sepharose-4B-L-tyrosine-sulfanilamide affinity chromatography for the purification of the two CA isozymes.[22,23] These isozymes have important roles in different tissues.[24-29] In many studies, they have been purified from different tissues. Theirs activity have been investigated with various chemicals, pesticides and drugs.[22,23,30-36] In this study, activities of purified hCAI and hCAII isoenzymes from human erythrocytes were determined by using the esterase activity method. And we used NPA as substrate as previous study.[36]

Activator effects of these drugs memantine (1) and donepezil (2) on enzyme activities were tested under *in vitro* conditions. %Activity / (drug concentration) curves was drawn (Figure 2, 3) and they was used at determination of activation constant (K_A) values of the drugs for CAI and II isoenzymes. The K_A values of memantine against hCAI was found to be 0.013 µM which whereas that of donepezil was of 1.8 µM. The K_A values of memantine against hCAII were found to be 0.045 µM whereas that of donepezil was of 3.7 µM (Table 1).

Histamine (3) which taken as the reference compound have

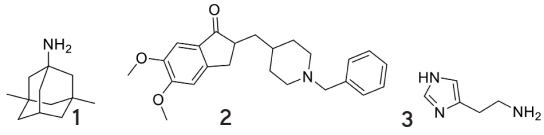

Figure 1. Chemical structures of memantine (1), donepezil (2) and histamine (3)

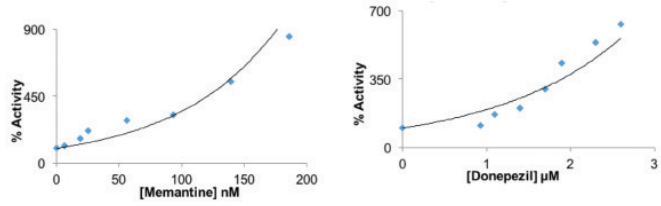

Figure 2. %Activity / (drug concentration) curves was used at determination of K_A values of the drugs for CAI isoenzyme

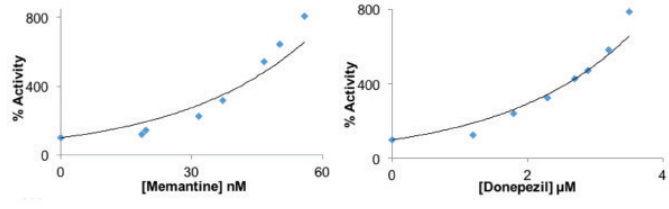

Figure 3. %Activity / (drug concentration) curves was used at determination of K_A values of the drugs for CAII isoenzyme

the K_A values against hCAI and hCAII of 2 µM, and 125 µM, respectively, being a highly potent activator against both the isoforms (Table 1).[37] The best activator of hCAI is memantine with respective K_A of 0.013 µM. Likewise, the best activator of hCAII is memantine with respective K_A of 0.045 µM. Donepezil activated hCAI almost the same rate compared with histamine. But it activated hCAII more activated than histamine (Table 1). As shown in Figure 1, memantine has bicyclic structure. Other structures are planar. Memantine has been easily interacted with the amino acids in active site of CA isoenzymes and these isoenzymes have been more active.

Memantine and donepezil acted as perfect activators for CAI and II isoenzymes like LHis, L-Adrenaline, D-DOPA, L-Tyr, and 4-amino-L-Phe. But these two isoenzymes more activated than L-Trp and dopamine have been demonstrated weak activating effects for different CAs.[2,12-15]

We reported here the first study on the activator effects of these drugs memantine (1) and donepezil (2) on the hCA esterase activity. The structures of active substances were shown in Figure 1. Consequently, memantine and donepezil are much more potent compared with histamine. These compounds may be used as leads for developing novel activators. This study will contribute to understand the relationship between CA isoenzymes and AD. Also, it will provide important information for the diagnosis of AD and its treatment.

EXPERIMENTAL

Chemicals

Sepharose-4B, protein assay reagents, 4-nitrophenylacetate and chemicals for electrophoresis were purchased from Sigma-Aldrich Co. All other chemicals were analytical grade and obtained from Merck.

Purification of carbonic anhydrase

Erythrocytes suspension was obtained from the Blood Center of the Research Hospital at Erzincan University. The red cells were washed twice with 0.9% NaCl, and hemolyzed with 1.5 volumes of ice-cold water. The ghost and intact cells were removed by centrifugation at 3100 g for 30 min at 4°C. The pH of the hemolysate was adjusted to 8.7 with a solid Tris base, and applied to the prepared Sepharose 4B-L-tyrosine-sulfonamide affinity column equilibrated with 25 mM Tris-HCl/22 mM Na_2SO_4 (pH 8.7).[22-25] The hCAI and hCAII isozymes were eluted with 1 M NaCl/25 mM Na_2HPO_4 (pH 6.3) and 0.1 M CH_3COONa/0.5 M $NaClO_4$ (pH 5.6), respectively. The absorbance of the protein in the column effluents was determined spectrophotometrically at 280 nm.[22,23,36]

Table 1. Activation constants of hCA isozymes I, and II with memantine, donepezil and histamine

Compound	K_A (µM)	
	hCAI	hCAII
Memantine	0.013	0.045
Donepezil	1.8	3.7
Histamine	2	125

K_A: Activation constant, hCA: Human carbonic anhydrase

CA activation assay

CA activity was assayed by following the change in absorbance at 348 nm of NPA to 4-nitrophenylate ion over a period of 3 min at 25°C using a spectrophotometer (Shimadzu UV-VIS) according to the method described by Verpoorte et al.[38] A reference measurement was obtained by preparing the same cuvette without enzyme solution.[39] The activation effects of memantine and donepezil were examined. Different activator concentrations were used. Stock solutions of activators (10 mM) were prepared in distilled-deionized water and dilutions up to 0.1-0.9 µM were done thereafter with the assay buffer. Then, %Activity / (drug concentration) curves was drawn (Figure 2, 3) and they was used at determination of K_A values of the drugs for CA I and II isoenzymes.

The K_A is defined similarly like the inhibition constant (K_i). It is obtained with the help of the classical Michaelis-Menten equation as shown below:

$$\upsilon = \upsilon_{max} / \{ 1 + \frac{K_M}{[S]\left(1 + \frac{[A]_f}{K_A}\right)} \}$$

$[A]_f$ is the free concentration of activator and can be represented in the form of the total concentration of the enzyme ($[E]_t$) and activator ($[A]_t$). Because we work at substrate concentrations considerably lower than K_M ($[S] \ll K_M$), the obtained competitive steady-state equation for determining the activation constant is given by the following equation:

$$\upsilon = \upsilon_o.K_A / \{K_A + [A]_t\}$$

$$-0.5\{([A]_t + [E]_t + K_A) - ([A]_t + [E]_t + K_A)2 - 4[A]_t.[E]_t)1/2\}$$

υ_o represents the initial velocity of the enzyme-catalyzed reaction without activator.[12,25,27]

Protein determination

We determined amount of protein during the purification steps according to the Bradford method. We measure it spectrophotometrically at 595 nm, using bovine serum albumin as the standard.[36,40-43] We have used ten tubes with different concentrations of albumin as shown in Figure 2. Then we mixed them with the Bradford reagent (Coomassie Brilliant Blue G-250) and measured the absorbance at 595 nm. Our unknown sample concentration was defined as µg/µL according to standard curve in Figure 4.

CONCLUSION

The K_A values of memantine against hCAI was found to be 0.013 µM which whereas that of donepezil was of 1.8 µM. The K_A

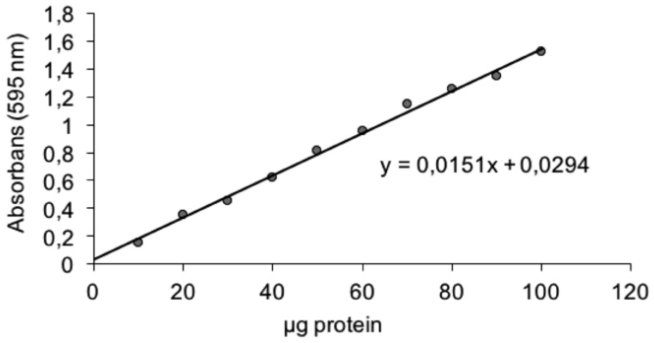

Figure 4. Protein standard curve displaying with just µg of protein at 595 nm

values of memantine against hCAII were found to be 0.045 µM whereas that of donepezil was of 3.7 µM (Table 1).

We used the histamine as the reference compound. It has the K_A values against hCAI and hCAII of 2 µM, and 125 µM, respectively. For two isoenzymes were reported that it is a highly potent activator.[37] It was reported that histamine attends the proton shuttling process and increases the activity of CA.[12]

Activation of these isoenzymes can be a potential target for drug development because of the physiological relevance of CAs.[2] CA activators may be designed as a derivative for increasing of synaptic efficacy.[37] The pharmacological effects of memantine and donepezil not yet been developed clinically for hCA I and hCA II isoenzymes. Thus, in the near future, the novel therapeutic applications will make for enzyme activators.

Conflict of Interest: No conflict of interest was declared by the author.

REFERENCES

1. Imtaiyaz Hassan M, Shajee B, Waheed A, Ahmad F, Sly WS. Structure, function and applications of carbonic anhydrase isozymes. Bioorg Med Chem. 2013;21:1570-1582.
2. Supuran CT, Vullo D, Manole G, Casini A, Scozzafava A. Designing of novel carbonic anhydrase inhibitors and activators. Curr Med Chem Cardiovasc Hematol Agents. 2004;2:49-68.
3. Supuran CT, Scozzafava A. Carbonic anhydrases as targets for medicinal chemistry. Bioorg Med Chem 2007;15:4336-4350.
4. Supuran CT. Carbonic anhydrases: novel therapeutic applications for inhibitors and activators. Nat Rev Drug Discov. 2008;7:168-181.
5. Innocenti A, Vullo D, Scozzafava A, Supuran CT. Carbonic anhydrase inhibitors: interactions of phenols with the 12 catalytically active mammalian isoforms (CAI-XIV). Bioorg Med Chem Lett. 2008;18:1583-1587.
6. Oztürk Sarikaya SB, Topal F, Sentürk M, Gülçin I, Supuran CT. *In vitro* inhibition of α-carbonic anhydrase isozymes by some phenolic compounds. Bioorg Med Chem Lett. 2011;21:4259-4262.
7. Nair SK, Ludwig PA, Christianson DW. Two site binding of phenol in the active site of human carbonic anhydrase II: structural implications for substrate association. J Am Chem Soc. 1994;116:3659-3660.
8. Casey JR. Why bicarbonate? Biochem Cell Biol. 2006;84:930-939.
9. Sun MK, Alkon DL. Carbonic anhydrase gating of attention: memory therapy and enhancement. Trends Pharmacol Sci. 2002;23:83-89.
10. Sultana R, Boyd-Kimball D, Poon HF, Cai J, Pierce WM, Klein JB, Merchant M, Markesbery WR, Butterfield DA. Redox proteomics identification of oxidized proteins in Alzheimer's disease hippocampus and cerebellum: an approach to understand pathological and biochemical alterations in AD. Neurobiology of Aging. 2006;27:1564-1576.
11. Briganti F, Mangani S, Orioli P, Scozzafava A, Vernaglione G, Supuran CT. Carbonic anhydrase activators: X-ray crystallographic and spectroscopic investigations for the interaction of isozymes I and II with histamine. Biochemistry. 1997;36:10384-10392.
12. Temperini C, Scozzafava A, Vullo D, Supuran CT. Carbonic anhydrase activators. Activation of isozymes I, II, IV, VA, VII, and XIV with l- and d-histidine and crystallographic analysis of their adducts with isoform II: engineering proton-transfer processes within the active site of an enzyme. Chemistry. 2006;12:7057-7066.
13. Abdülkadir Coban T, Beydemir S, Gülcin I, Ekinci D, Innocenti A, Vullo D, Supuran CT. Sildenafil is a strong activator of mammalian carbonic anhydrase isoforms I-XIV. Bioorg Med Chem. 2009;17:5791-5795.
14. Nishimori I, Onishi S, Vullo D, Innocenti A, Scozzafava A, Supuran CT. Carbonic anhydrase activators: the first activation study of the human secretory isoform VI with amino acids and amines. Bioorg Med Chem. 2007;15:5351-5357.
15. Dessirier JM, Simons CT, Carstens MI, O'Mahony M, Carstens E. Psychophysical and neurobiological evidence that the oral sensation elicited by carbonated water is of chemogenic origin. Chem Senses. 2000;25:277-284.
16. Ilies MI, Banciu MD, Ilies MA, Scozzafava A, Caproiu MT, Supuran CT. Carbonic anhydrase activators: design of high affinity isozymes I, II, and IV activators, incorporating tri-/tetrasubstituted-pyridinium-azole moieties. J Med Chem. 2002;45:504-510.
17. Briganti F, Iaconi V, Mangani S, Orioli P, Scozzafava A, Vernaglione G, Supuran CT. A ternary complex of carbonic anhydrase: X-ray crystallographic structure of the adduct of human carbonic anhydrase II with the activator phenylalanine and the inhibitor azide. Inorg Chim Acta. 1998:295-300.
18. Winblad B, Poritis N. Memantine in severe dementia: results of the 9M-Best Study (Benefit and efficacy in severely demented patients during treatment with memantine). Int J Geriatr Psychiatry. 1999;14:135-146.
19. Wilkinson D, Andersen HF. Analysis of the effect of memantine in reducing the worsening of clinical symptoms in patients with moderate to severe Alzheimer's disease. Dement Geriatr Cogn Disord. 2007;24:138-145.
20. Winblad B, Black SE, Homma A, Schwam EM, Moline M, Xu Y, Perdomo CA, Swartz J, Albert K. Donepezil treatment in severe Alzheimer's disease: a pooled analysis of three clinical trials. Curr Med Res Opin. 2009;25:2577-2587.
21. Birks J, Harvey RJ. Donepezil for dementia due to Alzheimer's disease. Cochrane Database Syst Rev. 2006:CD001190.
22. Çağlar S, Dilek E, Çağlar B, Adiguzel E, Temel E, Buyukgungor O, Tabak A. New metal complexes with diclofenac containing 2-pyridineethanol or 2-pyridinepropanol: synthesis, structural, spectroscopic, thermalproperties, catechol oxidase and carbonic anhydrase activities. Journal of Coordination Chemistry. 2016;69:3321-3335.
23. Burmaoğlu S, Dilek E, Yılmaz AO, Supuran CT. Synthesis of two phloroglucinol derivatives with cinnamyl moieties as inhibitors of the carbonic anhydrase isozymes I and II: an *in vitro* study. J Enzyme Inhib Med Chem. 2016;31(Suppl 2)208-212.

24. Supuran CT. Carbonic anhydrases: novel therapeutic applications for inhibitors and activators. Nat Rev Drug Discov. 2008;7:168-181.

25. Sly WS, Hu PY. Human carbonic anhydrases and carbonic anhydrase deficiencies. Annu Rev Biochem. 1995;64:375-401.

26. Ozensoy O, Arslan O, Sinan SO. A new method for purification of carbonic anhydrase isozymes by affinity chromatography. Biochemistry. 2004;69:216-219.

27. (a) Parkkila S, Parkkila AK, Carbonic anhydrase in the alimentary tract. Roles of the different isozymes and salivary factors in the maintenance of optimal conditions in the gastrointestinal canal. Scand J Gastroenterol. 1996;31:305-317. (b) Pastorekova S, Parkkila S, Pastorek J, Supuran CT. Carbonic anhydrases: current state of the art, therapeutic applications and future prospects. J Enzyme Inhib Med Chem. 2004;19:199-229.

28. Bülbül M, Hisar O, Beydemir S, Ciftçi M, Küfrevioğlu OI. The *in vitro* and *in vivo* inhibitory effects of some sulfonamide derivatives on rainbow trout (Oncorhynchus mykiss) erythrocyte carbonic anhydrase activity. J Enzyme Inhib Med Chem. 2003;18:371-375.

29. (a) Svastová E, Hulíková A, Rafajová M, Zat'ovicová M, Gibadulinová A, Casini A, Cecchi A, Scozzafava A, Supuran CT, Pastorek J, Pastoreková S. Hypoxia activates the capacity of tumor-associated carbonic anhydrase IX to acidify extracellular pH. FEBS Lett. 2004;577:439-445. (b) Cecchi A, Hulikova A, Pastorek J, Pastoreková S, Scozzafava A, Winum JY, Montero JL, Supuran CT. Carbonic anhydrase inhibitors. Design of fluorescent sulfonamides as probes of tumor-associated carbonic anhydrase IX that inhibit isozyme IX-mediated acidification of hypoxic tumors. J Med Chem. 2005;48:4834-4841.

30. Çelik I, Çamas H, Arslan O, Küfrevioglu Öİ. The effect of some pesticides on human and bovine erythrocyte carbonic anhydrase enzyme activities *in vitro*. J Environ Sci Health. 1996;31:2651-2657.

31. Vitale AM, Monserrat JM, Castilho P, Rodriguez EM. Inhibitory effects of cadmium on carbonic anhydrase activity and ionic regulation of the estuarine crab Chasmagnathus granulata (Decapoda, Grapsidae), Comp Biochem Physiol C Pharmacol Toxicol Endocrinol. 1999;122:121-129.

32. Gervais MR, Tufts BL. Characterization of carbonic anhydrase and anion exchange in the erythrocytes of bowfin (Amia calva), a primitive air-breathing fish. Comp Biochem Physiol A. 1999;23:343-350.

33. Hochster RM, Kates M, Quastel JH. Metabolic Inhibitors (ed). Academic Press; New York; 1973:66-82.

34. Ozdemir H, Uğuz MT. *In vitro* effects of some anaesthetic drugs on lactoperoxidase enzyme activity. J Enzyme Inhib Med Chem. 2005;20:491-495.

35. Christensen GM, Olson D, Riedel B. Chemical effects on the activity of eight enzymes: a review and a discussion relevant to environmental monitoring. Environ Res. 1982;29:247-255.

36. Bayram E, Senturk M, Kufrevioglu OI, Supuran CT. *In vitro* inhibition of salicylic acid derivatives on human cytosolic carbonic anhydrase isozymes I and II. Bioorg Med Chem. 2008;16:9101-9105.

37. Bertucci A, Zoccola D, Tambutté S, Vullo D, Supuran CT. Carbonic anhydrase activators. The first activation study of a coral secretory isoform with amino acids and amines. Bioorg Med Chem. 2010;18:2300-2303.

38. Verpoorte JA, Mehta S, Edsall JT. Esterase activities of human carbonic anhydrases B and C. J Biol Chem. 1967;242:4221-4229.

39. Innocenti A, Scozzafava A, Parkkila S, Pucceti L, De Simone G, Supuran CT. Investigations of the esterase, phosphatase, and sulfatase activities of the cytosolic mammalian carbonic anhydrase isoforms I, II, and XIII with 4-nitrophenyl esters as substrates. Bioorg Med Chem Lett. 2008;18:2267-2271.

40. Dilek EB, Küfrevioğlu Öİ, Beydemir Ş. Impacts of some antibiotics on human serum paraoxonase 1 activity. J Enzyme Inhib Med Chem. 2013;28:758-764.

41. Dilek E, Caglar S. Effects of mono and dinuclear copper (II) complexes derived from non-steroidal anti-inflammatory drug naproxen on human serum paraoxanase1 (PON1) activity. Int J Pharm Chem. 2015;5:189-195.

42. Dilek E, Polat MF. *In Vitro* Inhibition Of Three Different Drugs Used In Rheumatoid Arthritis Treatment On Human Serum Paraoxanase 1 Enzyme Activity. Protein Pept Lett. 2016;23:3-8.

43. Caglar S, Dilek E, Hamamci Alisir S, Çaglar B. New copper (II) complexes including pyridine-2,5-dicarboxylic acid: synthesis, spectroscopic, thermal properties, crystal structure and how these complexes interact with purified PON 1 enzyme, Journal of Coordination Chemistry. 2016;69:321-325.

Turk J Pharm Sci 2017;14(2):169-173
DOI: 10.4274/tjps.99609

ORIGINAL ARTICLE

In Vitro Evaluation of the Toxicity of Cobalt Ferrite Nanoparticles in Kidney Cell

Kobalt Ferrit Nanopartiküllerinin Böbrek Hücresi Üzerine Güvenliğinin *İn Vitro* Değerlendirmesi

Mahmoud ABUDAYYAK[1], Tuba ALTINÇEKİÇ GÜRKAYNAK[2], Gül ÖZHAN[1]*

[1]İstanbul University, Faculty of Pharmacy, Department of Pharmaceutical Toxicology, İstanbul, Turkey
[2]İstanbul University, Faculty of Engineering, Department of Chemical Engineering, İstanbul, Turkey

ABSTRACT

Objectives: The remarkable properties of hard magnetic cobalt ferrite nanoparticles ($CoFe_2O_4$-NPs) and their physicochemical stability lead to various applications in different industrial and medical fields. Although $CoFe_2O_4$-NPs have been reported to cause toxic effects, there is a serious lack of information concerning their effects on the kidneys. In this study, it was aimed to investigate the toxic effects of $CoFe_2O_4$-NPs on NRK-52E kidney cells.

Materials and Methods: The particle characterisation and cellular uptake were determined using transmission electron microscopy, dynamic light scattering and inductively coupled plasma-mass spectrometry. Then, the cytotoxicity was evaluated by MTT and neutral red uptake assays, the genotoxicity by comet assay, and the apoptotic potentials by Annexin V-FITC apoptosis detection assay with propidium iodide.

Results: After 24 h exposure to $CoFe_2O_4$-NPs (39±17 nm), it was observed they did not affect the cell viability at concentration ranging from 100 to 1000 µg/mL, but significantly induced DNA damage at concentration ≤100 µg/mL. No apoptotic or necrotic effect was observed in the exposed cells.

Conclusion: According to the results obtained, $CoFe_2O_4$-NPs are promising for safe use in various applications. However, further *in vivo* studies are needed to fully understand their mechanisms of action.

Key words: DNA damage, cell death, apoptosis, cobalt ferrite nanoparticle

ÖZ

Amaç: Sert manyetik kobalt ferrit nanopartiküllerinin ($CoFe_2O_4$-NP) dikkate değer özellikleri ve fizikokimyasal kararlılıkları farklı endüstri ve tıp alanlarında çeşitli uygulamalarda kullanılmalarına yol açmaktadır. $CoFe_2O_4$-NP'lerin bazı toksik etkilere neden olduğu bildirilmiş olsa da böbrek üzerindeki etkileri hakkında ciddi bilgi eksikliği vardır. Bu çalışmada, $CoFe_2O_4$-NPs'lerinin NRK-52E böbrek hücreleri üzerine toksik etki potansiyellerinin araştırılması amaçlanmıştır.

Gereç ve Yöntemler: Partikül karakterizasyonu ve hücresel alım transmisyon elektron mikroskopu, dinamik ışık saçılma tekniği ve indüktif eşleştirilmiş plazma-kütle spektrometrisi ile gerçekleştirildi. Sonra, sitotoksisite MTT ve nötral kırmızı alım testi, genotoksisite comet tekniği ve apoptotik potansiyel propidyum iyodürlü Annexin V-FITC apoptoz tayini ile değerlendirildi.

Bulgular: $CoFe_2O_4$-NP'lere (39±17 nm) 100-1000 µg/mL arasında değişen konsantrasyonlarda 24 saat süre ile maruz bırakılan böbrek hücrelerinde hücre canlılığının etkilenmediği, ancak ≤100 µg/mL'de önemli ölçüde DNA hasarı meydana geldiği gözlenmiştir. Maruz kalan hücrelerde apoptotik veya nekrotik etki gözlenmedi.

Sonuç: Elde edilen sonuçlara göre, $CoFe_2O_4$-NP'ler çeşitli uygulamalarda güvenli kullanımı vaat etmektedir. Bununla birlikte, etki mekanizmalarının tam olarak anlaşılabilmesi için *in vivo* çalışmalara ihtiyaç vardır.

Anahtar kelimeler: DNA hasarı, hücre ölümü, apoptoz, kobalt ferrit nanopartikülü

*Correspondence: **E-mail:** gulozhan@istanbul.edu.tr, **Phone:** +90 532 206 28 27
ORCID ID: orcid.org/0000-0002-6926-5723
Received: 25.11.2016, **Accepted:** 15.12.2016

INTRODUCTION

Today nanoparticles are important issue of concern with their widely application in industrial and medical sectors because of their special properties, which cause dramatic increases in intentional and inadvertent oral, dermal and inhalational human exposure. Also, nanoparticles can found as contaminant in water, air, and bulky materials as a result of the natural incident such as volcanic eruptions.[1,2] Research database provides that nanoparticles could cause DNA damage, cell death, oxidative stress and change cell function and morphology *in vitro*, damages and changes in liver, kidney, gastrointestinal and neuronal systems *in vivo*.[3,4]

The exceptional features of cobalt based nanoparticles motivate their uses in different technologies like sensors, catalysts, pigments, and magnetism and energy storage devices.[5,6] Because of the high physicochemical stability of cobalt ferrite nanoparticles ($CoFe_2O_4$-NPs), researchers also focus on using as drug carriers, anticancer treatment, and as magnetic resonance imaging contrast enhancement.[7-9] However, some researchers have shown that $CoFe_2O_4$-NPs could cause oxidative damage, cell death and inflammatory responses in exposed mice, guinea pigs, zebrafish and human cell lines.[10-14] Therewith, both *in vitro* and *in vivo* studies should be gradually carried out to get comprehensive toxicity profiles of nanoparticles to predict their effects on human. There is no study evaluating the effects of $CoFe_2O_4$-NPs or any other cobalt based nanoparticle on kidney. Therefore, we aimed to evaluate the toxic effects of $CoFe_2O_4$-NPs on kidney (NRK-52E) cells by *in vitro* assays.

MATERIALS AND METHODS

$CoFe_2O_4$-NPs (CAT. No: 773352), neutral red dye and MTT (3-[4,5-dimethylthiazol-2-yl]-2,5-diphenyl-tetrazolium bromide) were obtained from Sigma Chemical Co. Ltd. (St. Louis, MO, USA). Dulbecco's modified eagle medium (DMEM F-12), fetal bovine serum (FBS), phosphate buffered saline (PBS) and antibiotic solutions from Multicell Wisent (Quebec, Canada); Annexin V-FITC apoptosis detection kit with propidium iodide (PI) from Biolegend (San Diego, CA, USA); the other chemicals from Merck (NJ, USA) were purchased.

To particle size and distribution characterization, $CoFe_2O_4$-NPs were suspended in Milli-Q water and cell culture medium with 10% FBS, and measured by transmission electron microscopy (TEM) (Jem-2100 HR, JEOL, USA).[15-17] The average hydrodynamic size of $CoFe_2O_4$-NPs in cell culture medium was determined by dynamic light scattering (DLS) (ZetaSizer Nano-ZS, Malvern Instruments, Malvern, UK). One mg $CoFe_2O_4$-NPs was dispersed in cell culture medium, and then the suspension was sonicated at room temperature for 15 min at 40 W. Ten µL of the suspension were diluted with cell culture medium to reach final concentration 10 µg/mL, and sonicated for further 5 min. Then, DLS experiments performed.

NRK-52E rat kidney proximal tubular epithelial cells (CRL-1571) were obtained from American Type Culture Collection (Rockville, MD, USA). The cells were incubated in DMEM-12 medium supplemented with FBS (%10) and 100 U/mL antibiotic solution at 5% CO_2, 90% humidity and 37˚C for 24 h. The cell densities were from $1x10^4$ to $1x10^6$ cells/mL. $CoFe_2O_4$-NPs were freshly suspended at 1 mg/mL concentration in cell culture medium with 10% FBS and sonicated at room temperature for 15 min to avoid the aggregation/agglomeration of the nanoparticles before exposure.[15,16] The exposure times to the particle suspensions were 24 h.

The cellular uptake of nanoparticle was evaluated with inductively coupled plasma-mass spectrometry (ICP-MS) (Thermo Elemental X series 2, USA). After exposure to 200 µg/mL of nanoparticles, the cells were washed several times with equal volumes of PBS and counted by Luna cell counter (Virginia, USA).[15,16] The acid-digested samples were assayed for Co amount with ICP-MS. Also, Co content of the untreated cells for every cell line was measured.

The cytotoxic potentials of $CoFe_2O_4$-NPs were determined by MTT and neutral red uptake (NRU) assay based on different cellular mechanisms.[15,16,18,19] The cell exposed final concentrations of 0-1000 µg/mL. Optical density was read at 590 and 540 nm for MTT and NRU, respectively, using a microplate spectrophotometer system (Epoch, Germany). In every assay, the untreated cells were evaluated as negative control. It was calculated the inhibition of enzyme activity observed in cells compared with untreated (negative control) cells. Results were expressed as ratio of negative control.

The genotoxic potentials of $CoFe_2O_4$-NPs were determined by comet assay.[15,16,20,21] The cell exposed final concentrations of 0.1-100 µg/mL. Hydrogen peroxide (H_2O_2) (100 µM) and PBS were used as positive and negative controls, respectively. Briefly, the cells were layered on microscope slides coated with agarose gel. The slides were incubated for 1 h at 4˚C in lysis solution (2.5 M NaCl, 100 mM EDTA, and 10 mM tris-HCl, pH 10), added with 10% DMSO and 1% triton X-100. Then, DNA was unwinded for 20 min in cold-fresh electrophoresis buffer (0.3 M NaOH, 1 mM EDTA, pH 13) at 4˚C and electrophoresis was performed at 4˚C for 20 min (20 V / 300 mA). After electrophoresis, slides were neutralized with 0.4 M tris-HCl buffer (pH 7.5) 3 times for 5 min. The number of DNA breaks were scored under a fluorescent microscope (Olympus BX53, Olympus, Tokyo, Japan) at 400 magnification using an automated image analysis system (Comet Assay IV, Perceptive Instruments, Suffolk, UK). DNA damage to individual cells was expressed as a percentage of DNA in the comet tail (tail intensity %).

Annexin V-FITC apoptosis detection kit with PI was used to evaluate the cellular apoptosis or necrosis.[15,16] In every assay, negative controls and blank were evaluated. The cell exposed final concentrations of 0.1-100 µg/mL. The apoptotic or necrotic cells, distributed on the slides, were immediately counted at 400 magnification under a phase-contrast fluorescent microscope (Olympus BX53, Olympus, Tokyo, Japan). Results were expressed as percent of the total cell amount.

All experiments were done in triplicates and each assay as repeated four times. Data (n=12) was expressed as mean ± standard deviation. The significance of differences between

the untreated and treated cells with the nanoparticles was calculated by one-way ANOVA Dunnett t-test using SPSS version 17.0 for Windows (SPSS Inc., Chicago, IL). *p* values of less than 0.05 were selected as the levels of significance.

RESULTS

The aim of this study is to evaluate the toxicity profiles of $CoFe_2O_4$-NPs in NRK-52E kidney cells that could simulate specific target organ or system affected by occupational and environmental exposure to nanoparticles.

According to TEM images, the average size of $CoFe_2O_4$-NPs was 39±17 nm with narrow size distribution after dispersing in water (Figure 1). The nanoparticles slightly agglomerated and/or aggregated after dispersing in the culture medium, and their average sizes (range) increased to 101.5 nm (32.6 to 157.1 nm). The average hydrodynamic size of $CoFe_2O_4$-NPs was evaluated by DLS technique. The nanoparticle size was 183.6 nm (ranging from 5.6-342.1 nm), and 52% of the particles had a size lower than 33.6 nm. In addition, the cellular uptake of $CoFe_2O_4$-NPs was evaluated using ICP-MS. Results confirmed that nanoparticles were taken into the cells. Cobalt concentration was 8.3 µg/mL/10^5 cell compared to the negative control.

In the evaluation of their cytotoxic potential, it was shown that $CoFe_2O_4$-NPs did not decrease the cell viability at concentration ≤1000 µg/mL (Figure 2). Annexin V-FTIC apoptosis detection assay with PI was used to assess the cell death pathway. The maximum levels of apoptotic and necrotic induction were 4.02 and 2.25 fold, respectively. The induction level was statistically significant at 100 µg/mL. Our results showed that apoptosis could be the main cell death pathway in kidney NRK-52E cells exposed to $CoFe_2O_4$-NPs (Figure 3).

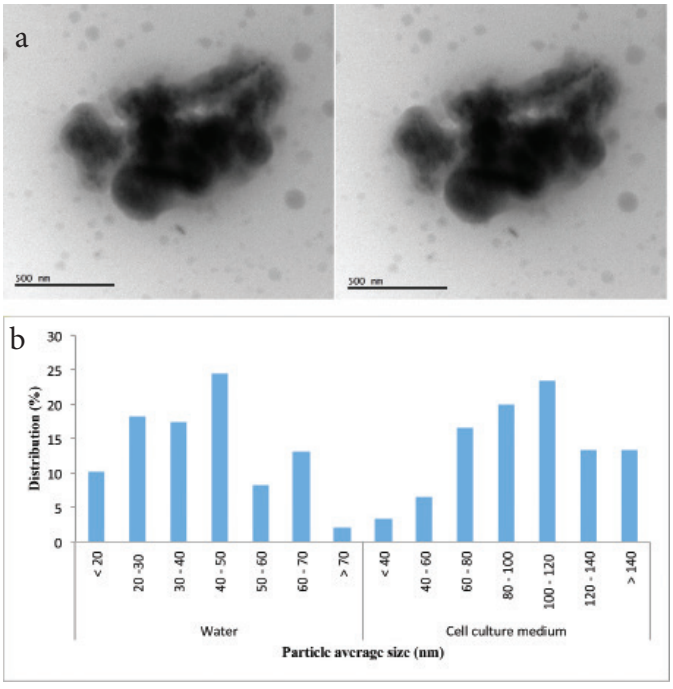

Figure 1. By transmission electron microscopy, the images and a) size distributions of $CoFe_2O_4$-NPs in water and b) cell culture medium

As to Comet assay results, $CoFe_2O_4$-NPs could be genotoxic because it was observed an increase in tail intensity, and induced DNA damage. The increase in DNA damage was significant in the range of 10-100 µg/mL, and occurred in a concentration-dependent manner (p<0.05). At the highest concentration of $CoFe_2O_4$-NPs (100 µg/mL), the tail intensity was approximately 1.7-fold of the negative control. In the positive controls (100 µM H_2O_2), the tail intensity was 16.9 (Figure 4).

DISCUSSION

$CoFe_2O_4$-NPs toxicity still controversial since the previous studies have contrary estimations. Horev-Azaria et al.[13] investigated the *in vitro* toxicological effects of $CoFe_2O_4$-NPs on lung (A549 and NCIH441), liver (HepG2), kidney (MDCK), intestine (Caco-2 TC7), and lymphoblast (TK6) cells in the concentration range of 11.7-281.5 mg/mL. They reported that $CoFe_2O_4$-NPs produced no toxic effects in all cell types at ≤46.9 mg/mL. In that study, a significant decrease in viability was

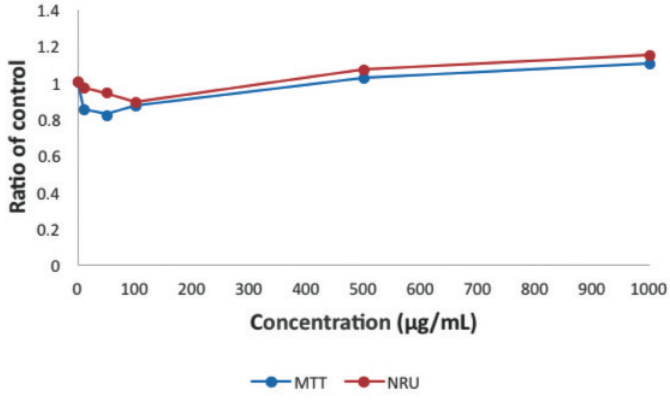

Figure 2. Effects of $CoFe_2O_4$-NPs on cell viability as assayed by MTT and NRU

All experiments were done in triplicates and each assay was repeated four times, The results are expressed as mean

NRU: Neutral red uptake

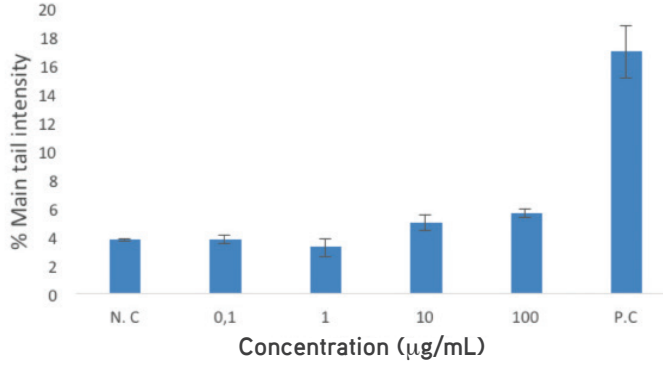

Figure 3. Evaluation of the apoptosis- and necrosis-inducing potentials of $CoFe_2O_4$-NPs as assayed by Annexin V-FTIC apoptosis detection assay with propidium iodide, Results are presented as percentage of the total cell amount, All experiments were done in triplicates and each assay was repeated four times, The results are presented as mean±standard deviation, *T≤0.05 were selected as the levels of significance by one-way ANOVA Dunnett t-test

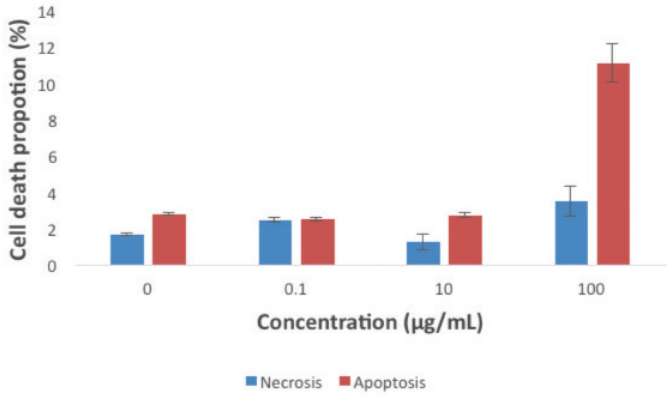

Figure 4. Evaluation of DNA damage potentials of $CoFe_2O_4$-NPs as assayed by comet assay

All experiments were done in triplicates and each assay was repeated four times, The results are presented as mean tail intensity (%) with ±standard deviation, NC and PC mean negative and positive controls, respectively, *p≤0.05 were selected as the levels of significance by one-way ANOVA Dunnett t-test

observed in NCIH441, HepG2, MDCK, and Caco-2 TC7 cells after 72 h, while there was no cytotoxic effect on A549 and TK6 cells even after 24 h of exposure.

Marmorato et al.[22] reported $CoFe_2O_4$ caused interference with lipid metabolism in Balb/3T3 cells depending on concentration. In another study, $CoFe_2O_4$-NPs were observed to have a weakly embryotoxic effect with an IC_{50} value of 243.91 and 20.05 mg/mL in mouse 3T3 fibroblast and D3 embryonic stem cell lines, respectively.[8] Human glioblastoma-astrocytoma (U87MG) cells were observed to have peculiar features including a white corona around the nucleus and other morphological changes after exposure to $CoFe_2O_4$-NPs at 58 and 235 mg/mL for 24 h. They suggested $CoFe_2O_4$-NPs caused cellular stress, and indicated the vesicles appeared to be lipid droplet organelles.[11]

The genotoxicity of $CoFe_2O_4$-NPs was evaluated by studying the interaction with Salmon sperm DNA.[23] It was reported the interaction between $CoFe_2O_4$-NPs and nucleic acid occurred, and the linkage was based on a coordination interaction of the phosphate groups and the oxygen atoms on the heterocyclic bases of DNA with metal ions on the particle surface.[24] Also, Ahmad et al.[10] pointed out the genotoxicity of $CoFe_2O_4$-NPs. Similarly, Colognato et al.[25] reported the induction of genotoxicity in human peripheral lymphocytes exposed those $CoFe_2O_4$-NPs.

CONCLUSION

In conclusion; $CoFe_2O_4$-NPs did not show cytotoxic potentials on the kidney cells, whereas only their highest concentration induced DNA damage. The intensity of toxicological effects of nanoparticles could be varied among different cell lines. In light of the results and previous researches, low but effective concentrations of $CoFe_2O_4$-NPs could be evaluated to be used safely in biomedicine, electronic, magneto-optic, sensor, data storage, catalysis and microwave applications. However, *in vivo* studies should be carried out to fully understand the mechanism of $CoFe_2O_4$-NPs toxicity.

ACKNOWLEDGEMENT

This work was supported by the Research Fund of İstanbul University (Project No: 40441).

Conflict of Interest: No conflict of interest was declared by the authors.

REFERENCES

1. Dhawan A, Sharma V. Toxicity assessment of nanomaterials: methods and challenges. Anal Bioanal Chem. 2010;398:589-605.
2. Kim YJ, Yu M, Park HO, Yang SI. Comparative study of cytotoxicity, oxidative stress and genotoxicity induced by silica nanomaterials in human neuronal cell line. Mol Cell Toxicol. 2010;6:337-344.
3. Arora S, Rajwade JM, Paknikar KM. Nanotoxicology and *in vitro* studies: the need of the hour. Toxicol Appl Pharmacol. 2012;258:151-165.
4. Brooking J, Davis SS, Illum L. Transport of nanoparticles across the rat nasal mucosa. J Drug Target. 2011;9:267-279.
5. Alarifi S, Ali D, Verma A, Alakhtani S, Ali BA. Cytotoxicity and genotoxicity of copper oxide nanoparticles in human skin keratinocytes cells. Int J Toxicol. 2013;32:296-307.
6. Alinovi R, Goldoni M, Pinelli S, Campanini M, Aliatis I, Bersani D, Lottici PP, Iavicoli S, Petyx M, Mozzoni P, Mutti A. Oxidative and pro-inflammatory effects of cobalt and titanium oxide nanoparticles on aortic and venous endothelial cells. Toxicol In Vitro. 2015;29:426-437.
7. Maaz K, Mumtaz A, Hasanain SK, Ceylan A. Synthesis and magnetic properties of cobalt ferrite (CoFe2O4) nanoparticles prepared by wet chemical route. J Magn Magn Mater. 2007;308:289-295.
8. Di Guglielmo C, López DR, De Lapuente J, Mallafre JM, Suarez MB. Embryotoxicity of cobalt ferrite and gold nanoparticles: a first *in vitro* approach. Reprod Toxicol. 2010;30:271-276.
9. Amiri S, Shokrollahi H. The role of cobalt ferrite magnetic nanoparticles in medical science. Mater Sci Eng C Mater Biol Appl. 2013;33:1-8.
10. Ahmad F, Yao H, Zhou Y, Liu X. Toxicity of cobalt ferrite (CoFe2O4) nanobeads in *Chlorella vulgaris*: interaction, adaptation and oxidative stress. Chemosphere. 2015;139:479-485.
11. Gianoncelli A, Marmorato P, Ponti J, Pascolo L, Kaulich B, Uboldi C, Rossi F, Makovec D, Kiskinova M, Ceccone G. Interaction of magnetic nanoparticles with U87MG cells studied by synchrotron radiation X-ray fluorescence techniques. X-Ray Spectrom. 2013;42:316-320.
12. Matsuda S, Nakanishi T, Kaneko K, Osaka T. Synthesis of cobalt ferrite nanoparticles using spermine and their effect on death in human breast cancer cells under an alternating magnetic field. Electrochim Acta. 2015;183:153-159.
13. Horev-Azaria L, Baldi G, Beno D, Bonacchi D, Golla-Schindler U, Kirkpatrick JC, Kolle S, Landsiedel R, Maimon O, Marche PN, Ponti J, Romano R, Rossi F, Sommer D, Uboldi C, Unger RE, Villiers C, Korenstein R. Predictive toxicology of cobalt ferrite nanoparticles: comparative *in vitro* study of different cellular models using methods of knowledge discovery from data. Part Fibre Toxicol. 2013;10:32.
14. Hwang DW, Lee DS, Kim S. Gene expression profiles for genotoxic effects of silica-free and silica-coated cobalt ferrite nanoparticles. J Nucl Med. 2012;53:106-112.
15. Abudayyak M, Altıncekic T, Özhan G. *In vitro* toxicological assessment of cobalt ferrite nanoparticles in several mammalian cell types. Biol Trace Elem Res. 2017;175:458-465.

16. Uzar NK, Abudayyak M, Akcay N, Algun G, Özhan G. Zinc oxide nanoparticles induced cyto- and genotoxicity in kidney epithelial cells. Toxicol Mech Methods. 2015;25:334-339.

17. Chattopadhyay S, Dash SK, Tripathy S, Das B, Mandal D, Pramanik P, Roy S. Toxicity of cobalt oxide nanoparticles to normal cells: an *in vitro* and *in vivo* study. Chem Biol Interact. 2015;226:58-71.

18. Repetto G, del Peso A, Zurita JL. Neutral red uptake assay for the estimation of cell viability/cytotoxicity. Nat Protoc. 2008;3:1125-1131.

19. Van Meerloo J, Kaspers GJ, Cloos J. Cell sensitivity assays: the MTT assay. Methods Mol Biol. 2011;731:237-245.

20. Collins AR. The comet assay for DNA damage and repair principles, applications, and limitations. Mol Biotechnol. 2004;26:249-261.

21. Speit G, Hartmann A. The comet assay (single-cell gel test): a sensitive genotoxicity test for the detection of DNA damage and repair. Methods Mol Biol. 1999;113:203-212.

22. Marmorato P, Ceccone G, Gianoncelli A, Pascolo L, Ponti J, Rossi F, Salomé M, Kaulich B, Kiskinova M. Cellular distribution and degradation of cobalt ferrite nanoparticles in Balb/3T3 mouse fibroblasts. Toxicol Lett. 2011;207:128-136.

23. Mariani V, Ponti J, Giudetti G, Broggi F, Marmorato P, Gioria S, Franchini F, Rauscher H, Rossi F. Online monitoring of cell metabolism to assess the toxicity of nanoparticles: the case of cobalt ferrite. Nanotoxicology. 2012;6:272-287.

24. Pershina AG, Sazonov AE, Novikov DV, Knyazev AS, Izaak TI, Itin VI, Naiden EP, Magaeva AA, Terechova OG. Study of DNA interaction with cobalt ferrite nanoparticles. J Nanosci Nanotechnol. 2012;11:2673-2677.

25. Colognato R, Bonelli A, Bonacchi D, Baldi G, Migliore L. Analysis of cobalt ferrite nanoparticles induced genotoxicity on human peripheral lymphocytes: comparison of size and organic grafting-dependent effects. Nanotoxicology. 2009;1:301-308.

Turk J Pharm Sci 2017;14(2):174-178
DOI: 10.4274/tjps.70299

ORIGINAL ARTICLE

Synthesis and Antioxidant Properties of New Oxazole-5(4*H*)-one Derivatives

Yeni Oksazol-5(4*H*)-one Türevlerinin Sentez ve Antioksidan Özellikleri

Canan KUŞ[1]*, Ezgi UĞURLU[1], Elçin D. ÖZDAMAR[2], Benay CAN-EKE[2]

[1]Ankara University, Faculty of Pharmacy, Department of Pharmaceutical Chemistry, Ankara, Turkey
[2]Ankara University, Faculty of Pharmacy, Department of Pharmaceutical Toxicology, Ankara, Turkey

ABSTRACT

Objectives: To synthesize and characterize 4-(substituted benzylidene)-2-(substituted phenyl)oxazol-5(4*H*)-one derivatives **(E1-E10)**, and evaluate them for antioxidant activity.

Materials and Methods: Required oxazole-5(4*H*)-one derivatives were synthesized in two steps to obtain novel hippuric acid derivatives **(7-13)**; glycine and acylated appropriate benzoic acid derivatives were used and then, final compounds were obtained with condensation of **7-13** with appropriate benzaldehydes **(E1-E10)**. These products were purified by column chromatography using ethyl acetate/n-hexane as eluent. All the compounds were unequivocally characterized using the combination of ^{1}H and ^{13}C-nuclear magnetic resonance, mass spectrometry (ESI-MS), and elemental analysis. The inhibition of lipid peroxidation and its effects on hepatic cytochrome P450-dependent ethoxyresorufin-O-deethylase (EROD) enzyme were determined in rats *in vitro*.

Results: The most active analogue on the microsomal EROD activity was **E3** which inhibited the microsomal EROD activity (89%) and was similarly better than that of the specific inhibitor caffeine (85%) at **10-3** M concentration.

Conclusion: The findings of this study indicate that the synthesized compounds, such as **E3,** display significant antioxidant activity.

Key words: Oxazolidinones, synthesis, antioxidant activity, lipid peroxidation, EROD activity

ÖZ

Amaç: Bu çalışma, 4-(sübstitüe benziliden)-2-(sübstitüefenil)oksazol-5(4*H*)-on (**E1-E10**) türevlerini sentezlemek, yapılarını aydınlatmak ve antioksidan etkilerini araştırmaktır.

Gereç ve Yöntemler: Oksazol-5(4*H*)-on türevleri iki yolak ile sentezlenmiştir. Yeni hippürik asit türevlerini (**7-13**) elde etmek için, glisin ve açillenmiş uygun benzoik asitler kullanıldı ve bu bileşiklerin (**7-13**) uygun benzaldehitler ile kondensasyon reaksiyonu ile de sonuç ürünlere (**E1-E10**) ulaşılmıştır. Bu ürünler etil asetat/n-hekzan solvan sistemi kullanılarak kolon kromatografisi ile temizlenmiştir. Tüm bileşikler için ^{1}H and ^{13}C-nükleer manyetik rezonans, mass spektrometresi (ESI-MS), elemental analiz yöntemleri kullanılarak yapıları tanımlanmıştır. Lipid peroksidasyon inhibisyonu ve karaciğer sitokrom P450 bağımlı Etoksirezorfin-O-deetilaz (EROD) enzimi üzerindeki etkileri sıçanlarda *in vitro* olarak tespit edildi.

Bulgular: Mikrozomal EROD aktivitesi üzerinde en aktif analog, EROD aktvitesini %89 ile inhibe eden **E3**'tür, benzer şekilde **10-3** M konsantrasyonda spesifik inhibitör kafeinden (%85) daha iyi idi.

Sonuç: Bu çalışmanın bulguları, **E3** gibi sentezlenen bileşiklerin, önemli antioksidan aktivite sergilediğini göstermektedir.

Anahtar kelimeler: Oksazolidinonlar, sentez, antioksidan aktivite, lipid peroksidasyon, EROD aktivite

*Correspondence: **E-mail:** profdrcanankus@gmail.com, **Phone:** +90 542 251 50 67
ORCID ID: orcid.org/0000-0001-6141-6788
Received: 18.10.2016, **Accepted:** 15.12.2016

INTRODUCTION

Oxazolone ring is an important scaffold in the area of drug discovery. Oxazolone and its derivatives make a prominent structure of number of well established marketed drugs such as rilmenidine, furazolidone, nifurantoin, oxaprozin, and especially linezolid, which is an active against methicillin-resistant *Staphylococcus aureus*. Indeed, oxazolone based derivatives have shown diverse biological and pharmacological applications such as anticancer[1,2], antibacterial[3], antimycobacterial against tuberculosis[4], and antioxidant[5,6] activity.

Free radicals, such as hydroxyl, superoxide anion (O_2^-), nitric oxide (NO) and peroxide ion (RO_2), reactive oxygen species, are involved in different physiological processes. Antioxidants can act as direct scavengers of free radicals and reactive oxygen species, or they can indirectly metabolize free radicals or their intermediates into harmless products. Oxidative damage to DNA and other macromolecules appears to have a major role in aging, degenerative diseases and cancer.[7-10] Due to oxidative cellular damage, development of cancers, cardiovascular diseases and ageing increase in the world. Antioxidant agents are able to either prevent or mitigate oxidative stress to cells that is an important area of investigation.

In light of the foregoing, novel oxazole-5(4*H*)-one derivatives were synthesized and evaluated their antioxidant activity. Molecular structure of designed compounds **(E1-E10)** is shown in Figure 1.

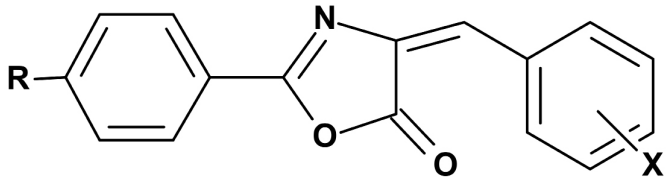

Figure 1. Molecular structure of designed compounds **(E1-E10)**
R= -H, 4-F, 4-CH_3, 4-NO_2, 4-Cl, 4-OCH_3, 4-Ph
X= -H, 2,4-di-F, 2,4-di-CH_3, 4-Cl

In this study, firstly some of hippuric acid derivatives **(7-13)** were synthesized according to the literature.[11-15] The synthetic route for hippuric acid derivatives **(7-13)** is displayed in Scheme 1.

In the second step, cyclization reactions of hippuric acide derivatives with corresponding benzaldehydes afforded the target compounds **(E1-E10)**, which are analogs of 4-(substituted benzylidene)-2-(substituted phenyl) oxazol-5(4*H*)-on, were synthesized (see Scheme 2). Among the synthesized compounds, 9 out of 10 were original except, **E1**. Compound **E1** was synthesized with one step reaction using hyppuric acid as starting material.[6-17]

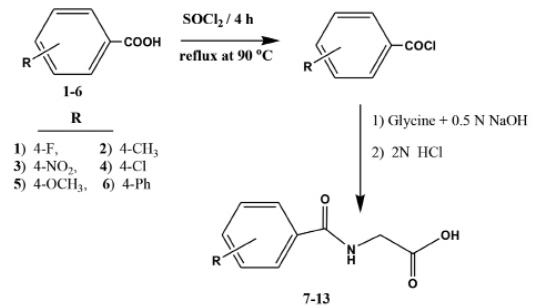

R	mp °C	Literature
7) -H	188	Commercial
8) 4-F	163-165	[11]
9) 4-CH_3	184	[12]
10) 4-NO_2	133-135	[11]
11) 4-Cl	176	[13]
12) 4-OCH_3	145-149	[14]
13) 4-Ph	218-219	[15]

Scheme 1. Synthesis of hippuric acide derivatives **(7-13)**

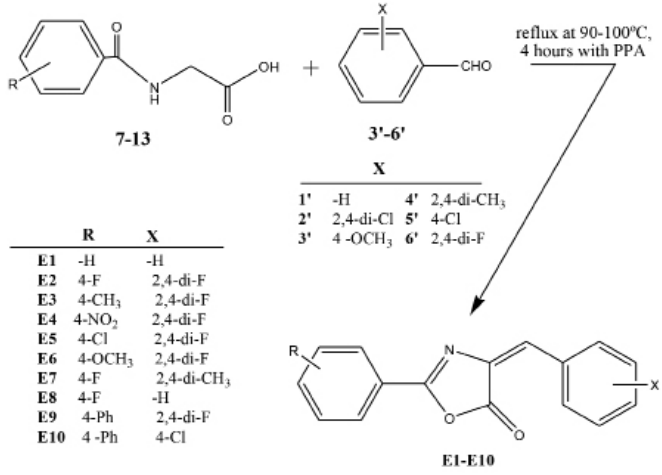

	R	X
E1	-H	-H
E2	4-F	2,4-di-F
E3	4-CH_3	2,4-di-F
E4	4-NO_2	2,4-di-F
E5	4-Cl	2,4-di-F
E6	4-OCH_3	2,4-di-F
E7	4-F	2,4-di-CH_3
E8	4-F	-H
E9	4-Ph	2,4-di-F
E10	4 -Ph	4-Cl

Scheme 2. Synthesis of the desired compounds **(E1-E10).**

EXPERIMENTAL

Chemical methods

Uncorrected melting points were measured on an Electrothermal 9100 capillary melting point apparatus. ^{1}H-NMR and ^{13}C-NMR spectra were recorded on a Varian Mercury 400 MHz and 100 MHz FT spectrometer, chemical shifts (δ) are in ppm relative to tetramethylsilane, and coupling constants (*J*) are reported in Hertz. Mass spectra were taken on a Waters Micromass ZQ using the Electrosprey Ionization (ESI) (+) method. Microanalyses were performed by Leco CHNS-932. All chemicals and solvents were purchased from commercial sources and used without furter purification. *p*-Fluorohippuric acid[11], *p*-methylhippuric acid[12], *p*-nitrohippuric acid[11], *p*-chlorohippuric acid[13], *p*-methoxyhippuric acid[14] and *p*-phenylhippuric acid[15] were prepared according to the literature.

Synthesis of hippuric acid derivatives **(7-13)**: One of appropriate benzoic acid derivatives **1-6** (1.5 mmol) was refluxed in benzene (5 mL) with $SOCl_2$ (5 mL) for 2 h at 80°C. Then solvent and excess of $SOCl_2$ were evaporated completely. Glycine (0.10 mol)

was dissolved in a 100 mL of 10% sodium hydroxide solution and appropriate benzoyl chloride (0.12 mol) was added portion-wise into it and the reaction mixture was shaked vigorously after each addition until all the chloride has been reacted for 1 h at 5°C and then at room temperature for 1 h, again. 2N HCl added to the reaction mixture, until it was acidic to litmus paper. The resulting precipitate of sufficient benzoyl glycine so obtained was filtered, washed several times with cold distilled water, dried and crystallized form carbon tetrachloride (see Scheme 1).

General procedure for the preparation of 4-(substituted benzylidene)-2-(substituted phenyl) oxazol-5(4H)-on derivatives **(E1-E10)**: Into a sample of polyphosphoric acid (0.01 mol), appropriate benzaldehyde **(1'-6')** and reasonable hippuric acid **(7-13)** (0.01 mol) were added. The mixture was heated in an oil bath (90°C) for 4 h followed by pouring water into the reaction mixture. The precipitate formed from the mixture was then washed several times with water, air-dried and then purified by column chromatography with convenient solvent.

4-Benzylidene-2-phenyloxazole-5(4H)-on **(E1)**: Light yellow crystal; (yield 75%); ethyl acetate/*n*-hexane= 1:4; mp: 169.4-169.9°C (168-169°C.[16,17] ^{1}H-NMR (Acetone-d_6): δ ppm: 7.30 (s, ^{1}H, =CH), 7.52-7.57 (m, ^{3}H), 7.62-7.67 (t, ^{2}H), 7.71-7.75 (t, ^{1}H), 8.20 (d, ^{1}H), 8.22 (s, ^{1}H), 8.35-8.37 (d, ^{2}H). ^{13}C NMR (Acetone-d_6): δ ppm: 171.7, 168.5, 138.6, 138.4, 138.3, 137.2, 135.96, 135.6, 134.0, 133.7, 132.9, 130.5; ESI-mass spectrometer (MS) m/z: 250.27 (M+1); Anal. Calculated for $C_{16}H_{11}NO_2$ (C, H, N): C 77.11, H 4.42, N 5.62; Found: C 76.77, H 4.26, N 5.97.

4-(2,4-Difluorobenzylidene)-2-(4-fluorophenyl)oxazole-5(4H)-on **(E2)**: Light yellow solid; (yield 13%), ethyl acetate/*n*-hexane= 1:9; mp: 229.4-231.3°C; ^{1}H-NMR (DMSO-d_6): δ ppm: 7.23 (s, ^{1}H, =CH), 7.31-7.36 (t, ^{1}H), 7.45-7.53 (m, ^{3}H), 8.21-8.24 (dd, ^{2}H), 8.87-8.9 (q, ^{1}H, H_5); ESI-MS m/z: 350.79 (M+47); Anal. Calculated for $C_{16}H_8F_3NO_2$ (C, H, N): C 63.37, H 2.64, N 4.62; Found: C 63.02, H 2.62, N 4.70, %.

4-(2,4-Difluorobenzylidene)-2-p-tolyloxazole-5(4H)-on **(E3)**: Light yellow solid; (yield 29.3%), ethyl acetate/*n*-hexane= 1:4; mp: 196.9°C. ^{1}H-NMR (DMSO-d_6): δ ppm: 2.44 (s, ^{3}H, -CH_3), 7.19 (s, ^{1}H, =CH), 7.32-7.36 (t, ^{1}H), 7.44-7.49 (m, ^{3}H), 8.04-8.06 (d, ^{2}H, J=8 Hz), 8.87-8.93 (q, ^{1}H); ESI-MS m/z: 346.81 (M+47); Anal. Calculated for $C_{17}H_{11}F_2NO_2$ (C, H, N): C 68.23, H 3.68, N 4.44; Found: C 68.03, H 3.54, N 4.78, %.

4-(2,4-Difluorobenzylidene)-2-(4-nitrophenyl)oxazole-5(4H)-on **(E4)**: Light yellow solid; (yield 13.7%); ethyl acetate/*n*-hexane= 1:4; mp: 227.5°C; ^{1}H-NMR (DMSO-d_6): δ ppm: 7.34 (s, ^{1}H, =CH), 7.37 (dd, ^{1}H, H_6, J=2 Hz), 7.51 (t, ^{1}H, H_3, J=2 Hz, J=8 Hz), 8.36-8.48 (m, ^{4}H, Ar-H), 8.86-8.94 (q, ^{1}H, H_5). ESI-MS m/z: 377.96 (M+47); Anal. Calculated for $C_{16}H_8F_2N_2O_4.0.1H_2O$: C 57.88, H 2.49, N 8.48; Found: C 57.48, H 2.59, N 8.29, %.

*4-(2,4-Difluorobenzylidene)-2-(4-chlorophenyl)oxazole-5(4H)-*on **(E5)**: Light yellow solid; (yield 17.7%); ethylacetate/*n*-hexane= 1:4; mp: 238-240°C; ^{1}H-NMR (DMSO-d_6): δ ppm: 7.22 (s, ^{1}H, =CH), 7.29-7.34 (t, ^{1}H), 7.43-7.48 (t, ^{1}H), 7.69-7.72 (d, ^{2}H, J=8 Hz), 8.11-8.14 (d, ^{2}H, J=8 Hz), 8.84-8.90 (q, ^{1}H, H_5); ESI-MS m/z: 366.79 (M+47); Anal. Calculated for $C_{16}H_8ClF_2NO_2$: C 60.11, H 2.52, N 4.39; Found: C 60.08, H 2.54, N 4.51, %.

4-(2,4-Difluorobenzylidene)-2-(4-methoxyphenyl)oxazole-5(4H)-on **(E6)**: Light yellow solid; (yield 22%), ethyl acetate/*n*-hexane= 1:4; mp: 197.7°C; ^{1}H-NMR (DMSO-d_6): δ ppm: 3.90 (s, ^{3}H, -OCH_3), 7.14 (s, ^{1}H, =CH), 7.18-7.21 (d, ^{2}H, J=8 Hz), 7.31-7.36 (t, ^{1}H), 7.43-7.49 (t, ^{1}H), 8.09-8.13 (d, ^{2}H, J=8 Hz), 8.87-8.94 (q, ^{1}H, H_5); ESI-MS m/z: 316.8 (M+1); Anal. Calculated for $C_{17}H_{11}F_2NO_3$: C 64.76, H 3.49, N 4.44; Found: C 64.51, H 3.54, N 4.43, %.

4-(2,4-Dimethylbenzylidene)-2-(4-fluorophenyl)oxazole-5(4H)-on **(E7)**: Light yellow solid; (yield 70.2%), ethyl acetate/*n*-hexane= 1:9; mp: 159.7-160.3°C; ^{1}H-NMR (DMSO-d_6): δ ppm: 2.34 (s, ^{3}H, -CH_3), 2.47 (s, ^{3}H, -CH_3), 7.18 (s, ^{1}H, H_3), 7.21 (d, ^{1}H, H_5, J=8.4 Hz), 7.39 (s, ^{1}H, =CH), 7.48 (t, ^{2}H, Ar-H), 8.16-8.19 (dd, ^{2}H, Ar-H), 8.65 (d, ^{1}H, H_6, J=8.4 Hz); ESI-MS m/z: 328.7 (M+33); Anal. Calculated for $C_{18}H_{14}FNO_2$: C 73.22, H 4.75, N 4.75; Found: C 73.18, H 4.58, N 4.84, %.

4-Benzylidene-2-(4-fluorophenyl)oxazole-5(4H)-on **(E8)**: Yellow solid; (yield 19.5%), ethyl acetate/*n*-hexane= 1:4; mp: 218.2°C; ^{1}H-NMR (DMSO-d_6): δ ppm: 7.33 (s, ^{1}H, =CH), 7.44-7.53 (m, ^{5}H), 8.17-8.20 (dd, ^{2}H), 8.27-8.30 (dd, ^{2}H, J=2.4 Hz, J=8.4 Hz); ESI-MS m/z: 300.9 (M+33); Anal. Calculated for $C_{16}H_{10}FNO_2.0.1H_2O$: C 71.42, H 3.82, N 5.21; Found: C 71.05, H 3.80, N 5.21, %.

4-(2,4-Difluorobenzylidene)-2-[(4-phenyl)phenyl]oxazole-5(4H)-on **(E9)**: Light yellow solid; (yield 14.6%), ethyl acetate/*n*-hexane= 1:4; mp: 213.4-215.9°C; ^{1}H-NMR (DMSO-d_6): δ ppm: 7.19 (s, ^{1}H, =CH), 7.31-7.36 (t, ^{1}H), 7.42-7.53 (m, ^{4}H), 7.76-7.87 (d, ^{2}H), 7.92-7.94 (d, ^{2}H, J=8.4 Hz), 8.17-8.19 (d, ^{2}H, J=8.4 Hz), 8.87-8.93 (q, ^{1}H); ESI-MS m/z: 362.9 (M+1); Anal. Calculated for $C_{22}H_{13}F_2NO_2$: C 73.13, H 3.60, N 3.88; Found: C 73.16, H 3.95, N 3.83, %.

4-(4-Chlorobenzylidene)-2-[(4-phenyl)phenyl]oxazole-5(4H)-on **(E10)**: Yellow solid; (yield 13.9%), ethyl acetat/*n*-hexane= 1:4; mp: 193.2-195.9°C; ^{1}H-NMR (DMSO-d_6): δ ppm: 7.39 (s, ^{1}H, =CH), 7.47 (t, ^{1}H), 7.53-7.57 (t, ^{2}H), 7.63 (d, ^{2}H, J=8.4 Hz), 7.81 (d, ^{2}H, J=7.2 Hz), 7.97 (d, ^{2}H, J=8.4 Hz), 8.22 (d, ^{2}H, J=8.4 Hz), 8.36 (d, ^{2}H, J=8 Hz); ^{13}C NMR ($CDCl_3$): δ ppm: 124.31, 127.48, 127.85, 128.73, 129.20, 129.29, 129.49, 130.04, 132.30, 133.74, 133.95, 137.47 139.86, 146.52, 163.97, 167.66; ESI-MS m/z= 360.7 (M+1); Anal. Calculated for $C_{22}H_{14}ClNO_2.0.2\ H_2O$: C 72.71, H 3.99, N 3.85; Found: C 72.71, H 4.18, N 3.90, %.

Biological methods

Assay of lipid peroxidation

Male albino Wistar rats (200-225 g) were used in the experiments. The animals were fed with standard laboratory rat chow and tap water add libitum. The animals were fasted for 24 h prior to sacrifice by decapitation under anesthesia. The livers were removed immediately and washed in ice-cold water and the microsomes were prepared, as described previously.[18]

NADPH-dependent lipid peroxidation (LP) was determined using the optimum conditions determined and described previously.[18] NADPH-dependent LP was measured spectrophotometrically by estimated the thiobarbituric acid reactant substances (TBARS). The amounts of TBARS were expressed in terms of nmol malondialdehyde/mg protein. The assay was essentially derived from the methods reported by Wills[19,20] and modified by Bishayee and Balasubramanian.[21] A typical optimized assay

mixture contained 0.2 nM Fe++, 90 mM KCl, 62.5 mM potassium-phosphate buffer (pH 7.4), a NADPH generating system consisting of 0.25 mM NADP+, 2.5 mM $MgCl_2$, 2.5 mM glucose-6-phosphate, 1.0 U glucose-6-phosphate dehydrogenase and 14.2 mM potassium phosphate buffer (pH 7.8) and 0.2 mg of the microsomal protein in a final volume of 1.0 mL.

Assay of ethoxyresorufin O-deethylase

Ethoxyresorufin *O*-deethylase (EROD) activity was measured by the spectrofluorometric method of Burke et al.[22]. A typical optimized assay mixture contained 1.0 mM ethoxyresorufin, 100 mM Tris-HCl buffer (pH 7.8), NADPH generating system consisting of 0.25 mM NADP+, 2.5 mM $MgCl_2$, 2.5 mM glucose-6-phosphate, 1.0 U glucose-6-phosphate dehydrogenase, and 14.2 mM potassium phosphate buffer (pH 7.8) and 0.2 mg liver microsomal protein in a final volume of 1.0 mL.

RESULTS

Carpy et al.[23] released that benzylic proton (Ar-CH=C) of 4-(2-chloro-4,5-dimethoxybenzylidene)-2-methyl-5-oxazolone was at 6.91 ppm and that if there were only one signal for the benzylic proton, this showed that *Z*-isomer existed. *E*-isomer is clarified by benzylic proton shift and absorbed magnetic resonance at up-field (~7.5 ppm). Similar results have also been published by other researchers.[24] Our final compounds showed parallel results at ^{1}H-NMR spectra as singlet Ar-CH= C protone at 7.14-7.40 ppm.

4-Benzylidene-2-phenyloxazole-5(4*H*)-on **(E1)** has 16 carbon atoms. 4-(4-chlorobenzylidene)-2-[(4-phenyl)phenyl]oxazole-5(4*H*)-on (**E10**) has 18 carbon atoms and there are only 12 and 16 signals at ^{13}C-NMR spectra, respectively. These findings are very normal and similar results were published by Younesi et al.[25].

To examine the mass analysis of the final compounds **(E1-E10)**, ESI-MS was used. Some of the desired compounds showed interesting results; **E7** and **E8** peaks were observed at (M+33) and **E2, E3, E4,** and **E5** peaks were observed at (M+47) at their mass spectra. These peaks were shown in the spectra of the molecules, because of keeping the solvents as methanol and ethanol. In 2003, Kawai et al.[26] explained these formations based on quantum chemical calculations. These findings are similar to other researchers' results.[27,28]

Compound **E10** has only one chlorine atom, because of that, as usual, M+ and M+2 (3:1) signals were observed in its mass spectrum.

For the EROD activity of the final compounds, **X** substitutents on the benzylidene moiety is more important than R substitutent, displayed in Scheme 2. As shown in Table 1, the most active compound on the microsomal EROD activity, **E3** has 2,4-di-F as **X** substitutents on the benzylidene moiety. This compound interestingly enhanced the LP levels and not consistent with EROD results. Biphenyl substitution led to a reduction in the EROD activity newertheless there is no observation like this in the LP levels. It can be said that there is no problem with biphenyl substitution for LP levels because these two compounds have somewhat moderate activity against LP.

Table 1. EROD and LP activity results of the final compounds E1-E10

Code	EROD (pmol/mg/min)	% of control	LP (nmol/mg/min)	% of control
E1	8.71±0.51	21	18.79±0.62	115
E2	13.23±2.57	32	15.89±2.06	98
E3	4.47±0.04	11	27.97±2.81	172
E4	11.13±1.27	28	26.59±3.21	163
E5	10.38±0.64	25	11.94±0.31	73
E6	12.72±0.76	30	9.01±0.86	55
E7	*	*	*	*
E8	9.79±0.57	24	6.91±0.86	43
E9	20.92±0.28	50	7.30±0.32	45
E10	28.85±1.36	69	9.40±0.32	58
BHT	-	-	5.68±0.22	35
Caffeine	6.41±0.99	15	-	-
DMSO	41.53±0.99	100	16.25±1.45	100

EROD: Ethoxyresorufin O-deethylase, LP: Lipid peroxidation, *Not tested

It is highly difficult to compare the results from different assays. The biggest problem is the lack of a validated assay that can reliably measure the antioxidant capacity of foods and biological samples, due to distinct antioxidant effects of chemicals which have already been noted in different *in vitro* assay systems.[29] Antioxidants scavenge and prevent the formation of free radicals so they are highly important for the treatment of these kind of diseases mentioned above. For this reason, there has been an increasing interest in finding novel antioxidant compounds in recent years.

The activity patterns of compounds on LP, and EROD activity were dissimilar because each method relates to the generation of a different radical, acting through a variety of mechanisms, and the measurement of a range of end points at a fixed time point or over a time period. It should also be realized that the analytical methods of measurement and the conditions can lead to variable results for the same compound.[30]

Compounds **E2** (2%), **E5** (27%), **E6** (45%), **E8** (57%), **E9** (55%) and **E10** (42%) displayed highly limited inhibitory effects on LP and the rest of the compounds enhanced LP levels. Similar results, where thiadiazole derivatives enhanced LP levels were obtained in another study of ours on liver LP levels, too.[31]

CONCLUSION

In conclusion, a series of 4-(substituted benzylidene)-2-(substituted phenyl) oxazole-5(4*H*)-on derivatives **(E1-E10)** were synthesized and their antioxidant activity were evaluated. The inhibition of LP, and its effects on hepatic cytochrome P450 dependent EROD enzyme were determined in rats *in vitro*. The most active analogue on the microsomal EROD activity was **E3**, which inhibited the microsomal EROD activity (89%) and was

similarly better than that of the specific inhibitor caffeine (85%) at 10^{-3} M concentration.

Compound **E3** displayed significant antioxidant activity so needs to study on its analogues.

ACKNOWLEDGEMENTS

This work was supported by Ankara University Research Fund (Grant No: *BAP 2005-08-030-50*). The Central Laboratory of the Faculty of Pharmacy, Ankara University, Turkey supported the acquisition of the NMR, and Mass spectra and elemental analyses in this work.

Conflict of Interest: No conflict of interest was declared by the authors.

REFERENCES

1. Zhu M, Gokhale VM, Szabo L, Munoz RM, Baek H, Bashyam S, Hurley LH, Von Hoff DD, Han H. Identification of a novel inhibitor of urokinase-type plasminogen activator. Mol Cancer Ther. 2007;6:1348-1356.
2. Kuzikov AV, Dugin NO, Stulov SV, Shcherbinin DS, Zharkova MS, Tkachev YV, Timofeev VP, Veselovsky AV, Shumyantseva VV, Misharin AY. Novel oxazolinyl derivatives of pregna-5,17(20)-diene as 17α-hydroxylase/17,20-lyase (CYP17A1) inhibitors. Steroids. 2014;88:66-71.
3. Das B, Rajarao AV, Sonalı R, Yadav A, Ray A, Pandya M, Rattan A, Mehta A. Synthesis and biological activity of novel oxazolidinones, Bioorg Med Chem Letters. 2009;19:6424-6428.
4. Diacon AH, Groote-Bidlingmaier F, Donald PR. A new 6-nitro-2,3-dihydroimidazo[2,1-*b*]oxazole for the management of tuberculosis resistant to at least isoniazid and rifampicin. Expert Opinion on Orphan Drugs. 2014;2:87-94.
5. Garg P, Chaudhary S, Milton MD. Synthesis of 2 aryl/heteroaryloxazolines from nitriles under metal and catalyst-free conditions and evaluation of their antioxidant activities. J Org Chem. 2014;79:8668-8677.
6. Temiz-Arpaci O, Coban T, Tekiner-Gulbas B, Can-Eke B, Yildiz I, Aki-Sener E, Yalcin I, Iscan MA. Study on the antioxidant activities of some new benzazole derivatives. Acta Biologica Hungarica. 2006;57:201-209.
7. Ames BN, Shigenaga MK, Hagen TM. Oxidants, antioxidants, and the degenerative disease of aging, Proc Natl Acad Sci USA. 1993;90:7915-7922.
8. Hagen TM, Yowe DL, Bartholomew JC, Wehr CM, Do KL, Park JY, Ames BN. Mitochondrial decay in hepatocytes from old rats: membrane potential declines, heterogeneity and oxidants increase. Proc Natl Acad Sci USA. 1997;94:3064-3069.
9. Hagen TM, Ingersoll RT, Wehr CM, Lykkesfeldt J, Vinarsky V, Bartholomew JC, Song MH, Ames BN. Acetyl-L-carnitine fed to old rats partially restores mitochondrial function and ambulatory activity. Proc Natl Acad Sci USA. 1998;95:9562-9566.
10. Beckman KB, Ames BN. The free radical theory of aging matures. Physiol Rev. 1998;78:547-581.
11. Benvenuti S, Severi F, Costanino L, Vampa G, Melegari M. Synthesis and aldose reductase inhibitory activity of benzoyl-amino acid derivatives. Farmaco. 1998;53:439-442.
12. Mıstry RN, Desai KR. Studies on Synthesis of Some Novel Heterocyclic Azlactone Derivatives and Imidazolinone Derivatives and their Antimicrobial Activity. E-Journal of Chemistry. 2005;2:42-51.
13. Novello NJ, Miriam SR, Sherwin CP. Comparative Metabolism of Certain Aromatic Acids. IX. Fate of some halogen derivatives of benzoic acid in the animal body. J Biol Chem. 1926;67:555-566.
14. Mariappan G, Saha BP, Datta S, Kumar D. Haldar PK. Design, synthesis and antidiabetic evaluation of oxazolone derivatives. J Chem Sci. 2011;123:335-334.
15. Tzschucke CC, Bannwarth W. Fluorous-silica-supported perfluoro-tagged palladium complexes catalyze Suzuki couplings in water. Helvetica Chimica Acta. 2004;87:2882-2889.
16. Oelschlaeger H, Seeling A, Radman M, Bockhard H. E/Z-ratio acid stability of halogenated benzylidene derivatives formed during the detection of glycine conjugates. Pharmazie. 2000;55:825-828.
17. Yu C, Zhou B, Su W, Xu Z. Erlenmeyer synthesis for azlactones catalyzed by Ytterbium (III) Triflate under solvent-free conditions. Synthetic Communications. 2006;36:3447-3453.
18. İşcan M, Arinç E, Vural N, İşcan MY. *In vivo* effects of 3-methylcholantrene, phenobarbital, pyretrum and 2,4,5-T isooctylester on liver, lung and kidney microsomal mixed-fuction oxidase system of guinea-pig: a comparative study. Comp Biochem Physiol. 1984;77:177-190.
19. Wills ED. Mechanism of lipid peroxide formation in animal tissues. Biochem J. 1966;99:667-676.
20. Wills ED. Lipid peroxide formation in microsomes. Relationship of hydroxylation to lipid peroxide formation. Biochem J. 1969;113:333-341.
21. Bishayee S, Balasubramanian AS. Lipid peroxide formation in rat brain. J Neurochem. 1971;18:909-920.
22. Burke MD, Thompson S, Elcombe CR, Halpert J, Haaparanta T, Mayer RT. Ethoxy-, Pentoxy-, and benzyloxyphenoxazones and homologues, a series of substrates to distinguish between different induced cytochromes P-450. Biochem Pharmacol. 1985;34:3337-3345.
23. Haasbroek PP, Oliver DW. Structure of 4-(2-chloro-4,5-dimethoxybenzylidine)-2-methyl-5-oxazolone X-ray and NMR stud. J Chem Cryst. 1998;28:811-814.
24. Päsha MA, Jayäshankara VP, Venugopala KN, Rao GK. Zinc Oxide (ZnO): An efficient catalyts for the synthesis of 4-arylmethylidene-2-phenyl 5(4*H*)-oxazolones having antimicrobial activity. J Pharm Toxicol. 2007;2:264-270.
25. Younesi A, Sorotskaya LN, Krapivin GD. Unexpected Spiroproducts from the Reaction of N-Benzoylglycine with ortho-Formylbenzoic Acids 3,5-dioxo-2-phenyl-1,3-dihydrospiro[indene-2,4-[1,3]oxazol]-1-yl Acetates: Establishments of Their Structure. J Chinese Chem Soc. 2009;56:619-625.
26. Kawai A, Tanaka H, Nakashima Y, Iimori T, Tsuji K, Obi K, Shibuya K. Protonation and multi-hydrogenation of benzophenone (BP) in BP/toluene and BP/ethanol binary cation clusters. Chemical Physics Letters. 2003;381:354-361.
27. Huang N, Siegel MM, Kruppa GH, Laukien FH, Automation of a Fourier Transform Ion Cyclotron Resonance Mass Spectrometer for Acquisition, Analysis, and E-mailing of High-Resolution Exact-Mass Electrospray Ionization Mass Spectral Data. J Am Soc Mass Spectrom. 1999;10:1166-1173.
28. Kobetic R, Gembarovski D, Baranovic G, Gabelica V. ESI-MS studies of mixed-ligand Fe (II) complexes containing 1,10-phenanthroline and 1,10-phenanthroline-5,6-dione as Ligands. J Mass Spectrom. 2008;43:753-764.
29. Ates-Alagoz Z. Antioxidant activities of retinoidal benzimidazole or indole derivatives *in vitro* model systems. Curr Med Chem. 2013;20:4633-4639.
30. Kuş C, Ayhan-Kilcigil G, Ozbey S, Kaynak FB, Kaya M, Coban T, Can-Eke B. Synthesis and antioxidant properties of novel N-methyl-1,3,4-thiadiazol-2-amine and 4-methyl-2H-1,2,4-triazole-3(4*H*)-thione derivatives of benzimidazole class. Bioorg Med Chem. 2008;16:4294-4303.
31. Kus C, Ayhan-Kilcigil G, Can-Eke B, Iscan M. Synthesis and antioxidant properties of some novel benzimidazole derivatives on lipid peroxidation in the rat liver. Arch Pharm Res. 2004;27:156-163.

Turk J Pharm Sci 2017;14(2):179-184
DOI: 10.4274/tjps.57070

ORIGINAL ARTICLE

Evaluation of Antioxidant Activities and Phenolic Compounds of *Scorzonera latifolia* (Fisch. & Mey.) DC. Collected from Different Geographic Origins in Turkey

Türkiye'nin Farklı Coğrafik Bölgelerinden Toplanmış *Scorzonera latifolia* (Fisch. & Mey.) DC. Örneklerinin Fenolik Bileşiklerinin ve Antioksidan Aktivitelerinin Değerlendirilmesi

Özlem Bahadır AÇIKARA[1]*, Burçin ERGENE ÖZ[1], Filiz BAKAR[2], Gülçin SALTAN ÇİTOĞLU[1], Serpil NEBİOĞLU[2]

[1]Ankara University, Faculty of Pharmacy, Department of Pharmacognosy, Ankara, Turkey
[2]Ankara University, Faculty of Pharmacy, Department of Biochemistry, Ankara, Turkey

ABSTRACT

Objectives: The chemical composition of plants is considered to be affected by many parameters. Therefore, the region where the samples are collected is likely to have an influence on the composition of phenolic compounds, so that their biological activities. In the present study, evaluation of antioxidant activity potentials of *Scorzonera latifolia* (Fisch. & Mey.) DC. aerial parts and roots, which were collected from different regions of Turkey, was aimed.

Materials and Methods: 1,1-diphenyl-2-picrylhydrazyl (DPPH) radical scavenging method and measurement of malondialdehyde (MDA) levels were used for determining antioxidant capacities of the tested extracts. In order to observe variations in the chemical composition of the investigated samples qualitatively as well as quantitatively, high performance liquid chromatography analyses were performed.

Results: Quantitative analysis showed that the amounts of chlorogenic acid and hyperoside in plants vary according to the regions where the samples were collected. As a result aerial parts of the *S. latifolia* collected from the Kars region have found to contain higher amount of chlorogenic acid (1246.78±3.20 µg/g) as well as hyperoside (652.32±2.48 µg/g) than other samples. The highest DPPH radical scavenging activity was determined with the IC_{50} value of 1.036 mg/mL for *S. latifolia* aerial parts of Kayseri sample. MDA level was detected as the lowest with treatment of *S. latifolia* Bayburt root sample (4.41 nmol/mL).

Conclusion: According to the antioxidant activity results, no significant difference was observed in the antioxidant potential between the samples collected from different locations except for *S. latifolia* collected from the Kars region.

Key words: DPPH, free radical scavenging activity, high performance liquid chromatography, MDA, *Scorzonera latifolia*

ÖZ

Amaç: Bitkilerin kimyasal içeriği pek çok parametreden etkilenmektedir. Bitkinin toplandığı bölge içerdiği fenolik bileşiklerin kompozisyonunu ve dolayısıyla aktivitelerini etkilemektedir. Bu çalışmada, Türkiye'nin farklı bölgelerinden toplanan *Scorzonera latifolia* (Fisch & Mey.) DC. kök ve toprak üstü kısımlarının antioksidan etki potansiyallerinin ölçülmesi amaçlanmıştır.

Gereç ve Yöntemler: Test edilen ekstrelerin antioksidan kapasiteleri 1,1-difenil-2-pikrilhidrazil (DPPH) radikal süpürücü etkileri ve malondialdehit (MDA) seviyesi üzerine etkilerinin ölçülmesiyle tespit edilmiştir. Araştırma konusu olan örneklerin kimyasal içeriğindeki değişiklikleri incelemek için kalitatif ve kantitatif yüksek performanslı sıvı kromatografisi analizleri yapılmıştır.

Bulgular: Kantitatif analiz sonuçları bitkilerde tespit edilen klorojenik asit ve hiperozit miktarlarının toplandığı bölgeye göre değiştiğini göstermiştir. *S. latifolia* Kars örneğinin diğer örneklere göre daha yüksek hiperozit (652.32±2.48 µg/g) ve klorojenik asit (1246.78±3.20 µg/g) içeriğine sahip olduğunu ortaya koymuştur. En yüksek DPPH radikal süpürücü etki 1.036 mg/mL IC_{50} değeri ile *S. latifolia* Kayseri örneğinde gözlenmiştir. En düşük MDA seviyesi ise *S. latifolia* Bayburt kök örneğinde (4.41 nmol/mL) belirlenmiştir.

Sonuç: Antioksidan aktivite sonuçları değerlendirildiğinde, farklı lokasyonlardan toplanan örnekler arasında, *S. latifolia* Kars kök örneği haricinde belirgin bir farklılık tespit edilememiştir.

Anahtar kelimeler: DPPH, serbest radikal süpürücü aktivite, yüksek performanslı sıvı kromatografisi, MDA, *Scorzonera latifolia*

*Correspondence: **E-mail:** obahadir@ankara.edu.tr, **Phone:** +90 312 203 31 03
ORCID ID: orcid.org/0000-0003-0809-784X
Received: 07.01.2016, **Accepted:** 26.01.2017

INTRODUCTION

It has been reported that the risk of various chronic diseases such as cancer, diabetes, cardiovascular diseases, aging, chronic inflammation, cataracts, atherosclerosis, Alzheimer's disease could be reduced by consumption of foods and beverages rich in natural antioxidants.[1-4] Although free radicals are generated by normal physiological processes and they are involved in phagocytosis, energy production and regulation of cell growth,[5] exogenous factors such as smoking, pollutants, ionising radiations, alcohol, synthetic pesticides, and solvent may increase the production of free radicals.[6] The overproduction of free radicals provokes oxidative damage on nucleic acids, proteins, lipids or DNA and causes degenerative diseases.[7] Natural antioxidants provide protection by their inhibitor and scavenger activities on free radicals.[4] Therefore, the plants containing natural antioxidants are considered to have therapeutic potential in treatment of many diseases and these findings have led to increased interest in the antioxidant activity studies of plants.[1-3]

Vitamin C, Vitamin E, carotenoids and phenolic compounds are recognized as the natural antioxidants found in plants.[8] The phenolic compounds consisting of flavonoids, isoflavones, flavones, anthocyanins, coumarins, lignans, catechins and isocatechins, etc.[9] have been shown to possess strong antioxidant activity.[5] Phenolic compounds exert their antioxidant activities mainly due to their redox properties that led to act them as reducing agents, hydrogen donors, singlet oxygen quenchers or metal chelators.[10,11] Different parameters such as time and period of sample collection, geographical origin and climatic conditions are considered as notable factors influencing the phenolic composition of plants.[11,12] The plants, cultivated with different conditions, exhibit an alteration in the quantity of phytochemicals and therefore display varied therapeutic effects.[13,14] The quality, uniformity and quantity of chemical constituents in plants are important parameters for the safety and effectiveness of herbal drugs.[14] The genus *Scorzonera* L. which consists of about 180 species belongs to *Asteraceae* family and is distributed in arid regions of Asia, Europe and Africa. It is represented by 50 species in Turkey.[15] The members of this genus are used as folk remedies against several diseases such as arteriosclerosis, kidney problems, hypertension and also for wound healing.[16,17] *Scorzonera latifolia* Fisc. & Mey. (*Asteraceae*) naturally grows in Central and East Anatolian Region and it is a widely known species from which a mastic named "yakı sakızı" is obtained. Yakı sakızı is known to be prepared from the latex of the plant roots and used as a folk medicine for its analgesic activity and against infertility externally as well as antihelmintic internally.[17] Antinociceptive, anti-inflammatory, wound healing, antioxidant and antimicrobial activities of *S. latifolia* have been reported.[18-21] *S. latifolia* roots contain terpenes; taraxasteryl myristate, taraxasteryl acetate, motiol, 3-β- hydroxy fern-8 en-7-one acetate, urs-12-en-11-one-3-acetyl, 3-β-hydroxy-fern-7-en-6-one-acetate, olean-12-en-11-one-3-acetyl, fern-7-en-3-β-one, leucodin, β-sitosterol[22-24], phenolic compounds; chlorogenic acid, chlorogenic acid methyl ester, 1,5-dicaffeoyl quinic acid, 3,5-dicaffeoyl quinic acid, methylester of 3,5-dicaffeoyl quinic acid, hydrangenol-8-*O*-glucoside, hydrangenol-4'-*O*-glucoside, scorzotomentosin-4'-*O*-glucoside and a new isocoumarine derivative[25] as well as scorzoveratrin 4'-*O*-β-glucoside, scorzoveratrin, scorzoveratrozit, 4,5-dicaffeoylquinic acid, 4,5-dicaffeoylquinic acid methyl ester and caffeic acid.[26] Aerial parts of the plant have been reported to contain phenolics which were identified as quercetin-3-*O*-β-glucoside, hyperoside, hydrangenol-8-*O*-glucoside, swertisin, 7-methylisoorientin, 4,5-*O*-dicaffeoyl-quinic acid, 3,5-di-*O*-caffeoyl-quinic acid and chlorogenic acid.[27]

In the current study, three samples of *S. latifolia* Fisc. & Mey. which were collected randomly from different locations of Turkey were evaluated for their antioxidant capacities and we also observed qualitative and quantitative variations in the chemical composition of samples by HPLC analysis.

EXPERIMENTAL

Plant materials

S. latifolia samples were collected from different locations of Turkey in flowering period. Identification of these plants was confirmed by Prof. Dr. H. Duman, in the Department of Biological Sciences, Faculty of Art and Sciences, Gazi University. Voucher specimens were stored in the herbarium of Ankara University, Faculty of Pharmacy (AEF) (Table 1).

Preparation of the extracts

Dried and powdered roots and aerial parts of the plants (0.25 g, each) were extracted in 10 mL of methanol:water (80:20) mixture by continuous stirring at room temperature for 8 hours. Obtained extracts were filtered and then concentrated to dryness under reduced pressure and low temperature (40-50˚C) on a rotary evaporator to give crude extracts. The crude extracts were dissolved in methanol-water mixture and adjusted to 10 mL in volumetric flask.

Phytochemical screening

HPLC analysis

For the HPLC analyses of the extracts of the roots and aerial parts of *Scorzonera* species, the method which was developed and validated by Küpeli Akkol et al.[19] was used. In accordance with this method, the analyses were carried out using Agilent LC 1100 model cromatograph (Agilent Technologies, California,

Table 1. Collection sites and herbarium numbers of the plants

Plant species	Locality	AEF no
S. latifolia (Kars)	Kars, Arpaçay, between Telekköy and Melekköy	23830
S. latifolia (Kayseri)	Kayseri, Erciyes Mountain, 1800-2000 m	25941
S. latifolia (Bayburt)	Bayburt, Kop Passage, 2000-2409 m	23827

USA) at the wavelength of 254 nm and peak areas were integrated by Agilent Software. A Supelcosil (250 mm x 4.6 mm; 5 µm) column was used with a gradient elution of acetonitrile (A) and water: 0 min, A-B (8:92, v/v); 0-10 min, linear change from A-B (8:92, v/v) to A-B (18:82); 10-20 min, a linear change from A-B (18:82) to A-B (20:80); 20-30 min, a linear gradient elution from A-B (20:80) to A-B (30:70). Phenolic acids including *p*-coumaric acid, ferulic acid, rosmarinic acid, caffeic acid, chlorogenic acid and flavonoids such as apigenin, luteolin, quercetin, rutin, hyperoside, hesperidin were used as standards.

DPPH radical scavenging activity

DPPH radical scavenging activity assays of the samples were carried out according to the method of Williams et al.[28] 0.01 g of sample was dissolved in 10 mL dimethylsulfoxide and seven different concentrations (1 mg/mL to 0.015 mg/mL) were prepared with ½ dilutions. 2.9 mL DPPH solution dissolved in 10^{-4} M ethanol was added into 0.1 mL of sample solutions. The mixture was shaken vigorously and incubated 30 min in a water bath adjusted to 30°C. Absorbance of the resulting solution was measured against the blank (the same mixture without the sample) at 517 nm UV-visible spectrophotometer (Shimadzu). All assays were carried out in triplicates and propylgallate is used as positive control. Percentage of inhibition determined as follows:

% DPPH radical-scavenging = [(Absorbance of control - Absorbance of sample) / Absorbance of control] x 100

According to this method, decrease at the absorbance of the reaction mixture indicates stronger DPPH radical-scavenging activity. For each sample, the IC_{50} values were calculated by linear regression analysis using % inhibition and concentration values.

Thiobarbituric acid reactive substances assay

The measurement of malondialdehyde (MDA) levels was performed spectrophotometrically according to the modified method of Puhl et al.[29] and Zhang et al.[30] 2.0 mg of plant extracts solved in dH_2O were incubated with 8.125 mM $CuSO_4$ solution. Following incubation, trichloroacetic acid (0.1 g/dL, final volume) and thiobarbituric acid (TBA) (0.67 g/dL, final volume) solutions were added and the absorbance was measured at 532 nm. Quantitation of TBA reactive substances (TBARS) was performed by comparison with a standard curve of MDA equivalents generated by acid-catalyzed hydrolysis of 1,1,3,3-tetraethoxypropane and the results were expressed as nmol/mL.

RESULTS AND DISCUSSION

Natural antioxidants from plant sources have been gaining more interest in recent years due to their important roles in the maintenance of health and protection from ageing-related degenerative diseases.[31,32] Plants serve as potential sources of compounds with antioxidant activity such as vitamin C, vitamin E, carotenoids, phenolic compounds, etc.[33] Phenolic compounds, one of the largest group of secondary metabolites, exhibit strong antioxidant activity as free radical scavengers, hydrogen donating sources or as singlet oxygen quenchers and metal ion chelators.[10,31]

In the current study, antioxidant activities of *S. latifolia* samples were evaluated by using two different methods. The DPPH method is the most common, cost-effective and quick method to evaluate antioxidant activities of natural products.[33,34] Scavenging activity against DPPH radical is considered as hydrogen donating ability of samples. DPPH is a stable free radical and accepts an electron on hydrogen radical to become a stable diamagnetic molecule.[33] The DPPH is decolorized by accepting an electron donated by an antioxidant.[12] DPPH radical scavenging activities of extracts are presented in Table 2. Among the root samples, *S. latifolia* Kars sample showed the highest DPPH radical scavenging activity with the IC_{50} value of 1.906 mg/mL as the highest activity among the tested aerial parts was determined for *S. latifolia* Kayseri sample (IC_{50}= 1.036 mg/mL).

Lipid oxidation plays an important role in the generation of reactive oxygen species and is considered as an important factor in the initiation and progression of several diseases.[35] TBARS assay is used to measure the degree of lipid peroxidation. TBA reacts with MDA which is a secondary product of lipid peroxidation, to give a red chromogen, than can be determined spectrophotometrically.[36] In the TBARS assay, the MDA levels for the root of *S. latifolia* samples from Bayburt, Kayseri, and Kars were determined as 4.41 nmol/mL, 4.66 nmol/mL, and 5.41 nmol/mL, respectively (Table 3).

The extracts of the aerial parts of all *S. latifolia* samples inhibited lipid peroxidation significantly and the lowest MDA level was detected in Kayseri sample as 5.15 nmol/mL (Table 3).

Table 2. IC_{50} values (mg/mL) of plant extracts in DPPH radical scavenging assay

Plant material	Root	Aerial parts
S. latifolia (Kars)	1.906	1.122
S. latifolia (Kayseri)	4.102	1.036
S. latifolia (Bayburt)	4.628	1.143
	Control	
Propylgallate	0.742	

DPPH: 1,1-difenil-2-pikrilhidrazil

Table 3. MDA levels of plant extracts, the results are given as nmol/mL concentrations

Plant material	Root	Aerial parts
S. latifolia (Kars)	5.41	6.14
S. latifolia (Kayseri)	4.66	5.15
S. latifolia (Bayburt)	4.41	5.90

MDA: Malondialdehit

The radical scavenging activities of the extracts were not found to be quite different except *S. latifolia* root Kars sample. Aerial part samples exhibited higher scavenger activities on DPPH radical compared to root samples (Table 2). The observed scavenger activities of aerial part samples were also close to the effect of propylgallate which is the positive control of the assay.

According to the HPLC results, root samples contain chlorogenic acid as one of the major constituent both in roots (Figure 1) and aerial parts (Figure 2) of *S. latifolia*. The highest amount was detected in the root of Kars sample as 1246.78±3.20 µg/g. None of the tested flavonoid standards were detected in root samples (Figure 3). However all aerial part samples contain chlorogenic acid as well as hyperoside as major compounds. Aerial part of *S. latifolia* was also found to contain higher amount of chlorogenic acid (652.32±2.48 µg/g) as well as hyperoside (305.71±1.70 µg/g) (Table 4).

Differences between the scavenging activity of root and aerial part extracts on DPPH radical may be explained by the flavonoid content of aerial part samples. It has been reported that, flavonoids which are widely distributed in plants have the ability to scavenge active oxygen radicals, superoxide and hydroxyl radicals by single electron transfer.[37] On the other hand in the TBARS assay, root samples were found to be more active when compared to aerial part samples. These results may be related to high amount of chlorogenic acid content of root extracts. Chlorogenic acid exhibits scavenging activity against reactive oxygen and nitrogen species[38] and inhibits the initiation of chain lipid peroxidations by free radicals.[39] Antioxidant activity of chlorogenic acid (5-CQA) against human LDL has also been reported.[36] Thus, chlorogenic acid may be considered to be one of the responsible compounds for the antioxidant activities of *S. latifolia* samples.

Qualitative and quantitative changes in the phytochemical composition of the *S. latifolia* root and aerial part samples which were collected from different localities of Anatolia were investigated by HPLC in the current study and the differences between the amounts of chlorogenic acid and hyperoside were observed. Results of present study have revealed that different samples of *S. latifolia* root and aerial parts have similar chemical composition however the quantity of the chlorogenic acid and hyperoside were different. A number of factors such as temperature, season, stages of maturity, geographical origin, climatic conditions and soil may affect the phytochemical content of plants.[11,12,40,41] Changes in the phytochemical composition may result variation in therapeutic effects of the medicinal plants.[13,14] According to the antioxidant activity results; we didn't find a significant correlation between the chlorogenic acid and/or hyperoside content and antioxidant capacities of samples.

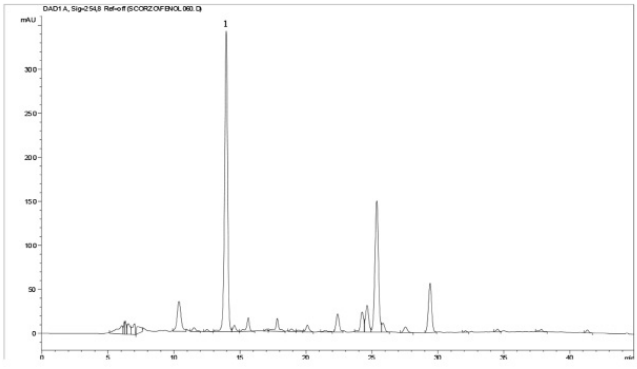

Figure 1. Chromatogram of the *S. latifolia* root (Kars sample) extract
1: Chlorogenic acid

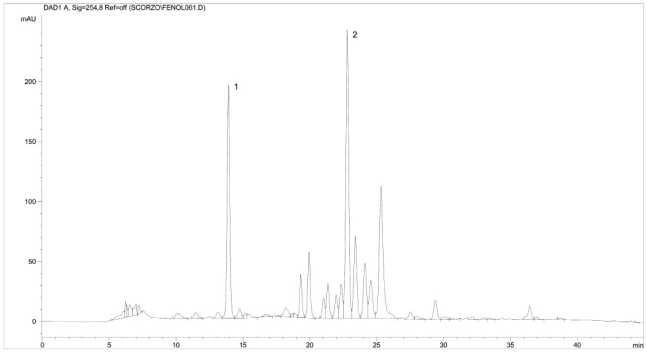

Figure 2. Chromatogram of the *S. latifolia* aerial part (Kars sample) extract
1: Chlorogenic acid, 2: Hyperoside

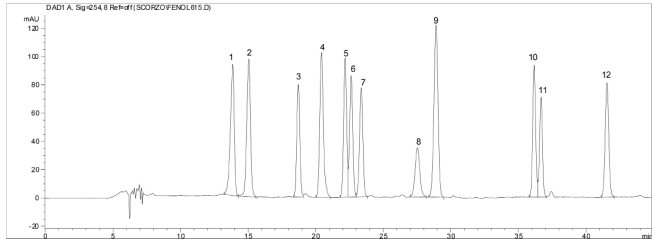

Figure 3. Chromatogram of the standart mixture
1: Chlorogenic acid, 2: Caffeic acid, 3: *p*-Coumaric acid, 4: Ferulic acid, 5: Rutin, 6: Hyperoside, 7: Luteolin-7-glucoside, 8: Hesperidin, 9: Rosmarinic acid, 10: Quercetin, 11: Luteolin, 12: Apigenin

Table 4. HPLC qualitative and quantitative data for roots and aerial parts of *Scorzonera samples* (µg/g)

Plant material		Chlorogenic acid (µg/g ± standart error)	Hyperoside (µg/g ± standart error)
S. latifolia (Kars)	R*	1246.78±3.20	-
	AE*	652.32±2.48	305.71±1.70
S. latifolia (Kayseri)	R*	988.070±3.78	-
	AE*	290.64±0.84	70.99±0.29
S. latifolia (Bayburt)	R*	541.96±2.56	-
	AE*	295.27±0.53	36.24±0.42

*R: Root, *AE: Aerial part

CONCLUSION

In conclusion, quantitative analyses have shown that same species collected from different localities may have different chemical composition. Therefore, the region chosen for the collection of a plant which is used as an herbal remedy is a very important parameter with respect to the effectiveness of an herbal drug.

Conflict of Interest: No conflict of interest was declared by the authors.

REFERENCES

1. Choi E, Hwang JK, Antiinflammatory, analgesic and antioxidant activities of the fruit of *Foeniculum vulgare*. Fitoterapia. 2004;75:557-565.
2. Gonçalves C, Dinis T, Batista MT. Antioxidant properties of proanthocyanidins of *Uncaria tomentosa* bark decoction: a mechanism for anti-inflammatory activity. Phytochemistry. 2005;66:89-98.
3. Conforti F, Sosa S, Marrelli M, Menichini F, Statti GA, Uzunov D, Tubaro A, Menichini F, Loggia RD. *In vivo* anti-inflammatory and *in vitro* antioxidant activities of Mediterranean dietary plants. J Ethnopharmacol. 2008;116:144-151.
4. Guha G, Rajkumar V, Mathew L, Kumar RA. The antioxidant and DNA protection potential of Indian tribal medicinal plants. Turk J Biol. 2011;35:233-242.
5. Narayanaswamy N, Balakrishnan KP. Evaluation of some medicinal plants for their antioxidant properties. Int J Pharm Tech Res. 2011;3:381-385.
6. Amiri H. Essential oils composition and antioxidant properties of three thymus species. Evid Based Complement Alternat Med. 2012;2012:728065.
7. Parakash A, Rigelhof F, Miller E, Antioxidant activity, Medallion Laboratories Analytical Progress. http://www.medlabs.com/Downloads/Antiox_acti_.pdf
8. Ara N, Nur H. *In vitro* antioxidant activity of methanolic leaves and flowers exracts of *Lippia alba*. Res J Med Sci. 2009;4:107-110.
9. Michalak A. Phenolic compounds and their antioxidant activity in plants growing under heavy metal stress. Polish J Environ Stud. 2006;15:523-530.
10. Teixeire EW, Message D, Negri G, Salatino A, Stringheta PC. Seasonal variation, chemical composition and antioxidant activity of Brazilian Propolis samples. Evid Based Complement Alternat Med. 2010;7:307-315.
11. Banerjee SK, Bonde CG. Total phenolic content and antioxidant activity of extracts of *Bridelia retusa* Spreng bark: Impact of dielectric constant and geographical location. J Med Plants Res. 2011;5:817-822.
12. Gull J, Sultana B, Anwar F, Naseer R, Ashraf M, Ashrafuzzaman M. Variation in antioxidant attributes at three ripening stages of guava (*Psidium guajava* L.) fruit from different geographical region of Pakistan. Molecules. 2012;17:3165-3180.
13. Sun YF, Liang ZS, Shan CJ, Viernstein H, Unger F. Comprehensive evaluation of natural antioxidants and antioxidant potentials in *Ziziphus jujube* Mill. var. spinosa (Bunge) Hu ex H.F. Chou fruits based on geographical origin by TOPSIS method. Food Chem. 2011;124:1612-1619.
14. Kolawole OT, Ayankunle AA. Seasonal variation in the anti-diabetic and hypolipidemic effects of *Momordica charantia* fruit extract in rats. European J Med Plants. 2012;2:177-185.
15. Duran A, Dogan B, Hamzaoglu E, Aksoy A. *Scorzonera coriacea* A. Duran & Aksoy (*Asteraceae*, *Cichorieae*), a new species from South Anatolia, Turkey. Candollea. 2011;62:353-359.
16. Sezik E, Yeşilada E, Tabata M, Honda G, Takaishi Y, Fujita T, Tanaka T, Takeda Y. Traditional medicine in Turkey VIII. Folk medicine in East Anatolia; Erzurum, Erzincan, Ağrı, Kars, Iğdır provinces, Econ Bot. 1997;51:195-211.
17. Baytop T. Therapy with medicinal plants in Turkey-past and present Ankara, Turkey, Nobel Publishers, 1999.
18. Sarı A, Özbek B, Özgökçe F, Antimicrobial activities of two *Scorzonera* species growing in Turkey, Asian J Chem. 2009;21:4785-4788.
19. Küpeli Akkol E, Acıkara OB, Süntar I, Citoglu GS, Keleş H, Ergene B. Enhancement of wound healing by topical application of *Scorzonera* species: Determination of the constituents by HPLC with new validated reverse phase method. J Ethnopharmacol. 2011;137:1018-1027.
20. Bahadır Ö, Saltan HG, Özbek H, Antinociceptive activity of some *Scorzonera* L. Species. Turk J Med Sci. 2012;42:861-866.
21. Erden Y, Kırbağ S, Yılmaz Ö. Phytochemical composition and antioxidant activity of some Scorzonera species. Proc Natl Acad Sci India Sect B Biol Sci. 2013;83:271-276.
22. Bahadir O, Citoğlu GS, Smejkal K, Dall'Acqua S, Ozbek H, Cvacka J, Zemlicka M. Analgesic compounds from *Scorzonera latifolia* (Fisch. and Mey.) DC. J Ethnopharmacol. 2010;131:83-87.
23. Acıkara ÖB, Çitoğlu GS, Dall'Acqua S, Smejkal K, Cvačka J, Zemlička M, A new triterpene from *Scorzonera latifolia* (Fisch. and Mey.) DC. Nat Prod Res. 2012;26:1892-1897.
24. Acikara OB, Citoğlu GS, Dall'Acqua S, Ozbek H, Cvacka J, Zemlicka M, Smejkal K. Bioassay-guided isolation of the antinociceptive compounds motiol and β-sitosterol from *Scorzonera latifolia* root extract. Pharmazie. 2014;69:711-714.
25. Bahadır Acıkara Ö, Smejkal K, Cvacka J, Budesinsky M, Dracinsky M, Saltan G. Secondary metabolites from *Scorzonera latifolia* roots. Planta Med. 2015;81:167.
26. Sarı A. Phenolic compounds from *Scorzonera latifolia* (Fisch. & Mey.) DC. Nat Prod Res. 2012;26:50-55.
27. Bahadır Acikara Ö, Hošek J, Babula P, Cvačka J, Budešínský M, Dračinský M, Saltan İşcan G, Kadlecová D, Ballová L, Šmejkal K. Turkish *Scorzonera* species extracts attenuate cytokine secretion via inhibition of NF-κB activation, showing anti-inflammatory effect *in vitro*. Molecules. 2015;21:43.
28. Williams WB, Cuvelier ME, Berset C. Use of free radical method to evaluate antioxidant activity. Food Sci Technol. 1995;28:25-30.
29. Puhl H, Waeg G, Esterbauer H. Methods to determine oxidation of low density lipoproteins. Method Enzymol. 1994;233:425-441.
30. Zhang A, Vertommen J, Van Gaal L, De Leeuw I. A rapid and simple method for measuring the susceptibility of low density lipoprotein and very low density lipoprotein to copper catalyzed oxidation. Clin Chim Acta. 1994;227:159-173.
31. Hsu CY, Chan YP, Chang J. Antioxidant activity of extract from Polygonum cuspidatum. Biol Res. 2007;40:13-21.

32. Charde MS, Shukla A, Bukhariya V, Chakole JMR. Herbal remedies as antioxidants: An overview. International Journal of Pharmacological Research. 2011;1:25-34.

33. Arulmozhi S, Mazumder PM, Narayanan LS, Thakurdesai PA. *In vitro* antioxidant and free radical scavenging activity of *Alstonia scholaris* Linn. R. Br. Int J PharmTech Res. 2007;6:191-196.

34. Singh DR, Singh S, Salim KM, Srivastava RC. Estimation of phytochemicals and antioxidant activity of underutilized fruits of Andaman Islands (India). Int J Food Sci Nutr. 2012;63:446-452.

35. Waqar MA, Mohmood Y. Anti- platelet, anti-hypercholesterolemic and anti-oxidant effects of ethanolic extracts of Brassica oleracea in high fat diet provided rats. World Appl Sci J. 2010;8:107-112.

36. Lakshmi A, Arawwawala LDA, Nandakumara A. Antioxidant and antifungal activities of essential oil of *Alpinia calcarata Roscoe* rhizomes. J Ayurveda Integr Med. 2012;3:199-202.

37. Chu YH, Chang CL, Hsu HF. Flavonoid content of several vegetables and their antioxidant activity. J Sci Food Agric. 2000;80:561-566.

38. Nakatani N, Kayano S, Kikuzaki, Sumino K, Katagiri K, Mitani T. Identification, quantitative determination and antioxidative activities of chlorogenic acid isomers in prune (*Prunus domestica* L). J Agric Food Chem. 2000;48:5512-5516.

39. Kono Y, Kobayashi K, Tagawa S, Adachi K, Ueda A, Sawa Y, Shibata H. Antioxidant activity of polyphenolics in diets. Rate constants of reactions of chlorogenic acid and caffeic acid with recative species of oxygen and nitrogen. Biochim Biophys Acta. 1997;1335:335-342.

40. Carmona JR, Yousef GG, Martinez-Peniche RA, Lila MA. Antioxidant capacity of fruit extracts of blackberry (*Rubus* sp.) produced in different climatic regions. J Food Sci. 2005;70:497-503.

41. Uzelac VD, Levaj B, Mrkic V, Bursac D, Boras M. The content of polyphenols and carotenoids in three apricot cultivars depending on stage of maturity and geographical region. Food Chem. 2007;102:966-975.

Turk J Pharm Sci 2017;14(2):185-190
DOI: 10.4274/tjps.79663

ORIGINAL ARTICLE

Assessment of Genotoxic Effects of Pendimethalin in Chinese Hamster Over Cells by the Single Cell Gel Electrophoresis (Comet) Assay

Pendimetalinin Genotoksik Etkilerinin Çin Hamster Over Hücrelerinde Tek Hücre Jel Elektroforez (Comet) Yöntemiyle Değerlendirilmesi

Nazlı DEMİR, Sevtap AYDIN, Ülkü ÜNDEĞER BUCURGAT*

Hacettepe University, Faculty of Pharmacy, Department of Pharmaceutical Toxicology, Ankara, Turkey

ABSTRACT

Objectives: Pendimethalin (*N*-(1-ethylpropyl)-3,4-dimethyl-2,6-dinitrobenzeneamine) is a dinitroaniline herbicide compound which selectively controls weeds. It is a cell division and growth inhibitor. It descends plants in a short time after seedling. It is a soil and water pollutant due to the widespread use of formulations in Turkey and around the world. Pendimethalin is manufactured in and imported by Turkey. Pendimethalin is a slightly toxic compound that is classified in toxicity class 3 by the United States Environmental Protection Agency (USEPA). Even though it is classified as group C (human possible carcinogen) compound by the USEPA, there are limited number of studies about its genotoxic effects. The aim of this study was to evaluate *in vitro* genotoxic effects of different concentrations of pendimethalin in Chinese hamster over (CHO) cells by the single cell gel electrophoresis (comet) assay.

Materials and Methods: The cells are incubated with 1, 10, 100, 1000 and 10000 µM concentrations of pendimethalin for 30 min at 37°C and DNA damage was compared with CHO cells untreated with pendimethalin. 50 µM hydrogen peroxide was used as positive control.

Results: No significant cytotoxic effects were observed within the concentration ranges studied. The DNA damage in CHO cells was significantly increased in the pendimethalin concentrations of 1, 100, 1000 and 10000 µM, however, a significant decrease was observed in 10 µM pendimethalin concentration.

Conclusion: Our results show that 1-10000 µM concentrations of pendimethalin induce DNA damage in CHO cells, which was assessed by comet assay.

Key words: Pendimethalin, herbicide, DNA damage, comet assay, CHO cells

ÖZ

Amaç: Pendimetalin (*N*-(1-etilpropil)-3,4-dimetil-2,6-dinitrobenzenamin) seçici bitki kontrolü yapan dinitroanilin türevi bir herbisit bileşiktir. Hücre bölünmesi ve büyümesi engelleyicisidir. Bitkilerin filizlenme aşamasından kısa süre sonra ölmelerine neden olur. Türkiye'de ve dünyada formülasyonlarının yaygın kullanımı nedeniyle toprak ve su kirleticisidir. Pendimetalin Türkiye'de üretilmekte ve ithal edilmektedir. Pendimetalin az toksik bir bileşiktir ve Amerika Birleşik Devletleri Çevre Koruma Ajansı'na (USEPA) göre toksisite sınıfı 3'tür. USEPA tarafından grup C (insanda olası kanserojen) olarak sınıflandırılmasına rağmen genotoksik etkileri sınırlı sayıda çalışılmıştır. Bu çalışmanın amacı, farklı konsantrasyonlardaki pendimetalinin Çin hamster over (CHO) hücrelerindeki *in vitro* genotoksik etkilerini tek hücre jel eletroforez (comet) yöntemiyle değerlendirmektir.

Gereç ve Yöntemler: Hücreler 1, 100, 1000 ve 10000 µM konsantrasyonlardaki pendimetalin ile 37°C'de 0.5 saat inkübe edilmiş ve DNA hasarı pendimetalin uygulanmayan CHO hücreleriyle karşılaştırılmıştır. 50 µM hidrojen peroksit pozitif kontrol olarak kullanılmıştır.

Bulgular: Çalışılan konsantrasyon aralığında önemli sitotoksik etki gözlenmemiştir. CHO hücrelerindeki DNA hasarı 1, 100, 1000 ve 10000 µM konsantrasyonlarda önemli derecede artarken, 10 µM pendimetalin DNA hasarını önemli derecede azaltmıştır.

Sonuç: Sonuçlarımız, 1-10000 µM konsantrasyon aralığındaki pendimetalinin CHO hücrelerinde comet yöntemiyle değerlendirilebilen DNA hasarını indüklediğini ortaya koymaktadır.

Anahtar kelimeler: Pendimetalin, herbisit, DNA hasarı, comet yöntemi, CHO hücreleri

*Correspondence: **E-mail:** uundeger@hacettepe.edu.tr, **Phone:** +90 312 309 29 58
ORCID ID: orcid.org/0000-0002-6692-0366
Received: 14.07.2016, **Accepted:** 06.10.2016

INTRODUCTION

Pendimethalin (PM), whose chemical name is (*N*-(1-ethylpropyl)-3,4-dimethyl-2,6-dinitrobenzeneamine), is a dinitroaniline herbicide. It is an inhibitor of cell division and cell elongation which selectively terminates weeds. This pre- and early post-emergence herbicide is used to control broadleaf weeds and grassy weed species in cabbage, carrots, celery, cereals, citrus, corn, cotton, garlic, lettuce, onions, peanuts, peas, pome fruits, potatoes, radish, rice, sorghum, soybeans, tomatoes, tobacco and stone fruits. Moreover, it is also used in nonagricultural areas, residential lawns and ornamentals. PM is a widely used herbicide in different formulations; so that, it can be detected as a contaminant in surface and ground water, in soil and air with increasing amount.[1,2] It may disperse through leaching, drift, evaporation and runoff after application to soil. It is also degraded by photo- and bio-degradation or volatilization.[3,4] PM is classified as a slightly toxic compound and also classified in group C carcinogen (human possible carcinogen) by Environmental Protection Agency.[5] In spite of this classification only a few works have been published on the genotoxic effects of PM. PM induces cytotoxicity in rat hepatocytes evaluated by altered mitochondrial respiration.[6] It also shows cytotoxic effect in FRTL 5 (rat thyroid)[7] and Chinese hamster over (CHO) cell line.[8] Dimitrov et al.[9] (2006) has shown that PM significantly increased the chromosomal aberrations at 489 mg/kg dose in mouse bone marrow. In addition, it induced the micronucleus frequency in plant cell and mouse bone marrow polychromatic erythrocytes. PM achieved, concentration dependent (0.1-100 mM) induction in DNA damage evaluated by Comet assay in CHO cells.[8] PM decreased the root bundle length and increased the mitotic index and the percentage of chromosome aberrations dose dependently in maize and onion.[10] It has been reported to be a contaminant for the environment and found highly toxic for fish and aquatic invertebrates.[11] PM exposure has been correlated with an increased incidence of cancer.[12,13] On the other hand, Hou et al.[14] detected no association of exposure of PM during lifetime either with specific cancer sites or with overall cancer incidence among pesticide applicators in North Carolina and Iowa.

The Alkaline Single-cell Gel Electrophoresis technique or comet assay is a versatile tool for assessing DNA damage. Comet assay measures strand breaks, incomplete excision repair events, alkaline labile sites and cross-linking in individual cells. It has been shown to be a method commonly used for measuring the genetic damage induced *in vitro* by different genotoxic agents and also for determining DNA repair under a variety of experimental conditions.[15,16] This assay is also widely used for the evaluation of DNA damage in studies to characterize DNA lesions with and without the addition of the repair enzymes such as formamidopyrimidine N-glycosylase (FPG). FPG is a base excision repair enzyme, it initiates the repair of oxidized bases by recognizing, excising them and cutting the sugar-phosphate backbone of the DNA molecule. At the location of oxidized DNA bases, additional DNA strand breaks occurs and these leads to DNA migration. The determination of FPG-sensitive DNA lesions indicates the appearence of oxidized purine bases.[17-19]

In this study, the genotoxic potentials of dinitroaniline herbicide PM is investigated at different concentrations in CHO cells by using the comet assay with and without the addition of the repair enzyme FPG.

EXPERIMENTAL

Chemicals

The cells were purchased from Republic of Turkey, Ministry of Food, Agriculture and Livestock. The chemicals used in the experiments were purchased from the following suppliers: Low melting agarose (LMA) and normal melting agarose (NMA) (respectively) from Boehringer Manheim (Manheim, Germany); sodium hydroxide (NaOH) and sodium chloride (NaCl) from Merck Chemicals (Darmstadt, Germany); RPMI 1640 medium, fetal calf serum (FCS), trypsin-EDTA, penicillin-streptomycin, dimethylsulfoxide (DMSO), hydrogen peroxide (H_2O_2), ethidium bromide, Triton X-100, phosphate-buffered saline tablets, ethylenediamine tetraacetic acid disodium salt dihydrate (EDTA), *N*-lauroyl sarcosinate, Tris HCl, bovine serum albumin (BSA) and FPG enzyme from Sigma-Aldrich (St. Louis, MO, USA); olive oil from Egaş (Ankara, Turkey).

Cell culture

CHO cells were seeded in 75 cm^2 flasks in 20 mL RPMI 1640 medium (phenol red-free, with L-glutamine and 10% FCS) for 24 h in a 5% CO_2 atmosphere at 37°C.

Treatment of cells

CHO cells were treated for 30 min with 1, 10, 100, 1000 and 10000 mM concentrations of PM which dissolved in 0.5% DMSO and 0.02% olive oil mixture. 0.5% DMSO and 0.02% olive oil mixture were used as (-) controls. As positive control, to create oxidative DNA damage, 50 mM H_2O_2 solution was applied to cells for 5 min on ice, then H_2O_2 solution was removed. CHO cells were disaggregated with trypsin EDTA and resuspendated in 10% FCS containing medium. Cells were centrifugated for 3 min at 3000 rpm, the supernatant was removed.

Evaluation of cell viability

Trypan blue dye exclusion technique was performed for evaluation of cell viability.[19]

Comet assay

The basic alkaline comet assay of Singh et al.[20], as later mentioned by Collins et al.[21], was performed in the standard version and post-treatment with FPG protein to evaluate oxidative DNA damage was used as described in.[16,22,23] The precipitated cells were resuspended and mixed with 80 mL of LMA for embedding on slides which were covered with 1% NMA. Approximately 25.000 cells mixed with 80 mL of 1% LMA were rapidly pipetted onto this slide as the second layer. Slides were covered with cover slips, then kept on an ice-cold flat tray for 5 min to solidify. Cover slips were removed and slides were immersed in cold lysing solution (2.5 M NaCl, 100 mM Na_2EDTA, 10 mM Tris, 1% sodium laurylsarcosinate, pH 10) with 1.5% Triton X-100 and 10% DMSO was added just before use, for a minimum period of 1 h at 4°C. H_2O_2 treated positive

control cells were immersed in a seperate cold lysing solution. Following lysis, slides were washed in enzyme buffer (20 mM Tris HCl, 1 mM Na_2EDTA, 100 mM NaCl, 0.5 mg BSA/mL, pH 7.5) at 4˚C, four times for 5 min, 20 min in total. Slides were covered with 200 mL of FPG protein (1 mg/mL) in enzyme buffer for detection of FPG-sensitive DNA lesions, and incubated for 30 min at 37˚C, then cover slips were removed. Slides were placed in a horizontal gel electrophoresis tank. The tank was filled with fresh electrophoresis solution (1 mM NaEDTA, and 300 mM NaOH, pH 13). Slides were left in the electrophoresis solution for 20 min to allow the unwinding of the DNA and expression of alkaline labile damage before electrophoresis. Electrophoresis was conducted at a low temperature for 20 min using 25 volts and adjusting the current to 300 miliamperes. All of the steps were carried out under dimmed light to prevent the occurrence of additional DNA damage. The slides were washed with neutralysing buffer, three times after electrophoresis. Following the slides were washed in distilled water, 50%, 75% and 99% ethanol (for 5 min each), they were allowed to dry at room temperature. 30 mL of EtBr solution (20 mg/mL) was added to each slide for staining. The slides were investigated thoroughly by the use of a Leica fluorescence microscope (Leica, Wetzlar, Germany) with 400-fold magnification. The tail length, intensity, moment and migration of 'comets' were measured with a computerised image analysis system-comet Assay III Perceptive Instruments (Suffolk, England) for randomly selected 100 cells, i.e. 50 cells from each of two replicate slides from each sample. And the mean value of these parameters was used for the evaluation of the DNA damage by repeating the experiments for three times.

Statistical analysis

The statistical analysis was performed by SPSS for Windows 11.5 software (SPSS Software, Chicago, IL, USA). The results from the DMSO+olive oil-treated negative control, H_2O_2-treated positive control, and test groups treated with different concentrations of PM were statistically compared by the use of one-way ANOVA and the post hoc analysis of the group differences was evaluated by the least significant difference test and finally the results were expressed as means ± standard error of the mean (SEM).

RESULTS

CHO cells are exposed to PM (1-10000 mM) for 30 min. Cell viability was greater than 90%. DNA damage is determined with comet assay in this study. In comet assay, the amount of DNA breakage in a cell is estimated from the migration extent (tail length) of the genetic material in the direction of anode.[20] Also, the DNA percentage in the tail (tail intensity) has been shown to be proportional to the frequency of DNA strand breaks.[24] Tail moment is a simple identifier calculated by the computerized image analysis system considering both the migration tail length as well as the fraction of DNA migrated in the tail.[25] The DNA damage in CHO cells following *in vitro* 30 min treatment with 1-10000 mM concentrations of PM and post treatment with 50 mM H_2O_2 and 50 mM H_2O_2+FPG protein after PM treatment are shown in Table 1, 2 and Figure 1a-d. Results are given as

Table 1. DNA damage as tail length and tail intensity in CHO cells treated with pendimetalin

		PM treated CHO cells	PM+H_2O_2 treated CHO cells	PM+H_2O_2+FPG treated CHO cells
	Comet parameter	Tail length		
1	(-) Control	17.25±0.35	28.17±0.45***	60.56±0.88$^{\#\#\#}$
2	1 µM PM	18.41±0.40^{+}	32.23±0.41***	61.55±0.72$^{\#\#\#}$
3	10 µM PM	15.66±0.36^{++}	31.39±0.35***	71.21±0.62$^{\#\#\#}$
4	100 µM PM	19.93±0.42^{+++}	29.88±0.32***	66.43±0.61$^{\#\#\#}$
5	1000 µM PM	19.13±0.39^{++}	29.18±0.37***	65.49±0.57$^{\#\#\#}$
6	10000 µM PM	20.65±0.50^{+++}	34.64±0.36***	65.60±0.59$^{\#\#\#}$
		Tail intensity		
1	(-) Control	7.89±0.54	15.23±0.99***	64.46±1.41$^{\#\#\#}$
2	1 µM PM	7.46±0.62	24.34±1.53***	56.79±1.32$^{\#\#\#}$
3	10 µM PM	6.06±0.54^{+}	34.81±1.37***	62.28±1.32$^{\#\#\#}$
4	100 µM PM	8.40±0.65	38.85±1.32***	62.52±1.33$^{\#\#\#}$
5	1000 µM PM	8.48±0.62	33.33±1.32***	59.01±1.25$^{\#\#\#}$
6	10000 µM PM	9.83±0.86	51.03±1.36***	57.75±1.33$^{\#\#\#}$

Data represent mean values (±standard error of the mean) of tail length, tail intensity, tail moment and tail migration of the alkaline comet assay and refers to 300 scores/concentration (100 scores/experiment, three experiments)

PM: Pendimetalin, CHO: Chinese hamster over, $^{+}p<0.05$, $^{++}p<0.01$, $^{+++}p<0.001$ significance of DNA damage in PM treated CHO cells compared with DMSO (0.5%) + olive oil (0.02%) treated negative control cells; $^{*}p<0.05$, $^{**}p<0.01$, $^{***}p<0.001$ significance of DNA damage in PM treated CHO cells compared with PM+H_2O_2 treated CHO cells; $^{\#}p<0.05$, $^{\#\#}p<0.01$, $^{\#\#\#}p<0.001$ significance of DNA damage in PM+H_2O_2 treated CHO cells with PM+H_2O_2+FPG treated CHO cells

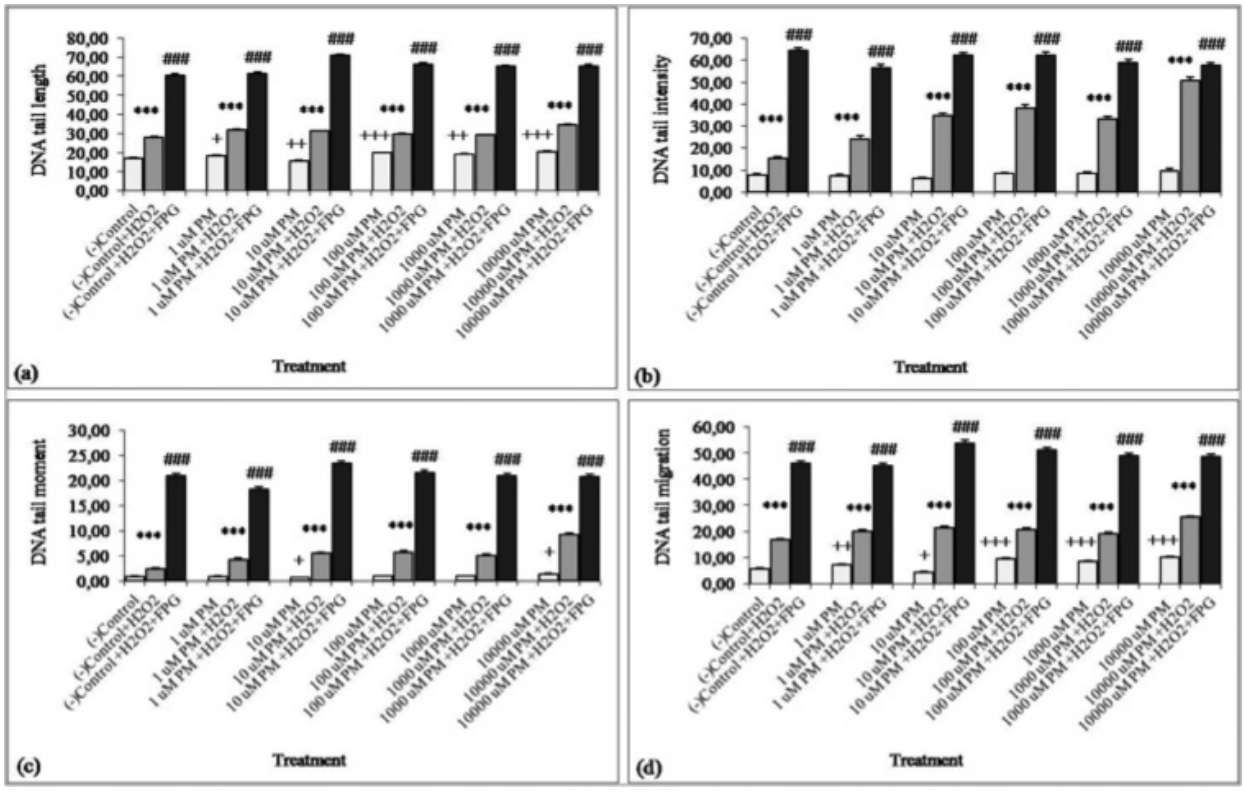

Figure 1. Genotoxic effects of pendimethalin for 30 min with or without Fpg in CHO cells, a) DNA damage was expressed as DNA tail length, b) DNA tail intensity (% DNA tail), c) DNA tail moment and d) DNA tail migration, results were given as the mean ± standard deviation

PM: Pendimethalin, FPG: Formamidopyrimidine *N*-glycosylase, $^{+}p<0.05$, $^{++}p<0.01$, $^{+++}p<0.001$, PM treatment compared to negative control [DMSO (0.5%) + olive oil (0.2%)], $^{*}p<0.05$, $^{**}p<0.01$, $^{***}p<0.001$, PM treatment compared to PM+50 µM H_2O_2, $^{\#}p<0.05$, $^{\#\#}p<0.01$, $^{\#\#\#}p<0.001$, PM+50 µM H_2O_2 treatment compared to PM+50 µM H_2O_2+FPG

Table 2. DNA damage as tail moment and tail migration in CHO cells treated with pendimetalin

		PM treated CHO cells	PM+H_2O_2 treated CHO cells	PM+H_2O_2+FPG treated CHO cells
	Comet parameter	Tail moment		
1	(-) Control	0.91±0.07	2.40±0.18**	20.85±0.53$^{\#\#\#}$
2	1 µM PM	0.90±0.08	4.24±0.28***	18.22±0.47$^{\#\#\#}$
3	10 µM PM	0.64±0.06^{++}	5.53±0.23***	23.34±0.54$^{\#\#\#}$
4	100 µM PM	0.98±0.08	5.78±0.22***	21.49±0.53$^{\#\#\#}$
5	1000 µM PM	1.00±0.08	5.11±0.24***	20.86±0.50$^{\#\#\#}$
6	10000 µM PM	1.37±0.15^{++}	9.20±0.27***	20.59±0.54$^{\#\#\#}$
		Tail migration		
1	(-) Control	5.67±0.35	16.75±0.46***	46.11±1.04$^{\#\#\#}$
2	1 µM PM	7.24±0.39^{++}	20.26±0.53***	45.33±0.92$^{\#\#\#}$
3	10 µM PM	4.36±0.35^{+}	21.41±0.47***	54.05±1.05$^{\#\#\#}$
4	100 µM PM	9.34±0.43^{+++}	20.78±0.44***	51.39±0.91$^{\#\#\#}$
5	1000 µM PM	8.57±0.39^{+++}	19.29±0.49***	49.04±0.90$^{\#\#\#}$
6	10000 µM PM	10.04±0.52^{+++}	25.42±0.53***	48.85±0.91$^{\#\#\#}$

Data represent mean values (±standard error of the mean) of tail length, tail intensity, tail moment and tail migration of the alkaline comet assay and refers to 300 scores/concentration (100 scores/experiment, three experiments)

PM: Pendimetalin, CHO: Chinese hamster over, $^{+}p<0.05$, $^{++}p<0.01$, $^{+++}p<0.001$ significance of DNA damage in PM treated CHO cells compared with DMSO (0.5%) + olive oil (0.02%)-treated negative control cells; $^{*}p<0.05$, $^{**}p<0.01$, $^{***}p<0.001$ significance of DNA damage in PM treated CHO cells compared with PM+H_2O_2 treated CHO cells; $^{\#}p<0.05$, $^{\#\#}p<0.01$, $^{\#\#\#}p<0.001$ significance of DNA damage in PM+H_2O_2 treated CHO cells with PM+H_2O_2+FPG treated CHO cells

the mean values (±SEM) of tail length, tail intensity, tail moment and tail migration.

According to the data obtained from three separate experiments, tail length and tail migration are significantly increased at all concentrations of the PM tested (1, 100, 1000 and 10000 µg/mL) when compared with those of untreated cells (Figure 1a, 1d, respectively). The tail length, tail intensity, tail moment and tail migration are significantly decreased at PM concentrations of 10 mM above the control values (Figure 1a-d). Moreover, the tail moment is significantly increased at PM concentrations of 10000 mM above the control values (Figure 1c).

Some inconsistencies among tail length, tail intensity, tail moment, tail migration and concentration are found (Figure 1a-d). Significant tail length and tail moment increases are found in CHO cells with 1, 100, 1000 and 10000 mM PM concentrations (Figure 1a, 1c, respectively). On the other hand, significant tail length, tail intensity, tail moment and tail migration decreases are found in these cells with only 10 mM PM concentration (Figure 1a-d). Generally, the genotoxic effects of the PM in CHO cells are appeared to be better reflected by tail length and tail migration than tail intensity and tail moment in this study. Post-treatment with H_2O_2+FPG protein reveals increases in all the investigated comet variables when compared to post-treatment with just H_2O_2, in previously 10, 100 and 1000 mM concentrations of PM treated CHO cells (Figure 1a-d). This finding shows that, DNA damage performed with 10, 100 and 1000 mM concentrations of PM+H_2O_2 treatment is an oxidative DNA damage which may be repaired by FPG protein.

DISCUSSION

DNA oxidative damage is a common type of damage of cells from reactive oxygen species (ROS) and it can lead to many different mutations and problems in DNA. Reactive oxygen species include hydrogen peroxide, superoxide anion radical, singlet oxygen, hydroxyl radical and nitric oxide. They are the consequence of normal body processes such as metabolism and also the consequence of interactions with toxic chemicals, certain drugs and radiation. ROS is not the only reason of oxidative DNA damage. Decreases in antioxidant defence and inhibition of repair of oxidative damage can also cause oxidation of DNA.[26] It is clear that oxidative DNA damage may lead to mutations upon cells. Mutations are very important step in carcinogenesis, and so elevated levels of oxidative DNA damage plays a critical role in the initiation, promotion and progression stages of carcinogenesis.[26,27] Oxidative DNA damage has also been associated with other diseases such as Alzheimer's disease, Huntington's disease, Parkinson's disease, hepatitis, atopic dermatitis, autoimmune diseases, atherosclerosis.[26-28] ROS may also cause sperm disfunction and plays a significant role in male infertility.[29] Additionally, it is suggested that the gradual accumulation of free-radical damage to biomolecules occurs aging.[26,30]

PM is widely used dinitroaniline herbicide in all continents of the world. On the other hand, scanty number of studies have been conducted on the genotoxic effects of PM. In this study, the DNA damage in all variables examined in CHO cells at various concentrations with PM application for 30 min, is created hormetic concentration-response (U shape concentration-response curve). Tail length and tail migration with 1 mM concentration of PM significantly increases as compared to negative controls ($p<0.05$ and $p<0.01$, respectively); while tail intensity and tail moment are decreased at 1 mM concentration of PM, this decrease is statistically insignificant. However, DNA tail length ($p<0.01$), tail intensity, tail moment and tail migration ($p<0.05$) values of CHO cells at 10 mM concentrations of PM application, significantly decreases compared to negative controls. In all the examined parameters, the DNA damage is increased with 100, 1000 and 10000 mM concentrations of PM applications when compared to negative controls. The increases in the DNA tail length and tail migration at three concentrations ($p<0.001$) and in the DNA tail moment for 1000 mM concentration ($p<0.05$) are statistically significant.

Our findings are in agreement with the results of the study conducted by Patel et al.[8] This study is the only other comet study in the literature performed in various concentrations of PM applied CHO cells. Patel et al.[8] were evaluated the cytotoxic effects of PM in CHO cells after application of PM for 3 h at 1, 10 , 100, 1000 and 10000 mM concentrations by MTT (*3-(4,5-Dimethylthiazol-2-yl)-2,5-diphenyltetrazolium bromide)* method, then they determined the DNA damage by comet assay. The results of this study show that, the IC_{50} value of PM is close to the 10000 mM. Moreover mitochondrial activity of CHO cells exposed to 10000 mM concentrations of PM for 3 h, shows a decrease of 54% compared to controls. The 90% cell viability after 3 h of exposure of PM is determined in 10-100 mM. Patel et al.[8] also report over 90% of cell survival by trypan blue staining method in CHO cells which are exposed to 0.01, 0.1, 1, 10 and 100 mM concentrations of PM for 3 h. The DNA damage is investigated by comet assay in terms of the arbitrary units, % tail DNA and tail length. PM is found to cause a significant concentration dependent increase in DNA damage in the studied variables, at the concentrations of 0.1 to 100 mM ($p<0.05$). In our study, unlike the work of Patel et al.[8], CHO cells are exposed to PM for 30 min and comet assay is performed by using FPG enzyme additionally. According to the results of our study, after 30 min application of PM in 1-10000 mM concentrations and following 50 mM H_2O_2 application for 5 min, the oxidative DNA damage which is formed in CHO cells can be repaired by FPG enzyme.

CONCLUSION

The data in the literature combined with our results show that commonly used dinitroaniline herbicides PM induced DNA damage in 1-10000 mM concentration in CHO cells can be detected by comet assay. Patel et al.[8] also conclude that PM may possess clastogenic effects such as some compounds having the same chemical structure of dinitroaniline herbicides. In this study, CHO cells are incubated with PM for 30 min. For more information about DNA damaging effects of PM, it will be useful to perform similar studies using longer incubation periods more than 30 min. In further studies, to refine the

data obtained in our study in the concentration range from 1 to 10000 mM and to be informed about the possible effects on close to human exposure concentrations, the DNA damage should be detected in concentrations below 10 mM. In addition, chromosomal aberration studies must be carried out for the detection of claimed clastogenic effects of PM.

Conflict of Interest: No conflict of interest was declared by the authors.

REFERENCES

1. Kegley S, Hill B, Orme S, Pendimethalin. PAN Pesticide Database, Pesticide Action Network, North America, San Francisco, CA, 2007, Available via ‹http://www.pesticideinfo.org›
2. Clarke J, Wynn S, Twinning S, Berry P, Cook S, Ellis S, Gladders P. Pesticide availability for cereals and oilseeds following revision of Directive 91/414/EEC, effects of losses and new research priorities, In: HGCA Research Review Nr 70. 2009.
3. Strandberg M, Scott-Fordsmand JJ. Effects of pendimethalin at lower trophic levels a review. Ecotoxicol Environ Safe. 2004;57:190-201.
4. Venkata Mohan S, Rama Krishna M, Muralikrishna P, Shailaja S, Sarma PN. Solid phase bioremediation of pendimethalin in contaminated soil and evaluation of leaching potential. Bioresour Technol. 2007;98:2905-2910.
5. US Environmental Protection Agency (US EPA), R.E.D. Facts: Pendimethalin, US EPA, Washington, DC, 1997.
6. Yamano T, Morita S. Effects of pesticides on isolated rat hepatocytes, mitochondria, and microsomes II. Arch Environ Contam Toxicol. 1995;28:1-7.
7. Pan H, Sun D, Wang J, Wu D. Using the FRTL-5 cell to screen the thyroxine disrupting effects of the two pesticides-ethylenethiourea and pendimethalin. Wei Sheng Yan Jiu. 2004;33:267-269.
8. Patel S, Bajpayee M, Pandey AK, Parmar D, Dhawan A. *In vitro* induction of cytotoxicity and DNA strand breaks in CHO cells exposed to cypermethrin, pendimethalin and dichlorvos. Toxicol In Vitro. 2007;21:1409-1418.
9. Dimitrov BD, Gadeva PG, Benova DK, Bineva MV. Comparative genotoxicity of the herbicides Roundup, Stomp and Reglone in plant and mammalian test systems. Mutagenesis. 2006;21:375-382.
10. Promkaev N, Soontornchainaksaeng P, Jampatong S, Rojanavipart P. Toxicity and genotoxicity of pendimethalin in maize and onion. Kasersart J (Nat Sci). 2010;44:1010-1015.
11. Singh B, Singh K. Microbial degradation of herbicides. Crit Rev Microbiol. 2014;42:1-17.
12. Hurley PM. Mode of carcinogenic action of pesticides inducing thyroid follicular cell tumors in rodents. Environ Health Perspect. 1998;106:437-445.
13. Alavanja MC, Dosemeci M, Samanic C, Lubin J, Lynch CF, Knott C, Barker J, Hoppin JA, Sandler PD, Coble J, Thomas K, Blair A. Pesticides and lung cancer risk in the agricultural health study cohort. Am J Epidemiol. 2004;160:876-885.
14. Hou L, Lee WJ, Rusiecki J, Hoppin JA, Blair A, Bonner MR, Lubin JH, Samanic C, Sandler DP, Dosemeci M, Alavanja MC. Pendimethalin exposure and cancer incidence among pesticide applicators. Epidemiology. 2006;17:302-307.
15. Fairbairn DW, Olive PL, O'Neill KL. The comet assay: a comprehensive review. Mutat Res. 1995;339:37-59.
16. Speit G, Hartmann A. The comet assay (single-cell gel test). A sensitive genotoxicity for the detection of DNA damage and repair. Methods Mol Biol. 1999;113:203-212.
17. Collins AR, Duthie SJ, Dobson VL. Direct enzymic detection of endogenous oxidative base damage in human lymphocyte DNA. Carcinogenesis. 1993;14:1733-1735.
18. Collins AR, Dusinska M, Gedik CM, Stetina R. Oxidative damage to DNA: do we have a reliable biomarker? Environ Health Perspect. 1996;104:465-469.
19. Tennant JR. Evaluation of the trypan blue technique for determination of cell viability. Transplantation. 1964;2:685-694.
20. Singh NP, McCoy MT, Tice RR, Schneider EL. A simple technique for quantitation of low levels of DNA damage in individual cells. Exp Cel Res. 1988;175:184-191.
21. Collins AR, Dobson VL, Dusinska M, Kennedy G, Stetina R. The comet assay: what can it really tell us? Mutat Res. 1997;375:183-193.
22. Undeğer U, Başaran A, Degen GH, Başaran N. Antioxidant activities of major thyme ingredients and lack of (oxidative) DNA damage in V79 Chinese hamster lung fibroblast cells at low levels of carvacrol and thymol. Food Chem Tox. 2009;47:2037-2043.
23. Aydın S, Tokaç D, Başaran N, Başaran AA. Effect of epigallocatechin gallate on oxidative DNA damage in human lymphocytes. Turk J Pharm Sci. 2015;12:19-28.
24. Olive PL, Banath JP, Durand RE. Heterogeneity in radiation-induced DNA damage and repair in tumor and normal cells measured using the 'comet' assay. Radiat Res. 1990;122:86-94.
25. Villarini M, Moretti M, Pasquini R, Scassellati-Sforzolini G, Fatigoni C, Marcarelli M, Monarca S, Rodriguez AV. *In vitro* genotoxic effects of the insecticide deltamethrin in human peripheral blood leukocytes: DNA damage ('comet' assay) in relation to the induction of sister-chromatid exchanges and micronuclei. Toxicology. 1998;130:129-139.
26. Azqueta A, Shaposhnikov S, Collins AR. Detection of oxidised DNA using DNA repair enzymes. In: Dhawan A, Anderson D, eds. The comet assay in toxicology. RSC Publishing; Cambridge; 2009:57-78.
27. Cooke MS, Evans MD, Dizdaroglu M, Lunec J. Oxidative DNA damage: mechanisms, mutation, and disease. FASEB J. 2003;17:1195-1214.
28. Olinski R, Gackowski D, Foksinski M, Rozalski R, Roszkowski K, Jaruga P. Oxidative DNA damage: assessment of the role in carcinogenesis, atherosclerosis, and acquired immunodeficiency syndrome. Free Radic Biol Med. 2002;33:192-200.
29. Shen HM Ong C. Detection of oxidative DNA damage in human sperm and its association with sperm function and male infertility. Free Radic Biol Med. 2000;28:529-536.
30. Harman D. Aging: a theory based on free radical and radiation chemistry. J Gerontol. 1956;11:298-300.

Turk J Pharm Sci 2017;14(2):191-200
DOI: 10.4274/tjps.69855

ORIGINAL ARTICLE

Ocular Application of Dirithromycin Incorporated Polymeric Nanoparticles: an *In Vitro* Evaluation

Diritromisin Yüklü Polimerik Nanopartiküllerin Oküler Uygulanması: *İn Vitro* Değerlendirme

Ebru BAŞARAN

Anadolu University, Faculty of Pharmacy, Department of Pharmaceutical Technology, Eskişehir, Turkey

ABSTRACT

Objectives: Ocular drug delivery is a difficult challenge especially with topical intillation which results in rapid drainage and non-productive drug absorption. For the improvement of the pre-corneal retention time and enhancing the corneal permeability, colloidal drug delivery systems play an important role in enhancement of the ocular bioavailability. In this study, dirithromycin incorporated Kollidon® SR-based polymeric nanoparticles, an antibacterial agent, were formulated for the efficient treatment of severe ocular bacterial infections.

Materials and Methods: In this study, dirithromycin was incorporated into the Kollidon® SR-based nanoparticles by spray drying method. *In vitro* characteristic properties were evaluated in detail during the storage period of three months at three different conditions.

Results: The results of *in vitro* analyses revealed that characteristic properties of the particles were remained unchanged during the storage period of three months.

Conclusion: Kollidon® SR-based polymeric nanoparticles are good candidates for drug delivery systems in the treatment of severe ocular bacterial infections with dirithromycin.

Key words: Dirithromycin, Kollidon® SR, polymeric nanoparticles, ocular drug delivery

ÖZ

Amaç: Özellikle gözyaşı üretimi ve kırpma refleksleri gibi gözün koruyucu mekanizmalarına bağlı olarak göze topik olarak uygulanan formülasyonların göz yüzeyinden hızla uzaklaştırılması ve korneal yüzeyden verimsiz absorbsiyonu söz konusu olmaktadır. Prekorneal tutunma süresinin ve korneal permeabilitenin arttırılması ile oküler biyoyararlanımın arttırılmasında kolloidal ilaç taşıyıcı sistemler büyük önem taşımaktadır. Bu çalışmada antibakteriyel etkili bir madde olan diritromisin yüklü Kollidon® SR yapılı polimerik nanopartiküller şiddetli oküler bakteriyel enfeksiyonların etkin tedavisi amacı ile hazırlanmıştır.

Gereç ve Yöntemler: Bu çalışmada diritromisin Kollidon® SR yapılı polimerik nanopartiküllere püskürterek kurutma yöntemi ile yüklenmiştir. Nanopartiküllerin *in vitro* karakteristik özellikleri üç farklı ortamda üç ay süresince detaylı olarak incelenmiştir.

Bulgular: *İn vitro* analiz sonuçları parçacıkların üç aylık saklama süresince karakteristik özelliklerini koruduklarını göstermiştir.

Sonuç: Kollidon® SR yapılı polimerik nanopartiküllerin şiddetli oküler bakteriyel enfeksiyonların diritromisin ile tedavisinde oldukça etkili ilaç taşıyıcı sistem adayları olduklarını göstermiştir.

Anahtar kelimeler: Diritromisin, Kollidon® SR, polimerik nanopartiküller, oküler ilaç taşıyıcı sistemler

*Correspondence: **E-mail:** ebcengiz@anadolu.edu.tr, **Phone:** +90 533 712 74 22
ORCID ID: orcid.org/0000-0003-2104-2069
Received: 17.01.2017, **Accepted:** 27.04.2017

INTRODUCTION

The topical instillation of the ocular formulations is the primary choice application method for ocular therapy.[1] However, the bioavailability of ophthalmic drugs via topical route result in a short duration at the therapeutic concentration, due to the several protective mechanisms of the eye like lacrimal secretion, high tear turnover and blinking reflex.[2,3] To overcome the poor bioavailability of drugs (5-10% of the applied dose) from ocular dosage forms after topical application, researchers mostly developed mucoadhesive colloidal drug delivery systems for extended corneal/conjuctival contact time.[4-7]

Most cases of acute infections, topical antibacterial treatment offers several benefits like shorter disease duration; prevention of spread of infection; reduction in side effects, and reduced disease recurrence.[8] In the eye bacterial, fungal and viral pathogens can produce severe disorders like conjunctivitis, keratitis, blepharitis, corneal ulcers and are one of the causes of ophthalmia neonatorum for the infants which may lead to the loss of an eye when being untreated sufficiently.[9,10]

Bacteria and other microorganisms are far more resistant to adverse situations than animal cells and can withstand environments that would be quickly lethal to us in many cases.[9]

Macrolides are one of the antibacterial agent group that are being used for the treatment of proposed disorders. All of the macrolides have a similar mechanism of action in that they selectively bind to the 50S subunit of the bacterial ribosome while not binding to the mammalian 80S ribosomal subunit, which accounts, in part, for their safety and selectivity of action.[11]

Erythromycin is the first member of the macrolide group and many derivatives were synthesized afterwards.[12] Dirithromycin is the second generation of semisynthetic macrolide derived from erythromycin with a 14-membered lactone ring.[13] It is acid stable and better absorbed with higher bioavailability than for erythromycin however its oral bioavailability results in between 6-14%.[11,14]

Furthermore, in addition to their antibacterial activities, macrolides such as azithromycin exhibit potent anti-inflammatory activities.[10] Despite being well tolerated, macrolides have a number of important side effects such as gastrointestinal adverse reactions QT interval prolongation, hepatotoxicity, ototoxicity, color vision loss and interactions with other drugs because of inhibition of drug metabolism.[15,16] For the enhancement of low bioavailability data and requirement of safer formulations dirithromycin was incorporated into polymeric nanoparticles in this study.

Kollidon® SR is polyvinyl acetate [polyvinyl alcohol (PVA), 80%] and [polyviniyl pyyrolidone (PVP), 20%] based mixture mostly used for pH-independent sustained release matrix tablets.[17-19] When PVA part gives to a tablet/particle structural integrity, water soluble PVP part leaches out forming pores where the active agent diffuses out.[17] Kollidon® SR has demonstrated to have no acute toxicity and to be not irritating to the skin or mucous membranes.[20] Kollidon® SR contains no ionic groups therefore its sustained release properties are unaffected by ions or salts.[21]

Considering the safety and the modification opportunities of the polymer novel application route for Kollidon® SR was studied for the first time in this study for efficient treatment of ocular bacterial infections using dirithromycin.

MATERIALS AND METHODS

Materials

Dirithromycin and Kollidon® SR was kindly gifted by Abdi İbrahim (İstanbul, Turkey) and by BASF (İstanbul, Turkey) respectively. Methanol was purchased from Merck (Darmstadt, Germany). *Staphylococcus aures* [American Type Culture Collection (ATCC 25923)] and *Pseudomonas aeruginosa* (ATCC 27853) strains were obtained from ATCC. All other reagents used were of analytical grade.

Methods

Preparation of nanoparticles

Spray-drying method was used for the preparation of nanoparticles.[22-24] Briefly, accurately weighed Kollidon® SR (1 g) was dissolved in methanol (60 mL). Dirithromycin was added to the mixture under mild agitation (150 rpm). Final transparent solution was then spray-dried using a Nano Spray Dryer (B-90, BUCHI Labortechnik AG, Flawil, Switzerland) with an inlet temperature of 90˚C±1˚C (outlet temperature of 35˚C±5˚C). White dry powders were collected and kept in tightly-closed and coloured vials at room temperature until being analyzed.

Placebo nanoparticles were prepared as described above without the addition of active agent.

Characterization of nanoparticles

Morphology

The microstructural characterization of the nanoparticles prepared were investigated using scanning electron microscope (SEM) (Carl Zeiss SUPRA 50 VP, Oberkochen, Germany) at 25˚C±2˚C.

Particle size and zeta potential

Particle size, polydispersity index (PDI) and zeta potential measurements were performed on freshly prepared samples using Malvern Nano ZS (Zetasizer Nano Series, Worcestershire, UK). Samples of all nanoparticles were dispersed in double-distilled water (adjusted to a constant conductivity of 50 μS/cm^2 using 0.9% NaCl) just prior to analyses.[25] All analyses were repeated in triplicate at 25˚C±2˚C.

pH value

*p*H values of the nanoparticle dispersions were analyzed at 25˚C±2˚C by WTW Profi Lab (pH 597, Weilheim, Germany). All analyses were repeated in triplicate.

Differential scanning calorimetry

Structural and crystallinity changes of dirithromycin and the Kollidon® SR due to the formulation steps were evaluated using differential scanning calorimetry (DSC) (DSC-60, Shimadzu Scientific Intruments, Columbia, MI, USA). Analyses were performed under nitrogen (flow rate of 50 mL/min) at 30-300˚C

temperature range with a constant heating rate of 10°C min^{-1}. DSC thermograms of pure materials were used as references for the comparison of the possibility of crystallinity changes of the structures.

X-ray diffractometry

For the evaluation of the crystallinity changes X-ray diffraction (XRD) analyses were performed (Rikagu Corporation D/Max-3C; Tokyo, Japan) within the range of 2-40° at 2θ with 2°/min scanning rate and using 40 kV voltage with 20 mA current intensity level. Analyses spectra of pure polymer and pure dirithromycin were used as references for evaluating the structural changes of the materials throughout formulation stages.

Fourier transform infrared spectrophotometry

IR Prestige-21 (Shimadzu, Tokyo, Japan) was used for fourier transform infrared (FTIR) analyses. Deuterated triglycine sulfate doped with L-alanine detector was used with Germanium-coated KBr plate beam splitter at 4000-500 cm^{-1} range. FTIR spectra of pure dirithromycin and polymer were used as references.

Nuclear magnetic resonance

For the evaluation of the interactions between the active agent and the polymer ^{1}H-NMR analyses were performed on UltraShield™ CPMAS NMR (Brucker, Rheinstetten, Germany) using deuterated chloroform ($CDCl_3$) as solvent. Spectra of pure dirithromycin and Kollidon® SR were used as references.

Determination of dirithromycin

A modified high-performance liquid chromatography (HPLC) method was used for the determination of dirithromycin.[26,27] Shimadzu 20 A (Tokyo, Japan) with Shimadzu Shim-Pack CLC-ODS column (Tokyo, Japan; column diameter: 4.6 mm, column length: 15.0 cm, particle diameter: 5 µm and particle size: 100 Å) was used as the instrument. Water:methanol:pbs buffer:acetonitrile (9:19:28:44, v/v/v/v, pH: 7.5) was used as the mobile phase with a flow rate of 1.0 mL/min. 20 µL constant amount of samples was injected via an Automatic Injector (Shimadzu, Tokyo, Japan) and Photodiode Array Detector (Shimadzu, Tokyo, Japan) was used at 205 nm. Column temperature was set to 30°C. Validation studies were performed for data reliability.

Drug loading and encapsulation efficiency

Accurately weighed particles (50 mg) were dissolved in 5 mL methanol while the same amount of particles were dispersed in 2-propanol (5 mL), vortexed for 1 min and centrifuged at 2000 rpm for 10 min for the determination of total dirithromycin content (DIR_T) and dirithromycin adsorbed on the nanoparticle surfaces (DIR_S), respectively. Supernatants were analyzed by HPLC after proper dilutions (n=3).

Drug loading and encapsulation efficiency (EE) were calculated according to Equation 1 and Equation 2 respectively.

$$\text{Drug loading (\%)} = [(DIR_T) / (\text{Particle weight})] \times 100$$

Equation (1)

$$\text{EE (\%)} = [(DIR_T - DIR_S) / (DIR_T)] \times 100$$

Equation (2)

In vitro release study

The dialysis bag diffusion method was used to analyze the *in vitro* drug release studies of dirithromycin incorporated Kollidon® SR nanoparticles.[28,29] *In vitro* release profiles of dirithromycin were investigated in freshly prepared simulated tear fluid (STF) at pH 7.4.[30-32] Briefly, spray-dried nanoparticles containing 5.0 mg dirithromycin were put in dialysis bags. Bags were closed tightly from both ends and were immersed in the dissolution medium containing 30 mL STF at 34°C±1°C on a water bath using continuous magnetic stirrer with a stirring rate of 150 rpm. 1 mL of samples were collectes at predetermined time intervals and dirithromycin content of the samples was analyzed using HPLC method as described at the previous section and release profile of the pure dirithromycin was used as a reference for better evaluation of the profiles. Each experiment was repeated three times.

Evaluation of the cytotoxicity

The toxicity of the nanoparticles prepared were evaluated by 3-(4,5-dimethylthiazol-2-yl)-2,5-diphenyltetrazoliumbromide (MTT) assay.[33,34] Briefly, cells were suspended in Dulbecco's Modified Eagle's Medium solution (containing 10% fetal bovine serum) and $2x10^4$ cells/mL were seeded into 96 well plates and cultured for 24 hrs. Formulations with different concentrations were added to the suspension and the mixtures were incubated at 37°C (under 5% CO_2 and 95% air) for 24 and 48 hrs. After the incubation period, 20 µL (5 mg/mL) of MTT dye was added to each well and incubated for more 2 hrs. (at 37°C) for the transformation of MTT to formazan salt by the presence of the living cells. Formazan crystals were extracted using 200 µL dimethyl sulfoxide (DMSO) and the amount of the dye was determined spectrophotometrically at λ=540 nm with microplate reader (Victor X5, Perkin Elmer, England).

Microbiological assay

The antifunfal activity of the formulations were evaluated with M27-A2 standard Microbroth Dilution Method.[35] Briefly formulations were dissolved in DMSO within the concentration of 400 µg/mL-0.78 µg/mL and transferred to the 96 well plates with a concentration of 100 µL. *S. aures* (ATCC 25923) and *P. aeruginosa* (ATCC 27853) were inoculated at the concentrations of $5x10^5$ CFU/mL. Positive and negative control groups were used as references. Resazurin was added to the plates up to the final concentration of 20 µg/mL after the 24 h incubation period at 36°C. The plates were analyzed with Synergy™ HT (Bio-Tek, USA) and the minimum inhibitory concentration (MIC) was evaluated as the lowest concentration that inhibits the visible microbial growth.[36]

Stability of the formulations

For the evaluation of the stability of the formulations prepared, samples were kept at different temperatures (25°C±2°C - 60%±5 RH; 40°C±2°C - 75%±5 RH, 5°C±3°C) during the storage period of 3 months and the particle size, PDI, zeta potential, pH and DSC analyses were evaluated on the day of production and at the end of 3 months for the evaluation of the changes in the characteristic properties of the nanoparticles.

RESULTS AND DISCUSSION

Compositions of the Kollidon® SR nanoparticles prepared were given in Table 1.

Duration of active agent on the ocular surface is mostly particle size dependent.[37] Drug can be absorbed into ocular tissues from precorneal pocket by small sized particles while on the other hand, longer retention times on the ocular surface and slow drug dissolution can be achieved by bigger sized particles. However condisering the irritation and tolerability issues particle sizes smaller than 10 µm are prerequisite for ocular administration.[37-39]

Particle size, zeta potential, pH and active agent contents of the Kollidon® SR based particles were summarized in Table 2.

Particle sizes of KD1 and KD2 formulations were found to be 329.6±6.8 nm and 522.2±24.4 nm, respectively, with relatively homogenous size distribution considering the PDI values (Table 2). Increased encapsulation has influenced the particle size however particle sizes remained in the nanometer range which will be convenient for topical ocular application. During the storage period of 3 months particle sizes were slightly changed (Table 2) showing that the storage conditions did not change the ocular applicability potential of the particles by remaining below the limit of 10 µm.[39]

Particle size and surface charge and are the two most frequently referred factors that are responsible for the enhanced biological effects of nanoparticles including cellular uptake, toxicity and dissolution.[40] Despite giving informations about the interactions with the ocular tissues, zeta potential values also gives preliminary data for the prediciton of the physical stability of particle dispersions.[41] Guidelines classifying nanoparticle dispersions with zeta potential values of ±0-10 mV, ±10-20 mV and ±20-30 mV and >±30 mV as highly unstable, relatively stable, moderately stable and highly stable, respectively.[40,42]

Since the corneal and conjunctival surfaces are negatively charged, main approach for the enhancement of ocular bioavailability cationic drug delivery systems are being preferred considering possesment of enhanced bioavailability due to the electrostatic interactions between the surfaces.[24,43-46] However anionic drug delivery systems also can enhance ocular bioavailability by the help of monocarboxylate transport which processes a proton or Na^+-coupled lactate systems in epithelial cells which may enhance the ocular bioavailability of the anionic drugs in a great extent.[47]

In this study zeta potentials were valued as -19.5±0.3 mV and -25.5±0.1 mV for KD1 and KD2 formulations respectively (Table 2). After 3 month storage period potentials were valued within the range of -20.1±4.1 mV and -26.5±0.3 mV indicating physical stability of the nanoparticles during the storage period (Table 2). Considering negatively charged polymeric nanoparticles prepeared, active transport might be the main mechanism of the enhanced bioavailability of dirithromycin by topical application.[47]

The pH and buffering of ocular formulations are very important since the pH changes are the main reason of the stability problems as well as the discomfort, safety and efficacy issues of the formulations prepared. Therefore ideally pH of the formulations would be buffered to pH 7.4 considering the physiological pH of the tear fluid.[48] Since the pH values of the formulations were 5.04±0.00 for placebo KD, 7.39±0.01 for KD1 and 7.90±0.00 for KD2 no adjustments were required for dirithromycin incorporated nanoparticle formulations in our study (Table 2). After 3 month storage period pH values were remained within the range of ocular tolerability.[49]

Dirithromycin was reported to crystallize into different polymorphic forms in different solvents, such as nonsolvated crystal forms (1 and 2), 1-propanol solvate, cyclohexane trisolvate and acetonitrile-trihydrate.[50,51] Therefore it is very important to evaluate morphological changes of dirithromycin and Kollidon® SR during and after formulation steps. In our study structural changes were evaluated by DSC analyses. Pure dirithromycin demonstrated a melting point at 191.3°C showing the crystalline structure (Figure 2a). No peaks were detected for both placebo formulation and pure Kollidon® SR as expected due to the amorphous structure of the polymer. DSC thermogram of the physical mixture of the dirithromycin with Kollidon® SR showed the stability of the active agent in the polymeric carrier owing to the presence of dirithromycin in crystalline structure. And the absence of the endothermic peak of dirithromycin in the formulations showing that the

Table 1. Composition of Kollidon® SR nanoparticles prepared

Code	Kollidon® SR (g)	Dirithromycin (g)	Methanol (mL)
Placebo KD	1	—	60
KD1	1	0.10	60
KD2	1	0.15	60

KD: Kollidon®, Dirithromycin

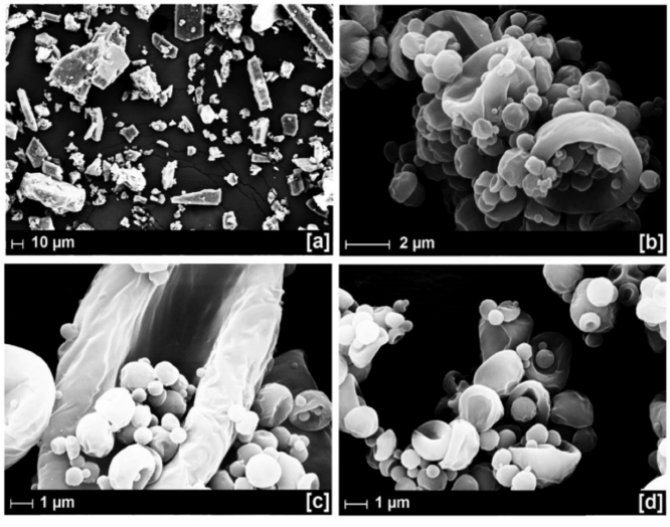

Figure 1. Scanning electron micrographs of pure dirithromycin and nanoparticles prepared, a) Dirithromycin, b) Placebo KD, c) KD1, d) KD2

KD: Kollidon®, Dirithromycin

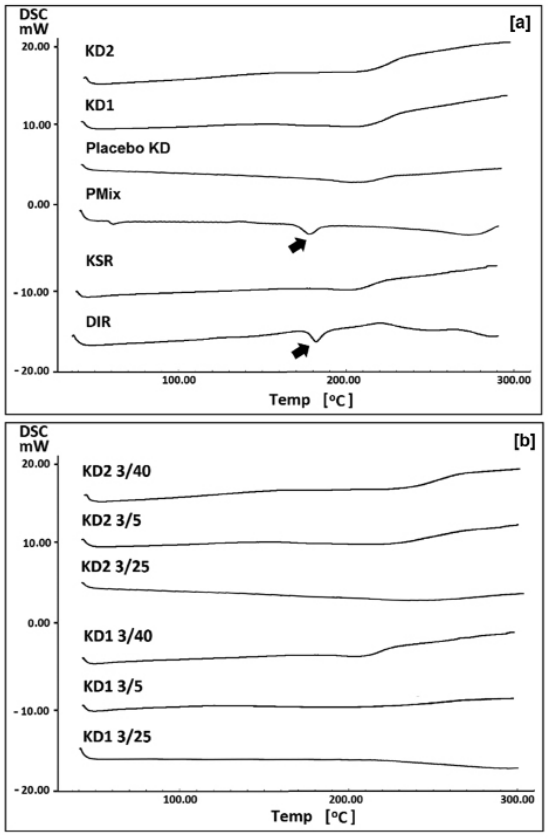

Figure 2. Differential scanning calorimetry thermograms of pure dirithromycin and the nanoparticles prepared, a) At the day of production, b) After the storage period of 3 months

DIR: Dirithromycin, KSR: pure Kollidon® SR, PMix: Physical mixture of dirithromycin with Kollidon® SR, Stability codes as x/y; x represents the storage month while y represents the storage conditions

dirithromycin was molecularly dispersed within the amorphous polymeric structure (Figure 2a). After the storage period of 3 months amorphous state of the polymeric structure remained unchanged showing that the particles were not affected from the storage conditions (Figure 2b).[52]

XRD is one of the most important characterization tools used in solid state chemistry and materials science for the determination of the size and the shape of the unit cell for polycrystals in nanoscale.[53,54] Diffraction pattern gives information of the crystalline/amorphous structure of the materials.[54] Since the polymorphic changes of the active agents are important factors which might affect the dissolution rate and the bioavailability of the applied drug, possibility of the structural changes must be monitored.[55] XRD also gives information about the size of the particles with the help of measurement of the smallest unfaulted regions or coherently scattering domains of the material.[56]

In XRD profiles dirithromycin showed sharp peaks at 2θ-scattered angles indicating crystalline structure (Figure 3). Pure Kollidon® SR showed semicrystalline structure (marked with arrows) however after spray drying process polymer transformed to the amorphous state which gives spaces for the incorporation of the active agent within the polymeric network. No signals were detected in the spectra of KD1 and KD2 (Figure 3) showing that the dirithromycin was dispersed within the amorphous polymer as indicated by DSC analyses results.

FTIR analysis method based on the selective absorption of light by the vibration modes of specific chemical bonds in the sample therefore FTIR analyses gives concise informations about the interactions occurred between the drug and polymer during the formation stages of nanoparticles by evaluating the alterations in frequency and intensity of the structures compared to FTIR signals of pure materials.[57]

Table 2. Particle size, polydispersity index, zeta potential, pH values and dirithromycin contents of Kollidon® SR nanoparticles prepared (n=3, mean ± standard error)

Code	PS (nm)	PdI	ZP (mV)	pH	DIR_S (%)	DIR_E (%)
Placebo KD	363.0±24.4	0.524±0.189	-19.6±4.1	5.04±0.01	-	-
KD1	329.6±6.8	0.425±0.080	-19.5±0.3	7.39±0.01	75.0±0.0	25.0±0.1
KD2	522.2±14.4	0.539±0.163	-25.5±0.1	7.90±0.00	55.6±0.1	44.4±0.1
Stability codes					**Total DIR loss (%)**	
Placebo KD-3/25	366.0±4.2	0.612±0.127	-20.6±1.1	5.54±0.10		
KD1-3/25	335.7±5.4	0.545±0.110	-21.5±0.2	7.42±0.01	0.18±0.02	
KD2-3/25	554.3±2.5	0.524±0.174	-26.1±1.1	7.98±0.02	1.2±0.01	
Placebo KD-3/40	373.0±5.1	0.628±0.199	-21.2±3.2	5.61±0.00		
KD1-3/40	348.6±7.8	0.614±0.092	-22.6±0.4	7.48±0.01	13.33±1.76	
KD2-3/40	562.4±6.3	0.654±0.183	-26.5±0.3	8.16±0.00	10.93±0.94	
Placebo KD-3/5	360.0±4.1	0.435±0.171	-20.1±4.1	5.74±0.02		
KD1-3/5	334.6±5.6	0.456±0.210	-21.4±0.3	7.56±0.01	1.69±0.90	
KD2-3/5	530.1±4.4	0.512±0.184	-26.4±0.1	7.88±0.01	1.77±0.22	

PS: Mean particle size, PdI: Polydispersity index, ZP: Zeta potential, DIR: Dirithromycin, DIR_S: Surface located DIR concentration, DIR_E: Encapsulated DIR concentration, Stability codes as x/y; x represents the storage month while y represents the storage conditions in °C

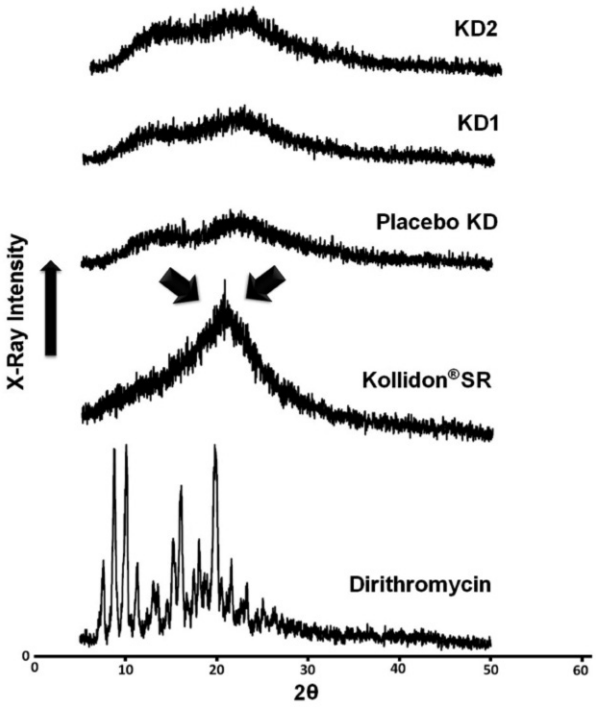

Figure 3. X-ray diffractometry spectra of dirithromycin, and nanoparticles prepared

KD: Kollidon®, Dirithromycin

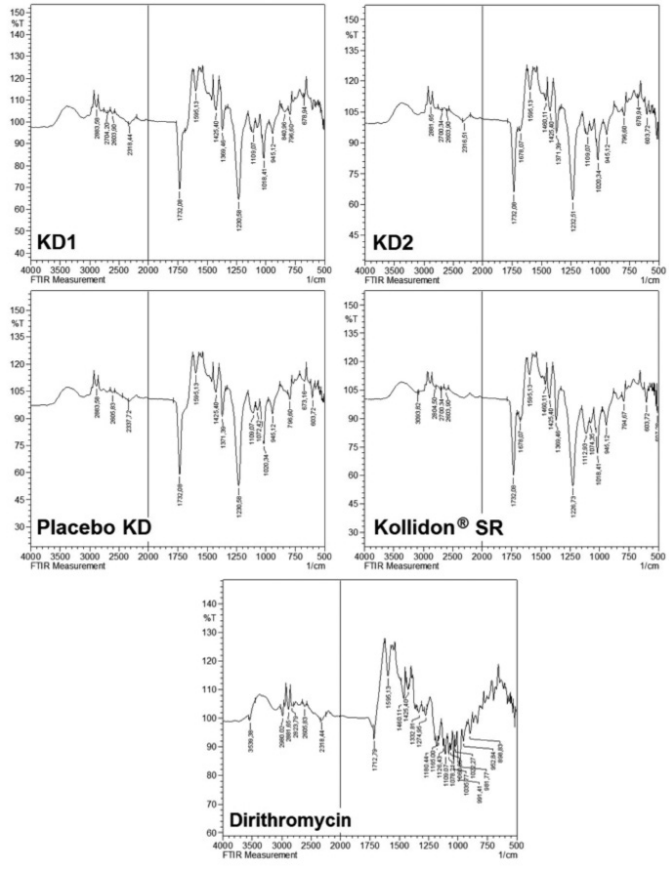

Figure 4. FTIR spectra of dirithromycin, and the nanoparticles prepared

KD: Kollidon®, Dirithromycin

Since the Kollidon® SR is a mixture of PVA and PVP, characteristic peaks were revealed for PVP N-C around 1230 cm^{-1} and PVA by C-O (stretch) at 1109 cm^{-1} and the C=O at 1732 cm^{-1} (Figure 4).[58,59]

Characteristic peaks of O-H streching at 3539 cm^{-1} observed in the pectrum of pure dirithromycin most probably due to the moisture content of the material.[60] C-H stretching (2980 cm^{-1}, 2881 cm^{-1}); C=O molecular vibration (1712 cm^{-1}) C=C (890-991 cm^{-1}) peaks were identified as the main groups (Figure 4).[20,61]

FTIR sptectra of pure materials were compared to KD1 and KD2 formulations and main signals were also detected in the spectra of formulations prepared therefore it showed that the formulation stages had no influence on the polymeric structure.

Intermolecular interactions of dirithromycin and Kollidon® SR was evaluated in this study also by ^{1}H-NMR.[62] Intensity of the peaks at 1-3 and 7-8 ppm ranges were increased slightly (marked with arrows) due to the presence of dirithromycin indicating the molecular distribution of dirithromycin within the polymeric structure (Figure 5).

Drug loading and encapsulation efficiency

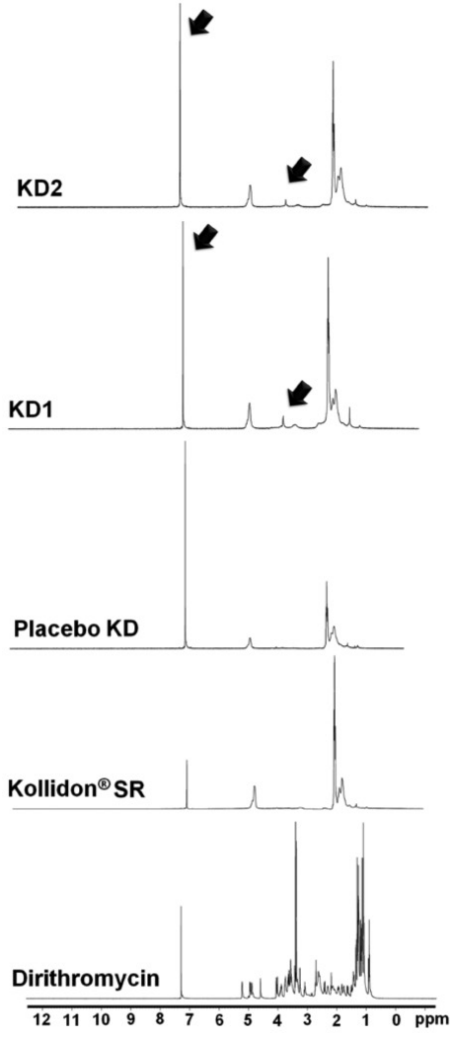

Figure 5. ^{1}H-NMR spectra of dirithromycin, and the nanoparticles prepared

As a result of HPLC method validation studies, linearity in methanol was y=1002.1x-1552.7 where r^2=0.997; accuracy was 97.8±1.9% for the concentrations of 5 µg/mL, precision was 4.9 and 5% for repeatability and reproducibility, respectively (n=3).

Dirithromycin amount of the nanoparticles prepared were presented at Table 2. Drug loading (%) and EE (%) were evaluated according to Equation 1 and Equation 2, respectively. Surface location was higher than the encapsulation for both formulations (75.0±0.0% and 55.6±0.1 for KD1 and KD2 respectively) (Table 2).

In vitro release study

Release profiles obtained for Kollidon® SR nanoparticles were given in Figure 6. The release profile of pure dirithromycin was used as a reference. According to the analysis results release rate of dirithromycin reached to 100% just after 2 hrs while the values for KD1 and KD2 formulations reached the highest points of 83.1% and 87.6% respectively after 6 hrs period (Figure 6). Initial burst releases were recorded from the nanoparticles as expected considering the surface location of the dirithromycin however drug releases were extended more than 3 fold which enhances the potential use of the nanoparticles for better treatment.

Realization of the *in vitro* release profiles with mathematical models that describes the dependence of release as a function of time gives valuable data about the *in vivo* release behaviour of the optimal delivery system.[63,64] Therefore *in vitro* release kinetics were also evaluated for the formulations prepared in comparison with pure Active pharmaceutical ingredient (API) using DDSolver Program (Table 3).[65] Best fitted models were selected considering the smaller Akaike information criterion (AIC) with higher adjusted R^2 values and the results were presented in Table 3.[63]

Pure dirithromycin's release kinetic was fitted to First Order which explains the release from the system where rate of drug release is concentration dependent.[66] Release kinetics of the formulations prepared were described by Baker-Lonsdale Model that describes the release kinetics from the matrixes of spherical in shape like many microparticle formulations (microcapsules and microspheres).[63,64] KD1 formulation also fitted to the Korsmeyer-Peppas Model which is a semi-empirical equation to describe drug release from polymeric systems when the release mechanism is not clear enough.[63] Considering the majority of the incorporated drug is located on the surface of KD1 formulation an initial burst effect was more obvious than KD2 formulation and therefore the difference between the release kinetics of the formulations can be attributed to the presence of more than one type of drug release of phenomenon was involved especially for KD1 formulation (Figure 6).[63] Kinetic models of both samples were also fitted to Weibull model which

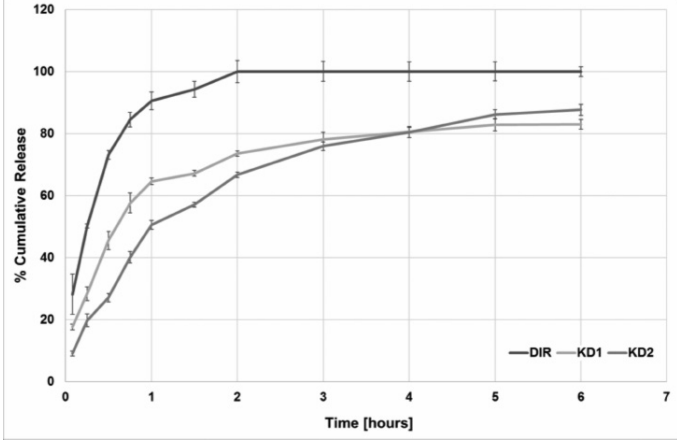

Figure 6. *In vitro* release profiles of dirithromycin from Kollidon® SR nanoparticles (n= 3, mean ± standard error)

DIR: Dirithromycin

Table 3. Best fitted *in vitro* release kinetic models of the dirithromycin and the formulations prepared

Code	Criteria	Zero order	First order	Higuchi	Korsmeyer-Peppas	Hopfenberg	Baker-Lonsdale	Weibull
DIR	k	0.025	0.003	0.56	0.045	0.00	0.000	α:0.00 β:0.001
	r^2	-0.003	0.001	0.000	-0.001	0.001	0.000	0.001
	AIC	0.113	0.061	0.100	0.106	0.092	0.096	0.050
KD1	k	0.020	0.001	0.043	0.056	0.00	0.000	α:0.001 β:0.000
	r^2	-0.001	0.001	0.001	0.001	0.00	0.001	0.001
	AIC	0.104	0.087	0.087	0.074	0.093	0.077	0.061
KD2	k	0.019	0.001	0.041	0.046	0.00	0.000	α:0.002 β:0.001
	r^2	0.000	0.001	0.001	0.001	0.001	0.001	0.001
	AIC	0.096	0.070	0.070	0.075	0.077	0.059	0.050

DIR: Dirithromycin, KD: Kollidon®

is an empirical model extensively used for fast and prolonged drug release profiles from matrix systems.[63,67] Weibull release kinetic model defined as the most applicable model almost all kinds of dissolution curves therefore has been subjected to some criticism.[64]

Evaluation of the cytotoxicity

Cytotoxicity of the nanoparticles prepared were evaluated by MTT method considering both dose and time dependancy on 3T3 mouse fibroblast cell lines.[68,69] At the highest dirithromycin concentration (0.25 µg/mL) the cell viability was found 83.36% and 63.36% after 24 and 48 hrs, respectively (Figure 7). Despite dirithromycin, no dramatic cell deaths were recorded for the Pure Kollidon® SR, Placebo KD, and KD1 formulations by valuing over 80% for all after the period of 48 hrs. However KD2 showed 88.01% and 63.48% cell viability after 24 and 48 hrs respectively considering the higher dirithromycin incorporation than KD1 (Figure 7). Analyses results showed that the concentration of the API has great influence on the cell viability. Achievement of the cell viability over 50% for all the formulations prepared showed that the formulations are safe to be applied to ocular the tissues.[33]

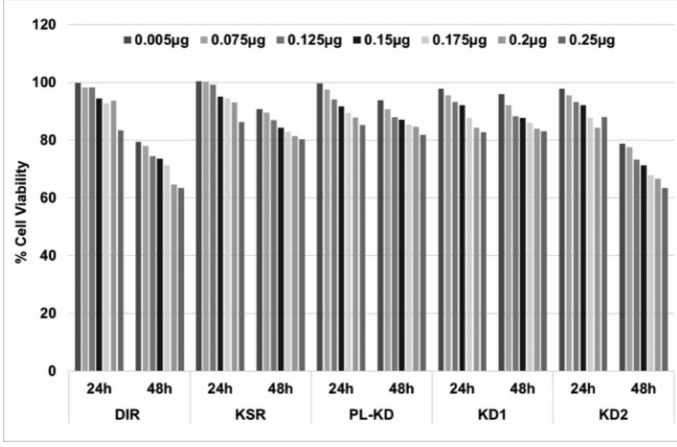

Figure 7. Cytotoxicity of dirithromycin, Kollidon® SR and nanoparticles prepared by MTT assay

DIR: Dirithromycin, KSR: Kollidon® SR, PL-KD: Placebo KD formulation, KD: Kollidon®, Dirithromycin

Microbiological assay

In vitro efficiency of the formulations were evaluated by Microbroth Dilution Method[35,36] on both gram positive and gram negative bacterias like *Staphylococcus aureus* (ATCC 25923) and *Pseudomonas aeruginosa* (ATCC 27853) respectively. The MIC values of the formulations were presented in Table 4.

Analyses results demonstrated that KD1 has MIC values of 200 µg/mL and 100 µg/mL while KD2 showed MIC values of 100 µg/mL and 50 µg/mL on *S. aureus* and on *P. aeruginosa* respectively showing that formulations are more effective on gram negative bacterias. Since the constant amount of the samples were evaluated in Micro-Broth Dilution tests, comparable results were recorded for KD1 and KD2 considering the API concentration of KD2 which was nearly two fold than KD1 formulation. Even the API concentration of KD1 and KD2 were approx. 1/2.5 and 1/5 respect to pure API, same MIC values were achieved for KD2 formulation showing that polymeric carrier has also influenced the potency of the dirithromycin. Analyses results revealed that the incorporation of dirithromycin into the polymeric nanoparticles gives possibility to degrease the applied dose considering the efficacy of the formulation with low API concentration.

Table 4. Micro-broth dilution test results of the formulations prepared

Codes	*S. aureus ATCC 25923*	*P. aeruginosa ATCC 27853*
	MIC (µg/mL)	MIC (µg/mL)
KD1	200	100
KD2	100	50
Placebo KD	400	400
DIR	100	50

DIR: Dirithromycin, KD: Kollidon®, Dirithromycin

CONCLUSION

Sufficient treatment of the severe ocular infections mostly are being hampered because of the locational and structural features of the human eye. Therefore novel approaches are requisite for the enhancement of ocular bioavailability of the active materials especially for topical instillations. In this study dirithromycin incorporated Kollidon® SR-based nanoparticles were formulated for topical application. *In vitro* characteristic properties of the nanoparticles were evaluated in detail and stability of the formulations were evaluated during the storage period of 3 months.

Analyses results demonstrated that nanometer sized spherical particles were achieved by spray drying method. DSC and XRD analyses revealed the amorphous structure of the polymer which is prerequisite for the incorporation higher amounts of active agents due to the unorganized spaced within the polymeric network. FTIR studies showed no drug-polymer interaction while ^{1}H-NMR analyses revealed the presence of the active agent within the amorphous polymeric structure. Due to the high encapsulation efficacy of the particles, dirithromycin release could be extended up to 6 hrs which will enhance the therapeutic efficacy of the formulations prepared. Cytotoxic evaluation revealed the safety of the particles with relatively high cell viability data. Microbiological experiments revealed the potency of the formulations prepared on both gram positive and gram negative bacterias.

Therefore analyses results can be concluded as Kollidon® SR-based nanoparticles are effective carrier candidates for the topical ocular application of dirithromycin. However *in vivo* analyses results are required for the final decision to be made.

ACKNOWLEDGEMENT

Author would like to acknowledge Res. Asst. Dr. Behiye Şenel for MTT tests, and Asst. Prof. Dr. Hülya Karaca Gençer for Micro-Broth Dilution tests. Author would like to thank to Faculty of Science, to Department of Materials Science and Engineering, to DOPNA-LAB and to BIBAM management for SEM, XRD, FTIR and ^{1}H-NMR analyses respectively.

Conflict of Interest: No conflict of interest was declared by the author.

REFERENCES

1. Liu R, Wang S, Sun L, Fang S, Wang J, Huang X, You Z, He X, Liu C. A novel cationic nanostructured lipid carrier for improvement of ocular bioavailability: Design, optimization, *in vitro* and *in vivo* evaluation. J Drug Deliv Sci Tec. 2016;33:28-36.
2. Ludwig A. The use of mucoadhesive polymers in ocular drug delivery. Adv Drug Deliv Rev. 2005;57:1595-1639.
3. Morsi N, Ghora D, Refai H, Teba H. Ketoroloac tromethamine loaded nanodispersion incorporated into thermosensitive *in situ* gel for prolonged ocular delivery. Int J Pharm. 2016;506:57-67.
4. He P, Davis SS, Illum L. *In vitro* evaluation of the mucoadhesive properties of chitosan Microspheres. Int J Pharm. 1998;166:75-68.
5. De Campos AM, Sanchez A, Alonso MJ. Chitosan nanoparticles: a new vehicle for the improvement of the delivery of drugs to the ocular surface Application to cyclosporin A. Int J Pharm. 2001;224:159-168.
6. Urtti A. Challenges and obstacles of ocular pharmacokinetics and drug delivery. Adv Drug Deliv Rev. 2006;58:1131-1135.
7. Başaran E, Demirel M, Sirmagül B, Yazan Y. Cyclosporine-A incorporated cationic solid lipid nanoparticles for ocular delivery. J Microencapsul. 2010;27:37-47.
8. Deschênes J, Blondeau J. Besifloxacin in the management of bacterial infections of the ocular surface. Can J Ophthalmol. 2015;50:184-191.
9. Hopkins G, Pierson R. Therapeutic drugs and their uses: Drugs For The Treatment Of Infections. In: Hopkins G, Pierson R, eds. Ophthalmic Drugs. 19103-2899, Elsevier's Health Sciences Rights Department, 1600 John F. Kennedy Boulevard, Suite 1800, Philadelphia: PA, USA; 2007.
10. Bremond-Gignac D, Chiambaretta F, Milazzo S. A European perspective on topical ophthalmic antibiotics: current and evolving options. Ophthalmol Eye Dis. 2011;3:29-43.
11. Scholar E. Macrolides. In: Scholar E, ed. Reference Module in Biomedical Sciences: The Comprehensive Pharmacology. Elsevier Inc; 2007:1-4.
12. Periti P, Mazzei T, Mini E, Novelli A. Pharmacokinetic drug interactions of Macrolides. Clin Pharmacokinet. 1992;23:106-131.
13. Cai HL, Wang F, Li HD, Peng WX, Zhu RH, Deng Y, Jiang P, Yan M, Hu SM, Lei SY, Chen C. Quantitative analysis of erythromycylamine in human plasma byliquid chromatography-tandem mass spectrometry and its application in a bioequivalence study of dirithromycin enteric-coated tablets with a special focus on the fragmentation pattern and carryover effect. J Chromatogr B. 2014;947:156-163
14. McConnell SA, Amsden GW. Review and comparison of advanced-generation macrolides clarithromycin and dirithromycin. Pharmacotherapy. 1999;19:404-415.
15. Abu-Gharbieh E, Vasina V, Poluzzi E, De Ponti F. Antibacterial macrolides: a drug class with a complex pharmacological profile. Pharmacol Res. 2004;50:211-222.
16. Neitz M, Neitz J. Color vision defects. Levin LA, Albert DM, eds. Ocular Disease: Mechanisms and Management. SAUNDERS an imprint of Elsevier Inc; 2010:478-485.
17. Bühler V. Kollidon® SR, Kollidon. In: Bühler V, ed. BASF SE Pharma Ingredients & Services: 67056 Ludwigshafen, Germany; 2008:255-270.
18. Sakr W, Alanazi F, Sakr A. Effect of Kollidon® SR on the release of Albuterol Sulphate from matrix tablets. Saudi Pharm J. 2011;19:19-27.
19. Song SH, Chae BR, Sohn SI, Yeom DW, Son HY, Kim JH, Kim SR, Lee SG, Choi YW. Formulation of controlled-release pelubiprofen tablet using Kollidon® SR. Int J Pharm. 2016;511:864-875.
20. Arias JL, Gómez-Gallo A, Delgado AV, Gallardo V. Study of the stability of Kollidon® SR suspensions for pharmaceutical applications. Colloid Surface A. 2009;338:107-113.
21. Arias JL, Gómez-Gallo A, Delgado AV, Ruiz MA. Kollidon® SR colloidal particles as vehicles for oral morphine delivery in pain treatment. Colloid Surface B. 2009;70:207-212.
22. Asada M, Takahashi H, Okamoto H, Tanino H, Danjo K. Theophylline particle design using chitosan by the spray drying. Int J Pharm. 2004;270:167-174.
23. Yenilmez E, Basaran E, Yazan Y. Release characteristics of vitamin E incorporated chitosan microspheres and *in vitro-in vivo* evaluation for topical application. Carbohydr Polym. 2011;84:807-811.
24. Başaran E, Yenilmez E, Berkman MS, Büyükköroğlu G, Yazan Y. Chitosan nanoparticles for ocular delivery of cyclosporine A. J Microencapsul. 2014;31:49-57.
25. Müller RH, Heinemann S. Fat emulsions for parenteral nutrition II: Characterisation and physical long-term stability of lipofundin MCT/LCT. Clin Nutr. 1993;12:298-309.
26. European Pharmacopeia 6.0 Directorate for the Quality of Medicines and healthcare of the Council of Europe (EDQM), Cedex, Frence 2007.
27. Diana J, Manyanga V, Hoogmartens J, Adams E. Development and validation of an improved liquid chromatographic method for the analysis of dirithromycin. Talanta. 2006;70:1064-1072.
28. Chourasiya V, Bohrey S, Pandey A. Formulation, optimization, characterization and *in vitro* drug release kinetics of atenolol loaded PLGA nanoparticles using 33 factorial design for oral delivery. Materials Discovery, Article in press 2016.
29. Kang BS, Choi JS, Lee SE, Lee JK, Kim TH, Jang WS, Tunsirikongkon A, Kim JK, Park JS. Enhancing the *in vitro* anticancer activity of albendazole incorporated into chitosan-coated PLGA nanoparticles. Carbohyd Polym. 2017;159:39-47.
30. Hägerström H, Paulsson M, Edsman K. Evaluation of mucoadhesion for twopolyelectrolyte gels in simulated physiological conditions using a rheological method. Eur J Pharm Sci. 2000;9:301-309.
31. Gürsoy AZ. Ocular drug delivery systems. In: Gürsoy AZ, ed. Controlled release Systems. İstanbul: 2002:197-217.
32. Shen J, Deng Y, Jin X, Ping Q, Su Z, Li L. Thiolated nanostructured lipid carriers as a potential ocular drug delivery system for cyclosporine A: Improving *in vivo* ocular distribution. Int J Pharm. 2010;402:248-253.
33. Eidi H, Joubert O, Attik G, Duval RE, Bottin MC, Hamouia A, Maincent P, Rihn BH. Cytotoxicity assessment of heparin nanoparticles in NR8383 macrophages. Int J Pharm. 2010;396:156-165.
34. Angius F, Floris A. Liposomes and MTT cell viability assay: an incompatible affair. Toxicol In Vitro. 2015;29:314-319.
35. Reference Method for Broth Dilution Antifungal Susceptibility Testing of Yeasts; Approved Standard In: Reference Method for Broth Dilution Antifungal Susceptibility Testing of Filamentous Fungi; Approved Standard - Second Edition, Clinical and Laboratory Standards Institute, 2008;22:1-30.

36. Gençer HK, Levent S, Acar Çevik U, Özkay Y, Ilgın S. New 1,4-dihydro[1,8] naphthyridine derivatives as DNA gyrase inhibitors. Bioorgan Med Chem Lett. 2017;27:1162-1168.
37. Patel A, Cholkar K, Agrahari V, Mitra AK. Ocular drug delivery systems: An overview. World J Pharmacol. 2013;2:47-64.
38. Zimmer A, Kreuter J. Microspheres and nanoparticles used in ocular delivery systems. Adv Drug Deliver Rev. 1995;16:61-73.
39. Jones D. Pharmaceutics-Dosage Form and Design. In: Jones D, ed. Ocular nasal and otic dosage forms. London, 2008:135-156.
40. Bhattacharjee S. In relation to the following article "DLS and zeta potential - What they are and what they are not?" Journal of Controlled Release, 2016, 235, 337-351? J Control Release. 2016;238;311-312.
41. Freitas C, Müller RH. Effect of light and temperature on zeta potential and physical stability in solid lipid nanoparticle (SLN™) dispersions. Int J Pharm. 1998;168:221-229.
42. Radomska-Soukharev A. Stability of lipid excipients in solid lipid nanoparticles. Adv Drug Deliver Rev. 2007;59:411-418.
43. Felt O, Furrer P, Mayer JM, Plazonnet B, Buri P, Gurny R. Topical use of chitosan in ophthalmology: tolerance assessment and evaluation of precorneal retention. Int J Pharm. 1999;180:185-193.
44. De Campos AM, Sanchez A, Alonso MJ. Chitosan nanoparticles: a new vehicle for the improvement of the delivery of drugs to the ocular surface. Application to cyclosporine A. Int J Pharm. 2001;224:159-168.
45. Başaran E, Demirel M, Sirmagül B, Yazan Y. Polymeric cyclosporine-A nanoparticles for ocular application. J Biomed Nanotechnol. 2011;7:714-723.
46. Başaran E, Yazan Y. Ocular application of chitosan. Expert Opin Drug Deliv. 2012;9701-712.
47. Sunkara G, Kompella UB. Membrane transport processes in the eye. In: Mitra AK, ed. Opthalmic drug delivery systems. 2nd ed. New York; 2003:13-58.
48. Missel PJ, Lang JC, Rodeheaver DP, Jani R. Design and Evaluation of Ophthalmic Pharmaceutical Products, In: Florence AT, ed. Modern Pharmaceutics Volume 2- Applications and Advances. Informa Healthcare USA Inc. 52 Vanderbilt Avenue. New York: NY, USA; 2009:101-189.
49. Gibson M. Ophthalmic dosage forms. In: Gibson M, ed. Pharmaceutical preformulation and formulation. CRC Press LLC, FL: USA; 2004:461-491.
50. Stephenson GA, Stowell JG, Toma PH, Dorman DE, Greene JR, Stephen R. Solid-state Analysis of Polymorphic, Isomorphic, and Solvated Forms of Dirithromycin. J Am Chem Soc. 1994;116:5766-5773.
51. Yi Q, Chen J, Le Y, Wang J, Xue C, Zhao H. Crystal structure and habit of dirithromycin acetone solvate: A combined experimental and simulative study. J Cryst Growth. 2013;372:193-198.
52. Casettari L, Vllasaliu D, Castagnino E, Stolnik S, Howdle S, Illum L. PEGylated chitosan derivatives: Synthesis characterizations and pharmaceutical applications. Prog Polym Sci. 2012;37:659-685.
53. Dorofeev GA, Streletskii AN, Povstugar IV, Protasov AV, Elsukov EP. Determination of Nanoparticle Sizes by X-ray Diffraction. Colloid J. 2012;74:675-685.
54. Ingham B. X-ray scattering characterisation of nanoparticles. Crystallogr Rev. 2015;21:229-303.
55. Kamble PR, Shaikh KS, Chaudhari PD. Application of Liquisolid Technology for Enhancing Solubility and Dissolution of Rosuvastatin. Adv Pharm Bull. 2014;4:197-204.
56. Akbari B, Tavandashti MP, Zandrahimi M. Particle Size Characterization of Nanoparticles A Practical Approach. IJMSE. 2011;8:48-56.
57. Devi TSR, Gayatahri S. FTIR and FT-RAMAN Spectral Analysis of Paclitaxel Drugs. IJPSR. 2010;2:106-110.
58. Kong J, Yu S. Fourier Transform Infrared Spectroscopic Analysis of Protein Secondary Structures. Acta Bioch Bioph Sin (Shanghai). 2007;39:549-559.
59. Kapse SV, Gaikwad RV, Samad A, Devarajan PV. Self nanoprecipitating preconcentrate of tamoxifen citrate for enhanced bioavailability. Int J Pharm. 2012;429:104-112.
60. Szente V, Baska F, Zelkó R, Süvegh K. Prediction of the drug release stability of different polymeric matrix tablets containing metronidazole. J Pharm Biomed Anal. 2011;54:730-734.
61. Erdik E. Kırmızıötesi (Infrared) Spektroskopisi, İçinde: Erdik E. Organik Kimyada Spektroskopik Yöntemler. Gazi Kitapevi Tic. Ltd. Şti. Ankara: Turkey; 2008:82-147.
62. Mayer C. Nuclear magnetic resonance on dispersed nanoparticles. Prog Nucl Mag Res Sp. 2002;40:307-366.
63. Bruschi ML. Mathematical models of drug release; In: Bruschi ML, ed. Strategies to Modify the Drug Release from Pharmaceutical Systems. Woodhead Publishing Limited is an imprint of Elsevier, Cambridge: UK; 2015:63-86.
64. Costa P, Sousa Lobo JM. Modeling and comparison of dissolution profiles. Eur J Pharm Sci. 2001;13:123-133.
65. Zhang Y, Huo M, Zhou J, Zou A, Li W, Yao C, Xie S. DDSolver: An Add-In Program for Modeling and Comparison of Drug Dissolution Profiles. AAPS J. 2010;12:263-271.
66. Bohrey S, Chourasiya V, Pandey A. Polymeric nanoparticles containing diazepam: preparation, optimization, characterization, *in vitro* drug release and release kinetic study. Nano Converg. 2016;3:3.
67. Jain A, Jain SK. *In vitro* release kinetics model fitting of liposomes: An insight. Chem Phys Lipids. 2016;201:28-40.
68. Xu L, Xu X, Chen H, Li X. Ocular biocompatibility and tolerance study of biodegradable polymeric micelles in the rabbit eye. ColloidS Surf Biointerfaces. 2013;112:30-34.
69. Uboldi C, Urbán P, Gilliland D, Bajaka E, Valsami-Jones E, Ponti J, Rossi F. Role of the crystalline form of titaniumdioxide nanoparticles: Rutile, and not anatase, induces toxic effects in Balb/3T3 mouse fibroblasts. Toxicol In Vitro. 2016;31:137-145.

Turk J Pharm Sci 2017;14(2):201-206
DOI: 10.4274/tjps.62207

REVIEW

Pharmacological and Toxicological Properties of Eugenol

Öjenolün Farmakolojik ve Toksikolojik Özellikleri

Solmaz MOHAMMADI NEJAD, Hilal ÖZGÜNEŞ, Nurşen BAŞARAN*

Hacettepe University, Faculty of Pharmacy, Department of Pharmaceutical Toxicology, Ankara, Turkey

ABSTRACT

Eugenol is a volatile phenolic constituent of clove essential oil obtained from *Eugenia caryophyllata* buds and leaves. It is a functional ingredient of numerous products which have been used in the pharmaceutical, food and cosmetic industry in restricted concentrations. Its derivatives have been used in medicine as a local antiseptic and anesthetic. The wide range of eugenol activities includes antimicrobial, anti-inflammatory, analgesic and antioxidant. Although eugenol is considered safe as a product, due to the vast range of different applications and extensive use, there has been a great concern about its toxicity in recent years. However, studies about cytotoxicity and genotoxicity of eugenol are very limited and controversial. The pharmacological and toxicological properties of eugenol will be discussed in this review.

Key words: Eugenol, clove oil, pharmacological activity, toxicity, cytotoxicity, genotoxicity

ÖZ

Öjenol, *Eugenia caryophyllata*'nın yaprak ve tomurcuklarından elde edilen, karanfil yağının fenolik yapıdaki uçucu bir bileşiğidir. İlaç, gıda ve kozmetik endüstrisinde sınırlı miktarlarda kullanılan, çok sayıda ürünün işlevsel bir bileşenidir. Türevlerinin lokal antiseptik ve anestezik olarak tıpta kullanımı bulunmaktadır. Geniş aralıktaki farmakolojik etkileri arasında antimikrobiyal, antiinflamatuvar, analjezik, antioksidan ve antikanser etkiler yer almaktadır. Öjenol genel olarak güvenli bir bileşik olarak değerlendirilir ancak çok farklı uygulamaları ve yaygın kullanım alanları nedeniyle, toksisitesi son yıllarda ilgi odağı olmuştur. Öjenolün sitotoksisitesi ve genotoksisitesi konusundaki çalışmalar da yetersiz ve çelişkilidir. Bu derlemede öjenolün farmakolojik ve toksikolojik özellikleri tartışılacaktır.

Anahtar kelimeler: Öjenol, karanfil yağı, farmakolojik aktivite, toksisite, sitotoksisite, genotoksisite

INTRODUCTION

Eugenol ($C_{10}H_{12}O_2$ or $CH_3C_6H_3$) is a volatile phenolic constituent of clove essential oil obtained from *Eugenia caryophyllata* buds and leaves, mainly harvested in Indonesia, India and Madagascar. The name supposedly is derived from the scientific name for clove *E. caryophyllata* tree which has large leaves and flower buds which turn to red color when they are ready for collection.[1,2] Eugenol is the main extracted constituent (70-90%) of cloves and is responsible for clove aroma.[1]

Eugenol, a phenylpropanoid, is pale yellow oil with a spicy aroma with the molecular weight of 164.2 g/mol. This molecule is a weak acid which is soluble in organic solvents and specially extracted from clove oil, nutmeg, cinnamon, basil and bay leaf.

There are different types of essential oil extracted from parts of clove. The oil derived from the flower buds of clove mainly consists of eugenol (60-90%), eugenyl acetate, caryophyllene and other substances, whereas oil derived from the leaves of the clove tree consists of eugenol (82-88%) and very little eugenyl acetate, and other minor constituents. The oil derived from the twigs of cloves consists of 90-95% of eugenol. Eugenol also can be produced synthetically by the allylation of guaiacol with allylchlorid.[3,4]

Since ancient times, clove oil has been used as an antimicrobial, antiseptic and antispasmodic in Chinese traditional medicine. Nowadays, there is also a wide range of use of eugenol for several purposes such as household products, fragrance in soaps and cosmetics, skin care products, flavoring substance for food, dental and pharmaceutical products.[1]

Eugenol causes an enhancement in skin penetration of diverse drugs. It is also used in agricultural applications to protect foods from microorganisms such as *Listeria monocytogenes* and *Lactobacillus* during storage, as a pesticide and fumigant.[5] Eugenol is useful for treatment of skin infections, skin lesions and inflammatory disorders. However, some reports show

*Correspondence: E-mail: nbasaran@hacettepe.edu.tr, Phone: +90 505 231 41 07
ORCID ID: orcid.org/0000-0001-8581-8933
Received: 16.06.2016, Accepted: 08.12.2016

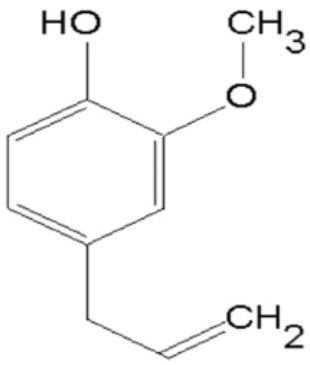

Figure 1. Chemical structure of eugenol ($C_{10}H_{12}O_2$)

that higher concentrations of undiluted clove oil may result in some symptoms. Indeed, an excessive dose of eugenol was considered as toxic.[2,5]

The US Food and Drug Administration approved the use of clove oil as a flavoring substance in the food industry, as a fragrance in cosmetics industry and in dentistry as a natural analgesic and antiseptic.[6]

There are relatively few human studies about the pharmacokinetic and effects of eugenol. Animal studies have suggested that after inhalation of the smoke of clove cigarettes, minor amounts of eugenol may be absorbed from the lung. Also some *in vitro* studies indicated that eugenol undergoes biotransformation in hepatocytes.[7] An investigation of male and female healthy volunteers demonstrated that eugenol was absorbed and metabolized after oral administration rapidly. It was almost completely excreted in the urine within 24 hours and the urine contained conjugates of eugenol. Results revealed that only less than 1% of administrated dose was excreted as non-metabolized in urine. Analysis of urine also demonstrated that more than 90% of metabolic products are phenolic conjugates and 50% of the conjugated metabolites were eugenol-glucuronide and eugenol-sulfate. Other observed metabolic routes were the epoxide-diol pathway, synthesis of a thiophenol and of a substituted propionic acid, allylic oxidation, and migration of the double bond.[8]

In an *in vitro* study, all assessed metabolites have been found to have an aromatic hydroxyl group. The reaction of the hydroxyl group with glucoronate or sulfate causes the formation of conjugates which are finally excreted in the urine. Similarities have been observed between the metabolism of eugenol in human and rodents.[9]

Guenette et al.[10] suggested that in rats, the half-life ($t_{1/2}$) of eugenol in plasma is about 14 hours and in blood is 18 hours.

Pharmacological activities of eugenol

Based on available experimental data, many phenolic compounds such as eugenol show antioxidant capacity and free radical scavenging activity.[5] The antioxidant activity of eugenol and one of its isomers isoeugenol has been studied by using iron-mediated lipid peroxidation and auto-oxidation of Fe^{2+}. Eugenol had the inhibitory effect on lipid peroxidation, with an IC_{50} value of about 80 μM, which was eightfold the value of isoeugenol however; this effect was less potent than the effect of isoeugenol. The functional mechanism of both compounds was evaluated and the obtained results indicated that the antioxidant activity of eugenol is potent to form complexes with reduced metals. Isoeugenol causes a decrease in the formation of iron-oxygen chelate complex, which is the initiating factor of lipid peroxidation.[11] In an experiment by using the hydroxyl radical scavenging tests, eugenol exhibited antioxidant capacity in a dose dependent manner.[12] Ogata et al.[13] suggested that the inhibitory mechanism of eugenol in lipid peroxidation has two steps. In fact, eugenol interferes with the chain reactions by trapping the active oxygen. Also eugenol is metabolized to dimer which inhibits lipid peroxidation.

In male rats, eugenol showed anesthetic effects and reports demonstrated a dose dependent anesthesia after administration of about 50-60 mg/kg i.v.[14]

Antibacterial activities of eugenol

The effects of eugenol on the growth of some species of Gram-positive *(Bacillus cereus; Bacillus subtilis; Staphylococcus aureus)* and Gram-negative *(Escherichia coli; Salmonella typhi; Pseudomonas aeruginosa)* bacteria were assessed by using the agar well diffusion method. Eugenol has shown an inhibitory effect on the growth of the *P. aeruginosa at the* concentration of 1000 μg/mL. The complete inhibitory effect against such bacteria is shown at 2000 μg/mL. In this study, ampicillin (1 mg/mL) is used as positive control and similar effects of eugenol also have confirmed against various pathogens such as *E. coli, B. cereus, Helicobacter pylori, S. aureus, Staphylococcus epidermidis, Streptococcus pneumoniae* and *Streptococcus pyogenes*.[15,16]

The combination of eugenol with a conventional antibiotic has been evaluated to detect the synergistic effect against Gram-negative bacteria. In the eugenol treated cells, 50% loss of membrane integrity was demonstrated which enhanced the activity of studied antibiotics. The combination of eugenol with two antibiotics, vancomycin and a β-lactam, showed an increased membrane damage in bacteria which means a synergistic effect. It has been also demonstrated that penetration of vancomycin and β-lactam, in combination with eugenol, has increased and resulted in more antimicrobial effect.[17]

In another experimental study, the antibacterial effect of several natural products; eugenol, cinnamaldehyde, thymol, carvacrol and a combination of all mentioned agents have been studied against the *E. coli*. The broth micro-dilution assay has been used for the evaluation. Results demonstrated that among mentioned substance, eugenol has the lowest antibacterial effect however, the combination of eugenol and cinnamaldehyde, thymol and carvacrol, showed a synergistic antibacterial activity.[18]

The mechanism action of eugenol on the bacterial membrane of *L. monocytogenes, S. pyogenes, Proteus vulgaris* and *E. coli* has been examined. Results displayed that eugenol induces cell lysis through the leakage of protein and lipid in the cell

membrane. Furthermore, it seems that the time of exposure of cells to eugenol is important. Because both the cell wall and membrane of the treated Gram-negative and Gram-positive bacteria were considerably damaged after about 120 min of exposure.[19]

Eugenol at the concentrations of 16 to 128 µg/mL, decreased the hemolytic activity and the release of tumor necrosis factor alfa (TNF-α) in a dose dependent manner. It is also found that depending on the concentration of eugenol, production of staphylococcal enterotoxin has been reduced significantly. As a result, it is suggested that eugenol could be used as a food additive because of the inhibitory effect on growth of bacteria and suppressive effect on the production of exotoxins of *S. aureus*.[20]

Anti-inflammatory effects of eugenol

Investigations of anti-inflammatory effects of eugenol, have suggested that this compound is able to suppress the expressions of cyclooxygenase II enzyme. Eugenol dimers can inhibit the expression of cytokines in macrophages, which are stimulated by polysaccharides. Eugenol also has an inhibitory effect on cell proliferation via suppression of NF-Kappa B (NF-κB). Eugenol suppresses the activation of NF-κB which induces reduction in the incidence of gastric tumors. Eugenol can also modulate the expression of NF-κB target genes which are responsible for the regulation of cell proliferation and cell survival. Because of these suggested activities, eugenol has been indicated to have chemo preventive effect.[21]

Macroscopic studies, clinical evidences of collagen-induced arthritis and treatment with eugenol in a murine model, showed that eugenol may have inhibitory effects on mononuclear cell infiltration into the knee joints of arthritic mice. Eugenol lowered the levels of cytokines such as TNF-α, interferon gamma and TNF-β in the ankle joints. The *in vitro* cell viability was assessed by MTT method and achieved results exhibited that cells were not affected by eugenol treatment. It is suggested that eugenol may have recovery effects on arthritis and can be useful as a beneficial supplement in the treatment of arthritis.[22]

Eugenol has been found to exert antipyretic activity in rabbits when given intravenously and intragastrically and may reduce fever through a similar central action to allopathic antipyretic drugs such as acetaminophen.[23]

Eugenol at the concentrations of 0.2-20 µm, is suggested to be able to produce a dose dependent and reversible vasodilator response that are partially dependent on the endothelium.[24] It has also been found to have a preventive effect on dopamine depression and lipid peroxidation, which can protect depression induced by 6-hydroxyl dopamine. Eugenol has prevented depression by decreasing the lipid peroxidation and stimulating reduced glutathione (GSH).[25]

Toxicity of eugenol

Eugenol is considered safe as a food additive, but due to the wide range of different applications and also the extensive use and availability of clove oil; there is a great concern about its toxicity in recent years.

Results of a case study indicated that ingestion of 5-10 mL of clove oil by a two-year boy resulted in distressing and crying and 3 h after ingestion, conditions were deteriorated. The acidosis marked and the patient was in deep coma. During 8 h, he suffered from a generalized seizure, and within 24 h, failure in liver function and also disseminated intravascular coagulopathy was noted. Within one week after ingestion and after severe symptomatic treatment, the patient gained consciousness and recovered. In terms of hepatotoxic effects, results showed some similarities between eugenol and paracetamol poisoning.[26]

Intravenous infusion of eugenol at 4 µL and 8 µL caused acute respiratory distress with hemorrhagic pulmonary edema in rats and it is suggested that at least a part of damage is related to oxidative stress.[27] In an *in vitro* experiment on isolated rat hepatocytes, after 5 h exposure to eugenol, hepatotoxicity and cell damage in more than 85% of cells were demonstrated. Administration of acetyl cysteine had preventive effects on cell death in the same cell line.[28]

Since cinnamon and clove have lipophilic properties, they are able to penetrate the cell membrane and then become accessible to intracellular organelles such as mitochondria. Recent studies indicated some inhibitory effects of such spices on the activity of Na^+/K^+ ATPase in kidney and intestine. It is also possible that spices have toxic effects on mitochondrial function which leads to decrease in ATP level. Reductions of ATP level can influence the mechanism of cell growth, viability and aging.[29]

Studies on the toxic effects of anesthetic doses of eugenol on African clawed frogs demonstrated damage in kidney and some morphological alteration and cell apoptosis in renal cells.[30]

The oral intake of eugenol in different doses during a 15 day period may cause some changes in blood chemistry. Moreover it causes an increase in aspartate aminotransferase, alanine aminotransferase, and total bilirubin levels, but it seems that such effects are not dose dependent.[31]

Cytotoxicity of eugenol

The cytotoxic effects of eugenol, induction of reactive oxygen species (ROS) production and reduced levels of GSH have been studied in human submandibular cell line. It is suggested that formation of benzyl radicals is the main cause of low GSH of eugenol is found to be related to ROS-independent mechanisms. Eugenol has been found to exert less cytotoxic effects compared to isoeugenol and such effects are dose dependent.[32]

Eugenol is also found potential to decrease the activity of dehydrogenase enzymes in human osteoblastic cells in a dose dependent manner.[33]

The cytotoxic effects of some of root canal sealer agents based on zinc-oxide eugenol (endofill) and sealer 26 were also studied. Results showed that both agents have cytotoxic effects, but the toxicity of "sealer 26" on macrophages is more than endofill.[34] Anpo et al.[35] evaluated the cytotoxic effects of eugenol on human pulp cells and also the expression of molecular markers in osteogenic differentiation. Observations suggested that eugenol used for endodontic treatment, may have cytotoxic effects on the normal function of stem cells.

Another study evaluated the apoptosis induced by eugenol in human breast cancer cells. Release of the lactate dehydrogenase enzyme, percentage of cell viability and cytotoxicity, morphological changes and quantitation of DNA fragments have been studied. The findings demonstrated that the increase of cell apoptosis and DNA fragmentation are dose dependent.[36]

The cytotoxicity of eugenol was studied in three different malignant and nonmalignant human derived cells. The malignant Hep G2 hepatoma cells, malignant Caco-2 colon cells and nonmalignant human VH10 fibroblasts were chosen to determine the cytotoxicity of eugenol. Eugenol was found to be toxic in human VH10 fibroblasts and Caco-2 colon cells but not in Hep G2 hepatoma cells. Eugenol at concentrations under 600 μM significantly caused an increase in DNA breaks in human VH10 fibroblast cells. But the degree of such damage in Caco-2 colon cells was found to be lower. The DNA damaging effect was not observed in Hep G2 cells.[37]

The effects of eugenol and a chemotherapeutic drug gemcitabine were investigated in colon cancer cells. The combination of eugenol and gemcitabine resulted in a decrease in cell viability of 84% (eugenol alone) to 47% (combination of eugenol-gemcitabine). Results showed that eugenol alone causes 84% decrease and gemcitabine causes 51% decrease in cell viability. The colon cancer cells were treated with eugenol resulted in increased lipid layer breaking. Furthermore, eugenol has been found to induce apoptosis by destruction the mitochondrial membrane potential and production of reactive oxygen species.[38]

Eugenol showed different degrees of cytotoxicity in HL-60 cancer cells and inhibited the cell growth by 50% at a concentration of 23.7 μM. Results demonstrated a significant increase of fragmented DNA caused by eugenol. Also eugenol has the potential to induce the induce ROS-dependent apoptosis in HL-60 cell line.[39]

It was found that eugenol is able to inhibit the proliferation of melanoma cells. Such effect resulted in a considerable delay in tumor growth and about 40% decrease in the size of tumor. Moreover, approximately 50% of the animals in the control group died because of metastatic growth, while no sign of metastasis was observed in the treatment group. Results of the experiments on the anti-proliferative mechanism of eugenol in the malignant melanoma cell line (WM1205L) in humans detected that eugenol arrests cells in the S phase of the cell cycle and induces apoptosis by this function.[40]

Genotoxicity of eugenol

Authors have suggested that a moderate to severe toxic effects of zinc oxide eugenol in V79 cell line and also demonstrated that these effects are dose dependent, suggesting that eugenol has genotoxic effects.[41] On the other hand, the chemopreventive effect of eugenol on DNA damage induced by 7,12 dimethylbenzanthracene (DMBA) has been evaluated in MCF-7 cells. The observations suggested that eugenol was potent to protect DNA against genotoxic damage induced by DMBA. Eugenol is able to suppress the DMBA activation and acts as a potential chemopreventive compound.[42]

After oral administration of eugenol (0.4% in the diet) for two weeks in rodents, the frequency of micronucleated erythrocytes was decreased significantly. The results provided that eugenol has the capacity of mutagenicity in male mouse and causes mutation, particularly in the anaphase of polychromatic erythrocytes of male mouse.[43]

The genotoxic capacity of various phenolic compounds such as eugenol, isoeugenol and safrole has been evaluated by using the wing spot test of *Drosophila melanogaster* (common fruit-fly). The results of this experiment demonstrated that at the same concentrations, isoeugenol clearly was not genotoxic. Observations also showed that eugenol and safrole are able to produce a positive recombinogenic response which is related to a high CYP P450 activation capacity. The genotoxicity of eugenol is related to reactive metabolites and recombinogenic compounds of it.[44]

The evaluation of antigenotoxicity effects of eugenol in mice with micronucleus test, suggests that the antigenotoxic effects of eugenol may be dose related.[45] In another experimental study, the effect of eugenol on tobacco-induced genotoxicity was evaluated by the Ames Salmonella/microsome test. The obtained data displayed that eugenol at concentrations of 0.5-1 mg/plate, has an inhibitory effect on tobacco-induced mutagenicity. But 150 mg/day of eugenol was ingested by ten non-smoking healthy male adults and findings suggested that eugenol has no antigenotoxic activity on human.[46]

Immunotoxicity of eugenol

Findings about the potency of eugenol and clove oil in inducing allergy and hypersensitivity are controversial. Several adverse effects have been observed after use of dental products which contain eugenol. Localized irritation of the skin; ulcers, allergic dermatitis, tissue necrosis and rarely even anaphylactic-like shock have been reported in different studies.[47]

The allergic capacity of eugenol containing fragrance was evaluated in approximately 24.000 individuals. Findings reported that 25.5% of health care workers, 16.5% of non-health care workers, 39.39% of metal workers and 16.3% of people in other occupations showed allergic reactions to eugenol.[48]

An 8 year old boy reported a type 1 immediate hypersensitive reaction to the eugenol after root canal was medicated with sodium hypochlorite and sealed with zinc oxide eugenol. About 1 min after the zinc oxide eugenol placement, the patient was anxious and excited, with evident erythema on the parts of the face, neck, torso, upper and lower limbs, itchiness and redness extending behind the ear. Cutaneous examination revealed extensive weal of various sizes and shapes with no angioedema or mucosal involvement. Owing to the fact that the erythema was noticed after the placement of zinc oxide eugenol, skin prick test for zinc oxide eugenol was performed and showed positive response for eugenol (10%) and negative responses for zinc oxide (10%), formaldehyde (1% aq) and sodium hypochlorite. Intravenous injection of 100 mg of

hydrocortisone hemi succinate was administrated immediately and zinc oxide eugenol temporary dressing was replaced with non-eugenol containing material. Forty-five minutes later, the patient presented reduced erythema on the face, neck and hands however; some studies also showed that eugenol alone or clove oil has a very low activity to induce these allergic effects.[49,50]

CONCLUSION

Eugenol has been recognized as a safe food additive in the generally recognized as safe substance classification under the sections of Federal Food, Drug and Cosmetics Administration. However, extensive toxicity studies should be performed to confirm that eugenol is safe for general public health. Research on the characteristics of clove oil and eugenol is still ongoing. Structurally eugenol is a simple molecule, but it is used extensively for varied purposes in various industries such as pharmaceutical, food and cosmetics, dentistry, agriculture and others.

Furthermore, some small changes in the molecular structure of eugenol, may lead in different molecular properties which can have different biological activities. Observations from several studies show synergistic effects of eugenol and other antimicrobial compounds which allow use of eugenol as a proper food additive. According to antimicrobial experiments, eugenol also is potent to damage the membranes of bacteria which may results in the increase of the penetration of some antibiotics.

Although there are extensive researches on plant toxicity, studies related to the toxic effects of eugenol and clove oil, are still very limited. Especially chronic toxicity, cytotoxicity and genotoxicity studies are lacking.

In conclusion, different properties and activities of eugenol are still undiscovered very well and should be further explored by more *in vitro* and *in vivo* long-term human research.

Conflict of Interest: No conflict of interest was declared by the authors.

REFERENCES

1. Barceloux DG. Medical Toxicology of Natural Substances: Foods, Fungi, Medicinal Herbs, Plants and Venomous Animals, Wiley: Hoboken; New Jersey; 2008.
2. Basch E, Gasparyan A, Giese N, Hashmi S, Miranda M, Sollars D, Seamon E, Tanguay-Colucci S, Ulbricht C, Varghese M, Vora M, Weissner W. Clove (*Eugenia aromatica*) and clove oil (eugenol). Natural standard monograph (www.naturalstandard.com) copyright© 2008. J Diet Suppl. 2008;5:117-146.
3. Barnes J, Anderson L, Phillipson D. Herbal Medicine. Pharmaceutical Press; London; 2007.
4. Oyedemi SO, Okoh AI, Mabinya LV, Pirochenva G, Afolayan AJ. The Proposed mechanism of bactericidal action of eugenol, α-terpineol and terpinene against Listeria monocytogenes, *Streptococcus pyogenes, Proteus vulgaris* and *Escherichia coli*. Afr J Biotechnol. 2009;8:1280-1286.
5. Kamatou GP, Vermaak I, Viljoen AM. Eugenol; from the remote Maluku Islands to the international market place: a review of a remarkable and versatile molecule. Molecules. 2012;17:6953-6981.
6. Chapter 6-Clove Oil (Eugenol), https://www.marinwater.org/Document Center/View/253, Acccessed: 20 September 2016.
7. Thompson DC, Constantin-Teodosiu D, Moldéus P. Metabolism and cytotoxicity of eugenol in isolated rat hepatocytes. Chem Biol Interact. 1991;77:137-147.
8. Fisher IU, von Unruh GE, Dangler HJ. The metabolism of eugenol in man. Xenobiotica. 1990;20:209-222.
9. Eugenol and Related Hydroxyallylbenzene Derivatives, http://www.inchem.org/documents/jecfa/jecmono/v56je09.pdf, Accessed: 10 August 2016.
10. Guenette SA, Ross A, Beaudry F, Vachon P. Pharmacokinetics of eugenol and its effects on thermal hypersensitivity in rats. Eur J Pharmacol. 2007;562:60-67.
11. Ito M, Murakami K, Yoshino M. Antioxidant action of eugenol compounds: role of metal ion in the inhibition of lipid peroxidation. Food Chem Toxicol. 2005;43:461-466.
12. Singh G, Maurya S, DeLampasona MP, Catalan CA. A comparison of chemical, anti-oxidant and antimicrobial studies of cinnamon leaf and bark volatile oils, oleoresins and their constituents. Food Chem Toxicol. 2007;45:1650-1661.
13. Ogata M, Hoshi M, Urano S, Endo T. Antioxidant activity of eugenol and related monomeric and dimeric compounds. Chem Pharm Bull (Tokyo). 2000;48:1467-1469.
14. Guenette SA, Beaudry F, Marier JF, Vachon P. Pharmacokinetics and anesthetic activity of eugenol in male sprague-dawley rats. J Vet Pharmacol Ther. 2006;29:265-270.
15. Leite AM, Lima EO, Souza EL, Diniz MFFM, Trajano VN, Medeiros IA. Inhibitory effect of β-pinene, α-pinene and eugenol on the growth of potential infectious endocarditis causing gram-positive bacteria. Braz J Pharmacol Sci. 2007;43:121-126.
16. Ali SM, Khan AA, Ahmed I, Musaddiq M, Ahmed KS, Polasa H, Rao LV, Habibullah, CM, Sechi LA, Ahmed N. Antimicrobial activities of eugenol and cinnamaldehyde against the human gastric pathogen *Helicobacter pylori*. Ann Clin Microbiol Antimicrob. 2005;4:20.
17. Hemaiswarya S, Doble M. Synergistic interaction of eugenol with antibiotics against Gram-negative bacteria. Phytomedicine. 2009;16:997-1005.
18. Pei RS, Zhou F, Ji BP, Xu J. Evaluation of combined antibacterial effects of eugenol, cinnamaldehyde, thymol, and carvacrol against *E. coli* with an improved method. J Food Sci. 2009;74:379-383.
19. Oyedemi SO, Okoh AI, Mabinya LV, Pirochenva G, Afolayan AJ. The proposed mechanism of bactericidal action of eugenol α-terpineol and terpinene against *Listeria monocytogenes, Streptococcus pyogenes*, *Proteus vulgaris* and *Escherichia coli*. Afr J Biotechnol. 2009;8:1280-1286.
20. Qiu J, Feng H, Lu J, Xiang H, Wang D, Dong J, Wang J, Wang X, Liu J, Deng X. Eugenol reduces the expression of virulence-related exoproteins in staphylococcus aureus. Appl Environ Microbiol 2010;76:5846-5851.
21. Leem HH, Kim EO, Seo MJ, Choi SW. Antioxidant and anti-inflammatory activities of eugenol and its derivatives from clove (*Eugenia caryophyllata* Thunb.) Korean J Food Sci. 2011;40:1361-1370.
22. Grespan R, Paludo M, Lemos Hde P, Barbosa CP, Bersani-Amado CA, Dalalio MM, Cuman RK. Anti-arthritic effect of eugenol on collagen-induced arthritis experimental model. Bio Pharm Bull. 2012;35:1818-1820.

23. Feng J, Lipton JM. Eugenol: antipyretic activity in rabbits. Neuropharmacology. 1987;26:1775-1778.

24. Criddle DN, Madeira SV, Soares de Moura R. Endothelium-dependent and independent vasodilator effects of eugenol in the rat mesenteric vascular bed. J Pharma Pharmacol. 2003;55:359-365.

25. Kabuto H, Yamanushi TT. Effects of zingerone [4-(4-hydroxy-3-methoxyphenyl)-2-butanone] and eugenol [2-methoxy-4-(2-propenyl) phenol] on the pathological progress in the 6-hydroxydopamine-induced Parkinson's disease mouse model. Neurochem Res. 2011;36:2244-2249.

26. Hartnoll G, Moore D, Douek D. Near fatal ingestion of oil of cloves. Arch Dis Child. 1993;69:392-393.

27. Wright SE, Baron DA, Heffner JE. Intravenous eugenol causes hemorrhagic lung edema in rats: proposed oxidant mechanisms. J Lab Clin Med. 1995;125:257-264.

28. Soundran V, Namagiri T, Manonayaki S, Vanithakumari G. Hepatotoxicity of eugenol. Anc Sci Life. 1994;13:213-217.

29. Usta J, Kreydiyyeh S, Bajakian K, Nakkash-Chmaisse H. *In vitro* effect of eugenol and cinnamaldehyde on membrane potential and respiratory chain complexes in isolated rat liver mitochondria. Food Chem Toxicol. 2002;40:935-940.

30. Goulet F, Vachon P, Helie P. Evaluation of the toxicity of eugenol at anesthetic doses in African clawed frogs (Xenopus laevis). Toxicol Pathol. 2011;39:471-477.

31. Li J, Yu Y, Yang Y, Liu X, Zhang J, Li B, Zhou X, Niu J, Wei X, Liu Z. A 15-day oral dose toxicity study of aspirin eugenol ester in Wistar rats. Food Chem Toxicol. 1980;50:1980-1985.

32. Atsumi T, Fujitsawa S, Tonosaki K. A comparative study of the antioxidant/prooxidant activities of eugenol and isoeugenol with various concentrations and oxidation conditions. Toxicol In Vitro. 2005;19:1025-1033.

33. Ho YC, Haung FM, Chang YC. Mechanisms of cytotoxicity of eugenol in human osteoblastic cells *in vitro*. Int Endod J. 2006;39:389-393.

34. Queiroz CE, Soares JA, Leonardo Rde T, Carlos IZ, Dinelli W. Evaluation of cytotoxicity of two endodontic cements in a macrophage culture. J Appl Oral Sci. 2005;13:237-242.

35. Anpo M, Shirayama K, Tsutsui T. Cytotoxic effect of eugenol on the expression of molecular markers related to the osteogenic differentiation of human dental pulp cells. Odontology. 2011;99:188-192.

36. Vidhya N, Devaraj SN. Induction of apoptosis by eugenol in human breast cancer cells. Indian J Exp Biol. 2011;49:871-878.

37. Slameňová, D, Horváthová, E, Wsólová, L, Šramková, M, Navarová J. Investigation of anti-oxidative, cytotoxic, DNA-damaging and DNA-protective effects of plant volatiles eugenol and borneol in human-derived HepG2, Caco-2 and VH10 cell lines. Mutat Res. 2009;677:46-52.

38. Jaganathan SK, Mazumdar A, Mondhe D, Mandal M. Apoptotic effect of eugenol in human colon cancer cell lines. Cell Biol Int. 2011;35:607-615.

39. Yoo CB, Han KT, Cho KS, Ha J, Park HJ, Nam JH, Kil UH, Lee KT. Eugenol isolated from the essential oil of *Eugenia caryophyllata* induces a reactive oxygen species-mediated apoptosis in HL-60 human promyelocytic leukemia cells. Cancer Lett. 2005;225:41-52.

40. Ghosh R, Nadiminty N, Fitzpatrick JE, Alworth WL, Slaga TJ, Kumar AP. Eugenol causes melanoma growth suppression through inhibition of E2F1 transcriptional activity. J Biol Chem. 2005;280:5812-5819.

41. Huang TH, Lee H, Kao CT. Evaluation of the genotoxicity of zinc oxide eugenol-based, calcium hydroxide-based, and epoxy resin-based root canal sealers by comet assay. J Endod. 2001;27:744-748.

42. Han EH, Hwang YP, Jeong TC, Lee SS, Shin JG, Jeong HG. Eugenol inhibit 7,12-dimethylbenz[a]anthracene-induced genotoxicity in MCF-7 cells: Bifunctional effects on CYP1 and NAD(P)H:quinone oxidoreductase. FEBS Lett. 2007;581:749-756.

43. Rompelberg CJ, Stenhuis WH, Vogel N, Osenbruggen WA, Schouten A, Verhagen H. Antimutagenicity of eugenol in the rodent bone marrow micronucleus test. Mutat Res. 1995;346:69-75.

44. Munerato MC, Sinigaglia M, Reguly ML, de Andrade HH. Genotoxic Effects of Eugenol, Isoeugenol and Safrole in the Wing Spot Test of Drosophila Melanogaster. Mutat Res. 2005;582:87-94.

45. Woolverton CJ, Fotos PG, Mokas MJ, Mermigas ME. Evaluation of eugenol for mutagenicity by the mouse micronucleus test. J Oral Pathol. 1986;15:450-453.

46. Sukumaran K, Kuttan R. Inhibition of tobacco-induced mutagenesis by eugenol and plant extracts. Mutat Res. 1995;343:25-30.

47. Sarrami N, Pemberton MN, Thornhill MH. Adverse reactions associated with the use of eugenol in dentistry. Brit Dent J. 2002;193:257-259.

48. Buckley DA, Rycroft RJ, White IR, McFadden JP. Fragrance as an occupational allergen. Occup Med (Lond). 2002;52:13-16.

49. Tammannavar P, Pushpalatha C, Jain S, Sowmya SV. An unexpected positive hypersensitive reaction to eugenol. BMJ Case Rep. 2013:2013.

50. Rothenstein AS, Booman KA, Dorsky J, Kohrman KA, Schwoeppe EA, Sedlak RI, Steltenkamp RJ, Thompson GR. Eugenol and clove leaf oil: a survey of consumer patch-test sensitization. Food Chem Toxicol. 1983;21:727-733.

Turk J Pharm Sci 2017;14(2):207-212
DOI: 10.4274/tjps.26349

REVIEW

Contribution of Rho-kinase and Adenosine Monophosphate-Activated Protein Kinase Signaling Pathways to Endothelium-Derived Contracting Factors Responses

Endotel Kaynaklı Kastırıcı Faktör Yanıtlarına Rho-kinaz ve Adenosin Monofosfatla Aktive Edilmiş Protein Kinaz Sinyal Yolaklarının Katkısı

Cennet BALCILAR*, Işıl ÖZAKCA, Vecdi Melih ALTAN

Ankara University, Faculty of Pharmacy, Department of Pharmacology, Ankara, Turkey

ABSTRACT

Vascular tonus is controlled by endothelium-derived relaxing factor (EDRF), endothelium-derived hyperpolarizing factor (EDHF) and endothelium-derived contracting factor (EDCF) under physiological circumstances. In pathological conditions, impairment of endothelium-derived relaxation can be caused by both decrease in EDRF release and increase in EDCF release. The increase in EDCF is observed with diseases such as hypertension and diabetes. The contribution of Rho-kinase and activated protein kinase (AMPK), which have opposite effects, to the increased EDCF responses was investigated. Rho-kinases are the effectors of Rho which is one of the small guanosine triphosphate-binding proteins. They increase cytosolic Ca^{+2} concentration and cause vascular smooth muscle to contract, keeping myosin light chain (MLC) in phosphorylated state by affecting myosin phosphatase target subunit which dephosphorylates the MLC. The activities of Rho-kinases increase with the increase of EDCF function. AMPK is the energy sensor of the cell. It provides a vasculoprotective effect by causing endothelium-dependent and endothelium-independent relaxation in smooth muscle. In contrast to Rho-kinase pathway activity, AMPK pathway activity decreases with diseases in which the EDCF function increases. In cases such as diabetes and hypertension that endothelial function impairs toward vasocontraction, it is considered that evaluating Rho-kinase and AMPK pathways which mediate contraction and relaxation in vascular smooth muscle respectively, would provide clues on choosing therapeutic target for pathologies in which endothelial dysfunction is observed.

Key words: AMPK, EDCF, endothelium, Rho-kinaz

ÖZ

Fizyolojik koşullarda vasküler tonus endotel kaynaklı rahatlatıcı faktörü (EDRF), endotel kaynaklı hiperpolarizasyon faktörü (EDHF) ve endotel kaynaklı kasılma faktörü (EDCF) tarafından kontrol edilmektedir. Patolojik durumlarda endotel kaynaklı gevşemenin azalması, EDRF üretimindeki azalmaya bağlı olabileceği gibi EDCF düzeyinin artmasına da bağlı olabilmektedir. EDCF hipertansiyon, diyabet gibi hastalıklarda artmaktadır. Diyabet, hipertansiyon gibi patolojik koşullarda artan EDCF yanıtına birbirine ters etki yapan Rho-kinaz ve aktive protein kinaz (AMPK) yolaklarının katkısı olabileceği düşünülmektedir. Rho-kinazlar küçük guanozin trifosfat-bağlı proteinlerden biri olan Rho'nun efektörüdür. Rho-kinazlar hafif zincir miyozini (MLC) defosforile eden miyozin fosfataz hedef altbirimine etki ederek MLC'nin fosforile halde kalmasının sağlayarak sitozolik Ca^{+2} konsantrasyonu artırır ve vasküler düz kasın kasılmasına neden olurlar. Rho-kinazların aktivitesi EDCF yanıtlarının arttığı hipertansiyon, kalp yetmezliği ve diyabet gibi hastalıklarda artmaktadır. AMPK ise hücrenin enerji sensörü olarak düşünülmektedir. Vasküler düz kasta endotel bağımlı ve bağımsız gevşemeyi sağlayarak vasküloprotektif etki sağlamaktadır. AMPK'nin aktivitesi Rho-kinaz yolağının aktivitesinin tersine EDCF fonksiyonunun arttığı hipertansiyon ve diyabet gibi hastalıklarda azalmaktadır. Endotel fonksiyonunun vazokonstriksiyon yönünde bozulduğu diyabet, hipertansiyon gibi tablolarda, damar düz kas dokusunda sırasıyla kasılma ve gevşemeye aracılık eden Rho-kinaz ve AMPK yolaklarının birlikte değerlendirilmesinin, endotel fonksiyon bozukluğunun gözlendiği patolojilerde terapötik hedef seçiminde ipuçları sağlayabileceği düşünülmektedir.

Anahtar kelimeler: AMPK, EDCF, endotel, Rho-kinaz

***Correspondence: E-mail:** cennetsnb@hotmail.com, **Phone:** +90 505 231 41 07
ORSID ID: orcid.org/0000-0002-0557-5853
Received: 01.12.2016, **Accepted:** 10.02.2017

INTRODUCTION

Under the normal physiological conditions, vascular tonus is controlled by endothelium-derived relaxation factors (EDRF) including nitric oxide (NO), endothelium-derived hyperpolarizing factor (EDHF) endothelium-derived contractile factor (EDCF).[1,2] The changes in these factors cause a change in the blood pressure. It is hypothesized that, the reduction of the endothelium-derived relaxation response in type II diabetes can be the result of the decrease EDRF production, as well as the increase of the EDCF level.[3]

Endothelium-derived relaxation factors

In 1980, Furchgott and Zawadzki[4], for the first time, proved that the endothelial cells are necessary for the relaxation of the vascular tissue via acetylcholine (ACH) and that the relaxation of the vascular muscle is provided via the secretion of the EDRF from endothelium. The neurotransmitters, hormones, and as a response to mechanical stress, the EDRF and/or EDCF can be secreted from the endothelial cells.[5] EDRF includes NO and prostaglandin I_2 [prostacyclin (PGI_2)].[6] EDRF induces the relaxation of the vascular smooth muscle via the activation of K^+ channels. PGI_2 and NO mediate the relaxation with the increase of the concentrations of the seconder messengers, such as cyclic adenosine monophosphate (AMP) and cyclic guanosine monophosphate inside the cell.[5]

Endothelium-derived hyperpolarizing factor

In addition to EDRF, EDHF also mediates the relaxation of the smooth muscle.[7] Although the molecular mechanism of the vasorelaxing activity of the EDHF has not been completely understood, it is thought that the mechanism is achieved via the occurence of the hyperpolarization as a result of the opening of the K^+ channels.[7] EDHF is defined as the endothelium-mediated relaxation response, which is observed after the PGI_2 - NO block is made.[7]

Endothelium-derived contractile factor

Endothelium-derived contraction happens via the cyclooxygenase (COX) products.[3] The COX's convert the arachidonic acid into endoperoxides. Endoperoxides, on the other hand, with the help of the appropriate enzymes are converted to various prostaglandins, such as, E_2 (PGE_2), prostaglandin D_2 (PGD_2), prostaglandin $F_{2\alpha}$ ($PGF_{2\alpha}$), and PGI_2 tromboxan A_2 (TxA_2). These prostanoids create the EDCF response by activating the thromboxane-prostanoid (TP), a receptor which is locked to the G-protein in smooth muscle. This contraction response occurs as a result of the increase of the amount of the Ca^{+2} ions entering the smooth muscle cells, which is achieved via the opening of the receptor-mediated and voltage dependent Ca^{+2} channels.[9] Under *in vitro* conditions the removal of the EDCF responses are removed via: (i) the incubation made with the COX inhibitors, which inturn results in the inhibition of the prostanoid production in endothelium and (ii) the incubation made with the antagonists of the TP receptors, which prevents the excitation of these receptors via prostanoids.[10] These results prove that the COX products and TP receptors are responsible from the EDCF-mediated response.[10]

EDCF response can be triggered by the ACH which excites the endothelium M_3- muscarinic receptors, and by vasoactive agonists like adenosine diphosphate, which activates purinergic receptors.[9] Just like these vasoactive agonists, Ca^{+2} ionophore A23187, an agent which increases the entrance of Ca^{+2} also triggers the creation of EDCF response. These agents are used for the evaluation of EDCF response, experimentally, under *in vitro* conditions (Figure 1).

The TP receptors belong to the family of the receptors locked to the Gq-protein. The endothelium-derived contraction responses created via the activation of TP receptors are associated with the increase of the sensitivity to Rho-kinase (ROCK)-mediated myofilaments.[10]

Rho-kinase pathway

The guanosine triphosphate (GTP)-locked proteins mediate the inside-cell pathways of the membrane receptors. These GTP-locked proteins include the Rho, Ras, Rab, Sarl/Arf and Ran families.[11] In the mammals, the RhoA, RhoB, RhoC, RhoD, RhoE and RhoG izoforms of the Rho family are defined.[12] RhoA is the most famous member of the Rho protein family. It participates in the organization of the actin, contraction, motility, proliferation and apoptosis.[12] In order for the RhoA-mediated cell response to occur, it plays the key role as the ROCK downstream effector in the interaction of inactive GDP and active GTP.[12] RhoA is activated via the conversion of guanine nucleotide from GDP to GTP. The proteins activating the GTP-ase excite the intrinsic GTP-ase activity, whereas they deactivate the RhoA. ROCK are the first and most important effectors of the RhoA.[13,14] There are two isoforms of ROCK, namely, ROCK1 and ROCK2.[14] Although

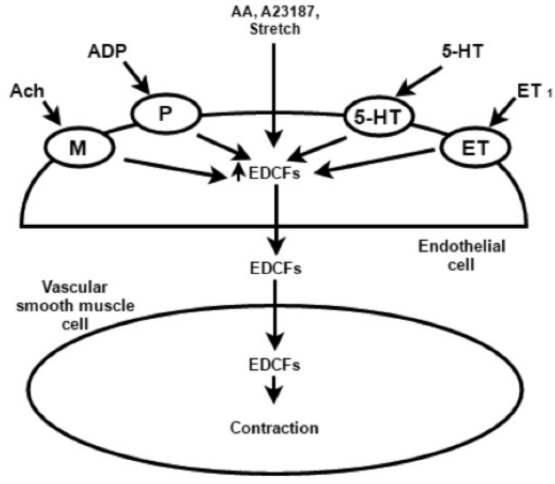

Figure 1. The creation and effect mechanism of endothelium-derived contractile factor, As a result of the bonding of some neuromediators to their corresponding receptors in endothelium cells, production of a Ca^{+2} ionophore A23187, arachidonic acid and an increase of the endothelium-derived contractile factor production occurs, which then results in the contraction of the smooth muscle[9]

Ach: Acetylcholine, ADP: Adenosine diphosphate, AA: Arachidonic acid, ET_1: Endothelin$_{-1}$, M: Muscarinic receptor, P: Purinergic receptor, 5-HT: 5-hydroxytryptamine, EDCF: Endothelium-derived contractile factor

these two isoforms are located with different concentrations at different tissues, no functional difference between them has been defined.[15] The activity of the RhoA/Rho associated protein kinase pathway is increased in diabetes, as well as it is occurred in hypertension, coroner vasospasm, stroke, atherosclerosis and heart failure.[16] This situation makes the ROCK a new and important theurapeutic aim.[16]

The targets of ROCK, such as myosin phosphatase target subunit (MYPT-1), myosin light chain (MLC) and calponin play the key role in the contraction of the smooth muscle cells. MYPT-1 is the major effector in the contraction of the smooth muscle for the ROCK associated Ca^{+2} sensitivity.[10] In addition, MLC, C-kinase potentiated protein phosphatase-1 inhibitor (CPI-17) and the phosphorylation of the calponin contribute to the ROCK associated smooth muscle contraction. In the vascular smooth muscle, the MLC is phosphorylated by the MLC kinase, (MLCK) which is activated by Ca^{+2}-calmoduline-dependent kinase, and dephosphorylated by the Ca^{+2}-independent MLC phosphatase (MLCP).[13,14] The MLC, which gets phosphorylated with the activation of the MLCK, mediates the increase of the cytosolic Ca^{+2} concentration and the vascular smooth muscle contraction occurs (Figure 2).[12]

ROCK inhibits the production of NO from the endothelium cells. The activation of RhoA/ROCK decreases the endotelial NO synthase (eNOS) expression by inhibiting the eNOS mRNA stability.[13] It was shown that the eNOS expression increases during the treatment of human umbilical vein endothelial cells channel via the incubation of ROCK inhibitor Y27632 (10 µmol/L).[17] Among the ROCK inhibitors, only the fasudil is approved for the clinical use in the cerebral vasospasm endication.[18] In addition to fasudil, Y-27632 is another ROCK inhibitor whose activity is also proven and which has been used in several studies.[18]

There are several studies demonstrating that the ROCK pathway activity increases in parallel to the EDCF response. For instance, in the spontaneously hypertensive rats the inhibitors of the ROCK inhibit the increasing EDCF response in the carotid arter, under *in vitro* conditions,[10] and in STZ-diabetic rats the application of fasudil treatment (5 mg/kg/day, oral) for a period of 16 weeks decreases the vascular contraction response.[19]

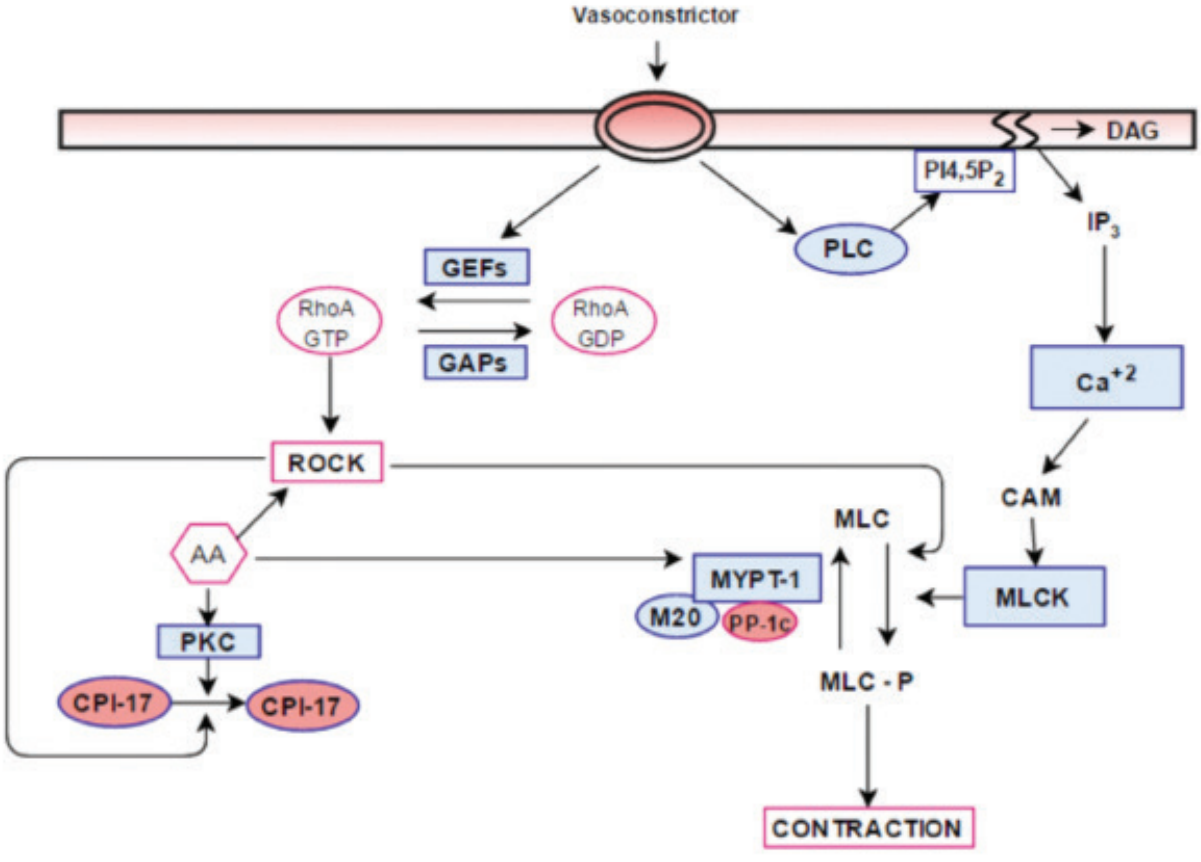

Figure 2. The contraction signal mechanism of the vascular smooth muscle cells, The contraction is induced by an increase of 20-kDa in myosin light chain phosphorylation, Excitation of the receptor locked to the G protein, by the vasoconstrictor agent increases the Ca^{+2} concentration in the cell, thereby inhibiting the myosin light chain phospatase, via the excitation of the myosin light chain kinase, myosin light chain phospatase consists of 3 parts, These subunits are the catalytic subunit PP-1c, myosin phosphatase target-1 and 20-kDa subunit M20, Vasoconstrictor increases the the agent induced myosin light chain phospatase inhibition and activation of RhoA and Rho-kinase[12]

PKC: Protein kinase C, GEF: Guanine nucleotide exchange factor, GAP: GTPase-activation protein, PLC: Phospholipase C, DAG: Diacylglycerol, $PI4,5P_2$: Phosphatidylinositol 4,5-biphosphate, IP3: Inositol 1,4,5-triphophate, CAM: Calmodulin, MLC: Myosin light chain, MLCK: Myosin light chain kinase, MLCP: Myosin light chain phospatase, MYPT: Myosin phosphatase target, ROCK: Rho-kinases, AA: Arachidonic acid, GTP: Guanosine triphosphate

Adenosine monophosphate-activated protein kinase pathway

Another pathway which is hypothesized to be related to EDCF is adenosine monophosphate-activated protein kinase (AMPK). AMPK term was introduced in 1988, by Sim and Hardie[20], for the first time. Being a serine/threonine kinase AMPK regulates all of the cellular events and is though as the energy sensor of the cell.[21,22]

AMPK consists of 3 subunits, namely, α, β and γ. α and β subunits consist of 2 isoforms, whereas γ subunit has 3 isoforms.[22] These isoforms have different placements in different tissues at different expression levels. Each isoform is coded by a different genes. α is the catalytic subunit; whereas, β and γ are regulatory subunits. α subunit consists of a autoinhibitor region, which inhibits the catalytic kinase region of N terminal, and the activity of the C terminal when the regulatory part AMP is not present, and a region which is connected to the β, and γ subunits. α_1 subunit is dominant at adipose tissue, in the pancreas island cells, at endothelium and vascular smooth muscle, α_2 subunit on the other hand is dominant in skeletal and heart muscles. β subunit works as a sketelon which connects the α and γ subunits. γ subunit, on the other hand, carries the connection parts of AMP and adenosine triphosphate (ATP).[21]

The activity of AMPK increases in the situations where the need of ATP increases; such situations are exercise, hunger, inflammation and hypoxia. AMPK effects the metabolisms of lipid, carbohydrate, and proteins. Activation of AMPK regulates the lipid methabolism by ensuring the fat oxidation, producing the cholesterol in liver, decreasing the synthesis of the fatty acids and increasing the lipolysis in adipocytes. The effect of AMPK on carbohydrate metabolism can be summarized as the increase of the glucose uptake in the skeleton muscle and at heart, with the activation of AMPK, the excitation of glucogeneogenesis enzym in the liver and the regulation of the insulin secretion of the β cells in pancreas. In addition to these effects, the activation of AMPK increases the NO production at heart and vascular endothelium. Long periods of AMPK activation might cause modifications in protein synthesis via the modulation of transcription factors, like myocyte enhancer factor-2, mammalian target of rapamycin and eukaryotic elongation factor 2.[23]

Antidiabetic agents, such as, metformin[24], thiazolidinediones, glukagon like peptid-1 agonists, dipeptidyl peptidase-4 inhibitors, statins, adiponectin and the leptin hormone increase the AMPK activation.[25,26] Experimentally, 5-aminoimidazole-4-carboxamide ribonucleoside is used for the AMPK activation[24], whereas the dorsomorphine (compound C) is used for the inhibition.

AMPK increases the eNOS activity in the smooth muscle, which in turn increases the NO-mediated endothelium-dependent relaxation. The endothelium independent relaxation, on the other hand, is ensured by AMPK via the decrease in the Ca^{+2} sensitivity of the MLCK in the smooth muscle cell (Figure 3). It therefore shows a vasoprotective effect.[25-27] It is thought that the vasoprotective effects of the therapeutic agents like, metformin[24], thiazolidinediones and statins also occur via the AMPK activation.[21] AMPK activation causes the NO-mediated

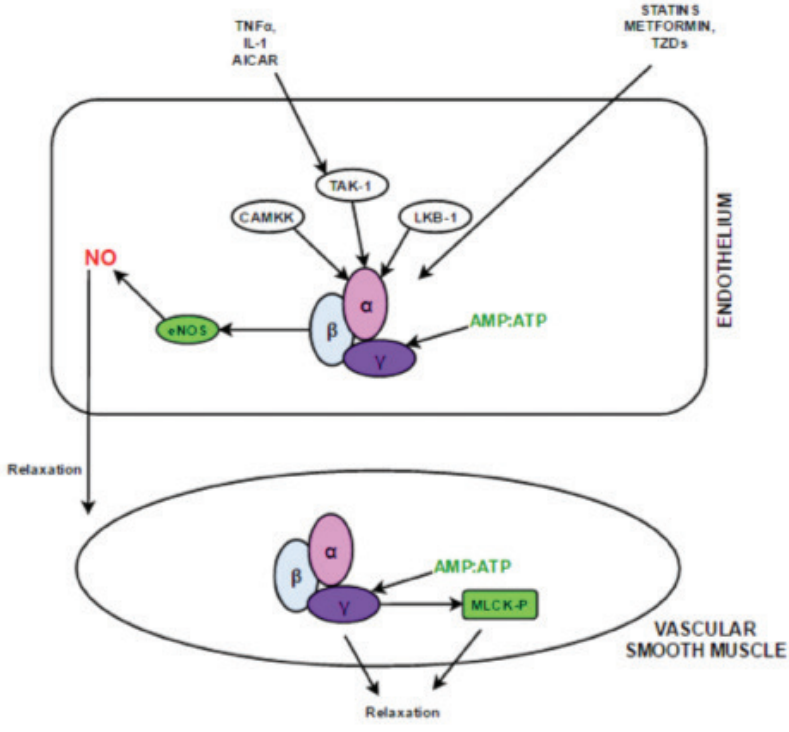

Figure 3. The vascular effect of the AMPK activation and the agents activating AMPK[21]

TNF-α: Tumor necrosis factor-alpha, IL: Interleukin, AICAR: 5-aminoimidazole-4-carboxyamide-1-β-D-ribofuranoside, CAMKK: Calmodulin-dependent kinase kinase, TAK: Transforming growth factor β-activated kinase, LKB: Liver kinase B, MLCK: Myosin light chain kinase, AMP: Adenosine monophosphate, ATP: Adenosine triphosphate, NO: Nitric oxide

relaxation in the spontaneously hypertensive rats.[25-28] AMPK, at the same time, causes the endothelium independent vascular smooth muscle relaxation in the aort preparations of the Mouse.[27]

Rho-kinase and adenosine monophosphate-activated protein kinase interaction

In the pathologies with hyperglycemia and hypertension, the inverse effects of AMPK and ROCK pathways results in the speculations that these two pathways are related to each other.

Increase in ROCK activation suppresses production of NO in endothelium cells and indirectly causes contraction in vascular smooth muscle. This is related with ROCK activation's effects of decreasing eNOS expression and mRNA stability. ROCKs effect on MYPT-1 also plays role in this pathway. By keeping MYPT-1 inactive, ROCK triggers MLC phosphorylation, cytosolic Ca^{+2} level increase and as a result it's contraction.[13] AMPKs vascular effect is the opposite of this. In contrast to ROCKs effect, AMPK activation increases the activity of eNOS in arterial smooth muscle. It causes endothelium dependent relaxation by increasing the production of NO. On the other hand, it causes endothelium independent relaxation by decreasing intracellular Ca^{+2} sensitivity and vascular tonus through activating MLCK in vascular smooth muscle cell.[25-27] In summary, ROCK activation makes hypertension and diabetes like pathologies more critical by causing increase in vascular contraction. Increase in the AMPK activation, can help fixing vascular complications caused by these pathologies with its vasculoprotective effect. From this point of view, it is believed that in pathologies in which vascular tonus increases, inhibition of ROCK activity and activation of AMPK can be beneficial. That is why ROCK inhibitors and agents that are increasing the activation of AMPK are considered as new therapeutic targets.[18-25]

ROCK and AMPK is related also because the molecules below are up-regulated ROCK inhibition. And these molecules are the downstream targets of AMPK (Figure 4)[29]:

Cpt1a and Cpt1b that play role in obtaining energy through lipolysis and carrying fatty acids from outer membrane of mitochondria to cytosol, Cycs (cytochrome C) and Cox4i1 (cytochrome C oxidase lower unit 4i1), transmembrane proteins in mitochondria and last receiver of the electron transfer chain, Slc2a4, glucose transporter which is found in muscle tissue and adipose tissue.

Additionally, it is another finding that shows the relationship between these pathways that, as a ROCK inhibitor hydroxyfasudil increase the NAD^+/NADH rate and Sirtuin-1 activity (Figure 4) which are AMPK's downstream target.[29]

In experimental models and humans, observing metformin, which causes AMPK activation, decrease body weight and serum lipid levels like fasudil does, is another sign of the interaction.[29]

Below studies are made in order to enlighten the relationship between AMPK and ROCK pathways:

In hypertensive rats that angiotensin are induced, it is observed that resveratrol treatment stabilizes the blood pressure by decreasing ROCK activity and AMPK activation.[30]

Metabolic disorders observed in rats that are fed with high fat diet, are fixed with ROCK inhibitor and AMPK mediated.

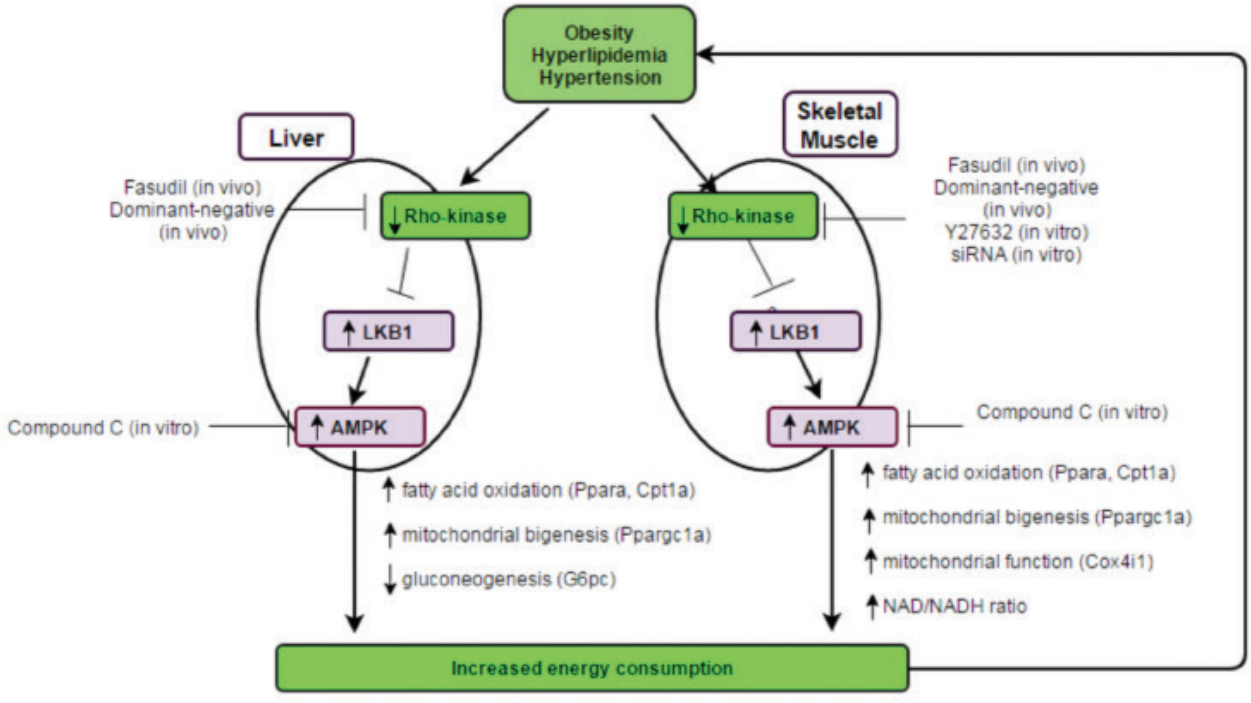

Figure 4. Rho-kinase inhibition increases energy consumption by activating AMPKα2 through liver kinase B-1, effect of change in Rho-kinase activity on adenosine monophosphate-activated protein kinase activity[29]

LKB: Liver kinase B, AMPK: Adenosine monophosphate-activated protein kinase

And positive effects of the treatment with ROCK inhibitor are disappeared in rats AMPK gene is deleted.[29]

DISCUSSION

In pathologies that endothelium functions impair, ROCK activity increases in parallel with EDCF response while AMPK pathway activity decreases. It is thought that, having these pathways response to the same pathologies adversely might mean that there is a relationship between them. It is seen as a sign of relationship between pathways in following researches: hypertensive rats with induced angiotensin, it is observed that resveratrol treatment stabilizes the blood pressure by decreasing ROCK activity and AMPK activation[30], metabolic disorders observed in rats that are fed with high fat diet, are fixed with ROCK inhibitor and AMPK mediated. And positive effects of the treatment with ROCK inhibitor are disappeared in AMPK gene deleted rats.[29] ROCK activation makes hypertension and diabetes like pathologies more critical by causing increase in vascular contraction. Increase in AMPK activation contributes recovery of vascular complications related with these pathologies by providing a vasculoprotective effect. That is why, in pathologies with vascular tonus increase, it is thought that ROCK activity inhibition and AMPK activity activation might be beneficial. Hence, ROCK inhibitors and AMPK activating agents are considered as new therapeutic targets.[18-25] Evaluating ROCK and AMPK pathways together can provide hints about therapeutic target selection in the pathologies in which endothelium function impairs.

Conflict of Interest: No conflict of interest was declared by the authors.

REFERENCES

1. Feletou M, Vanhoutte PM. Endothelial dysfunction: a multifaceted disorder (The Wiggers Award Lecture). Am J Physiol Heart Circ Physiol. 2006;291:985-1002.
2. Pieper GM. Review of alterations in endothelial nitric oxide production in diabetes: protective role of arginine on endothelial dysfunction. Hypertension. 1998;31:1047-1060.
3. Matsumoto T, Kobayashi T, Kamata K. A therapeutic target for microvascular complications in diabetes: endothelium-derived hyperpolarizing factor. Curr Cardiol Rev. 2006;2:185-191.
4. Furchgott RF, Zawadzki JV. The obligatory role of endothelial cells in the relaxation of arterial smooth muscle by acethylcholine. Nature. 1980;288:373-376.
5. Shen B, Ye CL, Ye KH, Liu JJ. Mechanism underlying enhanced endothelium-dependent vasodilatation in thoracic aorta of early stage streptozotocin-induced diabetic mice. Acta Pharmacol Sin. 2003;24:422-428.
6. Kang KT. Endothelium-derived relaxing factors of small resistance arteries in hypertension. Toxicol Res. 2014;30:141-148.
7. Ohashi J, Sawada A, Nakajima S, Noda K, Takaki A, Shimokawa H. Mechanism for enhanced endothelium-derived hyperpolarizing factor-mediated responses in microvessels in mice. Circ J. 2012;76:1768-1779.
8. Vanhoutte PM. Vascular biology. Old-timer makes a comeback. Nature. 1998;396:213-216.
9. Vanhoutte PM, Feletou M, Taddei S. Endothelium-dependent conractions in hypertension. Br J Pharmacol. 2005;144:449-458.
10. Denniss SG, Jeffery AJ, Rush JW. RhoA-Rho kinase signaling mediates endothelium and endoperoxide dependent contractile activities characteristic of hypertensive vascular dysfunction. Am J Physiol Heart Circ Physiol. 2010;298:1391-1405.
11. Shinmokawa H, Takeshita A. Rho-kinase is an important therapeutic target in cardiovascular medicine. Arterioscler Thromb Vascl Biol. 2005;25:1767-1775.
12. Loirand G, Guèrin P, Pacaud P. Rho kinases in cardiovascular physiology and pathophysiology. Circ Res. 2006;98:322-334.
13. Loirand G. Rho Kinases in Health and Disease: From Basic Science to Translational Research. Pharmacol Rev. 2015;67:1074-1095.
14. Shimokawa H, Sunamura S, Satoh K. RhoA/Rho-Kinase in the Cardiovascular System. Circ Res. 2016;118:352-366.
15. Hahmann C, Schroeter T. Rho-kinase inhibitors as therapeutics: from pan inhibition to isoform selectivity. Cell Mol Life Sci. 2010;67:171-177.
16. Zhou H, Li YJ. Rho kinase inhibitors: potential treatments for diabetes and diabetic complications. Curr Pharm Des. 2012;18:2964-2973.
17. Eto M, Barandier C, Rathgeb L, Kozai T, Joch H, Yang Z, Lüscher TF. Thrombin suppresses endothelial nitric oxide synthase and upregulates endothelin-converting enzyme-1 expression by distinct pathways: role of Rho/ROCK and mitogen-activated protein kinase. Circ Res. 2001;89:583-590.
18. Surma M, Wei L, Shi J. Rho kinase as a therapeutic target in cardiovascular disease. Future Cardiol. 2011;7:657-671.
19. Li T, Yang GM, Zhu Y, Wu Y, Chen XY, Lan D, Tian KL, Liu LM. Diabetes and hyperlipidemia induce dysfunction of VSMCs: contribution of the metabolic inflammation/miRNA pathway. Am J Physiol Endocrinol Metab. 2015;308:257-269.
20. Sim AT, Hardie DG. The low activity of acetyl-CoA carboxylase in basal and glucagon-stimulated hepatocytes is due to phosphorylation by the AMP-activated protein kinase and not cyclic AMP-dependent protein kinase. FEBS Lett. 1988;233:294-298.
21. Ewart MA, Kennedy S. AMPK and vasculoprotection. Pharmacol Ther. 2011;131:242-253.
22. Li J, Li S, Wang F, Xin F. Structural and biochemical insight into the allosteric activation mechanism of AMP-activated protein kinase. Chem Biol Drug Des. 2016:1-7.
23. Hardie DG, Alessi DR. LKB1 and AMPK and the cancer-metabolism link - ten years after. BMC Biol. 2013;15:11-36.
24. Yan T, Zhang J, Tang D, Zhang X, Jiang X, Zhao L, Zhang Q, Zhang D, Huang Y. Hypoxia Regulates mTORC1-Mediated Keratinocyte Motility and Migration via the AMPK pathway. Plos One. 2017;12:e0169155.
25. Ford RJ, Rush JW. Endothelium-dependent vasorelaxation to the AMPK activator AICAR is enhanced in aorta from hypertensive rats and is NO and EDCF dependent. Am J Physiol Heart Circ Physiol. 2011;300:64-65.
26. Batchuluun B, Inoguchi T, Sonoda N, Sasaki S, Inoue T, Fujimura Y, Miura D, Takayanagi R. Metformin and liraglutide ameliorate high glucose-induced oxidative stress via inhibition of PKC-NAD(P)H oxidase pathway in human aortic endothelial cells. Atherosclerosis. 2014;232:156-164.
27. Goirand F, Solar M, Athea Y, Viollet B, Mateo P, Fortin D, Leclerc J, Hoerter J, Ventura-Clapier R, Garnier A. Activation of AMP kinase alpha1 subunit induces aortic vasorelaxation in mice. J Physiol. 2007;581:1163-1171.
28. Ford RJ, Teschke SR, Reid EB, Durham KK, Kroetsch JT, Rush JW. AMP-activated protein kinase activator AICAR acutely lowers blood pressure and relaxes isolated resistance arteries of hypertensive rats. J Hypertens. 2012;30:725-733.
29. Noda K, Nakajima S, Godo S, Saito H, Ikeda S, Shimizu T, Enkhjargal B, Fukumoto Y, Tsukita S, Yamada T, Katagiri H, Shimokawa H. Rho-kinase inhibition ameliorates metabolic disorders through activation of AMPK pathway in mice. Plos One. 2014;9:e110446.
30. Cao X, Luo T, Luo X, Tang Z. Resveratrol prevents AngII-induced hypertension via AMPK activation and RhoA/ROCK suppression in mice. Hypertens Res. 2014;37:803-810.